Cardiac development in relation to clinical supraventricular arrhythmias : focus on structure-function relations

Kolditz, D.P.

Cardiac Development in Relation to Clinical Supraventricular Arrhythmias: Focus on Structure-Function Relations

Denise Pamela Kolditz

Cardiac Development in Relation to Clinical Supraventricular Arrhythmias: Focus on Structure-Function Relations

Colophon

The studies described in this thesis were performed at the department of Cardiology, Pediatric Cardiology and Anatomy & Embryology of the Leiden University Medical Center, Leiden, The Netherlands.

Cover:
Denise P. Kolditz, Leiden, The Netherlands

Layout:
Denise P. Kolditz, Leiden, The Netherlands

Printing:
Zalsman Kampen BV, Kampen, The Netherlands

Production:
Cicero Grafisch Productiebureau, Haren, The Netherlands

ISBN: 978-90-9024068-8

Cardiac Development in Relation to Clinical Supraventricular Arrhythmias: Focus on Structure-Function Relations

PROEFSCHRIFT

ter verkrijging van
de graad van Doctor aan de Universiteit van Leiden,
op gezag van Rector Magnificus prof. mr. P.F. van der Heijden,
volgens besluit van het College voor Promoties
te verdedigen op woensdag 8 april 2009
klokke 16:15 uur

door

Denise Pamela Kolditz

geboren te Maassluis
in 1982

Promotiecommissie

Promotores:	Prof. Dr. M.J. Schalij Prof. Dr. A.C. Gittenberger-de Groot
Leden:	Prof. Dr. R.N.W. Hauer *(Universitair Medisch Centrum Utrecht)* Prof. Dr. D.L. Ypey *(Leids Universitair Medisch Centrum)* Prof. Dr. N.A. Blom *(Leids Universitair Medisch Centrum)*

Financial support by the Netherlands Heart Foundation for the publication of this thesis is gratefully acknowledged.

“EX OVO OMNIA”

William Harvey (1651), Exercitationes de generatione animalium.

Table of Contents

Chapter 1

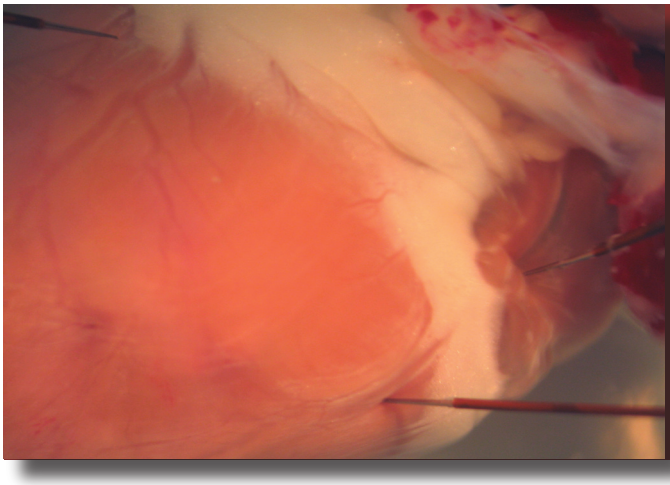

Denise P. Kolditz[1,2]

[1]Department of Cardiology, Leiden University Medical Center

[2]Department of Anatomy and Embryology, Leiden University Medical Center

General Introduction & Outline of the Thesis

Outline General Introduction

Supraventricular tachycardias (SVTs) are amongst the most commonly encountered cardiac arrhythmias in clinical practice in both children and adults.[1, 2] The causative mechanisms underlying the appearance of most of these SVTs have however still remained as intriguing as they are unexplained. In this thesis, cardiac development is analyzed in relation to the etiology of clinical supraventricular arrhythmias with a special focus on structure-function relations.

Firstly, in **PART I** of this thesis, both the (patho) physiological development of the annulus fibrosus cordis and the etiological origin of clinical accessory AV pathway (AP) mediated AVRT in children and adults is analyzed in experimental animal models and human sections. Secondly, in **PART II** of this thesis a review of the different ontogenic theories on the embryonic development of the AV Node (AVN) in literature is followed by an experimental study postulating a new concept on the developmental origin of the AVN in relation to the etiology of AV Nodal Reentrant Tachycardia (AVNRT).

As a general introduction to both these 'basic research' (**I** & **II**) and the 'clinical' (**III**) parts of this thesis, structural cardiac development in avians (with references to equivalent mouse and human developmental timelines) (**Figure 1**) will first be described since the development of the cardiac conduction system (CCS) and structural cardiogenesis are intimately related. Next, the developmental transitions in impulse propagation and the construction of the individual components of the specialized CCS and the AVN in particular will be shortly outlined. Following a description of the changes in electrocardiograms (ECGs) during cardiogenesis, current concepts on the transitions in ventricular activation sequences during embryogenesis will be discussed. Thereafter, contemporary knowledge on the development of the isolating annulus fibrosis, the key structure involved in AP persistence, in relation to general CCS development will be reviewed. Subsequently, relevant general characteristics of the different animal models and the immunohistochemical markers used in this thesis are briefly discussed. Following the description of the structural basics of cardiogenesis, attention will be focused on current knowledge of clinical SVTs in neonates and children and the treatment of these arrhythmias. These therapeutic clinical issues will be further outlined in **PART III** of this thesis.

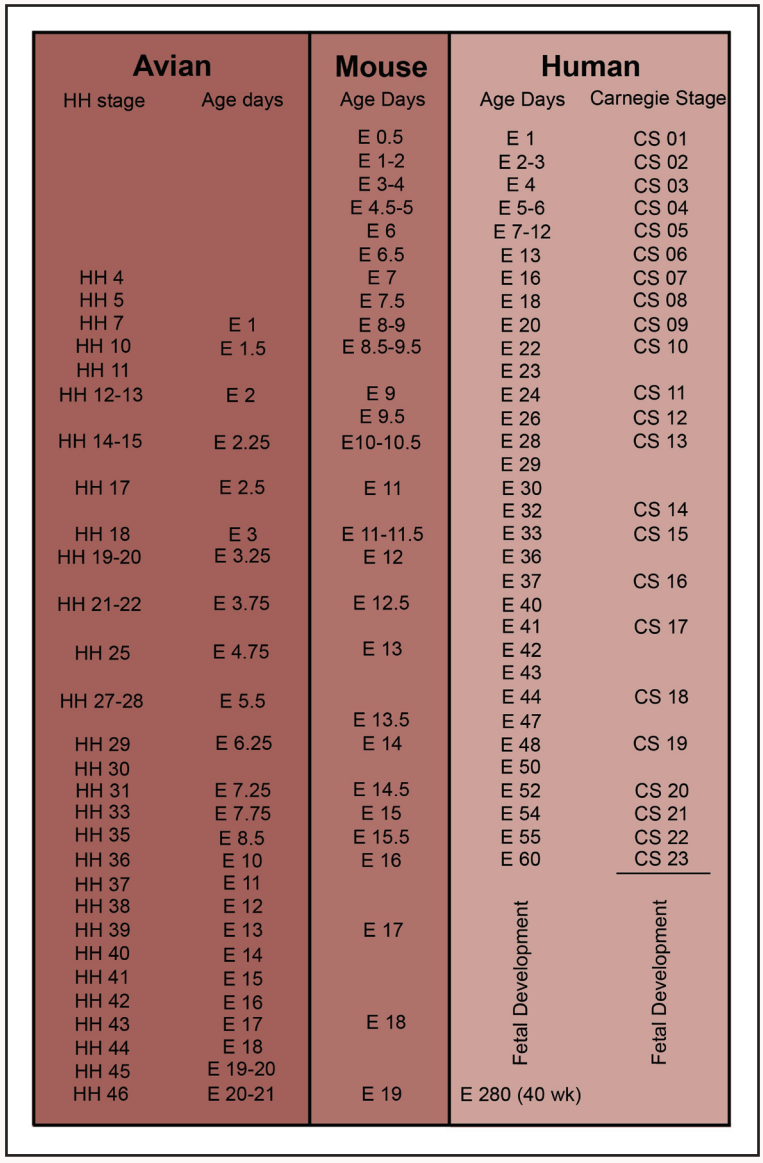

Avian		Mouse	Human	
HH stage	Age days	Age Days	Age Days	Carnegie Stage
		E 0.5	E 1	CS 01
		E 1-2	E 2-3	CS 02
		E 3-4	E 4	CS 03
		E 4.5-5	E 5-6	CS 04
		E 6	E 7-12	CS 05
		E 6.5	E 13	CS 06
HH 4		E 7	E 16	CS 07
HH 5		E 7.5	E 18	CS 08
HH 7	E 1	E 8-9	E 20	CS 09
HH 10	E 1.5	E 8.5-9.5	E 22	CS 10
HH 11			E 23	
HH 12-13	E 2	E 9	E 24	CS 11
		E 9.5	E 26	CS 12
HH 14-15	E 2.25	E10-10.5	E 28	CS 13
			E 29	
HH 17	E 2.5	E 11	E 30	
			E 32	CS 14
HH 18	E 3	E 11-11.5	E 33	CS 15
HH 19-20	E 3.25	E 12	E 36	
			E 37	CS 16
HH 21-22	E 3.75	E 12.5	E 40	
			E 41	CS 17
HH 25	E 4.75	E 13	E 42	
			E 43	
HH 27-28	E 5.5		E 44	CS 18
		E 13.5	E 47	
HH 29	E 6.25	E 14	E 48	CS 19
HH 30			E 50	
HH 31	E 7.25	E 14.5	E 52	CS 20
HH 33	E 7.75	E 15	E 54	CS 21
HH 35	E 8.5	E 15.5	E 55	CS 22
HH 36	E 10	E 16	E 60	CS 23
HH 37	E 11			
HH 38	E 12			
HH 39	E 13	E 17	Fetal Development	Fetal Development
HH 40	E 14			
HH 41	E 15			
HH 42	E 16			
HH 43	E 17	E 18		
HH 44	E 18			
HH 45	E 19-20			
HH 46	E 20-21	E 19	E 280 (40 wk)	

Figure 1. Schematic overview of the major staging systems of embryonic development in the avian, mouse and human embryonic developmental timeline. *Sources: Hamburger V, Hamilton HL. A series of normal stages in the development of the chick embryo. J Morphol. 1951;88:49-92, Fishman MC, et al. Development.1997;124:2099-2117, O'Rahilly R. Early human development and the chief sources of information on staged human embryos. Eur J Obstet Gynecol Reprod Biol. 1979;9:273-80, Edinburgh Human Developmental Anatomy (EHDA) Human versus Mouse Developmental Stage Comparison, University of New South Wales (UNSW) Carnegie Stage Comparison, University of New South Wales (UNSW) Chicken Developmental Stages.*

STRUCTURAL CARDIOGENESIS AND TRANSITIONS IN ELECTRICAL WIRING OF THE DEVELOPING HEART

1.1. Structural Heart Development

During cardiogenesis intriguing processes of cell recruitment, fusion, looping and septation, ultimately facilitate the formation of the four-chambered heart. The first cardiac progenitor cells can already be identified even before gastrulation in the epiblast layer as it is separating from the hypoblast.[3, 4] These heart precursor cells will invaginate through the rostral half of the primitive streak and are amongst the first embryonic cells to gastrulate.[5-9] In avians, the gastrulation process sets off at Hamburger-Hamilton (HH) stage 4 to 5 (human embryonic day (E) ~16-18, mouse ~E 7-7.5), with the recruitment of the cardiac progenitor cells from the primitive streak.[10-13] These cells will subsequently migrate to the bilateral splanchic mesodermal crescent-like primary heart fields, that express cardiac-specific genes like Nkx2.5 and GATA 4-6,[11, 14, 15] already indicating their potential to terminally differentiate into myocardial cells.[16]

At about HH stage 8 to 9 (human ~E 20-21, mouse ~E 8-9), the bilateral heart fields will fuse in the ventral midline in cephalocaudal direction to ultimately give rise to the primitive linear heart tube.[12, 17] The process of fusion of the bilateral heart fields is a sequential process, since fusion of these endocardial primordia spatiotemporally highly depends on definitive closure of the floor of the developing foregut. As a consequence, the heart tube is formed in a cephalocaudal sequence, first forming the truncoventricular portion, then the atrium and last of all the sinus venosus.[18-20] The ultimate straight heart tube contains an outer myocardium and an inner endocardium (derived from the remaining endothelial cells of the embryo that are recruited for vascular development) separated by an extracellular matrix (ECM) known as the cardiac jelly. The dorsal mesocardium, which will later on be separated to form the arterial and venous pole connections, links the primary heart tube to the dorsal body wall. Cranially the heart tube is connected to the pharyngeal arches and caudally to the omphalomesenteric veins.[12, 13]

The myocardium of the tubular and later looped heart forms a single or double cell layer at the circular periphery and is not yet covered by epicardium. However already at these early stages, anisotropic arrangement of the cardiomyocytes is clearly evident; the inner cell layer is more differentiated[21] and along the length of the heart tube preferential circular alignment of the myofibrils is seen in the AV canal and outflow tract region.[22]

The primitive heart tube will begin it's rightward folding process at about HH stage 10 (human ~E 22, mouse ~E 8.5-9.5), first transforming in a C-shaped and than in a more S-shaped structure in order to facilitate adequate mature positioning of the cardiac chambers (e.g. positioning of the future right atrium above the future right ventricle).[17, 23] This looping program is regulated by a cascade of genes of which the exact interactions are still largely unclear, but that are also critical for the left and right programming of the embryo itself.[14, 24]

Whilst the heart tube undergoes its dextral looping phase (HH stage 9-34), the cardiac jelly lining the inside of the myocardium is unevenly remodeled over the full length of the heart tube into endocardial cushions in the AV canal and the outflow tract, which are subsequently invaded by mesenchymal cells derived from the endocardium by Epithelial-Mesenchymal-Transformation (EMT).[25]

During looping, the heart tube consists of several cardiac segments: the left and right sinus venosus horns, the primitive atrium, the ventricular inlet segment and the ventricular outlet segment. These segments are divided by so-called transitional zones, brought together in the inner curvature of the heart by the looping process.[25] With continued looping, the cardiac chambers will further differentiate, a process controlled by a different subset of genes and transcription factors,[26, 27] which subsequently results in positioning of the ventricles and outflow tract of the heart in an anterior/ventral position and of the atria in a dorsal/posterior position. **Figure 2** schematically demonstrates the location of the transitional zones during the major developmental stages in cardiogenesis.

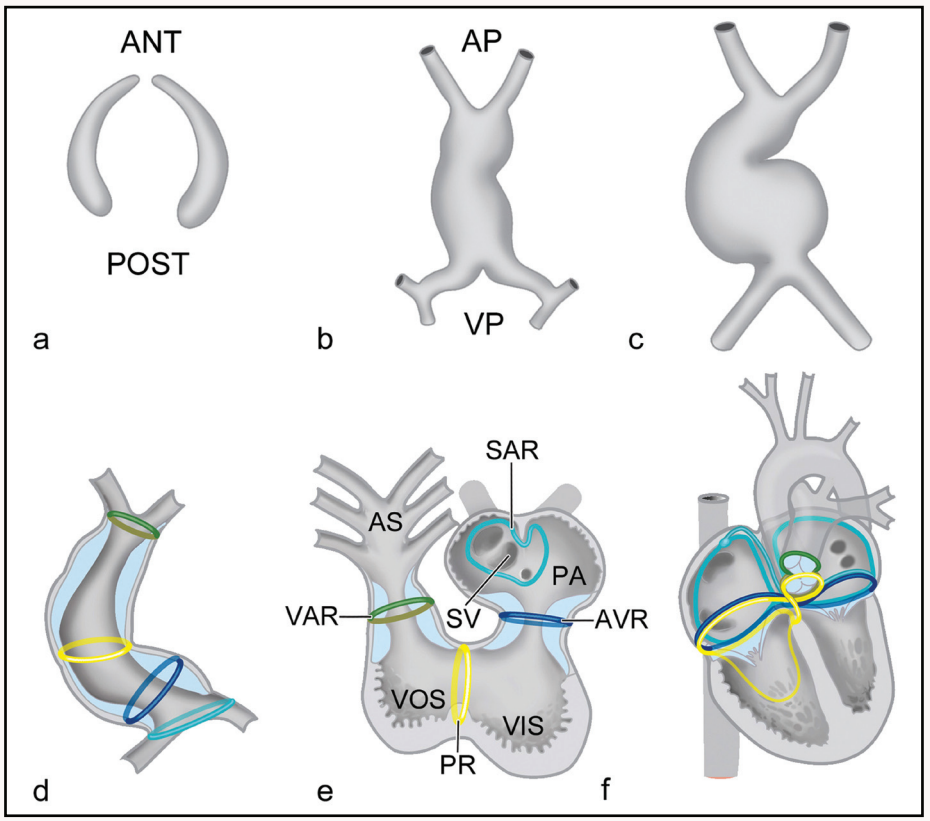

Figure 2. Schematic representation of the spatiotemporal relation of the transitional zones in cardiogenesis. The bilateral cardiogenic plates are derived from the splanchic mesoderm (a). These bilateral plates fuse in the ventral midline in cephalo-caudal direction to form the primitive linear heart tube (b). Subsequently, the linear heart tube undergoes dextral looping, that transforms the heart in a C-shape and later in a S-shape (c). After looping, the transitional zones or rings dividing the different putative chambers of the heart can be recognized, being the sinu-atrial transition (SAR), the atrioventricular ring (AVR), the primary ring (PR) and the ventriculo-arterial transition (VAR) (e-f). AP=arterial pole, VP=venous pole, PA=primitive atrium, AS=arterial segment, VOS= ventricular outflow segment, VIS= ventricular inflow segment. *Adapted from: Gittenberger-de Groot AC, et al. Pediatr Res. 2005;57:169-176.*

The next stage in ventricular morphogenesis involves the development of trabeculation, needed to increase the surface area to increase diffusion potential for nourishing the still avascular myocardium, allow the myocardial mass to increase, coordinate intraventricular conduction, enhance contractility and effectively route blood flow.[28-30] The bulk of compact myocardium is subsequently formed by trabecular compaction, which coincides with the onset of ventricular septation and the now compulsory development of coronary circulation.[29, 31]

At this time, in order to construct a mature four-chambered heart, septation is initiated at the level of the atrium, the ventricle and the arterial pole. Moreover, at the venous pole the sinus venosus becomes incorporated in the dorsal wall of the right and left atrium and receives the venous inflow of the left and right superior cardinal veins as well as the pulmonary veins.[23, 32] In the human heart, as development proceeds, the left cardinal vein regresses becoming the ligament of Marshall and oblique vein, while the remaining proximal portion (with part of the left sinus horn) becomes the coronary sinus (CS), which will open via the sinoatrial foramen into the right atrium.[10, 32-36]

As a result of subsequent endocardial cushion remodeling, the AV cushions take part in formation of the AV septal structures and AV valves (mitral and tricuspid valve), while the cushion tissues in the outflow tract are essential for the formation of the semilunar valves of the aorta and pulmonary artery and contribute to outflow tract septation.[35, 37] Due to the resultant formation of the cardiac septa and of the mitral and tricuspid valve and aortic and pulmonary valve, a functional four-chambered heart can now direct the future separate systemic and pulmonary circulation. **Figure 3** summarizes the transitions in alignment of the cardiac segments during cardiogenesis.

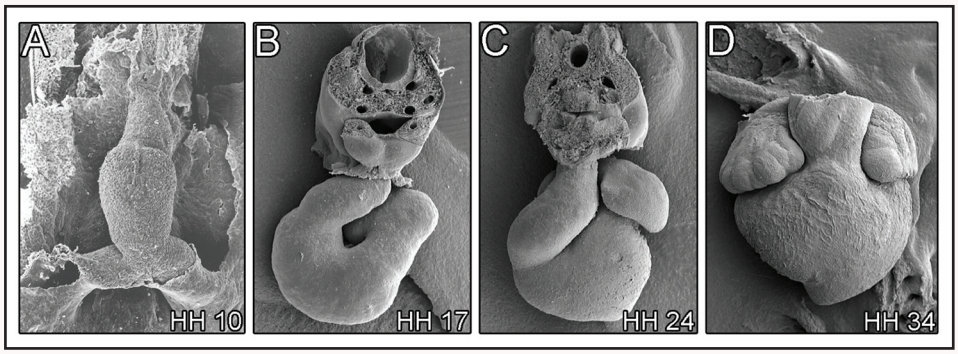

Figure 3. Transitions in alignment of the cardiac segments during cardiogenesis. **A.** At HH 10 the primitive heart tube begins it's rightward folding process. **B.** Around HH 17 the C-shaped heart tube is still in the midst of its looping phase. **C.** At HH 24, the right atrium becomes positioned above the right ventricle, whilst the left atrium is positioned above the left ventricle. **D.** Around HH 34 a four-chambered heart has been formed, which can now separate the future systemic and pulmonary circulation.

Figure 4. (right) Schematic representation of the primary linear heart tube (in brown) and the secondary added myocardium derived from the second heart field (in yellow).The second heart field is subdivided in the anterior heart field (arterial pole), the secondary heart field (arterial pole) and the posterior heart field (venous pole).The pro-epicardial organ (PEO), the source of Epicardium-Derived-Cells (EPDCs) is also derived from the posterior heart field at the venous pole of the heart. Cardiac neural crest cells (blue) enter the heart at both the arterial and venous pole. AVC=atrioventricular canal, CV=cardinal veins, CCS=cardiac conduction system, DOT=distal outflow tract, LV=left ventricle, OFT=outflow tract, PAA=pharyngeal arch arteries, ggl=ganglions, POT=proximal outflow tract, PV=pulmonary veins, RV=right ventricle, SAN=sinoatrial node, SV=sinus venosus. *Adapted from: Jongbloed MRM, et al. Development of the cardiac conduction system and the possible relation to predilection sites of arrhythmogenesis. The Scientific World Journal. 2008;8:239-269.*

1.2. Secondary & Extracardiac Contributions to the Heart

1.2.1. Secondary Contributions to the Heart

The major cardiac segments of the linear primitive heart tube - the left ventricle (LV), the AV canal (AVC) and part of the atria - are derived from the bilateral splanchic mesodermal primary heart fields (first heart field), as described above (**Figure 4**). The pharyngeal mesoderm provides the heart with a second cardiac progenitor pool (second heart field) that enters the heart at both the venous and arterial pole (**Figure 5**).[38-40] The second heart field can be subdivided in the anterior heart field (AHF) and the secondary heart field (SHF) at the arterial pole[41-43] and the posterior heart field (PHF) at the venous pole (**Figure 4**).[20, 32, 44-51]

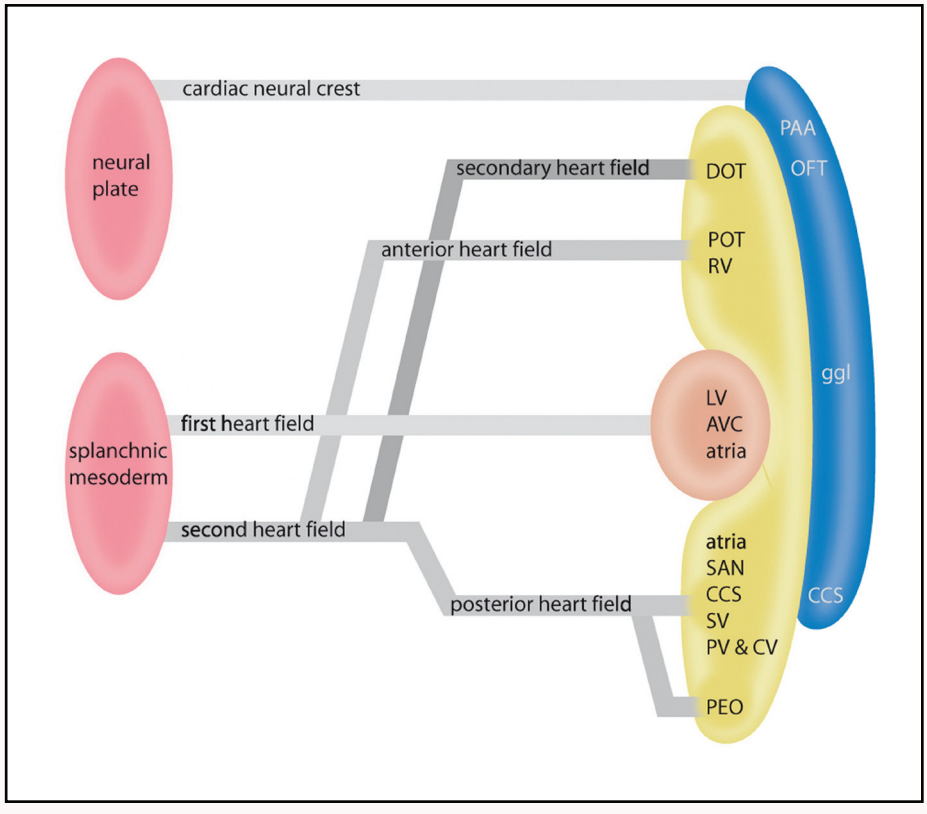

The cardiac outflow tract (OFT) myocardium and a large part of the right ventricle (RV) are one of the last segments of the heart to form and will be added to the arterial pole of the primitive heart tube. These cardiac structures arise from a cellular population of the pharyngeal mesoderm, which initially starts migrating to the conotruncal area between HH stage 7 (human ~E 20, mouse ~E 8.0) and HH stage 13-14 (human ~E 26, mouse ~E 9.5), prior to neural crest cell invasion.[38-40, 52]

Cardiac progenitor cells derived from the posterior heart field added to the heart at the venous pole, have been shown to contribute to the formation of the atria, interatrial septum (IAS), pulmonary veins (PV), cardinal veins (CV), sinus venosus (SV) and the components of the CCS (**Figure 4,5**).[20, 32, 40-53]

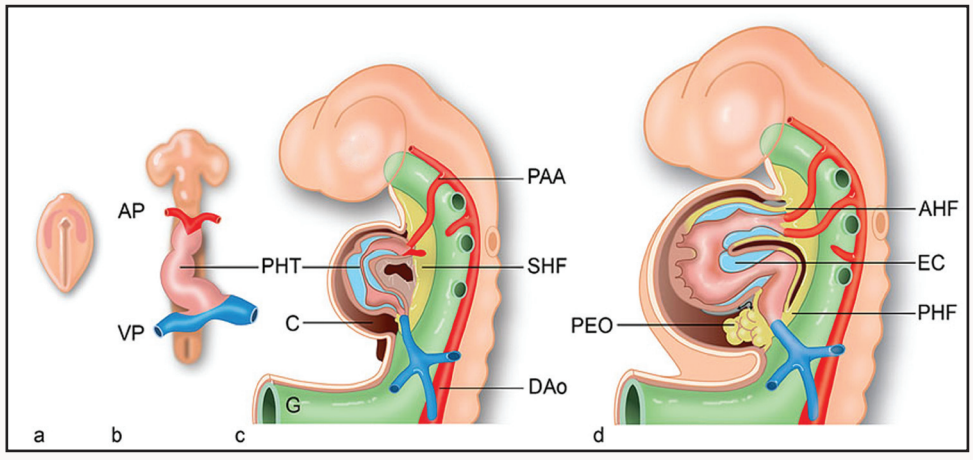

Figure 5. Schematic figure depicting the contribution of the primary (pink & blue) and secondary (yellow) heart-forming fields. The second heart field (SHF) can be divided into the anterior heart field (AHF) at the arterial pole of the heart and the posterior heart field (PHF) at the venous pole of the heart. The Pro-Epicardial-Organ (PEO) develops as part of the PHF (yellow). AP=arterial pole, VP=venous pole, PHT=primary heart tube, PAA=pharyngeal arch arteries, DAo=dorsal aorta, C=coelomic cavity, EC=endocardial cushions, G=gut. *Adapted from: Gittenberger-de Groot AC, et al. Cardiac morphogenesis. In Fetal Cardiology. 2nd ed. Yagel S, Silverman NH and Gembruch U, Eds. Taylor and Francis. London, 2008, in press.*

1.2.2. Epicardium-Derived-Cells (EPDCs)

Classically, Epicardium-Derived-Cells (EPDCs), derived from the Pro-Epicardial-Organ (PEO), have been considered as one of the extracardiac contributors to the developing heart.[54] In view of recent new concepts on the spatiotemporal addition of cells from the different heart forming fields, the true extracardiac origin of EPDCs can be debated.[47, 54] The posterior heart field (derived from the splanchic mesoderm) is located at the site where the sinus venosus enters the pericardial cavity, which is also the site where de PEO originates.[47, 55] In **Figure 6** the spatial relation of the primary and secondary (anterior and posterior) heart fields, the neural crest cells and the PEO is depicted.

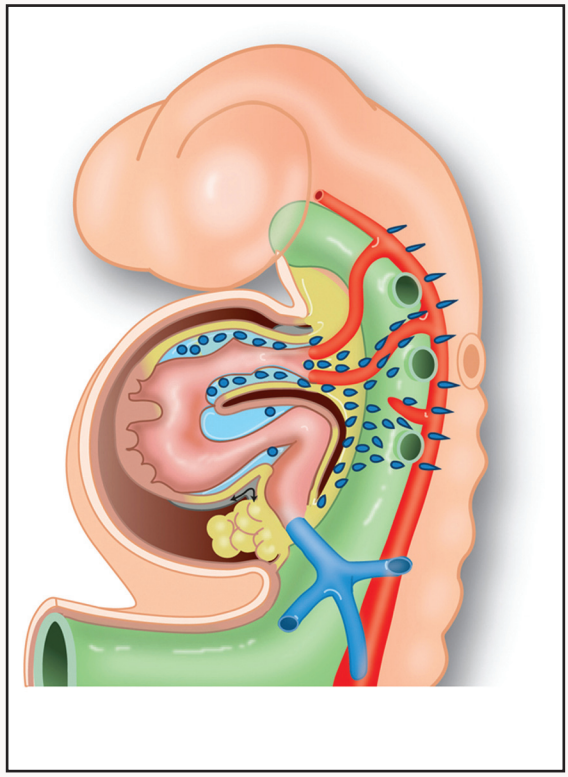

Figure 6. Spatial relation of the primary and secondary heart fields, the neural crest and PEO. Extracardiac contribution of the cardiac neural crest cells to the arterial and venous pole of the heart (blue cells). The secondary heart field is depicted in yellow. *Adapted from: Gittenberger-de Groot AC, et al. Cardiac morphogenesis. In. Fetal Cardiology. 2nd ed. Yagel S, Silverman NH and Gembruch U, Eds. Taylor and Francis. London; in press.*

During embryonic development, the epicardium is formed from the splanchnopleural mesoderm of the PHF by formation of a cauliflower like villous structure known as the pericardial serosa, proepicardium or Pro-Epicardial-Organ (or PEO) on the pericardial wall covering the SV and venous pole of the heart. The PEO protrudes from the pericardial mesothelium into the pericardial cavity in the direction of the looped heart.[56-61]

Both in mammalian and avian embryos, the PEO is initially formed as paired bilateral symmetrical structures on the transverse septum (mouse) and sinus venosus (avian). In chicken, the left PEO Anlage does however not persist, whereas the right PEO will develop into the cauliflower like protrusion (PEO).[62, 63]In avians, around HH stage 16, EPDCs will migrate to the naked heart tube by means of a tissue bridge which is formed between the SV and the dorsal wall of the AV canal of the looped heart and initially forms a mesothelial outside covering of the myocardium. After attachment to the myocardial surface, the cells start to migrate radially and start to circumvent the AV region, the inner curvature and the dorsal side of the outflow tract.[61, 64, 65] After covering the last parts of the heart – the left atrium and parts of the distal outflow tract - the heart will be completely covered by mesothelium by HH stage 26.[61] **Figure 7** schematically demonstrates the temporal relations in cardiogenesis and EPDC formation.

From HH stage 19 onwards, immediately after the onset of spreading of EPDCs over the myocardial surface, the epicardial mesothelial sheet will undergo Epithelium-to-Mesenchymal Transformation (EMT).[64, 66, 67] Initially, the resultant mesenchymal EPDCs reside in the subepicardial matrix. In chicken embryos, the subepicardum is relatively thin (one to three cell layers) at the atrial and ventricular myocardium, while it is very thick in the AV sulcus where abundant EMT is needed to provide EPDCs for coronary formation.[66]

Mesenchymal EPDCs will subsequently invade the myocardium in a spatiotemporally regulated fashion.[64, 66, 67] While the precise temporal regulation of EPDC migration has remained unknown, two distinct influxes into the myocardium of the chicken heart have been described. The first influx directly follows the process of EMT and formation of the subepicardium and takes place between HH stage 19 and HH stage 31, while the second influx takes place between HH stage 31 and HH stage 43. First influx EPDCs will take up subendocardial positions in the atrium and ventricle and will migrate into the myocardial interstitial spaces, whereas EPDCs from the second influx will mainly migrate into the AV cushions (**Figure 7**).[64, 68]

From previous studies in epicardial quail-chicken chimeras, we know that at HH stage 35, most EPDCs will have taken up their final position: around the coronary arteries as smooth muscle cells (SMCs) and fibroblasts,[66, 69-71] in the ventricular myocardium as interstitial fibroblasts,[64, 68, 70] in the AV cushions[68, 70] and in the subendocardium of the ventricular trabeculae and atria.[68]

Numerous studies in experimental models in which epicardial development has been disturbed mechanically or genetically, have proven the functional significance of EPDCs in cardiac development.[67, 72-83] In this respect, EPDCs have been inferred to play crucial roles in the development of the coronary vasculature, the AV valves, the myocardial architecture, the peripheral conduction system (Purkinje fibers) and in the formation of the isolating AV annulus fibrosis (**Figure 8**)(see also **Chapter 3**, *this thesis*).

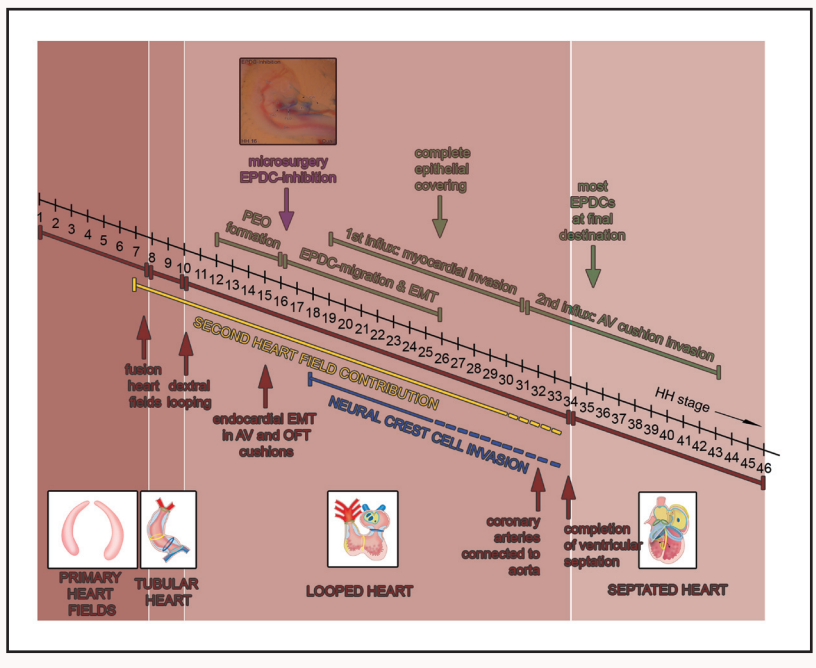

Figure 7. Temporal timeline in avian cardiogenesis and formation of Epicardium-Derived-Cells (EPDCs). The different stages of cardiogenesis are indicated by red blocks (primary heart fields, tubular heart, looped heart and septated heart) and schematic figures outlining the overall structure of the heart. At the bottom of the timeline, major events in cardiogenesis are indicated (red). Additionally, ingrowth of the second heart field population of cells and the extracardiac NCCs is indicated in yellow and blue, respectively. Contemporary processes of PEO-formation, EPDCs migration and myocardial invasion are indicated at the top of the timeline (green).

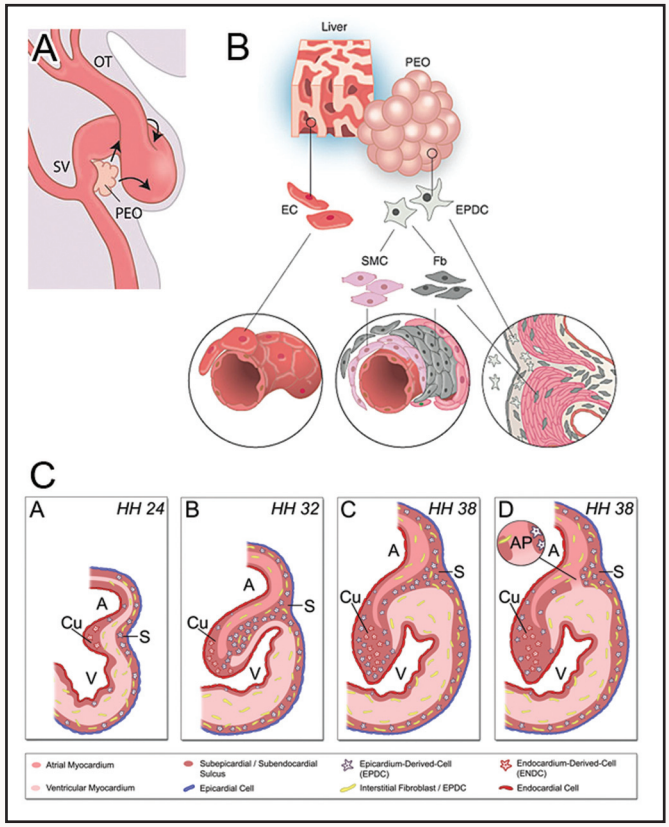

Figure 8. Schematic figure depicting EPDC fate and function. A. In avians, around HH stage 16, EPDCs will migrate to the naked heart tube from the sinus venosus region to the dorsal wall of the AV canal of the looped heart. After attachment to the myocardial surface, the cells start to migrate radially and start to circumvent the atrioventricular region, the inner curvature and the dorsal side of the outflow tract. After covering of the left atrium and parts of the distal outflow tract, the heart will be completely covered by HH stage 26. **B.** The proepicardial cells migrate from the Pro-Epicardial-Organ (PEO) to the heart tube. After migration, epithelium-mesenchymal-transformation (EMT) and formation of the subepicardium, the EPDCs start migrating into the myocardium and differentiate into smooth muscle cells (SMCs) in the media and adventitia of the coronary vessels and fibroblasts in the interstitium and the fibrous heart skeleton. **C.** From HH32 onwards, subepicardial EPDCs in the AV sulcus (S) migrate through the continuous AV junctional myocardium to ultimately populate the endocardial AV cushions (Cu). In the normal 4-chambered heart, EPDCs continue populating the AV cushions and favour 2 positions: 1) the myocardial/endocardial cushion interface and 2) the subendocardially at the luminal face of the AV cushions. *Figure A,B Adapted from: Winter EM, et al. Epicardium-derived cells in cardiogenesis and cardiac regeneration. Cell Mol Life Sci. 2007;64:692-703. Figure C adapted from Kolditz DP, et al. Epicardium-Derived-Cells (EPDCs) in Annulus Fibrosis Development and Persistence of Accessory Pathways. Circulation 2008;117:1508-1517.*

1.2.3. Extracardiac Contributions to the Heart – Neural Crest Cells (NCCs)

After looping of the single linear heart tube, the true extracardiac contributors to heart development, the pluripotent neural crest cells (NCCs), migrate from the neural crest into the arterial and venous pole of the developing heart (**Figure 6**).[84-86] Neural crest cells or ectomesenchymal cells have been traced to various parts of the embryo, including the face, thymus and the thoracic great vessels.[25] It is well established that NCCs originating from the posterior rhombencephalic segments of the neural tube (from the otic placode to the third somite) contribute to multiple aspects of cardiac development and function. However, the contribution of these cardiac NCCs has been suggested to be mostly instructive rather than constructive since the majority of NCCs are destined for apoptosis.[87] The contribution of NCCs to the vessels of the arterial pole however is substantiated, since the major part of the smooth muscle cells have a NCC origin.[88]

The mesenchymal NCCs first arrive at the outflow tract (arterial pole) and thereafter populate the inflow tract of the heart (venous pole).[25] Seminal work using NCC extirpation and analysis of quail-chick chimeras, demonstrated that NCCs entering the heart through the pharyngeal arches at the arterial pole, contribute to the neurons of the cardiac autonomic nervous system, aortopulmonary septum, the tunica media of the great arteries, the outflow tract septum and the semilunar valves.[88-97] The cardiac NCCs entering the heart at the venous pole, migrate to the dorsal mesenchymal protrusion forming the vestibular spine, from where they contribute to the base of the atrial septum and the condensed mesenchyme that is forming the membranous part of the ventricular septum.[98-100] Furthermore, NCCs entering the heart at the venous pole have been observed in vicinity of putative elements of the CCS before they undergo their fate of apoptosis. [99, 101, 102] Interestingly, neural crest ablation in the chick was recently shown to result in a lack of differentiation of the compact lamellar organization of the His bundle, which separates this essential structure from the surrounding working myocardium.[103]

1.3. Impulse Propagation During Cardiogenesis

1.3.1. Tubular Heart

In the avian embryo, when only 7 to 10 somites have yet developed (HH stage 9, equivalent age in human ~E 21-22 and mouse ~E 8.5), a small dominant pacemaking area already becomes established at the posterior inflow side of the heart (the presumptive atrium and SV region), well before formation of the tubular heart is completed and contraction is initiated.[104-106] The posterior inflow tract myocardium thus becomes electrically active, long before the primitive myocardium of the heart tube acquires the ability to contract.[107]

The very first faint and slow but rhythmic contractions (approximately 24 beats/min. in avians) will subsequently appear in the cephalic ventricular myocardium (first fused cardiac segment) around HH stage 10 (equivalent to 9-10 somites, human ~E 22, mouse ~E 8.5-9.5) even before cephalocaudal fusion of the paired primordia is complete in the atrial region.[18, 108-110] At this developmental stage, the atria and SV do not yet exist as a differentiated part of the heart, but are merely represented by endocardial primordia which are still widely separated from each other in the bilateral heart fields.[18]

These early pulsations are however still inefficient to set the blood in motion through the developing blood vessels and merely consist of non-propagating local twitchings that initially appear as fibrillar contractions along the right margin of the bulboventricular region and then coalesce to produce a concerted movement of the entire right side of the ventricle.[18, 111] Next, the left side of the ventricle becomes involved in these twitchings and subsequently the entire primitive ventricle displays synchronous contractions. These early contractions are however not yet regularly occurring, but are interrupted by rest periods, which will become progressively shortened as a slow regular rhythm gradually becomes established.[111]

The continuing Anlage of the fusing caudal cardiac segments is spatiotemporally correlated to the onset of myocardial contractions with progressively higher intrinsic pulsation rates along the anteroposterior axis, reaching its peak after final fusion of the sinus primordia at the venous pole.[105, 107, 111-113] Pacemaker dominance thus spatiotemporally spreads to the different cardiac regions in the same sequence in which they are formed by continued caudal fusion of the bilateral heart fields.[18]

In the completely fused primitive heart tube (HH stage 10), equivalent to ~23 days post conception (dpc) in humans (mouse ~E 8.5), stronger and regular

peristaltic caudal to cranial contractions, finally facilitating the first efficient propulsion of blood from the venous to the arterial pole of the heart, will be seen. At this developmental stage, when the atrial primordia have fused, spontaneous action potentials are generated in a dominant area of pacemaker cells in the left posterior inflow-site of the heart (atria and SV region).[13, 105, 111, 114-117]

Only some time after the beginning of circulation, the SV is formed (> HH stage 10) and ultimately starts to dominate the pacemaking rate. At this stage, the cardiac impulse is efficiently conducted through the heart with a constant conduction velocity from the most caudal SV inflow site of the heart (or most posterior site), through the future atrial segment, the direct myocardial AV connection between the future atria and ventricles, through the ventricles and finally to the outflow site of the heart (or most anterior site).[111]

In short, in the primary myocardium of the embryonic tubular heart, each myocardial cell inherently possesses intrinsic pacemaker activity, which on the cellular level is reflected by action potentials displaying slow depolarizations typical of slow voltage-gated calcium ion channels (reminiscent of pacemaker action potentials). The regional differences in intrinsic beat rates, reflected in their characteristic action potential shapes and underlying action currents, most likely result from the differential expression of largely unknown gene products in different regions of the heart that cause the individual segments to have diverse types and numbers of channels and pumps.[118-120] In general, impulse propagation through the primary myocardium of the tubular heart is relatively slow, due to poor intercellular coupling in the embryonic myocardium at this developmental stage.[121-123]

1.3.2. Looped Heart

As the developing heart transforms from a tubular to a looped morphology, the pattern and speed of ventricular activation also undergo their first changes. The pattern of universally slow propagation along the primitive tubular heart develops heterogeneities in conduction properties in the different cardiac segments.[124-126] In avians, by 42 hours of development (equivalent to HH stage 11, human ~E 23, mouse ~E 8.5) as looping proceeds, a slowly conducting AV canal is forming separating the synchronous activation of the atrial and ventricular segments.[127-129] Concordantly emerging are action potentials in the atrial and ventricular working myocardium with a fast rising phase and high amplitude, characteristic of fast voltage-gated sodium channels.[122, 130]

As a consequence, the emerging atrium and ventricle in the looped heart start displaying fast conduction, while the myocardium of the AV junction is characterized by slow conduction, which is thought to result from a lack of fast sodium channels and a relative lack of the gap junctional protein connexin-43.[18, 111, 131] In the looped heart, the cardiac impulse is thus propagated with alternating conduction velocities form base-to-apex through the different segments of the looped heart resulting in a sequential contraction pattern still following the direction of the blood flow (from inflow to outflow tract).[124]

Interestingly, the cellular electrophysiology of the embryonic AV junctional tissue is already quite similar to adult nodal tissues,[132] e.g. it responds to adenosine with a reduction in action potential amplitude and dV/dt_{max}.[133] Histologically, like the Sino Atrial Node (SAN) and AVN and unlike the working myocardium, the AV junctional myocardium is relatively devoid of connexin-43.[134] Myocytes at the AV junction preferentially however express connexin 45,[135] a low conductance gap junction channel that is also expressed in the SAN as well as in the AVN of the mature heart.[136]

Coincident with the emergence of ventricular trabeculation and the formation of the primordia of the interventricular septum (IVS),[28, 137] preferential temporal anterior and posterior myocardial AV activation pathways can be identified between HH stages 16 and 24 of avian embryogenesis (human ~E 30-42, mouse ~E 11-13).[138] As development proceeds, these pathways are masked by the appearance of more trabeculae and will finally be superseded by functioning of the mature His-Purkinje system.[138] The anterior activation pathway (or anterior septal branch), is not unique to the chick heart but has also been functionally demonstrated in the embryonic rat E 11.5 heart and the embryonic mouse heart.[138, 139]

Functionally, in the looped heart the dominant pacemaking area remains localized in the left sinus primordium up to 5-6 days of incubation (HH stage 27-29, human ~E 44-48, mouse ~E 13-14), with resultant left atrial depolarization preceding right atrial depolarization.[105, 106, 140-142] Morphologically, nodal cells are also found in the right sinushorn around the 4th day of incubation (HH stage 24, human ~E 41, mouse ~E12.5) temporarily remaining functionally quiescent.[142, 143] With the outgrowth of the right atrium, between 6 and 7 days of avian development (HH stage 29-31, human ~E 48-52, mouse ~E 14-15), the SV completes its shift to the right and becomes submerged in the right atrium. Around this developmental stage, the myocardium in the dorsal mesocardium has completely developed excluding the large veins from the atria only leaving contact with the non-cardiac dorsal mesoderm at the arterial and venous pole and impulse generation switches to the adult right position.[140]

The AVN and His bundle, of mainly unestablished origin, also start to develop around this developmental stage.[144] Additionally, the atria and ventricles become subjected to chamber differentiation and trabeculation and start expressing the inward-rectifier potassium current (I_{K1}) stabilizing a strongly negative resting potential suppressing excitability, which ultimately renders the atria and ventricles electrically quiescent while the rate and rhythm will exclusively be controlled by the compact nodes.[145] Concomitantly (HH 28-29), the IVS and AV cushions have started to fuse,[146, 147] completing ventricular septation around HH stage 34.[127]

1.3.3. Septated Heart

By the stage at which the ventricles have septated (> HH stage 34), the AVN and His bundle will have formed and attained their definitive positions close to the inferior edge of the atrial septum, while the annulus fibrosis still has to undergo extensive developmental changes (see also **Chapters 2-5**, *this thesis*). To facilitate propulsion of blood into the arterial trunks of the four-chambered heart, the initial base-to-apex direction of impulse propagation is reversed to a more mature apex-to-base oriented conduction and myocardial contraction (which will be further outlined in paragraph **1.6. "Transitions in Ventricular Activation During Cardiogenesis"**).

1.4. Development of the Specialized Cardiac Conduction System (CCS)

The specialized Cardiac Conduction System (CCS) is comprised of separate subcomponents with distinct functions and has mainly been studied in avian embryos.[141, 142] Firstly, the SAN generates the cardiac impulse and sets the leading pacemaker rate. The electrical impulse will subsequently be conducted via the internodal pathways to the AVN. After a short AV delay, the cardiac impulse is then rapidly transmitted to the His bundle, bundle branches and Purkinje fiber network.

1.4.1. The Origin of the CCS

The origin of the CCS has been a subject of debate for many years now. In the debate of the 19th century, both "*myogenic*" and "*neurogenic*" origins of the CCS were suggested. Temporarily, with the discovery of the existence of intraventricular neurons in the early 19th century, the balance was tipped in the neurogenic direction.[148, 149] Again, a quite similar debate arose at the end of the 20th century with the demonstration of neural cell-type gene expression in the cells of the CCS, now proposing the neural crest cell (NCC) as a candidate parental population for the developing CCS.[99, 150-153]

An elegant series of 20th century retroviral lineage studies has however unambiguously demonstrated that cardiomyocytes are the true and sole progenitors of the CCS cells.[99, 154] Indeed, cardiomyocytes of the CCS share with the cardiomyocytes of the ordinary working myocardium four basic elements: 1) contraction, 2) autorhythmicity, 3) intercellular conduction and 4) electromechanical coupling.[120] The still unresolved question however remains, if the CCS cardiomyocytes are derived from the division of differentiated (pre-specified) conduction cells (*the"specification"-model*) or are recruited from a pool of multipotent undifferentiated cardiomyogenic cells (*the "recruitment"-model*).[155]

1.4.2. CCS Development and The 4-Ring Theory

In an attempt to distinguish the working myocardium from the myocardium of the specialized CCS, the observation was made that after looping of the heart tube, 4 rings of 'special' tissue could be distinguished from the working myocardium, as was described by Wenink and others.[156-158] These rings or transitional zones consist of: 1) the sinoatrial ring in between the SV segment and the primitive atrium, 2) the AV ring in between the primitive atrium and primitive left ventricle, 3) the primary ring or fold separating the primitive left ventricle from

the primitive right ventricle and 4) the ventriculo-arterial ring positioned at the junction of the primitive right ventricle with the truncus or putative outflow tract of the heart (**Figure 2**).

This 'ring-theory', hypothesized that these 4 rings of 'special' tissue are the precursors of the CCS. During development these rings will come together in the inner curvature of the heart and partly loose their specialized character, while the remaining parts are identified as putative parts of the mature CCS.[158] Classically, in this theory, the SA ring was thought to contribute to formation of the SAN, the SA ring and the AV ring to contribute to the AVN and the primary ring to give rise to the His bundle and bundle branches.[23, 25, 37, 48, 52, 158] This theory has however been the subject of discussion and controversy for many years. Later on, contemporary marker studies could again confirm the important contribution of the SA ring to the developing SAN and AVN by HNK-1 expression patterns in the developing human embryo and analysis of CCS-LacZ and MinK-LacZ expression in the mouse embryo identified the SA ring, AV ring and primary ring as important contributors to CCS development.[23,25,37,48,52]

1.4.3. Molecular Markers for CCS Development

In the early embryonic heart, the individual cells of the CCS can hardly be distinguished from the surrounding myocardium by unique histological features, while their separate arrangement and topography can in some cases be helpful.[159-162] Histologically, in the adult heart nodal cardiomyocytes of the CCS display some characteristics comparable to embryonic working cardiomyocytes: they are small compared to the cardiomyocytes of the surrounding adult working myocardium and have poorly organized actin and myosin filaments and a scantily developed sarcoplasmatic reticulum.[159]

By applying the criteria established by Monckeberg and Aschoff in 1910, using the AV conduction axis as the paradigm, discrete specialized conduction tracts in the postnatal heart: 1) are histologically distinct, 2) can be followed from section to section and 3) are insulated from the adjacent working myocardium by fibrous tissue.[163] While these criteria permit adequate recognition of the specialized components of the CCS in the postnatal human heart, identification of the embryologic conduction tissues in the developing heart has remained fairly challenging. A multitude of transgenes, such as minK-LacZ,[49] Engrailed2-lacZ/CCS-LacZ[48, 164] has however been consistently proposed to reflect the arrangement of the developing CCS.

Moreover, each subcomponent of the CCS expresses a distinct set of

discriminating ion channels,[165, 166] channel-associated proteins,[167] connexins,[136, 168-172] cytoskeletal components[173, 174] and transcriptional regulators,[175, 176] useful for immunohistological recognition. Additionally, important known signaling and transcription factors implicated in the induction, maturation and patterning of the CCS including endothelin (ET),[177-182] neuregulin,[139, 183] Notch,[183] Wnt,[184] Msx,[185] Nkx,[44, 186-188] Hop,[189] Id-2,[50] podoplanin[47] and Tbx and GATA gene families[190-193] can also be of help. State-of-the-art studies focusing on the transcription factors involved in cardiogenesis have made evident that myocardial differentiation to CCS cells cannot be dependent on a single gene, but should be considered as a multifactorial process in which a multitude of different gene families must contribute.

1.4.4. The Individual Components of the CCS

1.4.4.1. The Sino Atrial Node (SAN)

In humans and other mammals, the first morphological signs of the developing SAN are present at Carnegie stage 15 (~5 weeks of human development, avians ~HH stage 18, mouse ~E 11.5)[120] in the anteromedial wall of the right common cardinal vein, which will ultimately give rise to the superior caval vein.[160, 194]

In the adult heart, the SAN is located in the crista terminalis (representing the internal fusion-line of the SV and the primitive atrium) near the superior caval entrance into the right atrium.[119, 195] During formation of the SAN, a considerable portion of the right horn of the SV becomes incorporated in the dorsal wall of the right atrium. The SAN myocardium, thus represents myocardium which was originally associated with the right sinus horn. Interestingly, as described above, in the early stages of development the sinus horns belong to the most caudal regions of the cardiac primordia harboring the highest cephalocaudal pacemaking rate.[111]

While all adult heart muscle cells retain the capacity to rhythmically beat without an external stimulus, the cells of the SAN are those with the most rapid intrinsic rate of excitation (the dominant pacemaking rate).[196] In generating the pacemaker action potential of the SAN, the hyperpolarization activated I_f (pacemaker or "funny") current plays a major role. Furthermore, the pacemaking action potential is regulated by several genes, including those for the T- and L-type calcium currents and the sustained inward current, producing a slow and diastolic depolarization.[166, 197] From genetic studies in human and mouse we know that Hyperpolarization-activated Cyclic Nucleotide gated (HCN)

channels are required to generate the I_f current or normal pacemaking current, but it is however still unclear how the complex expression of HCN channels is induced and regulated at specific regions of the developing heart.[198, 199]

1.4.4.2. The Internodal Tracts

Considerable controversy and debate, lasting for almost a century, has surrounded the mostly semantic discussion on the existence of specialized, insulated internodal tracts in the atrium between the SAN and AVN. Within the right atrium three internodal tracts for preferential interatrial conduction have been demonstrated between the SAN and AVN: 1) the anterior bundle running through the septum spurium (SS),[23,46,48] which connects to *Bachmann's bundle*[200-202] running in a retroaortic position connecting the right atrium to the left atrium, 2) the posterior bundle running through the right venous valve (RVV)[23,46,48] partly corresponding to the posterior bundle or *Thorel's bundle* localized along the crista terminalis and 3) the posterior bundle running through the left venous valve (LVV)[26] partly corresponding to the middle bundle or *Wenckebach's bundle*.[23, 46, 48, 158, 200-202]

Currently, it is well established that preferential conduction between the cardiac nodes (SAN and AVN), through the ultrastructural and electrophysiological heterogenic atrial myocardium, highly depends on the nonuniform anisotropic arrangement of the normal working myocardial fibers,[203] instead of on the existence of truly specialized insulated atrial internodal tracts. These non-specialized internodal atrial tracts are made up in part of transitional cells, which interpose between the working atrial myocardium and the unequivocally histologically specialized compact AV Node.[204] While structurally these tracts have been extensively demonstrated,[23, 46, 48, 49] their functionality has still not been shown.

1.4.4.3. The Atrioventricular Node (AVN)

In the human embryo, the developing AVN becomes gradually identifiable from Carnegie stage 16/17 (~5/6 weeks of human development) onwards.[161, 162, 205] Early in the sixth week of human development (~HH stage 25, mouse ~E 13) a compact cluster of cells makes its appearance in the posterior wall of the AV canal, towards its right side.[206] This cluster of cells is thought to represent the primitive AVN, which is in cellular continuity with the atrial muscle and AV bundle.

The architecture of the adult AV conduction axis was first described by Sunao

Tawara in 1906.[149] In the mature heart, the compact AVN is positioned in the apex of the triangle of Koch at the base of the interatrial septum, where it lies only a few millimeters anterior to the coronary sinus (CS) ostium and directly beneath the right atrial septal endocardium and the septal attachment of the tricuspid valve where it rests on the central fibrous body, which forms the anchor for the septal portion of the mural leaflet of the mitral valve. The atrial margin of the AVN is apposed to the myocardialized vestibular spine, containing the tendon of Todaro, while the ventricular margin of the AVN is continuous with the bundle of His.[207, 208]

The triangle of Koch occupies the atrial component of the muscular AV septum and is limited by three anatomical landmarks: 1) superiorly by the tendon of Todaro (the fibrous commissure of the flap guarding the openings of the inferior caval vein and the CS), 2) inferiorly by the attachment of the septal leaflet of the tricuspid valve and 3) at the base by the mouth of the CS. The apex of the triangle of Koch overlies the membranous component of the AV septum and lies at the center of the short axis of the heart.[209] The triangle of Koch not only harbors the AV nodal tissues but also the remnants of the embryologic primordium of the specialized myocardium that surrounds the primary interventricular foramen (primary ring), extending rightward and inferiorly from the compact node.[204]

The main functions of the adult AVN are: 1) gathering the incoming signals from the SAN, 2) directing the signals through the AVN to the His bundle, 3) maintaining an AV delay, 4) generating an escape rhythm when needed and 5) responding to the autonomic nervous system and humoral signals.[210, 211]

The ontogenic development of the AV specialized tissues has, since the first detailed report on the AVN by Tawara in 1906, been studied for over 100 years now. In the debate of the 20th century, competing theories based on observations in different species complicated by the use of variable terminology for identification and non-specific staining, however failed to provide a resolution on this subject. The developmental origin of the AVN will more extensively be reviewed and analyzed in **Chapter 6 & 7** of this thesis.

1.4.4.4. The His Bundle and Bundle Branches (His & BBs)

From the AVN, propagation of the electrical impulse is subsequently accelerated along the AV bundle (His bundle) and bundle branches. Around 6 weeks of human development (avians ~HH stage 25, mouse ~E 13), the AV bundle can first be found to run across the top of the thick IVS, behind and under the dorsal endocardial cushion. Subsequently, after 8 weeks of human development (avians

~HH stage 35, mouse ~E 15.5), the bundle branches arise from the terminal end of the His bundle.[212]

The His bundle in the adult heart, as first described in the mammalian heart by His in 1893, originates at the posterior right atrial wall near the atrial septum above the AV groove and than passes over the upper margin of the ventricular septal muscle, where its fibers intermingle with the cardiomyocytes. Near the aorta it subsequently bifurcates in the right and left bundle branch, the later terminating at the base of the aortic leaflet of the mitral valve.[149, 176, 213]

Controversy concerning the development of the His bundle has led to various proposals on the origin of the His bundle: 1) Viragh and Challice demonstrated in 1976 that the AVN and His bundle develop simultaneously,[205, 214] while 2) others found that the AVN develops first and the AV bundle arises later as an outgrowth of the AVN,[206, 215-217] 3) others have suggested that the AV bundle develops first and than the AVN develops as an outgrowth of its proximal portion[218-220] and 4) in the classical 'ring theory', the AVN and AV bundle have been shown to originate independently from the AV and bulboventricular ring respectively and join secondarily.[158, 221, 222]

1.4.4.5. The Purkinje Fibers

In the human embryo, Purkinje fibers do not appear until rather late, between the 10th and 15th week of development.[206] The original description of the Purkinje fiber in 1845 by Purkinje stated that these special cells can ultrastructurally be identified as cardiac fibers without transverse tubules.[223] Since the Purkinje fibers have been found to co-express both myogenic and neurogenic gene products, the origin of the Purkinje fiber system has also been a subject of longstanding controversies.

Individual Purkinje fibers are scattered throughout the myocardium but can be distinguished from the working myocardium by their distinct electrophysiological and molecular characteristics. Functionally, these cells of the fast conduction system are electrically coupled to neighboring muscle cells via gap junctions and exhibit a faster action potential upstroke, a prolonged action potential duration, a higher membrane diastolic potential and greater electrical restitution properties in comparison to the slow conducting components of the CCS.[178, 182, 224]

While the proximal components of the Purkinje system run subendocardially regardless of species, the presence and distribution of the more distal intramyocardial branches of the fast conduction network is highly variable among species.[120, 174] Furthermore, in avian hearts in addition to the subendocardial Purkinje fibers, intramyocardial Purkinje fibers penetrate along the coronary artery branches (periarterial Purkinje fibers).[154, 176, 182, 225, 226]

Cell tracing studies have demonstrated that Purkinje fiber recruitment from the myocardium takes place at two restricted sites: periarterially and subendocardially.[71] In this respect, recent studies have shown that Purkinje fiber differentiation is tightly regulated by hemodynamic alterations, while endothelin-1 (ET-1) and ET-converting enzyme 1 (ECE1) were identified as inductive molecules.[179, 182, 227] Concomitant retroviral expression of mature ET-1 and ECE1 was even shown to be sufficient for the ectopic conversion of adjacent cardiomyocytes into Purkinje fibers.[182] Prompted by the periarterial and interstitial arrangement of EPDCs in the developing heart, an instrumental role of EPDCs in Purkinje fiber differentiation could recently also be demonstrated.[68, 77]

Figure 9. (right) **Scanning electron microscopic photographs of the developing chicken heart with matching electrocardiograms** (*adapted from Seidl W, et al. A few remarks on the physiology of the chick embryo heart (Gallus gallus). Folia Morphol. 1981;29:237–242).* At Hamburger Hamilton (HH) stage 11, a linear peristaltic contracting heart tube has developed, from which a matching sinusoidal electrocardiogram can be derived. At HH stage 14, a sharp downward deflection approximately 80 ms ahead of the QRS-complex can be recorded (presumptive inverted P-wave). When the ventricular loop is subsequently looped backward, around HH 18, and becomes to be positioned caudal to the outflow tract, the P-wave appears above the iso-electric line and an adult type electrocardiogram can be recorded. ap = arterial pole; A = atrium; avc = atrioventricular canal; oft = outflow tract; V = ventricle; vp = venous pole. *Adapted and modified from Moorman AFM, et al. Anatomic substrates for cardiac conduction. Heart Rhythm 2005;2:875– 886.*

1.5. The Electrocardiogram (ECG) in Cardiogenesis

The youngest embryo of which a primitive ECG has been recorded, is a chick embryo of only 15 somites (33-36 hours of development, HH stage 9-10), a developmental stage at which the heart tube almost solely consists of the common ventricle. The ECG recorded at this developmental stage, shows a sinusoidal curve dropping below and above the isoelectric line, reflecting the vector of myocardial contractions in caudocephalic direction.[111, 128, 228, 229] In **Figure 9**, an example of such a sinusoidal ECG recorded in the developing tubular chick heart is shown, reflecting linear and isotropic impulse conduction with constant low velocity resulting in the typical primitive peristaltic unidirectional contraction pattern.[230, 231]

With progression in caudal fusion of the cardiac primordia, the SV is formed and becomes positioned posterior to the atrium and a sharp downward deflection approximately 80 ms ahead of the QRS-complex can be recorded (presumptive inverted P-wave). When the ventricular loop is subsequently looped backward and becomes positioned caudal to the outflow tract (day 4 or HH stage 23-24), the P-wave starts to appear above the isoelectric line (**Figure 9**).[128]

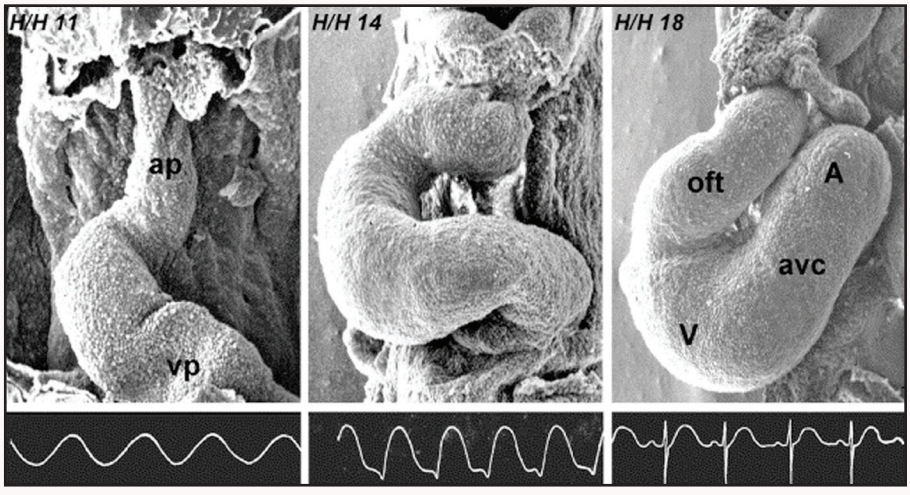

As described above, in the looped embryonic heart, the different cardiac segments will contract sequentially and conduct the electrical impulse with distinct conduction velocities - slow conduction in the AV canal and outflow myocardium and fast conduction in the future atrial and ventricular myocardium - from the ventricular base to the ventricular apex of the developing heart.[124] As a consequence, the electrocardiogram of a 3 to 4 day old chick (~HH stage 18-22) already reveals the presence of a PR interval (AV delay) in the absence of a structural AVN.[230, 232] In the looped embryonic heart, an adult type electrocardiogram including a P-wave reflecting atrial activation, an AV delay caused by slow conduction in the AV junctional myocardium and a QRS complex reflecting fast ventricular activation, can thus be recorded.[107, 230]

The first electrocardiographic tracings in the human fetal heart have been recorded in the 1930-ies with direct chest leads from fetuses removed by hysterectomy. An adult type tracing could be obtained from an embryo of between 6 and 7 weeks of gestation (avians ~HH stage 25-30, mouse ~E 13-14) and of about 16 mm Crown-Romb-Length (CRL) (**Figure 10**). At this developmental stage, the AVN and His bundle are morphologically recognizable but their differentiation is still far from complete yet. [233, 234]

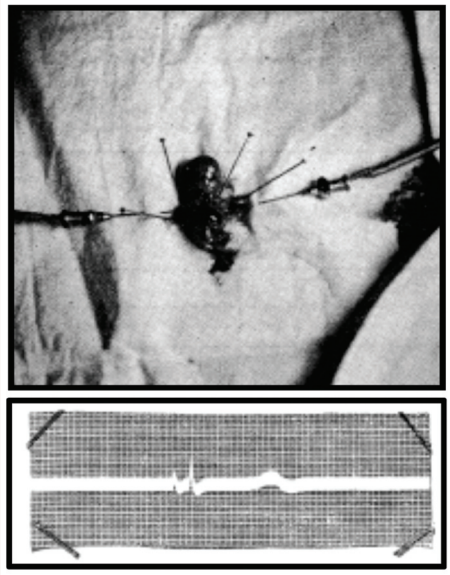

Figure 10. The first electrocardiographic tracings in the human fetal heart, recorded in the 1930-ies with direct chest leads form a foetus of 6-7 weeks of gestation (avians ~HH stage 25-29, mouse ~E 13-14) removed by hysterectomy. *Adapted from: Marcel MP, Exchaquet JP. L'electrocardiogramme du foetus human. Arch Ml Coeur. 1938;1:52.*

1.6. Transitions in Ventricular Activation During Cardiogenesis

During cardiogenesis, the ventricular activation sequence changes concomitantly with changes in ventricular geometry and microarchitecture, from a slow peristaltoid base-to-apex pattern in the tubular heart, through a sequential base-to-apex pattern in the looped trabeculated heart and ultimately to the mature apex-to-base sequention in the septated heart.[138, 235] Generally, myocardial activation proceeds from the venous inflow towards the arterial outflow end of the heart and thus consistently follows the direction of the blood flow (**Figure 11**).

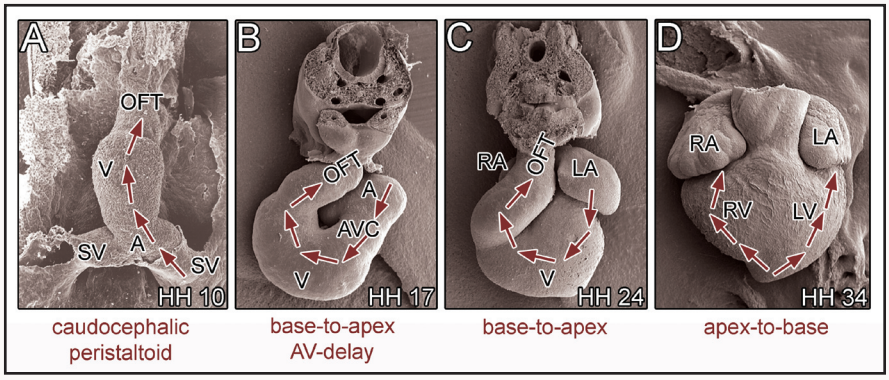

Figure 11. Transitions in ventricular activation sequences during cardiogenesis. The ventricular activation sequence changes from a slow peristaltoid caudocephalic base-to-apex pattern in the tubular heart (**A**), to a sequential base-to-apex pattern in the looped trabeculated heart due to the development of an AV delay (**B&C**) and ultimately to the mature apex-to-base sequention in the septated heart (**D**).

As described above, at the earlier stages of development the heart resembles a tube rather than an ellipsoid with a widely separated inflow and outflow tract. In the tubular heart, the primitive slow caudocephalic peristaltic contractions are sufficient to facilitate efficient slow propulsion of blood from the venous to the arterial pole.

Subsequent configuration of the alternating slow- and fast conducting segments in the looped heart, inherently subjected to progressive spatiotemporal changes in chamber arrangement, guarantees that the downstream ventricular segment does not start contracting before contraction of the upstream atrial segment is terminated. This electrical configuration also ensures that relaxation of the atrial or ventricular segment does not occur before contraction of a downstream flanking segment. This sphincter-like prolonged peristaltic contraction of the slow conducting flanking segments in a way substitutes for the adult type of one-way valves.[124]

In the septated heart, the inflow and outflow tract ultimately become more closely aligned at the top of the ventricles and a morphogenetic division between the atrial and ventricular chambers (annulus fibrosis) dissociating direct morphological coupling between the atrial and ventricular chambers is laid down, necessitating the start of ventricular activation from the apex to the base of the ventricle to efficiently propulse the blood towards the aortic and pulmonary arterial outlet. This apex-to-base sequence of ventricular activation is not only thought to increase ventricular pumping efficiency but is also used as a marker for the anatomical presence of a mature and functional His-Purkinje-System (HPS). More precisely, apex-to-base conduction functionally marks the emergence of mature “apex-first” epicardial breakthrough, near the termini of first the right (at HH stage 29) and secondly the left bundle branch.[227, 236]

The ventricles of the mammalian looped heart are however already capable to contract from apex-to-base even before ventricular septation is completed.[164, 237] In a developmental timeline, apex-to-base conduction might thus already be facilitated before completion of formation of the four-chambered heart and complete structural maturation of the His-Purkinje-System (HPS).

Furthermore, functional activation of the working muscle of the ventricle and its ensuing contraction, also proceed from the right or left ventricular apex in the primitive heart of lower vertebrates (e.g. the African lungfish, bullfrog and crocodilian) in whom the existence of an anatomically distinct organized specialized ventricular conduction system has never been demonstrated.[238-240] Coordinated contraction of the ventricular myocardium from apex-to-base or

from inflow to outflow tract, the common functional principle in the ventricular conduction system of all species, thus already seems to be realized early in vertebrate evolution, suggesting the presence of non-specialized preferential pathways of conduction.[241]

Moreover, the physiological transition in ventricular activation sequence is highly influenced by epigenetic factors affecting general hemodynamics. For instance, maturation of HPS functioning has been shown to be accelerated in the setting of increased pressure load at distinct developmental stages, an effect that is probably mediated by endothelin signaling.[178, 179, 227] Conversely, bundle branch maturation can be delayed by a decreased workload in experimental left heart hypoplasia and inhibition of stretch-sensitive cation channels by gadolinium.[193]

Despite the onset of preferential conduction through the central AV-conduction axis, the occurrence of immature base-to-apex conduction in the developing postseptated heart is not an exceptional phenomenon (*this thesis*).

1.7. Annulus Fibrosis Development: State-of-the-Art

Coincidently with maturation of the His-Purkinje system, completion of ventricular septation and the transition to an apex-to-base ventricular activation sequence, the AV myocardial continuity, which is present around the entire circumference of the slow conducting AV junction disappears as a result of annulus fibrosis formation.[237, 242] It is well established that this AV junctional myocardium is incorporated in the atrial myocardium forming the smooth walled lower atrial rim leading toward the valvular orifices.[243] A small part of the AV canal myocardium however remains in situ and contributes to the AVN and normally this structure constitutes the only site of myocardial continuity with the ventricular conduction system.[243]

The exact signaling processes that underlie atrial and ventricular myocardium dissociation are still incompletely understood and the tissues responsible for the formation of the annulus fibrosis have largely remained unknown. It is however well established that the development of this isolating structure involves several processes in which fusion of the endocardial AV cushions lining the luminal side of the primitive AV canal and the epicardially located AV sulcus tissue at the ventricular site of the AV junction play an important role.[243-245] State-of-the-art in literature postulates critical roles for bone-morphogenetic-protein (BMP) signaling and periostin (an osteoblast specific factor) expression in formation of the isolating annulus fibrosis (see also **Chapters 2-5**, *this thesis*).[246-251] Moreover, recently the important role of the

multipotent EPDCs, migrating through the developing AV dissociated border, in structural formation and electrical isolation of the annulus fibrosis was further established by electrophysiological studies in the EPDC-inhibited quail embryo (see also **Chapter 3**, *this thesis*).[68, 251]

Around the 7th week of human development, the process of AV dissociation at the primitive AV canal has started. From the 12th week of development onwards, the atrial and ventricular myocardium will be completely separated by the annulus fibrosis, through which the AV conduction axis should be the only remaining AV myocardial continuity in postnatal life (see also **Chapter 5**, *this thesis*).[245, 248]

The isolating annulus fibrosis is part of the fibrous skeleton of the heart, which additionally consists of the AV valve annuli, the arterial orifices and the central fibrous body (CFB) or trigonum fibrosum (a triangular mass of fibrous tissue), which connects the AV and aortic valve annuli. Ingrowth of tissue from the dorsal mesocardium contributes to the atrial part of the CFB and is continuous with the tendon of Todaro - a strip of connective tissue originating in the anterior CFB - directly above the junction of the AVN and bundle of His, and passing posteriorly through the atrial septum.[252]

The ventricular part of the CFB is formed by invagination of AV sulcus tissue from the posterior AV sulcus towards the dorsocaudal extension of the bulbar ridge. In this process, a small part of endocardial AV cushion tissue on top of the ventricular septum is trapped and incorporated in the CFB. The AVN passes through the CFB beneath the endocardial cushions and becomes separated from the atrial tissues and directly contacts the bundle of His.[252]

1.8. Accessory Pathway (AP) Persistence

It is certainly not uncommon for annulus fibrosis formation to be incomplete at birth, resulting in postnatal AP persistence providing a possible substrate for clinical AVRTs. During physiological embryonic development, remnants of the primitive AV connections bypassing the insulating AV groove, have morphologically been described in the post-septated embryonic and adult quail (see also **Chapters 2 & 3**, *this thesis*),[125, 225, 249, 251] mouse (see also **Chapter 4**, *this thesis*)[253] and human heart (see also **Chapter 5**, *this thesis*).[248, 254-260] Interestingly, a conducting right-sided AV myocardial continuity was demonstrated in postseptated CCS-LacZ transgenic mice, providing a possible explanation for the occurrence of functional atriofascicular bypass tracts via the moderator band, as a possible substrate for Mahaim tachycardias.[23] Additionally, another

electrophyiological study in wildtype mice has demonstrated the onset of AP mediated AVRT at early stages of mouse development[261]

The structural characteristics and electrophysiological properties of persistent myocardial APs have however not been studied systematically and will be further described in **Chapters 2-5** of *this thesis*.

1.9. Animal Models (Used in This Thesis)

Genetic pathways that dictate cardiac development are highly conserved across vastly diverse species from flies to humans.[27] Despite diversities of body structures in different species, a common genetic program for the early formation of a circulatory system seems to exist. The cardiovascular system seems to have adapted increasing complexity in order to adapt to specific environments.[262, 263]

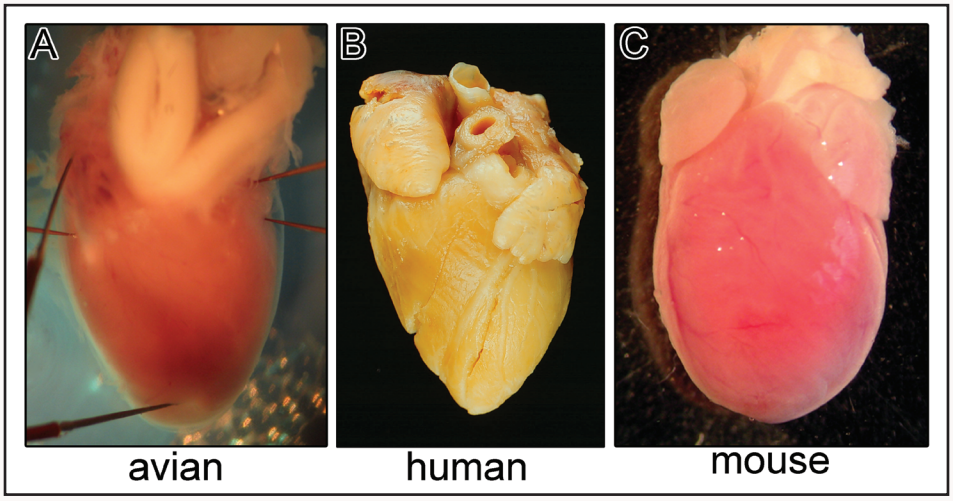

Figure 12. External shape of the embryonic avian, mouse and human heart. A. Externally, the overall shape of the avian heart closely resembles that of the human heart (**B**), while the elipsoidal mouse heart (**C**) is externally differently shaped in comparison to the more pyramidal human and avian developing heart.

1.9.1. Avians (Aves, Amniota, Diapsida)

Since the days of antiquity, the chick embryo has been a very popular model for studying morphology and (patho)physiology of the developing heart.[28, 264] Birds belong to the only class of vertebrates (*Aves*) that consists exclusively of oviparous forms, which makes the avian embryo a vertebrate model always ready at hand. Aristotle, whose work was written toward the end of the fourth century B.C., described many observations on the development of birds and was probably the first to compare the embryology of avians with that of other vertebrates.

The *Gallus domesticus* (chick) and *Coturnix coturnix japonica* (Japanese quail) are among the most frequently used avian strains in experimental research. Externally, the overall shape of the avian heart closely resembles that of the human heart (**Figure 12**). While birds do not have a diaphragm, the relatively large size of the liver leaves little free space in the pericardial and peritoneal cavity, which explains the similar pyramidal shape of the avian heart in comparison to the human heart, which rests on the diaphragm.

Despite the obvious differences in size, the morphological plan of the avian (nonmammlian vertebrate heart) and the mammalian vertebrate heart is quite similar.[35] In comparison to the mammalian heart, the avian heart has valuable advantages as a research model: 1) experimental work with avian embryos (eggs) is much more practical than with mammalian embryos, 2) avians have a very rapid reproduction cycle (5 generations/year) and a very high offspring production (80-90 per 100 days) and 3) the avian embryonic heart has a relatively large size compared to hearts of mammalian embryos at equivalent developmental stages.

Furthermore, the anatomy of the avian CCS is well characterized,[142, 226, 265-268] since the components of the conduction system of the birds heart can be more easily recognized histologically in contrast to the conducting cells in the mammalian heart.[269] Additionally, the electrophysiology of the avian CCS has also been extensively characterized using microelectrodes as well as optical mapping with voltage sensitive dyes.[124, 131, 179, 227, 237, 266, 270, 271] Functionally, the ventricular activation patterns in the avian and mammalian model show remarkable spatiotemporal homology.[227, 253, 272, 273]

As is the case with all animal models, there are however also some differences in anatomy between the avian and mammalian heart: 1) the interventricular septum (IVS) of the bird is an entirely muscular bulky structure, while the upper part of the IVS in the human heart is a thin fibrous structure, 2) the right AV valve (tricuspid valve) of avians is not a fibrous, cusped valve as

in mammals, but consists of a large, single, sickle shaped muscular flap and 3) the bird heart has a very generous subendocardial and intramural distribution of diffuse Purkinje cells throughout the walls and septa of both the atria and ventricles, which is not seen in the mammalian heart.[226]

1.9.2. Mouse (Mus, Amniota, Synapsida)

Due to the increasing availability of tools for genetic manipulation, the mouse has become one of the most popular and most used animal models for studying normal and abnormal cardiac development. Enormous advances in mouse genetics have led to the production of numerous mutants with cardiac abnormalities resembling those seen in human congenital heart disease.[35] Apart from differences in heart rate (adult mouse 300-800 bpm vs. adult human 80-100 bpm) and size (adult mouse heart 0.5 grams vs. adult human heart 250-400 grams), the most pronounced difference between the mouse and human heart is found in their overall shape (**Figure 12**).

As described above, in humans, the heart rests on the diaphragm, which is reflected by a more pyramidal shape and a flat dorsal (or inferior) shape. The heart of the four-legged mouse, in comparison, does not rest on the diaphragm and has more room in the pericardial cavity to more freely move around which is reflected in a more ellipsoidal shape. Moreover, the atria in the human heart are very prominent, whilst in the mouse heart the atrial chambers and atrial appendages are very small.[35]

While the cardiac anatomy of the mouse and human heart is considered remarkably similar, there are however small variations: 1) the AV septum (AVS) of the mouse is a relatively thick and mostly muscular structure, while in the human heart the AVS is a thin fibrous structure known as the membranous septum, 2) the muscular part of the IVS in the human heart is a massive and compact muscular structure, while this structure in the mouse is not quite as compact or massive, 3) in the human but not in the mouse, there is a pronounced difference in the morphology of the trabeculae in the right (coarse) versus left (relatively thin) ventricle, 4) whereas the left atrium of the human heart receives four pulmonary veins, in the mouse heart the pulmonary veins join in a pulmonary confluence behind the left atrium and 5) in the mouse heart the left superior cardinal vein (LSCV) persists into postnatal life, while this structure regresses in the human heart and becomes the ligament of Marshall and oblique vein.[35]

1.10. Immunohistochemical Markers (Used in This Thesis)

1.10.1. Atrial Myosin Light Chain 2 (MLC2a)

Atrial Myosin Light Chain 2 (MLC2a) is a protein, which is predominantly expressed in atrial myocardium and to a lesser extent in the ventricular myocardium and outflow tract of the heart.[274] Embryonic and adult cardiac muscle express two major isoforms of myosin light chain 2, MLC2v (MYL2 – Mouse Genome Informatics) and MLC2a (MYLC2A – Mouse Genome Informatics).

During cardiogenesis, MLC2v is expressed exclusively in ventricular and AV junctional myocardium. Ablation of MLC2v results in disruption of ventricular function at embryonic day 11.5 and embryonic lethality at E 12.5.[275] MLC2a is initially expressed throughout the heart at E 7.5 (human ~E 18) and becomes restricted to the atria after E 12.5 (human ~E 40).[274] In the embryonic and adult avian heart however, MLC2a expression does not become restricted to the atria but demonstrates an expression gradient in which the atria express more MLC2a in comparison to the ventricular myocardium.

1.10.2. Nk2 transcription factor related locus 5 (Nkx 2.5)

Nk2 transcription factor related locus 5 (Nkx2.5), also known as Cardiac specific homeobox protein (Csx), is a homeodomain-containing transcription factor of the Nkx-2 gene family. Nxk2.5 is expressed early during embryogenesis, and although not exclusively found in embryonic regions destined to be heart tissue, it helps to define the cardiogenic field.[276] In many organisms, its expression persists in the heart throughout development. The function of Nkx2.5 and its relatives has been examined in a variety of ways. For instance, the loss of the fly homologe *tinman* gene prevented the development of the dorsal vessel in flies.[277] Mice without functional Nkx2.5 formed small hearts that failed to loop, failed to septated, had underdeveloped ventricles and malformed AV canals.[278] These null studies are complemented by overexpression studies carried out in Xenopus that showed that increased Nkx2.5 levels lead to enlarged hearts in early embryos.[279]

Mutations in the Nkx2.5 gene have also been reported in humans with congenital heart disease. Human individuals were found to be heterozygous for the mutations, indicating that the mutations are either dominant or the result of haploinsufficiency. The phenotypes of patients are varied. Two specific Nkx2.5 mutations (Nkx2-5 Gln170ter and Gln198ter) have been found to lead to problems that included atrial septal defects, AV heart block (conduction system defects), and less commonly, tetralogy of Fallot, mitral valve defects, left ventricular

hypertrophy, pulmonary atresia, and ventricular septal defects.[188] Interestingly, recent studies have identified the contribution of a Nkx2.5 negative myocardial population to the developing sinus venosus and SAN.[47, 192]

1.10.3. Periostin

Periostin was originally isolated as an osteoblast-specific factor that functions as a cell adhesion molecule involved in osteoblast recruitment, attachment and spreading. Expression of periostin mRNA was later also found in the embryonic mouse and chicken heart in the endocardial cushions that ultimately divide the primitive heart tube in a four-chambered heart.[246, 250] Additionally, periostin expression was found to be maintained within the valves of the adult mouse heart.[250] Periostin is secreted during cushion mesenchym formation.[280] Expression of periostin is significantly increased in response to BMP and TGF-β signaling in mesenchymal cells undergoing differentiation.[281, 282] Induction of periostin expression has also been shown following myocardial infarction in the adult heart.[283] In a recent study, a 40-fold increase in periostin mRNA expression in mouse hearts subjected to cardiovascular overload was described.[284] Moreover, in a rat cardiac dilatation model, a decrease in periostin expression was correlated with an increased survival rate and left ventricular function.[285] In literature, periostin has been suggested to induce myocardium to transform into mesenchym of a mixed phenotype, which can subsequently transdifferentiate into cells with a fibrous identity, possibly in response to shear stress during cardiac development,[246, 280] while at late stages of development, periostin may also serve to maintain the integrity of the fibrous tissues of the heart.[280] At the boundary where myocardial cells directly interface endocardial cushion tissue at the AV junction, periostin expression is enhanced and myocardial cells are replaced over time by dense fibrous periostin-positive tissue.[286]

1.10.4. Connexin 43 (Cx43)

Connexin 43 (Cx43) is one of the 4 major connexins in the mammalian heart: connexin 40 is expressed in fast conducting cardiac tissues and in the atria,[287] connexin 45 is expressed in slow conducting pathways and in the myocardium of the primary heart tube,[135, 136, 168] connexin 30.2 is expressed in the AVN and contributes to slowing of propagation of excitation in the AVN[288] and connexin 43 is expressed in the slower conducting working myocardium of the atria and ventricles and in the distal part of the CCS.[289] The expression of connexins is highly variable between species and varies during different stages of development.[287]

Connexin 43 expression in the avian heart is subject to considerable controversy in literature. Expression of connexin 43 in the developing avian embryo has been demonstrated in the smooth muscle cells in the media of the vessel walls of the arterial outflow tract of the heart (aorta, pulmonary arteries, brachiocephalic arteries) and the smooth muscle cells of the coronary arteries.[290, 291] Additionally, persistent Cx43 expression throughout development and in the mature avian heart has been reported in a Northern blotting study of the developing chick heart and persisted at significant levels.[292]

In contrast, complete absence of Cx43 expression in the myocardial tissues of the developing and adult chick heart has also been described in literature[290, 291] and can possibly be explained by the use of mammalian antibodies and slight differences in the Cx43-isoform between avians and mammals.[292] Freeze-fracture studies of avian embryonic myocardium have indicated that its gap-junctions are very tiny and infrequent,[293] which might have a restrictive effect on the ability to properly detect Cx43 in the developing avian heart. Moreover, gap-junctional expression seems to follow an ontogenic sequence since a developmental increase in the density of gap junctions in prenatal rat hearts has been observed[294] and electrophysiological studies of isolated cell pairs from developing avian hearts have noted a change in the regulation of gap junctions between embryonic days 4 (~HH 24) and 18 (~HH 44).[295]

1.10.5. Sodium Channel, voltage-gated, type V, alpha subunit (SCN5a)

The Sodium Channel, voltage-gated, type V, alpha subunit (SCN5a) gene encodes for the Nav1.5 sodium ion channel protein and is responsible for the rapid influx of sodium ions (inward sodium current, I_{Na}) that initiates and propagates the cardiac action potential in the heart.[296, 297] The SCN5A gene is located on the short (p) arm of chromosome 3 at position 21. The encoded protein provides instructions for making a sodium channel that is abundant in heart muscle and is responsible for the initial upstroke of the action potential. These channels open and close at specific times to control the flow of sodium ions into cardiac muscle cells.[298-300]

SCN5a mRNA can first be detected at stage E 9.5 of mouse heart development, peaks at E11.5, than decreases and steadily increases from E17.5 onwards. Mutations in the SCN5a gene are associated with diverse channelopathies, such as long QT syndrome type 3 (LQT3), Brugada syndrome, and idiopathic ventricular fibrillation.[301]

1.10.6. Periodic-Acid-Schiff (PAS)-Staining

Periodic Acid Schiff (PAS) is a staining method used for histology in Pathology. This method is primarily used to identify glycogen in tissues. Glycogen is a high-molecular-weight polysaccharide that serves as a repository of glucose units for utilization in times of metabolic need. In PAS staining, the reaction of periodic acid selectively oxidizes the glucose residues and creates aldehydes that react with the Schiff reagent and than creates a purple-magenta color.

The first glycogen in the muscular tissue of chick embryos becomes recognizable at about the time that cardiac contraction begins (9 somite stage).[302] Unlike in mammals, little or no glycogen is found in the specialized CCS tissues of the avian heart, while the atrial and ventricular myocardium have a high glycogen content.[303-306]

CLINICAL ASPECTS OF SUPRAVENTRICULAR TACHYCARDIAS IN CHILDREN AND ADULTS

1.11. Clinical SVTs in Children and Adults

Supraventricular tachycardia is the most common cardiac arrhythmia in both children and adults, with an estimated prevalence of 2.25 per 1000 in the normal population.[1, 2] The prevalence of SVTs in children is estimated at one in 500 children worldwide.[307] In adults, AV Nodal Reentrant Tachycardia (AVNRT) accounts for approximately 80% of all SVTs,[308] yet it accounts for only 5% of SVT cases in infants and toddlers and comprises only 13–16% of SVTs in children and adolescents.[309] Conversely, macroreentry through an accessory AV pathway (Atrioventricular Reentrant Tachycardia, AVRT) accounts for ~30 % of SVT cases in adults, but is by far the most common (80%) mechanism of SVT in children.[2, 310] Much less prevalent forms of SVTs include Permanent-Junctional-Ectopic-Tachycardia (PJET), Ectopic-Atrial-Tachycardia (EAT) and Intra-Atrial-Reentrant-Tachycardia (IART) or Atrial Flutter.

1.12. Symptoms of SVTs in Children and Adults

Symptoms of SVT in infancy differ from those in childhood or adolescence. Newborns may present with a history of fetal tachycardia, signs of left ventricular dysfunction or even with hydrops foetalis representing severe heart failure from persistent rapid fetal tachycardia (see also **Chapter 9**, *this thesis*).[311, 312] Neonates can also present with new onset incessant and difficult to treat tachycardia at birth with no history of any fetal tachycardias.[307] Moreover, neonates with SVTs are at high risk for sudden cardiac arrest, since cardiac reserve in neonates is very small and typical SVTs with heart rates exceeding 200/min. can lead to life threatening myocardial dysfunction within several days. [313]

In infants, symptoms of SVTs are inconspicuous and masquerade those of many other common illnesses in infancy and include irritatebility, poor feeding, tachypnea, diaphoresis and poor color. Most infants with SVT have structurally normal hearts, while in 15% of patients tachycardia is associated with heart disease, drug administration or febrile illness.[307] Older children and adolescents complain of palpitations (in excess of 150/min.), general malaise, indistinct pressure or discomfort in the throat, isolated headaches, fatigue, chest discomfort, shortness of breath or lightheadedness. Syncope is unusual and may indicate life-threatening arrhythmia. In adolescence, typical SVTs are characterized by a sudden onset (often in rest) and sudden termination of tachycardia.

1.13. Treatment of SVTs in Children and Adults

Regardless of SVT type, maneuvers that increase parasympathetic (vagal) tone, slow down conduction through the AVN and break the reentry circuit responsible for SVT, apply to all patients. Different measures may be successful in different children and include placing an ice-bag around the nose and mouth or abdomen, immersion in ice-cold water, applying the Valsalva maneuver (take a deep breath and bear down), pressure on the abdomen, carotid sinus massage or blowing on a thumb.[307]

Acute treatment with intravenous administration of adenosine as a rapid bolus is safe in children of all ages and usually breaks the SVT. When symptoms however resume, beta-blockers (e.g. propranolol), procainamide, a calcium blocker (e.g.verapamil) or amiodarone should additionally be administrated.[314]

Chronic management of SVTs should be individualized, but in general prophylactic treatment with antiarrhythmic medication is prescribed to infants younger than 1 year of age. At the age of 1 year, this prophylactic treatment is temporarily discontinued in order to see if tachycardia recurs.[315] Elimination of the arrhythmogenic substrate and permanent cure from almost all forms of SVT can be achieved by percutaneous radiofrequency catheter ablation (RFCA) or surgery.[307, 316, 317]

During a RFCA procedure, the cardiac tissue is locally heated to 50-60 ˚C by alternating current (350 kHz to 1 MHz) delivered by the small metal tip of a RF catheter, producing a permanent small scar measuring approximately 4 mm in diameter and 4 mm in depth.[318] The initial success rates of RFCA exceed 90%.[312] In **Chapter 8** of this thesis the therapeutic issues in pediatric SVT are further outlined.

1.14. AV Reentrant Tachycardias in Children and Adults

AV Reentrant Tachycardia (AVRT) is by far the most common (80%) mechanism of SVT in children,[1, 2] and accounts for ~30% of SVTs in adults.[310]

1.14.1. Arrhythmogenic Substrate in AVRT

AV Reentrant Tachycardia (AVRT) involves the presence of an accessory myocardial AV pathway (AP) that bypasses the annulus fibrosis. The overall incidence of APs in the general population is 0.1-0.3% and 3.4% in first degree relatives of patients with ventricular preexcitation on ECG.[319]

Commonly, the APs are “concealed” bypass tracts, which are capable of conducting solely in the retrograde direction (from the ventricles to the atria).

The ECG of a patient with a concealed AP during sinus rhythm is normal (no signs of ventricular preexcitation). Accessory pathways in patients with the Wolff-Parkinson-White (WPW) syndrome are however usually capable of both antegrade and retrograde conduction and give rise to ventricular preexcitation on ECG recordings during sinus rhythm.[307]

Other, less frequently encountered APs include substrates with decremental (nodal) properties mostly located in the septal or inferior half of the tricuspid valve, Mahaim fibers producing ventricular preexcitation resembling left bundle branch block and slow conducting APs giving rise to Permanent Junctional Reciprocating Tachycardia (PJRT).[307]

1.14.2. Natural Course of AVRTs

In approximately 60% of pediatric patients, the first episode of AVRT occurs before birth or in infancy and appears to spontaneously resolve completely in two thirds of cases before the age of 1 year, while more than 80-90% of patients become asymptomatic after the first year of life.[1, 2] Relapse during follow-up is however observed in 20-30% of these cases.[320] A second new onset AVRT incidence peak is seen around the age of 8-12 years, in which case spontaneous regression of symptoms is only observed in approximately 20% of cases.[321]

1.14.3. Arrhythmia Mechanism in AVRT

Orthodromic AVRT is the most common tachycardia mechanism in AVRT in both children and adults. In orthodromic AVRT, antegrade conduction occurs through the normal AV conduction system, while retrograde conduction to the atria occurs via the AP. Antidromic AVRT is far less common and utilizes the AP as the antegrade pathway of circus movement conduction. Reentrant tachycardia may also involve multiple APs, providing both antegrade and retrograde conduction.[322]

Besides an anatomical substrate two additional conditions are required for functional preexcitation during sinus rhythm to occur: 1) electrical coupling between adjacent ventricular and atrial myocytes, and 2) a higher conduction velocity through the AP than in the normal ventricular conduction system. Reentry tachycardia can occur when: 1) at least two functionally distinct conduction pathways are present, 2) unidirectional block is induced in one pathway and 3) conduction time is slow enough over the nonblocked pathway to allow recovery of excitability in the blocked pathway, thereby permitting retrograde conduction over the blocked pathway and completing the reentry circuit.[322, 323]

1.14. The Wolff-Parkinson-White (WPW) Syndrome

1.14.4.1. Epidemiology of WPW Syndrome

The estimated prevalence of typical WPW syndrome is 0.1 to 3.1 per 1000 persons.[324, 325] Because of its intermittent pattern, the precise incidence of WPW is unknown.[326] The incidence of WPW in males is more than twice that in females.[324, 326-328] Additionally, in female patients, an incidence peak around the age of 7 years has been reported, while men are significantly younger at first presentation than women.[326]

The AP in WPW, known as the bundle of Kent, is usually located in the lateral rings of the annulus fibrosis and consists of a thin muscular segment that does not posses decremental properties.[254, 329-331] Approximately 10% of patients may have two or more AV bypass tracts. Most patients with typical WPW syndrome demonstrate isolated ventricular preexcitation in a structurally normal heart.[332] In a small percentage of patients with WPW, APs however occur in association with other cardiac abnormalities or congenital heart disease.[333] WPW is more prevalent in children with Epstein anomaly of the tricuspid valve, AV septal defects and ventricular septal defects, while occasionally the WPW syndrome may be inherited.[328, 334] Moreover, coronary artery disease was found to be associated with WPW in 6% of patients.[326]

1.14.4.2. Genetics in WPW Syndrome

The inherited form of WPW syndrome is an autosomal dominant trait of which the gene has been identified on chromosome 7q34-q36.[335, 336] A point mutation in the PRKAG2 gene, which encodes the regulatory γ-subunit of AMP-activated protein kinase (AMPK), results in the substitution of glutamine for arginine (R302Q).[335] These mutations cause glycogen-storage hypertrophic cardiomyopathy (HCM) associated with Wolff-Parkinson-White ventricular preexcitation syndrome and progressive cardiac conduction system disease.[337] In other hereditary forms of ventricular preexcitation associated with glycogen storage hypertrophic cardiomyopathy, mutations in the Lysosome associated protein 2 (LAMP2) and α-galactosidase A (GLA) have been identified.[338-340]

14.4.4.3. Arrhythmia Mechanism in WPW Syndrome

The macroreentry circuit in WPW syndrome is produced in the atrial muscle, AVN, ventricular muscle and the AP itself. This circuit facilitates continuous alternate depolarization of the atrial and ventricular myocardium.

In typical orthodromic reciprocating AV tachycardia, the electrical impulse proceeds from the atria to the ventricles through the AVN and retrograde back up to the atria from the ventricle via the AP. In this type of AVRT, the effective refractory period of the AP exceeds that of the normal AV Nodal His-Purkinje pathway.[341] In orthodromic AVRT, the QRS complexes are narrow and a retrograde P wave can be seen embedded in the early portion of the T wave (best seen in leads II and V2).[307]

Infrequently, the reentry circuit in WPW can proceed in the opposite direction and produce antidromic AVRT. In this type of AVRT the effective refractory period of the AP is shorter than that of the normal HPS pathway.[341] The ECG demonstrates very abnormally wide QRS complexes resembling those seen in ventricular tachycardia.[307]

14.4.4. The WPW Syndrome ECG

The typical ECG recorded during sinus rhythm in a patients with WPW syndrome shows ventricular preexcitation manifested by: 1) a short PR interval, 2) a wide QRS complex, and 3) initial slurring (delta wave) of the QRS complex. Ventricular preexcitation during sinus rhythm is produced by a fast wave of depolarization, which prematurely enters one of the ventricles through the AP. In most patients, ventricular preexcitation is present at all times and all heart rates, while in some cases preexcitation is intermittent. In the later, preexcitation is usually only present at lower heart rates.[322]

14.4.5. Atrial Fibrillation in WPW Syndrome

Episodes of atrial fibrillation are reported in 20% to 30% of adult patients with WPW syndrome, while atrial fibrillation is uncommon in children.[342, 343] These episodes are clinically important, since extreme rapid rates may occur over the bypass tract, leading to hemodynamic deterioration or ventricular fibrillation. In case of atrial fibrillation, the AP conducts the atrial rate to the ventricles, which in this case can exhibit extremely rapid rates, possibly resulting in ventricular fibrillation and cardiac arrest. Patients are considered to be at high risk for ventricular fibrillation when the shortest interval between two subsequent preexcited ventricular beats during atrial fibrillation is less than 220 ms .[344, 345]

14.4.6. Treatment Options in WPW Syndrome

Currently, conservative treatment with class I anti-arrhythmic drugs, beta-blockers (class II) and/or amidarone (class III) achieves a 70-80% efficacy in prevention of arrhythmia relapse.[346] Patients with WPW syndrome should not be treated with medications which shorten refractoriness along the bypass tract, such as calcium channel blockers and digoxin.[326]

After thorough evaluation of the risk/benefit ratio, radiofrequency (RF) ablation has been shown to also be a highly effective definitive treatment in the pediatric age group.[346] Since the risk of fatal complications is estimated to be up to 0.3% in children less than 4-5 years of age, the Pediatric Radiofrequency Catheter Ablation Registry advises to restrict the indication for RF ablation to children older than 10-12 years.[346] Currently, main concerns in pediatric RF ablation focus on X-ray exposure and possible damage to the CCS,[346] in which respect new systems of 3D mapping or the 'non-contact' system and the introduction of cryoablation are promising.[347-349]

1.14.4.7. Sudden Infant Death in WPW Syndrome

Sudden death (SD) in ventricular preexcitation syndrome is rare with an overall risk rate of 0.006 per patient-year, and mostly occurs in young and otherwise healthy individuals and can be the first manifestation of the WPW syndrome in previously asymptomatic patients.[256, 324, 328, 350-354] In a clinicopathological series on 273 SDs in children and young adults (aged < 35 years), a 3.6% prevalence of ventricular preexcitation syndrome was reported.[355] The fatal event was not preceded by warning symptoms in 40% of patients and death almost invariably occurred at rest and often during sleep. In 50% of these SD patients additional isolated acute atrial myocarditis was found on histological examination.[355]

Pathophysiologically, in most cases SD results from a rapid ventricular response to atrial fibrillation over an AP with a short refractory period.[354] In these cases, atrial fibrillation might be triggered by a primary atrial pathology or be secondary to AV reentrant tachycardia (AVRT).[354] Additionally, strenuous physical activities shorten the refractory period of the bypass tract and may precipitate atrial fibrillation or flutter.[326]

Syncope in patients with WPW might indicate high risk of sudden death. Successful ablation of the AP eliminates the risk of sudden death from WPW.

1.14.4.8. Animal WPW-Models

Most electrophysiological characteristics of APs and their role in causing AVRT have been obtained from clinical studies in humans. Extensive electrophysiological experiments in dogs have provided additional detailed insights in types A and B ventricular preexcitation.[341] Moreover, since the mutation for familial WPW syndrome was identified transgenic technology has been used to generate transgenic models for WPW. [335, 336]

Transgenic mice overexpressing the mutated PRKAG2 gene, were recently found to nicely recapitulate the human phenotype of familial WPW syndrome and glycogen storage cardiac hypertrophy.[335, 338] In this model, the mutated PRKAG2 gene, which encodes for the γ-2 subunit of AMP-activated-protein-kinase (AMPK), was cloned along side a powerful alpha-myosin heavy chain promoter. Histopathology demonstrated glycogen filled cardiomyocytes disrupting the annulus fibrosis and functionally giving rise to ventricular preexcitation. Additionally, in a similar transgenic mouse model overexpressing the PRKGA2 mutation, the preexcitation phenotype was reproduced and SVTs could be induced.[356]

Furthermore, deletion of the ALK3 gene (BMP receptor type IA), which encodes for the type 1a receptor for bone morphogenetic proteins (BMPs), in the AV canal cardiomyocytes during development causes ventricular preexcitation, possibly indicating an important role for the ALK3 gene in the etiology of the WPW syndrome.[247, 357]

1.15. AV Nodal Reentrant Tachycardias in Children and Adults

1.15.1. Epidemiology in AVNRT

AV Nodal Reentrant Tachycardia (AVNRT) is the most common form of SVT in adolescence and adulthood, while its very unusual in infants and toddlers (<5 %) and only school-aged children may present with AVNRT.[2, 308]

1.15.2. Arrhythmogenic Substrate in AVNRT

AV Nodal Reentrant Tachycardia (AVNRT) is based on the concept of AV Nodal conduction dichotomy, which implies that AV Nodal conduction is longitudinally dissociated in a slow and fast pathway. Functionally, the slow (α) and fast (β) pathways have distinct conduction velocities and refractory periods, while their precise anatomic boundaries are unknown. The fast pathway conducts rapidly and has a relatively long refractory period in the antegrade direction, while the slow pathway conducts relatively slowly and has a shorter refractory period than the fast pathway.[358] The polemic in dual AV nodal pathways concentrates on confinement of the slow and fast pathway to the AVN itself or the presence of an upper common pathway in the adjacent atrial tissues to complete the reentry circuit.

The dual input to the AVN seems to be a normal, physiological finding. Large studies on the inducebility of echoes or repetitive reentry in normal hearts do not exist. It is said that dual pathways existing in response to atrial extrastimulation may be found in up to 25% of patients without SVT.[325] In arrhythmia free children with congenital heart disease, the prevalence of dual antegrade AV Nodal pathways was 35%.[359] Moreover, dual AV Nodal physiology was found to be present in 62% of pediatric patients with AVNRT.[349]Interestingly, dual AV Nodal conduction pathways have been identified in up to 12% of patients with WPW-syndrome.[360]

The slow pathway is predominantly posteroinferiory located between the ostium of the CS and the septal leaflet of the tricuspid valve, while the fast pathway allegedly starts anterosuperiorly in the interatrial septum. These pathways converge onto the AVN at sites known as the posterior and anterior nodal inputs.[361] In addition, left-sided atrial inputs were implicated and proved in the structurally normal human heart.[362]

1.15.3. Arrhythmia Mechanism in AVNRT

In patients with AVNRT, the physiological conduction properties of the slow and fast pathway are such that they allow for a microreentry circuit at the entrance of the AVN.[307]

Subforms of AVNRT based on the location of earliest atrial activation include: 1) the most common subform, slow-fast conduction (antegrade conduction over the slow pathway and retrograde conduction over the fast pathway, 81,4%), 2) the slow-slow form (both antegrade and retrograde conduction over a slow pathway, 13,7%) and 3) the fast-slow form (antegrade conduction over the fast pathway and retrograde conduction over the slow pathway, 4,9%).[363]

1.15.4. The ECG in AVNRT

In patients with AVNRT, the ECG recorded during sinus rhythm is normal. An ECG recorded during an episode of AVNRT however shows normal but usually narrow QRS complexes. In these ECGs, the P waves are not clearly seen since activation of the atria and ventricles occurs at the same time and P waves are thus embedded in the QRS complexes.[307]

On electrophysiological study, the classic clinical finding of AV Nodal dual pathway electrophysiology – the 50 ms jump in the AH (atrium-His) interval for a 10 ms decrement in AA (atrium-atrium) interval during atrial stimulation- is applicable to 60-85% of cases with AVNRT.[364, 365] A second but far less specific parameter to show the presence of a slow AV Nodal pathway is a PR greater than or equal to RR during atrial overdrive pacing. In adults with AVNRT, this finding is present in 93% of cases.[366]

1.15.5. Treatment Options in AVNRT

In the initial attempts of RF ablation for AVNRT, the fast pathway was targeted by application of RF energy superior and anterior to the His bundle region, with success rates of 80-90% but with AV block induction in as many as 21% of patients. Currently slow pathway ablation, first introduced by Jackman et al., is targeted to cure AVNRT. With this technique the slow pathway is targeted by placing the catheter over the posteroinferior septum in the region of the CS and has reached success rates of 99% in experienced centers.[365, 367-371] In **Chapter 8** RF ablation in pediatric AVNRT is further outlined.

Aim and Outline of the Thesis

This thesis focuses on structure-function relations in cardiogenesis in relation to clinical arrhythmia etiology. The aim of the first two parts of this thesis is to correlate the results of basic experimental studies in the developing avian, mouse and human heart to the etiology of clinical AV Reentrant Tachycardias (AVRT) and AV Nodal Reentrant Tachycardias (AVNRT) in both children and adults. In the third part of this thesis, therapeutic clinical issues in pediatric supraventricular tachycardia (SVT) will be outlined.

In **PART I,** Chapter 2 describes the physiological development of the isolating annulus fibrosis and the persistence of functional APs in the postseptated embryonic avian heart in relation to the etiology of AVRTs in neonates and children. In Chapter 3, the pathological development of the isolating annulus fibrosis was studied in an experimental avian model in which the outgrowth of Epicardium-Derived-Cells (EPDCs) was delayed by an *in-ovo* microsurgical technique. In this model the persistence of APs was analyzed in relation to the etiology of AVRTs in adolescents and adults. Chapter 4 subsequently extrapolates the acquired avian data to mammalian heart development and describes the persistence of APs in mouse heart development as a possible anatomical substrate for perinatal SVTs. In Chapter 5**,** the postulated etiological considerations described in the previous 'basic experimental' chapters are extrapolated to humans by a systematical immunohistochemical analysis of the physiological development of the annulus fibrosis in serial sections of the developing human heart at consequent stages of embryonic development.

In **PART II**, Chapter 6 provides a historical review of the different theories on the ontogenic development of the AVN in relation to AVNRT etiology. In Chapter 7, the developmental origin of the AVN was subsequently analyzed in an experimental study in the avian embryo, providing a new concept on the origin of the adult AV nodal region.

Chapter 8 in **PART III**, describes the treatment options, success-, complication- and recurrence rates for pediatric SVTs. Finally, in Chapter 9 an illustrative case report of incessant AP mediated SVT in a premature neonate with hydrops foetalis, is presented.

References

1. Morady F. Catheter ablation of supraventricular arrhythmias: state of the art. *J Cardiovasc Electrophysiol.* 2004;15(1):124-139.

2. Ko JK, Deal BJ, Strasburger JF, Benson DW. Supraventricular tachycardia mechanisms and their age distribution in pediatric patients. *Am J Cardiol.* 1992;69(12):1028-1032.

3. Hatada Y, Stern CD. A fate map of the epiblast of the early chick embryo. *Development.* 1994;120(10):2879-2889.

4. Yutzey KE, Kirby ML. Wherefore heart thou? Embryonic origins of cardiogenic mesoderm. *Dev Dyn.* 2002;223(3):307-320.

5. Garcia-Martinez V, Schoenwolf GC. Primitive-streak origin of the cardiovascular system in avian embryos. *Dev Biol.* 1993;159(2):706-719.

6. Tam PP, Steiner KA. Anterior patterning by synergistic activity of the early gastrula organizer and the anterior germ layer tissues of the mouse embryo. *Development.* 1999;126(22):5171-5179.

7. Schoenwolf GC, Garcia-Martinez V. Primitive-streak origin and state of commitment of cells of the cardiovascular system in avian and mammalian embryos. *Cell Mol Biol Res.* 1995;41(4):233-240.

8. Rosenquist GC. Location and movements of cardiogenic cells in the chick embryo: the heart-forming portion of the primitive streak. *Dev Biol.* 1970;22(3):461-475.

9. Davidson BP, Kinder SJ, Steiner K, Schoenwolf GC, Tam PP. Impact of node ablation on the morphogenesis of the body axis and the lateral asymmetry of the mouse embryo during early organogenesis. *Dev Biol.* 1999;211(1):11-26.

10. Hamburger V, Hamilton HL. A series of normal stages in the development of the chick embryo. 1951. *Dev Dyn.* 1992;195(4):231-272.

11. Rawless M. The heart-forming areas of the early chick blastoderm. *Physiol Zool.* 1943;16:22-41.

12. de Ruiter MC, Poelmann RE, van der Plas-de Vries I, Mentink MM, Gittenberger-de Groot AC. The development of the myocardium and endocardium in mouse embryos. Fusion of two heart tubes? *Anat Embryol.* 1992;185(5):461-473.

13. Fishman MC, Olson EN. Parsing the heart: genetic modules for organ assembly. *Cell.* 1997;91(2):153-156.

14. Olson EN, Srivastava D. Molecular pathways controlling heart development. *Science.* 1996;272(5262):671-676.

15. Laverriere AC, MacNeill C, Mueller C, Poelmann RE, Burch JB, Evans T. GATA-4/5/6, a subfamily of three transcription factors transcribed in developing heart and gut. *J Biol Chem.* 1994;269(37):23177-23184.

16. Abu-Issa R, Waldo K, Kirby ML. Heart fields: one, two or more? *Dev Biol.* 2004;272(2):281-285.

17. Männer J. Cardiac looping in the chick embryo: a morphological review with special reference to terminological and biomechanical aspects of the looping process. *Anat Rec.* 2000;259(3):248-262.

18. Patten BM. Initiation and early changes in the character of the heart beat in vertebrate embryos. *Physiol Rev.* 1949;29(1):31-47.

19. Zaffran S, Kelly RG, Meilhac SM, Buckingham ME, Brown NA. Right ventricular myocardium derives from the anterior heart field. *Circ Res.* 2004;95(3):261-268.

20. Galli D, Domínguez JN, Zaffran S, Munk A, Brown NA, Buckingham ME. Atrial myocardium derives from the posterior region of the second heart field, which acquires left-right identity as Pitx2c is expressed. *Development.* 2008;135(6):1157-1167.

21. Shiraishi I, Takamatsu T, Fujita S. Three-dimensional observation with a confocal scanning laser microscope of fibronectin immunolabeling during cardiac looping in the chick embryo. *Anat Embryol.* 1995;191(3):183-189.

22. Thompson RP, Reckova M, deAlmeida A, Bigelow MR, Stanley CP, Spruill JB, Trusk TT, Sedmera D. The oldest, toughest cells in the heart. *Novartis Found Symp.* 2003;250:157-174; discussion 174-156, 276-159.

23. Jongbloed MR, Wijffels MC, Schalij MJ, Blom NA, Poelmann RE, van der Laarse A, Mentink MM, Wang Z, Fishman GI, Gittenberger-de Groot AC. Development of the right ventricular inflow tract and moderator band: a possible morphological and functional explanation for Mahaim tachycardia. *Circ Res.* 2005;96(7):776-783.

24. Capdevila J, Johnson RL. Hedgehog signaling in vertebrate and invertebrate limb patterning. *Cell Mol Life Sci.* 2000;57(12):1682-1694.

25. Gittenberger-de Groot AC, de Ruiter MC, Bartelings MM, Poelmann RE. Embryology of congenital heart disease. In: Crawford MH, DiMarco, J.P., Paulus, W.J., ed. *Cardiology*: Richard Furn; 2004:1217-1227.

26. Bruneau BG. Transcriptional regulation of vertebrate cardiac morphogenesis. *Circ Res.* 2002;90(5):509-519.

27. Srivastava D, Olson EN. A genetic blueprint for cardiac development. *Nature.* 2000;407(6801):221-226.

28. Sedmera D, Pexieder T, Hu N, Clark EB. Developmental changes in the myocardial architecture of the chick. *Anat Rec.* 1997;248(3):421-432.

29. Rychter Z, Ostádal B. Fate of "sinusoidal" intertrabecular spaces of the cardiac wall after development of the coronary vascular bed in chick embryo. *Folia morphologica.* 1971;19(1):31-44.

30. Rychterová V. Principle of growth in thickness of the heart ventricular wall in the chick embryo. *Folia morphologica.* 1971;19(3):262-272.

31. Vrancken Peeters MP, Gittenberger-de Groot AC, Mentink MM, Hungerford JE, Little CD, Poelmann RE. The development of the coronary vessels and their differentiation into arteries and veins in the embryonic quail heart. *Dev Dyn.* 1997;208(3):338-348.

32. de Ruiter MC, Gittenberger-de Groot AC, Wenink AC, Poelmann RE, Mentink MM. In normal development pulmonary veins are connected to the sinus venosus segment in the left atrium. *Anat Rec.* 1995;243(1):84-92.

33. Webb S, Brown NA, Wessels A, Anderson RH. Development of the murine pulmonary vein and its relationship to the embryonic venous sinus. *Anat Rec.* 1998;250(3):325-334.

34. Wessels A, Anderson RH, Markwald RR, Webb S, Brown NA, Viragh S, Moorman AF, Lamers WH. Atrial development in the human heart: an immunohistochemical study with emphasis on the role of mesenchymal tissues. *Anat Rec.* 2000;259(3):288-300.

35. Wessels A, Sedmera D. Developmental anatomy of the heart: a tale of mice and man. *Physiol Genomics.* 2003;15(3):165-176.

36. Douglas YL, Jongbloed MR, Gittenberger-de Groot AC, Evers D, Dion RA, Voigt P, Bartelings MM, Schalij MJ, Ebels T, de Ruiter MC. Histology of vascular myocardial wall of the left atril body after pulmonry venous incorporation. *Am J Cardiol.* . 2006(97):66-70.

37. Gittenberger-de Groot AC, Bartelings MM, de Ruiter MC, Poelmann RE. Basics of cardiac development for the understanding of congenital heart malformations. *Pediatr Res.* 2005;57:169-176.

38. Mjaatvedt CH, Nakaoka T, Moreno-Rodriguez RA, Norris RA, Kern MJ, Eisenberg CA, Turner D, Markwald RR. The outflow tract of the heart is recruited from a novel heart-forming field. *Dev Biol.* 2001;238(1):97-109.

39. Waldo KL, Kumiski DH, Wallis KT, Stadt HA, Hutson MR, Platt DH, Kirby ML. Conotruncal myocardium arises from a secondary heart field. *Development.* 2001;128(16):3179-3188.

40. Kelly RG, Brown NA, Buckingham ME. The arterial pole of the mouse heart forms from Fgf10-expressing cells in pharyngeal mesoderm. *Dev Cell.* 2001;1(3):435-440.

41. Kelly RG. Molecular inroads into the anterior heart field. *Trends Cardiovasc Med.* 2005;15(2):51-56.

42. Waldo KL, Hutson MR, Ward CC, Zdanowicz M, Stadt HA, Kumiski D, Abu-Issa R, Kirby ML. Secondary heart field contributes myocardium and smooth muscle to the arterial pole of the developing heart. *Dev Biol.* 2005;281(1):78-90.

43. Mesbah K, Harrelson Z, Théveniau-Ruissy M, Papaioannou VE, Kelly RG. Tbx3 Is Required for Outflow Tract Development. *Circ Res.* 2008.

44. Thomas PS, Kasahara H, Edmonson AM, Izumo S, Yacoub MH, Barton PJ, Gourdie RG. Elevated expression of Nkx-2.5 in developing myocardial conduction cells. *Anat Rec.* 2001;263(3):307-313.

45. Blaschke RJ, Hahurij ND, Kuijper S, Just S, Wisse LJ, Deissler K, Maxelon T, Anastassiadis K, Spitzer J, Hardt SE, Schöler H, Feitsma H, Rottbauer W, Blum M, Meijlink F, Rappold G, Gittenberger-de Groot AC. Targeted mutation reveals essential functions of the homeodomain transcription factor Shox2 in sinoatrial and pacemaking development. *Circulation.* 2007;115(14):1830-1838.

46. Blom NA, Gittenberger-de Groot AC, de Ruiter MC, Poelmann RE, Mentink MM, Ottenkamp J. Development of the cardiac conduction tissue in human embryos using HNK-1 antigen expression: possible relevance for understanding of abnormal atrial automaticity. *Circulation.* 1999;99(6):800-806.

47. Gittenberger-de Groot AC, Mahtab EA, Hahurij ND, Wisse LJ, Deruiter MC, Wijffels MC, Poelmann RE. Nkx2.5-negative myocardium of the posterior heart field and its correlation with podoplanin expression in cells from the developing cardiac pacemaking and conduction system. *Anat Rec.* 2007;290(1):115-122.

48. Jongbloed MR, Schalij MJ, Poelmann RE, Blom NA, Fekkes ML, Wang Z, Fishman GI, Gittenberger-de Groot AC. Embryonic conduction tissue: a spatial correlation with adult arrhythmogenic areas. *J Cardiovasc Electrophysiol.* 2004;15(3):349-355.

49. Kondo RP, Anderson RH, Kupershmidt S, Roden DM, Evans SM. Development of the cardiac conduction system as delineated by minK-lacZ. *J Cardiovasc Electrophysiol.* 2003;14(4):383-391.

50. Moskowitz IP, Kim JB, Moore ML, Wolf CM, Peterson MA, Shendure J, Nobrega MA, Yokota Y, Berul C, Izumo S, Seidman JG, Seidman CE. A molecular pathway including Id2, Tbx5, and Nkx2-5 required for cardiac conduction system development. *Cell.* 2007;129(7):1365-1376.

51. Watanabe M, Timm M, Fallah-Najmabadi H. Cardiac expression of polysialylated NCAM in the chicken embryo: correlation with the ventricular conduction system. *Dev Dyn.* 1992;194(2):128-141.

52. Jongbloed MR, Mahtab EA, Blom NA, Schalij MJ, Gittenberger-de Groot AC. Development of the cardiac conduction system and the possible relation to predilection sites of arrhythmogenesis. *ScientificWorldJournal.* 2008;8:239-269.

53. Snarr BS, O'Neal JL, Chintalapudi MR, Wirrig EE, Phelps AL, Kubalak SW, Wessels A. Isl1 expression at the venous pole identifies a novel role for the second heart field in cardiac development. *Circ Res.* 2007;101(10):971-974.

54. Lie-Venema H, van den Akker NM, Bax NA, Winter EM, Maas M, Kerarainen T, Hoeben RC, de Ruiter MC, Poelmann RE, Gittenberger-de Groot AC. Origin, fate and function of Epicardium-Derived-Cells (EPDCs) in normal and abnormal cardic development. *ScientificWorldJournal.* 2007;7:1777-1798.

55. Kruithof BP, van Wijk B, Somi S, Kruithof-de Julio M, Pérez Pomares JM, Weesie F, Wessels A, Moorman AF, van den Hoff MJ. BMP and FGF regulate the differentiation of multipotential pericardial mesoderm into the myocardial or epicardial lineage. *Dev Biol.* 2006;295(2):507-522.

56. Manasek FJ. Embryonic development of the heart. II. Formation of the epicardium. *J Embryol Exp Morphol.* 1969;22(3):333-348.

57. Ho E, Shimada Y. Formation of the epicardium studied with the scanning electron microscope. *Dev Biol.* 1978;66(2):579-585.

58. Hiruma T, Hirakow R. Epicardial formation in embryonic chick heart: computer-aided reconstruction, scanning, and transmission electron microscopic studies. *Am J Anat.* 1989;184(2):129-138.

59. Männer J. The development of pericardial villi in the chick embryo. *Anat Embryol.* 1992;186(4):379-385.

60. Virágh S, Challice CE. The origin of the epicardium and the embryonic myocardial circulation in the mouse. *Anat Rec.* 1981;201(1):157-168.

61. Vrancken Peeters MP, Mentink MM, Poelmann RE, Gittenberger-de Groot AC. Cytokeratins as a marker for epicardial formation in the quail embryo. *Anat Embryol.* 1995;191(6):503-508.

62. Männer J, Pérez-Pomares JM, Macías D, Muñoz-Chápuli R. The origin, formation and developmental significance of the epicardium: a review. *Cells Tissues Organs* 2001;169(2):89-103.

63. Schulte I, Schlueter J, Abu-Issa R, Brand T, Männer J. Morphological and molecular left-right asymmetries in the development of the proepicardium: a comparative analysis on mouse and chick embryos. *Dev Dyn.* 2007;236(3):684-695.

64. Lie-Venema H, Eralp I, Maas S, Gittenberger-de Groot AC, Poelmann RE, de Ruiter MC. Myocardial heterogeneity in permissiveness for epicardium-derived cells and endothelial precursor cells along the developing heart tube at the onset of coronary vascularization. *Anat Rec.* 2005;282(2):120-129.

65. Virágh S, Gittenberger-de Groot AC, Poelmann RE, Kálmán F. Early development of quail heart epicardium and associated vascular and glandular structures. *Anat Embryol.* 1993;188(4):381-393.

66. Vrancken Peeters MP, Gittenberger-de Groot AC, Mentink MM, Poelmann RE. Smooth muscle cells and fibroblasts of the coronary arteries derive from epithelial-mesenchymal transformation of the epicardium. *Anat Embryol.* 1999;199(4):367-378.

67. Pérez-Pomares JM, Carmona R, González-Iriarte M, Atencia G, Wessels A, Muñoz-Chápuli R. Origin of coronary endothelial cells from epicardial mesothelium in avian embryos. *Int J Dev Biol.* 2002;46(8):1005-1013.

68. Gittenberger-de Groot AC, Vrancken Peeters MP, Mentink MM, Gourdie RG, Poelmann RE. Epicardium-derived cells contribute a novel population to the myocardial wall and the atrioventricular cushions. *Circ Res.* 1998;82(10):1043-1052.

69. Poelmann RE, Gittenberger-de Groot AC, Mentink MM, Bökenkamp R, Hogers B. Development of the cardiac coronary vascular endothelium, studied with antiendothelial antibodies, in chicken-quail chimeras. *Circ Res.* 1993;73(3):559-568.

70. Männer J. Does the subepicardial mesenchyme contribute myocardioblasts to the myocardium of the chick embryo heart? A quail-chick chimera study tracing the fate of the epicardial primordium. *Anat Rec.* 1999;255(2):212-226.

71. Mikawa T, Gourdie RG. Pericardial mesoderm generates a population of coronary smooth muscle cells migrating into the heart along with ingrowth of the epicardial organ. *Dev Biol.* 1996;174(2):221-232.

72. Gittenberger-de Groot AC, Vrancken Peeters MP, Bergwerff M, Mentink MM, Poelmann RE. Epicardial outgrowth inhibition leads to compensatory mesothelial outflow tract collar and abnormal cardiac septation and coronary formation. *Circ Res.* 2000;87(11):969-971.

73. Kwee L, Baldwin HS, Shen HM, Stewart CL, Buck C, Buck CA, Labow MA. Defective development of the embryonic and extraembryonic circulatory systems in vascular cell adhesion molecule (VCAM-1) deficient mice. *Development.* 1995;121(2):489-503.

74. Yang JT, Rayburn H, Hynes RO. Cell adhesion events mediated by alpha 4 integrins are essential in placental and cardiac development. *Development.* 1995;121(2):549-560.

75. Lie-Venema H, Gittenberger-de Groot AC, van Empel LJ, Boot MJ, Kerkdijk H, de Kant E, de Ruiter MC. Ets-1 and Ets-2 transcription factors are essential for normal coronary and myocardial development in chicken embryos. *Circ Res.* 2003;92(7):749-756.

76. Eralp I, Lie-Venema H, de Ruiter MC, van den Akker NM, Bogers AJ, Mentink MM, Poelmann RE, Gittenberger-de Groot AC. Coronary artery and orifice development is associated with proper timing of epicardial outgrowth and correlated Fas-ligand-associated apoptosis patterns. *Circ Res.* 2005;96(5):526-534.

77. Eralp I, Lie-Venema H, Bax NA, Wijffels MC, van der Laarse A, de Ruiter MC, Bogers AJ, van den Akker NM, Gourdie RG, Schalij MJ, Poelmann RE, Gittenberger-de Groot AC. Epicardium-derived cells are important for correct development of the Purkinje fibers in the avian heart. *Anat Rec.* 2006;288(12):1272-1280.

78. Kastner P, Grondona JM, Mark M, Gansmuller A, LeMeur M, Decimo D, Vonesch JL, Dollé P, Chambon P. Genetic analysis of RXR alpha developmental function: convergence of RXR and RAR signaling pathways in heart and eye morphogenesis. *Cell.* 1994;78(6):987-1003.

79. Männer J, Schlueter J, Brand T. Experimental analyses of the function of the proepicardium using a new microsurgical procedure to induce loss-of-proepicardial-function in chick embryos. *Dev Dyn.* 2005;233(4):1454-1463.

80. Merki E, Zamora M, Raya A, Kawakami Y, Wang J, Zhang X, Burch J, Kubalak SW, Kaliman P, Belmonte JC, Chien KR, Ruiz-Lozano P. Epicardial retinoid X receptor alpha is required for myocardial growth and coronary artery formation. *Proc Natl Acad Sci USA.* 2005;102(51):18455-18460.

81. Sucov HM, Dyson E, Gumeringer CL, Price J, Chien KR, Evans RM. RXR alpha mutant mice establish a genetic basis for vitamin A signaling in heart morphogenesis. *Genes Dev.* 1994;8(9):1007-1018.

82. Tevosian SG, Deconinck AE, Tanaka M, Schinke M, Litovsky SH, Izumo S, Fujiwara Y, Orkin SH. FOG-2, a cofactor for GATA transcription factors, is essential for heart morphogenesis and development of coronary vessels from epicardium. *Cell.* 2000;101(7):729-739.

83. Watt AJ, Battle MA, Li J, Duncan SA. GATA4 is essential for formation of the proepicardium and regulates cardiogenesis. *Proc Natl Acad Sci USA.* 2004;101(34):12573-12578.

84. Erickson CA, Reedy MV. Neural crest development: the interplay between morphogenesis and cell differentiation. *Curr Top Dev Biol.* 1998;40:177-209.

85. Huang X, Saint-Jeannet JP. Induction of the neural crest and the opportunities of life on the edge. *Dev Biol.* 2004;275(1):1-11.

86. Kulesa P, Ellies DL, Trainor PA. Comparative analysis of neural crest cell death, migration, and function during vertebrate embryogenesis. *Dev Dyn.* 2004;229(1):14-29.

87. Poelmann RE, Mikawa T, Gittenberger-de Groot AC. Neural crest cells in outflow tract septation of the embryonic chicken heart: differentiation and apoptosis. *Dev Dyn.* 1998;212:373-384.

88. Bergwerff M, Verberne ME, de Ruiter MC, Poelmann RE, Gittenberger-de Groot AC. Neural crest cell contribution to the developing circulatory system: implications for vascular morphology? *Circ Res.* 1998;82(2):221-231.

89. Bartelings MM, Gittenberger-de Groot AC. The outflow tract of the heart--embryologic and morphologic correlations. *Int J Cardiol.* 1989;22(3):289-300.

90. Bockman DE, Kirby ML. Dependence of thymus development on derivatives of the neural crest. *Science.* 1984;223(4635):498-500.

91. Boot MJ, Steegers-Theunissen RP, Poelmann RE, van Iperen L, Gittenberger-de Groot AC. Cardiac outflow tract malformations in chick embryos exposed to homocysteine. *Cardiovasc Res.* 2004;64(2):365-373.

92. Farrell M, Waldo K, Li YX, Kirby ML. A novel role for cardiac neural crest in heart development. *Trends Cardiovasc Med.* 1999;9(7):214-220.

93. Firulli AB, Conway SJ. Combinatorial transcriptional interaction within the cardiac neural crest: a pair of HANDs in heart formation. *Birth Defects Res Part C Embryo Today.* 2004;72(2):151-161.

94. Hood LC, Rosenquist TH. Coronary artery development in the chick: origin and deployment of smooth muscle cells, and the effects of neural crest ablation. *Anat Rec.* 1992;234(2):291-300.

95. Kirby ML, Waldo KL. Neural crest and cardiovascular patterning. *Circ Res.* 1995;77(2):211-215.

96. Li WE, Waldo K, Linask KL, Chen T, Wessels A, Parmacek MS, Kirby ML, Lo CW. An essential role for connexin43 gap junctions in mouse coronary artery development. *Development.* 2002;129(8):2031-2042.

97. Verberne ME, Gittenberger-de Groot AC, Poelmann RE. Lineage and development of the parasympathetic nervous system of the embryonic chick heart. *Anat Embryol.* 1998;198(3):171-184.

98. Komatsu K, Wakatsuki S, Yamada S, Yamamura K, Miyazaki J, Sehara-Fujisawa A. Meltrin beta expressed in cardiac neural crest cells is required for ventricular septum formation of the heart. *Dev Biol.* 2007;303(1):82-92.

99. Poelmann RE, Gittenberger-de Groot AC. A subpopulation of apoptosis-prone cardiac neural crest cells targets to the venous pole: multiple functions in heart development? *Dev Biol.* 1999;207(2):271-286.

100. Poelmann RE, Molin D, Wisse LJ, Gittenberger-de Groot AC. Apoptosis in cardiac development. *Cell Tissue Res.* 2000;301(1):43-52.

101. Gittenberger-de Groot AC, Blom NM, Aoyama N, Sucov H, Wenink AC, Poelmann RE. The role of neural crest and epicardium-derived cells in conduction system formation. *Novartis Found Symp.* 2003;250:125-134; discussion 134-141, 276-129.

102. Poelmann RE, Jongbloed MR, Molin DG, Fekkes ML, Wang Z, Fishman GI, Doetschman T, Azhar M, Gittenberger-de Groot AC. The neural crest is contiguous with the cardiac conduction system in the mouse embryo: a role in induction? *Anat Embryol.* 2004;208(5):389-393.

103. Gurjarpadhye A, Hewett KW, Justus C, Wen X, Stadt H, Kirby ML, Sedmera D, Gourdie RG. Cardiac neural crest ablation inhibits compaction and electrical function of conduction system bundles. *Am J Physiol Heart Circ Physiol.* 2007;292(3):H1291-1300.

104. Hirota A, Fujii S, Kamino K. Optical monitoring of spontaneous electrical activity of 8-somite embryonic chick heart. *Jpn J Physiol.* 1979;29(5):635-639.

105. Kamino K, Hirota A, Fujii S. Localization of pacemaking activity in early embryonic heart monitored using voltage-sensitive dye. *Nature.* 1981;290(5807):595-597.

106. Kamino K, Komuro H, Sakai T. Regional gradient of pacemaker activity in the early embryonic chick heart monitored by multisite optical recording. *J Physiol* 1988;402:301-314.

107. Van Mierop LH. Location of pacemaker in chick embryo heart at the time of initiation of heartbeat. *Am J Physiol.* 1967;212(2):407-415.

108. Johnstone PN. Studies on the physiological anatomy of the embryonic heart. I. The demonstration of complete heart block in chick embryos during the second, third, and fourth days of incubation. *Bull Johns Hopkins Hospital.* 1924;35:87.

109. Johnstone PN. Studies on the physiological anatomy of the embryonic heart. II. An inquiry into the development of the heart beat in chick embryos, including the development of irritatability to electrical stimulation. *Bull Johns Hopkins Hospital.* 1925;35:299.

110. Sabin FR. Studies on the origin of blood-vessels and of red blood-corpuscles as seen in the living blastoderm of chicks during the second day of incubation. *Contrib Embryol.* 1920;9:213-262.

111. Patten BM. The initiation of contraction in the embronic chick heart. *Am J Anat.* 1933;53(3):349-375.

112. Barry A. Intrinsic pulsation rates of fragments of embryonic chick heart. *J Exp Zool.* 1942;91:119-130.

113. Satin J, Fujii S, DeHaan RL. Development of cardiac beat rate in early chick embryos is regulated by regional cues. *Dev Biol.* 1988;129(1):103-113.

114. de Haan H. Cardia bifida and the development of pacemaker function in the early chick heart. *Dev Biol.* 1959;1:586-602.

115. Goss CM. The physiology of the embryonic mammalian heart before circulation. *Am J Physiol.* 1942;137:146-152.

116. Hirota A, Kamino K, Komuro H, Sakai T, Yada T. Early events in development of electrical activity and contraction in embryonic rat heart assessed by optical recording. *J Physiol* 1985;369:209-227.

117. Sakai T, Hirota A, Fujii S, Kamino K. Flexibility of regional pacemaking priority in early embryonic heart monitored by simultaneous optical recording of action potentials from multiple sites. *Jpn J Physiol.* 1983;33(3):337-350.

118. de Haan H. *Spiegel Historiael.* 1980;15(10):554-560.

119. Moorman AF, Christoffels VM, Anderson RH. Anatomic substrates for cardiac conduction. *Heart Rhythm* 2005;2(8):875-886.

120. Moorman AF, de Jong F, Denyn MM, Lamers WH. Development of the cardiac conduction system. *Circ Res.* 1998;82(6):629-644.

121. Galper JB, Smith TW. Properties of muscarinic acetylcholine receptors in heart cell cultures. *Proc Natl Acad Sci USA.* 1978;75(12):5831-5835.

122. Sperelakis N. Developmental changes in membrane electrical properties of the heart. In: Sperelakis N, ed. *Physiol Pathophysiol Heart*. The Hague, The Netherlands: Martinus-Nijhoff; 1984:543-573.

123. Wobus AM, Rohwedel J, Maltsev V, Hescheler J. Development of cardiomyocytes expressing cardiac-specific genes, action potentials, and ionic channels during embryonic stem cell-derived cardiogenesis. *Ann N Y Acad Sci.* 1995;752:460-469.

124. de Jong F, Opthof T, Wilde AA, Janse MJ, Charles R, Lamers WH, Moorman AF. Persisting zones of slow impulse conduction in developing chicken hearts. *Circ Res.* 1992;71(2):240-250.

125. Lieberman M, Paes de Carvalho, A. The electrophysiological organization of the embryonic chick heart. *J Gen Physiol.* 1965;49:365-379.

126. Lieberman M, Paes de Carvalho, A. The spread of excitation in the embryonic chick heart. *J Gen Physiol.* 1965;49:365-379.

127. Gourdie RG, Harris BS, Bond J, Justus C, Hewett KW, O'Brien TX, Thompson RP, Sedmera D. Development of the cardiac pacemaking and conduction system. *Birth Defects Res Part C Embryo Today.* 2003;69(1):46-57.

128. Hoff EC, Kramer, T.C., Dubois, D., Patten, B.M. The development of the electrocardiogram of the embryonic heart. *Am Heart J.* 1939;17:471-488.

129. Robb JS. The elemental character of embryonic electrocardiograms. *Am J Physiol.* 1929;90:496.

130. Galper JB, Catterall WA. Developmental changes in the sensitivity of embryonic heart cells to tetrodotoxin and D600. *Dev Biol.* 1978;65(1):216-227.

131. Argüello C, Alanís J, Pantoja O, Valenzuela B. Electrophysiological and ultrastructural study of the atrioventricular canal during the development of the chick embryo. *J Mol Cell Cardiol.* 1986;18(5):499-510.

132. Clemo HF, Belardinelli L. Effect of adenosine on atrioventricular conduction. I: Site and characterization of adenosine action in the guinea pig atrioventricular node. *Circ Res.* 1986;59(4):427-436.

133. McGuire MA, de Bakker JM, Vermeulen JT, Moorman AF, Loh P, Thibault B, Vermeulen JL, Becker AE, Janse MJ. Atrioventricular junctional tissue. Discrepancy between histological and electrophysiological characteristics. *Circulation.* 1996;94(3):571-577.

134. Oosthoek PW, Virágh S, Mayen AE, van Kempen MJ, Lamers WH, Moorman AF. Immunohistochemical delineation of the conduction system. I: The sinoatrial node. *Circ Res.* 1993;73(3):473-481.

135. Alcoléa S, Théveniau-Ruissy M, Jarry-Guichard T, Marics I, Tzouanacou E, Chauvin JP, Briand JP, Moorman AF, Lamers WH, Gros DB. Downregulation of connexin 45 gene products during mouse heart development. *Circ Res.* 1999;84(12):1365-1379.

136. Coppen SR, Kodama I, Boyett MR, Dobrzynski H, Takagishi Y, Honjo H, Yeh HI, Severs NJ. Connexin45, a major connexin of the rabbit sinoatrial node, is co-expressed with connexin43 in a restricted zone at the nodal-crista terminalis border. *J Histochem Cytochem.* 1999;47(7):907-918.

137. de la Cruz MV, Castillo MM, Villavicencio L, Valencia A, Moreno-Rodriguez RA. Primitive interventricular septum, its primordium, and its contribution in the definitive interventricular septum: in vivo labelling study in the chick embryo heart. *Anat Rec.* 1997;247(4):512-520.

138. Sedmera D, Reckova M, Bigelow MR, deAlmeida A, Stanley CP, Mikawa T, Gourdie RG, Thompson RP. Developmental transitions in electrical activation patterns in chick embryonic heart. *Anat Rec.* 2004;280(2):1001-1009.

139. Rentschler S, Morley GE, Fishman GI. Molecular and functional maturation of the murine cardiac conduction system. *Cold Spring Harb Symp Quant Biol.* 2002;67:353-361.

140. Hait G, Licata RH. Sequence of atrial depolarization at different stages of development of the chick embryo. *Circ Res.* 1967;20(2):204-213.

141. Kamino K, Komuro H, Sakai T, Hirota A. Functional pacemaking area in the early embryonic chick heart assessed by simultaneous multiple-site optical recording of spontaneous action potentials. *J Gen Physiol.* 1988;91(4):573-591.

142. Lamers WH, de Jong F, De Groot IJ, Moorman AF. The development of the avian conduction system, a review. *Eur J Morphol.* 1991;29(4):233-253.

143. Patten BM. The development of the sinoventricular conduction system. *Medical Bulletin* 1956;22(1):1-21.

144. Argüello C, Alanis J, Valenzuela B. The early development of the atrioventricular node and bundle of His in the embryonic chick heart. An electrophysiological and morphological study. *Development.* 1988;102(3):623-637.

145. Kubo Y, Reuveny E, Slesinger PA, Jan YN, Jan LY. Primary structure and functional expression of a rat G-protein-coupled muscarinic potassium channel. *Nature.* 1993;364(6440):802-806.

146. de la Cruz MV, Giménez-Ribotta M, Saravalli O, Cayré R. The contribution of the inferior endocardial cushion of the atrioventricular canal to cardiac septation and to the development of the atrioventricular valves: study in the chick embryo. *Am J Anat.* 1983;166(1):63-72.

147. Waldo K, Miyagawa-Tomita S, Kumiski D, Kirby ML. Cardiac neural crest cells provide new insight into septation of the cardiac outflow tract: aortic sac to ventricular septal closure. *Dev Biol.* 1998;196(2):129-144.

148. Keith A, Flack M. The Form and Nature of the Muscular Connections between the Primary Divisions of the Vertebrate Heart. *J Anat Physiol.* 1907;41(Pt 3):172-189.

149. Tawara S. Das reizleitungssystem des saugetierherzens. Eine anatomisch-histologische studie uber das atrioventrikularbundel und die Purkinjeschen faden. Verslag von Gustav Fischer; 1906.

150. Gorza L, Schiaffino S, Vitadello M. Heart conduction system: a neural crest derivative? *Brain Res.* 1988;457(2):360-366.

151. Gorza L, Vitadello M. Distribution of conduction system fibers in the developing and adult rabbit heart revealed by an antineurofilament antibody. *Circ Res.* 1989;65(2):360-369.

152. Vitadello M, Colpo P, Gorza L. Rabbit cardiac and skeletal myocytes differ in constitutive and inducible expression of the glucose-regulated protein GRP94. *Biochem J.* 1998;332 (Pt 2):351-359.

153. Vitadello M, Matteoli M, Gorza L. Neurofilament proteins are co-expressed with desmin in heart conduction system myocytes. *J Cell Sci.* 1990;97 (Pt 1):11-21.

154. Gourdie RG, Mima T, Thompson RP, Mikawa T. Terminal diversification of the myocyte lineage generates Purkinje fibers of the cardiac conduction system. *Development.* 1995;121(5):1423-1431.

155. Gourdie RG, Harris, B.S., Bond, J., Edmondson, A.M., Cheng, G., Sedmera, D., O'Brien, T.X., Mikawa, T., Thompson, R.P. His-Purkinje lineage and development. *Novartis Found Symp.* 2003;250:110-122.

156. Anderson RH, Taylor, I.M. Development of the atrioventricular specialized issue in human heart. *Br Heart J.* 1972;34(12):1205-1214.

157. Benninghof A. Uber die beziehungen des reitzleitungssystem und der papillarmuskeln zu der konturfasern des herzschlauches. *Anatomischer Anzeicher* 1923;57:185-208.

158. Wenink AC. Development of the human cardiac conducting system. *J Anat.* 1976;121(Pt 3):617-631.

159. Canale ED, Campbell, G.R., Smolich, J.J., Campbell, J.H. *Cardic Muscle*. Berlin, Germany: Spinger Verslag; 1986.

160. Virágh S, Challice CE. The development of the conduction system in the mouse embryo heart. *Dev Biol.* 1980;80(1):28-45.

161. Virágh S, Porte A. The fine structure of the conducting system of the monkey heart (Macaca mulatta). I. The sino-atrial node and the internodal connections. *Zeitschrift für Zellforschung und mikroskopische Anatomie* 1973;145(2):191-211.

162. Virágh SZ, Porte A. On the impulse conducting system of the monkey heart (Macaca mulatta). II. The atrio-ventricular node and bundle. *Zeitschrift für Zellforschung und mikroskopische Anatomie* 1973;145(3):363-388.

163. Monckebreg JG. Beitrage zur normalen und pathologischen anatomie des herzens. *Verh Disch Pathol Ges.* 1910;14:64-71.

164. Rentschler S, Morley GE, Fishman GI. Patterning of the mouse conduction system. *Novartis Found Symp.* 2003;250:194-205; discussion 205-199, 276-199.

165. Callewaert G, Vereecke J, Carmeliet E. Existence of a calcium-dependent potassium channel in the membrane of cow cardiac Purkinje cells. *Pflugers Arch.* 1986;406(4):424-426.

166. Kaupp UB, Seifert R. Molecular diversity of pacemaker ion channels. *Annu Rev Physiol.* 2001;63:235-257.

167. Kupershmidt S, Yang T, Anderson ME, Wessels A, Niswender KD, Magnuson MA, Roden DM. Replacement by homologous recombination of the minK gene with lacZ reveals restriction of minK expression to the mouse cardiac conduction system. *Circ Res.* 1999;84(2):146-152.

168. Coppen SR, Severs NJ, Gourdie RG. Connexin45 (alpha 6) expression delineates an extended conduction system in the embryonic and mature rodent heart. *Dev Genet.* 1999;24(1-2):82-90.

169. Gourdie RG. A map of the heart: gap junctions, connexin diversity and retroviral studies of conduction myocyte lineage. *Clin Sci.* 1995;88(3):257-262.

170. Gourdie RG. Connexin diversity in the human conduction system. *J Cardiovasc Electrophysiol.* 1996;7(4):382-383.

171. Gourdie RG, Cheng G, Thompson RP, Mikawa T. Retroviral cell lineage analysis in the developing chick heart. *Methods Mol Biol.* 2000;135:297-304.

172. Gros DB, Jongsma HJ. Connexins in mammalian heart function. *Bioessays.* 1996;18(9):719-730.

173. Alyonycheva T, Cohen-Gould L, Siewert C, Fischman DA, Mikawa T. Skeletal muscle-specific myosin binding protein-H is expressed in Purkinje fibers of the cardiac conduction system. *Circ Res.* 1997;80(5):665-672.

174. Welikson RE, Fischman DA. The C-terminal IgI domains of myosin-binding proteins C and H (MyBP-C and MyBP-H) are both necessary and sufficient for the intracellular crosslinking of sarcomeric myosin in transfected non-muscle cells. *J Cell Sci.* 2002;115(Pt 17):3517-3526.

175. Davis DL, Edwards AV, Juraszek AL, Phelps A, Wessels A, Burch JB. A GATA-6 gene heart-region-specific enhancer provides a novel means to mark and probe a discrete component of the mouse cardiac conduction system. *Mech Dev.* 2001;108(1-2):105-119.

176. Pennisi DJ, Rentschler S, Gourdie RG, Fishman GI, Mikawa T. Induction and patterning of the cardiac conduction system. *Int J Dev Biol.* 2002;46(6):765-775.

177. Gassanov N, Er F, Zagidullin N, Hoppe UC. Endothelin induces differentiation of ANP-EGFP expressing embryonic stem cells towards a pacemaker phenotype. *FASEB J.* 2004;18(14):1710-1712.

178. Gourdie RG, Wei Y, Kim D, Klatt SC, Mikawa T. Endothelin-induced conversion of embryonic heart muscle cells into impulse-conducting Purkinje fibers. *Proc Natl Acad Sci USA.* 1998;95(12):6815-6818.

179. Hall CE, Hurtado R, Hewett KW, Shulimovich M, Poma CP, Reckova M, Justus C, Pennisi DJ, Tobita K, Sedmera D, Gourdie RG, Mikawa T. Hemodynamic-dependent patterning of endothelin converting enzyme 1 expression and differentiation of impulse-conducting Purkinje fibers in the embryonic heart. *Development.* 2004;131(3):581-592.

180. Kanzawa N, Poma CP, Takebayashi-Suzuki K, Diaz KG, Layliev J, Mikawa T. Competency of embryonic cardiomyocytes to undergo Purkinje fiber differentiation is regulated by endothelin receptor expression. *Development.* 2002;129(13):3185-3194.

181. Patel R, Kos L. Endothelin-1 and Neuregulin-1 convert embryonic cardiomyocytes into cells of the conduction system in the mouse. *Dev Dyn.* 2005;233(1):20-28.

182. Takebayashi-Suzuki K, Yanagisawa M, Gourdie RG, Kanzawa N, Mikawa T. In vivo induction of cardiac Purkinje fiber differentiation by coexpression of preproendothelin-1 and endothelin converting enzyme-1. *Development.* 2000;127(16):3523-3532.

183. Milan DJ, Giokas AC, Serluca FC, Peterson RT, MacRae CA. Notch1b and neuregulin are required for specification of central cardiac conduction tissue. *Development.* 2006;133(6):1125-1132.

184. Bond J, Sedmera D, Jourdan J, Zhang Y, Eisenberg CA, Eisenberg LM, Gourdie RG. Wnt11 and Wnt7a are up-regulated in association with differentiation of cardiac conduction cells in vitro and in vivo. *Dev Dyn.* 2003;227(4):536-543.

185. Chan-Thomas PS, Thompson RP, Robert B, Yacoub MH, Barton PJ. Expression of homeobox genes Msx-1 (Hox-7) and Msx-2 (Hox-8) during cardiac development in the chick. *Dev Dyn.* 1993;197(3):203-216.

186. Jay PY, Harris BS, Maguire CT, Buerger A, Wakimoto H, Tanaka M, Kupershmidt S, Roden DM, Schultheiss TM, O'Brien TX, Gourdie RG, Berul CI, Izumo S. Nkx2-5 mutation causes anatomic hypoplasia of the cardiac conduction system. *J Clin Invest.* 2004;113(8):1130-1137.

187. Pashmforoush M, Lu JT, Chen H, Amand TS, Kondo R, Pradervand S, Evans SM, Clark B, Feramisco JR, Giles W, Ho SY, Benson DW, Silberbach M, Shou W, Chien KR. Nkx2-5 pathways and congenital heart disease; loss of ventricular myocyte lineage specification leads to progressive cardiomyopathy and complete heart block. *Cell.* 2004;117(3):373-386.

188. Schott JJ, Benson DW, Basson CT, Pease W, Silberbach GM, Moak JP, Maron BJ, Seidman CE, Seidman JG. Congenital heart disease caused by mutations in the transcription factor NKX2-5. *Science.* 1998;281(5373):108-111.

189. Ismat FA, Zhang M, Kook H, Huang B, Zhou R, Ferrari VA, Epstein JA, Patel VV. Homeobox protein Hop functions in the adult cardiac conduction system. *Circ Res.* 2005;96(8):898-903.

190. Bakker ML. Transcription factor Tbx3 is required for the specification of the atrioventricular conduction system. *Circ Res.* 2008;102(11):1340-1349.

191. Bruneau BG, Logan M, Davis N, Levi T, Tabin CJ, Seidman JG, Seidman CE. Chamber-specific cardiac expression of Tbx5 and heart defects in Holt-Oram syndrome. *Dev Biol.* 1999;211(1):100-108.

192. Christoffels VM, Burch JB, Moorman AF. Architectural plan for the heart: early patterning and delineation of the chambers and the nodes. *Trends Cardiovasc Med.* 2004;14(8):301-307.

193. Moskowitz IP, Pizard A, Patel VV, Bruneau BG, Kim JB, Kupershmidt S, Roden D, Berul CI, Seidman CE, Seidman JG. The T-Box transcription factor Tbx5 is required for the patterning and maturation of the murine cardiac conduction system. *Development.* 2004;131(16):4107-4116.

194. de Groot IJM, Wessels A, Viragh S, Lamers WH, Moorman AFM. The relation between isomyosin heavy chain expression pattern and the architecture of sinoatrial nodes in chicken, rat and hman embryos. In: U C, ed. *Sarcomeric and non-sarcomeric muscles: basic and applied research prospects for the 90s*. Padova, Italy: Unipress; 1988:305-310.

195. Moorman AF, Soufan AT, Hagoort J, de Boer PA, Christoffels VM. Development of the building plan of the heart. *Ann N Y Acad Sci.* 2004;1015:171-181.

196. Mikawa T, Hurtado R. Development of the cardiac conduction system. *Semin Cell Dev Biol.* 2007;18(1):90-100.

197. Yasui K, Liu W, Opthof T, Kada K, Lee JK, Kamiya K, Kodama I. I(f) current and spontaneous activity in mouse embryonic ventricular myocytes. *Circ Res.* 2001;88(5):536-542.

198. Schulze-Bahr E, Neu A, Friederich P, Kaupp UB, Breithardt G, Pongs O, Isbrandt D. Pacemaker channel dysfunction in a patient with sinus node disease. *J Clin Invest.* 2003;111(10):1537-1545.

199. Ueda K, Nakamura K, Hayashi T, Inagaki N, Takahashi M, Arimura T, Morita H, Higashiuesato Y, Hirano Y, Yasunami M, Takishita S, Yamashina A, Ohe T, Sunamori M, Hiraoka M, Kimura A. Functional characterization of a trafficking-defective HCN4 mutation, D553N, associated with cardiac arrhythmia. *J Biol Chem.* 2004;279(26):27194-27198.

200. James TN. The connecting pathways between the sinus node and A-V node end between the right and left atrium in the human heart. . *Am Heart J.* 1963;66:498-508.

201. James TN. The internodal pathways of the human heart. *Prog Cardiovasc Dis.* 2001;43(6):495-535.

202. Sherf L, James, T.N. Fine structure of cells and their histologic organization within intranodal pathways of the heart: clinical and electrcardiographic implications. *Am J Cardiol.* 1979;44(2):345-369.

203. Spach MS, Kootsey JM. The nature of electrical propagation in cardiac muscle. *Am J Physiol.* 1983;244(1):H3-22.

204. Anderson RH, Ho SY, Becker AE. Anatomic boundaries between the atrioventricular node and the atrioventricular bundle. *J Cardiovasc Electrophysiol.* 1998;9(2):225-228.

205. Virágh S, Challice CE. The development of the conduction system in the mouse embryo heart. II. Histogenesis of the atrioventricular node and bundle. *Dev Biol.* 1977;56(2):397-411.

206. Walls EW. The development of the specialized conducting tissue of the human heart. *J Anat.* 1947;81:91-110.

207. Anderson RH, Becker AE, Brechenmacher C, Davies MJ, Rossi L. The human atrioventricular junctional area. A morphological study of the A-V node and bundle. *Eur J Cardiol.* 1975;3(1):11-25.

208. Anderson RH, Janse MJ, van Capelle FJ, Billette J, Becker AE, Durrer D. A combined morphological and electrophysiological study of the atrioventricular node of the rabbit heart. *Circ Res.* 1974;35(6):909-922.

209. Janse MJ, Anderson RH, McGuire MA, Ho SY. "AV nodal" reentry: Part I: "AV nodal" reentry revisited. *J Cardiovasc Electrophysiol.* 1993;4(5):561-572.

210. Meijler FL, Janse MJ. Morphology and electrophysiology of the mammalian atrioventricular node. *Physiol Rev.* 1988;68(2):608-647.

211. Zipes DP, Mendez C, Moe GK. Evidence for summation and voltage dependency in rabbit atrioventricular nodal fibers. *Circ Res.* 1973;32(2):170-177.

212. de Haan H. Differentiation of the atrioventricular conducting system of the heart. *Circulation.* 1961;24:458-470.

213. His W. Die Tatigkeit des embryonalen Herzens und deren Bedcutung fur die Lehre von der Herzbewegung beim Menschen. *Arbeiten aus der mediziischen klinik zu Leipzig.* 1893:23.

214. Viragh S, Challice CE. The development of the conduction system in the mouse embryo heart. I. The first embryonic A-V conduction pathway. *Dev Biol.* 1977;56:382-396.

215. Retzer R. The anatomy of the conductive system in the mammalian heart. *Bull Johns Hopkins Hospital.* 1908;19:208-215.

216. Shaner RF. The development of the atrioventricular node, bundle of His and sinoatrial node in the calf, with a description of a third embryonic node-like structure. *Anat Rec.* 1929;44:85-99.

217. Tandler J. The development of the human heart. In: Kiebel F, Mall, F.P., ed. *Manual of human embryology.* Vol 2. Mexico: J.B. Lippincott; 1912.

218. Field EJ. The development of the conducting system in the heart of sheep. *Br Heart J.* 1951;13(2):129-147.

219. Muir AR. The development of the ventricular part of the conducting tissue in the heart of the sheep. *J Anat.* 1954;88(3):381-391.

220. Navartnam V. The ontogenesis of cholinesterase activity within the heart and cardiac ganglia in man, rat and guinea-pig. *J Anat.* 1965;99:459-467.

221. Anderson RH, Becker AE, Wilkinson JL, Gerlis LM. Morphogenesis of univentricular hearts. *Br Heart J.* 1976;38(6):558-572.

222. Anderson RH, Wenick AC, Losekoot TG, Becker AE. Congenitally complete heart block. Developmental aspects. *Circulation.* 1977;56(1):90-101.

223. Purkinje JE. Mikroskopisch-neurologische beobachtunghen. *Arch Anat Physiol Wiss Med.* 1845;12:281-295.

224. Dangman KH, Danilo P, Hordof AJ, Mary-Rabine L, Reder RF, Rosen MR. Electrophysiologic characteristics of human ventricular and Purkinje fibers. *Circulation.* 1982;65(2):362-368.

225. Davies F. The Conducting System of the Bird's Heart. *J Anat.* 1930;64(Pt 2):129-146.127.

226. Vassall-Adams PR. The developing atrioventricular bundle and its branches in relation to small induced ventricular septal defects in the heart of chick embryos. *J Anat.* 1982;134(Pt 2):209-214.

227. Reckova M, Rosengarten C, deAlmeida A, Stanley CP, Wessels A, Gourdie RG, Thompson RP, Sedmera D. Hemodynamics is a key epigenetic factor in development of the cardiac conduction system. *Circ Res.* 2003;93(1):77-85.

228. Bogue JY. The heart rate of the developing chick. *J Exp Biol.* 1932;9:351.

229. Bogue JY. The electrocardiogram of the developing chick. *J Exp Biol.* 1933;10:286-292.

230. Paff GH, Boucek RJ, Harrell TC. Observations on the development of the electrocardiogram. *Anat Rec.* 1968;160(3):575-582.

231. Seidl W, Schulze, M., Steding, G., Kluth, D. A few remarks on the physiology of the chick embryo heart. *Folia morphologica.* 1981;29(3):237-242.

232. Boucek RJ, Murphy WP, Paff GH. Electrical and mechanical properties of chick embryo heart chambers. *Circ Res.* 1959;7:787-793.

233. Heard JD. Electrocardiograms derived from eleven fetuses through the medium of direct leads. *Am Heart J.* 1936;11:41-48.

234. Marcel MP, Exchaquet, J.P. L'electrocardiogramme du foetus human. *Arch Ml Coeur.* 1938;1:52.

235. Sedmera D, Reckova M, Rosengarten C, Torres MI, Gourdie RG, Thompson RP. Optical mapping of electrical activation in the developing heart. *Microsc Microanal.* 2005;11(3):209-215.

236. Watanabe M, Chuck ET, Rothenberg F, Rosenbaum DS. Developmental transitions in cardiac conduction. *Novartis Found Symp.* 2003;250:68-75; discussion 76-69, 276-279.

237. Chuck ET, Watanabe M. Differential expression of PSA-NCAM and HNK-1 epitopes in the developing cardiac conduction system of the chick. *Dev Dyn.* 1997;209(2):182-195.

238. Arbel ER, Liberthseon, R., Langendorf, R., Pick, A., Lev, M., Fishman, A.P. Electrophysiological and anatomical observation on the heart of the African lungfish. *Am J Physiol.* 1977;232(1):24-34.

239. Christian E, Grigg GE. Electrical activation of the ventricular myocardium of the crocodylus johnstoni: a combined microscopic and electrophysiological study. *Comp Biochem Physiol A Mol Integr.* 1999;123(1):17-23.

240. Dillon S, Morad M. A new laser scanning system for measuring action potential propagation in the heart. *Science.* 1981;214(4519):453-456.

241. Randall DJ. The circulatory system. In: Hoar WS, Randall, D.J., ed. *Fish Physiology*. New York: Academic Press; 1970.

242. Rothenberg F, Watanabe M, Eloff B, Rosenbaum D. Emerging patterns of cardiac conduction in the chick embryo: waveform analysis with photodiode array-based optical imaging. *Dev Dyn.* 2005;233(2):456-465.

243. Kim JS, Virágh S, Moorman AF, Anderson RH, Lamers WH. Development of the myocardium of the atrioventricular canal and the vestibular spine in the human heart. *Circ Res.* 2001;88(4):395-402.

244. Wenink AC, Gittenberger-de Groot AC. Embryology of the mitral valve. *Int J Cardiol.* 1986;11(1):75-84.

245. Wessels A, Markman MW, Vermeulen JL, Anderson RH, Moorman AF, Lamers WH. The development of the atrioventricular junction in the human heart. *Circ Res.* 1996;78(1):110-117.

246. Norris RA, Kern CB, Wessels A, Moralez EI, Markwald RR, Mjaatvedt CH. Identification and detection of the periostin gene in cardiac development. *Anat Rec.* 2004;281(2):1227-1233.

247. Gaussin V, Morley GE, Cox L, Zwijsen A, Vance KM, Emile L, Tian Y, Liu J, Hong C, Myers D, Conway SJ, Depre C, Mishina Y, Behringer RR, Hanks MC, Schneider MD, Huylebroeck D, Fishman GI, Burch JB, Vatner SF. Alk3/Bmpr1a receptor is required for development of the atrioventricular canal into valves and annulus fibrosus. *Circ Res.* 2005;97(3):219-226.

248. Hahurij ND, Gittenberger-de Groot AC, Kolditz DP, Bokenkamp R, Schalij MJ, Poelmann RE, Blom NA. Accessory atrioventricular myocardial connections in the developing human heart: relevance for perinatal supraventricular tachycardia. *Circulation.* 2008;117(22):2850-2858.

249. Kolditz DP, Wijffels MC, Blom NA, van der Laarse A, Markwald RR, Schalij MJ, Gittenberger-de Groot AC. Persistence of functional atrioventricular accessory pathways in postseptated embryonic avian hearts: implications for morphogenesis and functional maturation of the cardiac conduction system. *Circulation.* 2007;115(1):17-26.

250. Kruzynska-Frejtag A, Machnicki M, Rogers R, Markwald RR, Conway SJ. Periostin (an osteoblast-specific factor) is expressed within the embryonic mouse heart during valve formation. *Mech Dev.* 2001;103(1-2):183-188.

251. Kolditz DP, Wijffels MC, Blom NA, van der Laarse A, Hahurij ND, Lie-Venema H, Markwald RR, Poelmann RE, Schalij MJ, Gittenberger-De Groot AC. Epicardium-Derived Cells in Development of Annulus Fibrosis and Persistence of Accessory Pathways. *Circulation.* 2008;117(12):1508-1517.

252. van Gils FA. The fibrous skeleton in the human heart: embryological and pathogenetic considerations. *Virchows Archiv A, Pathological anatomy and histology.* 1981;393(1):61-73.

253. Rentschler S, Vaidya DM, Tamaddon H, Degenhardt K, Sassoon D, Morley GE, Jalife J, Fishman GI. Visualization and functional characterization of the developing murine cardiac conduction system. *Development.* 2001;128(10):1785-1792.

254. Becker AE, Anderson RH, Durrer D, Wellens HJ. The anatomical substrates of wolff-parkinson-white syndrome. A clinicopathologic correlation in seven patients. *Circulation.* 1978;57(5):870-879.

255. James TN. Normal and abnormal consequences of apoptosis in the human heart. From postnatal morphogenesis to paroxysmal arrhythmias. *Circulation.* 1994;90(1):556-573.

256. Klein GJ, Hackel DB, Gallagher JJ. Anatomic substrate of impaired antegrade conduction over an accessory atrioventricular pathway in the Wolff-Parkinson-White syndrome. *Circulation.* 1980;61(6):1249-1256.

257. Ohnell RF. Pre-excitation, a cardiac abnormality. *Acta Med Scand.* 1944;52:1-167.

258. Peters NS, Rowland E, Bennett JG, Green CR, Anderson RH, Severs NJ. The Wolff-Parkinson-White syndrome: the cellular substrate for conduction in the accessory atrioventricular pathway. *Eur Heart J.* 1994;15(7):981-987.

259. Truex RC, Bishof JK, Hoffman EL. Accessory atrioventricular muscle bundles of the developing human heart. *Anat Rec.* 1958;131(1):45-59.

260. Wood FC. Histologic demonstration of accessory muscular connections between auricle and ventricle in a case of short PR interval and prolonged QRS complex. *Am Heart J.* 1942;25:454-462.

261. Valderrábano M, Chen F, Dave AS, Lamp ST, Klitzner TS, Weiss JN. Atrioventricular ring reentry in embryonic mouse hearts. *Circulation.* 2006;114(6):543-549.

262. Chien KR, Olson EN. Converging pathways and principles in heart development and disease. *Cell.* 2002;110(2):153-162.

263. Srivastava D. Genetic regulation of cardiogenesis and congenital heart disease. *Ann Rev Pathol.* 2006;1:199-213.

264. Hu N, Clark EB. Hemodynamics of the stage 12 to stage 29 chick embryo. *Circ Res.* 1989;65(6):1665-1670.

265. Cheng G, Litchenberg WH, Cole GJ, Mikawa T, Thompson RP, Gourdie RG. Development of the cardiac conduction system involves recruitment within a multipotent cardiomyogenic lineage. *Development.* 1999;126(22):5041-5049.

266. Davies F. The conducting system of the bird's heart. *J Anat.* 1929;64:129-146.

267. de Groot IJ, Hardy GP, Sanders E, Los JA, Moorman AF. The conducting tissue in the adult chicken atria. A histological and immunohistochemical analysis. *Anat Embryol.* 1985;172(2):239-245.

268. Lu Y, James TN, Bootsma M, Terasaki F. Histological organization of the right and left atrioventricular valves of the chicken heart and their relationship to the atrioventricular Purkinje ring and the middle bundle branch. *Anat Rec.* 1993;235(1):74-86.

269. Truex RC, Smythe MQ. Comparative morphology of the cardiac conduction tissue in animals. *Ann N Y Acad Sci.* 1965;127(1):19-33.

270. Kamino K. Optical approaches to ontogeny of electrical activity and related functional organization during early heart development. *Physiol Rev.* 1991;71(1):53-91.

271. Vassall-Adams PR. The development of the atrioventricular bundle and its branches in the avian heart. *J Anat.* 1982;134(Pt 1):169-183.

272. Durrer D, Formijne P, van Dam R, van Lier A, Buller J, Meyler FL. The electrocardiogram in normal and some abnormal conditions; in revived human fetal heart and in acute and chronic coronary occlusion. *Am Heart J.* 1961;61:303-316.

273. Witkowski FX, Clark RB, Larsen TS, Melnikov A, Giles WR. Voltage-sensitive dye recordings of electrophysiological activation in a Langendorff-perfused mouse heart. *Can J Cardiol.* 1997;13(11):1077-1082.

274. Kubalak SW, Miller-Hance WC, O'Brien TX, Dyson E, Chien KR. Chamber specification of atrial myosin light chain-2 expression precedes septation during murine cardiogenesis. *J Biol Chem.* 1994;269(24):16961-16970.

275. Chen J, Kubalak SW, Chien KR. Ventricular muscle-restricted targeting of the RXRalpha gene reveals a non-cell-autonomous requirement in cardiac chamber morphogenesis. *Development.* 1998;125(10):1943-1949.

276. Bartlett HL, Sutherland L, Kolker SJ, Welp C, Tajchman U, Desmarais V, Weeks DL. Transient early embryonic expression of Nkx2-5 mutations linked to congenital heart defects in human causes heart defects in Xenopus laevis. *Dev Dyn.* 2007;236(9):2475-2484.

277. Bodmer R. The gene tinman is required for specification of the heart and visceral muscles in Drosophila. *Development.* 1993;118(3):719-729.

278. Lyons I, Parsons LM, Hartley L, Li R, Andrews JE, Robb L, Harvey RP. Myogenic and morphogenetic defects in the heart tubes of murine embryos lacking the homeo box gene Nkx2-5. *Genes Dev.* 1995;9(13):1654-1666.

279. Cleaver OB, Patterson KD, Krieg PA. Overexpression of the tinman-related genes XNkx-2.5 and XNkx-2.3 in Xenopus embryos results in myocardial hyperplasia. *Development.* 1996;122(11):3549-3556.

280. Kern CB, Hoffman S, Moreno R, Damon BJ, Norris RA, Krug EL, Markwald RR, Mjaatvedt CH. Immunolocalization of chick periostin protein in the developing heart. *Anat Rec.* 2005;284(1):415-423.

281. Horiuchi K, Amizuka, N., Takeshita, S., Tamamatsu, H., Katsuura, M., Ozawa, H., Toyama, Y., Bonewald, L.F., Kudo, A. Identification and characterization of novel protein periostin, with restricted expression to periosteum and periodontal ligament and increased expression by transforming growth factor beta. *J Bone Miner Res.* 1999;14(7):1239-1249.

282. Ji X, Chen D, Xu C, Harris SE, Mundy GR, Yoneda T. Patterns of gene expression associated with BMP-2-induced osteoblast and adipocyte differentiation of mesenchymal progenitor cell 3T3-F442A. *J Bone Miner Metab.* 2000;18(3):132-139.

283. Stanton LW, Gerrard LJ, Damm D, Garrick BL, Lam A, Kapoun AM, Zheng O, Protter AA, Schreiner GF, White RT . Altered patterns of gene expression in response to myocardial infarction. *Circ Res.* 2000;86(9):939-945.

284. Wang D, Oparil S, Feng JA, Li P, Perry G, Chen LB, Dai M, John SW, Chen YF. Effects of pressure overload on extracellular matrix expression in the heart of the atrial natriuretic peptide-null mouse. *Hypertension.* 2003;42(1):88-95.

285. Katsuragi N, Morishita R, Nakamura N, Ochiai T, Taniyama Y, Hasegawa Y, Kawashima K, Kaneda Y, Ogihara T, Sugimura K. Periostin as a novel factor responsible for ventricular dilation. *Circulation.* 2004;110(13):1806-1813.

286. Litvin J, Zhu S, Norris R, Markwald R. Periostin family of proteins: therapeutic targets for heart disease. *Anat Rec.* 2005;287(2):1205-1212.

287. Delorme B, Dahl E, Jarry-Guichard T, Marics I, Briand JP, Willecke K, Gros D, Théveniau-Ruissy M. Developmental regulation of connexin 40 gene expression in mouse heart correlates with the differentiation of the conduction system. *Dev Dyn.* 1995;204(4):358-371.

288. Kreuzberg MM, Willecke K, Bukaukas FF. Connexin-mediated cardiac impulse propagation: connexin 30.2 slows atrioventricular conduction in mouse heart. *Trends Cardiovasc Med.* 2005;16(8):266-272.

289. Miquerol L, Dupays L, Théveniau-Ruissy M, Alcoléa S, Jarry-Guichard T, Abran P, Gros D. Gap junctional connexins in the developing mouse cardiac conduction system. *Novartis Found Symp.* 2003;250:80-98; discussion 98-109, 276-109.

290. Gourdie RG, Green CR, Severs NJ, Anderson RH, Thompson RP. Evidence for a distinct gap-junctional phenotype in ventricular conduction tissues of the developing and mature avian heart. *Circ Res.* 1993;72(2):278-289.

291. Minkoff R, Rundus VR, Parker SB, Beyer EC, Hertzberg EL. Connexin expression in the developing avian cardiovascular system. *Circ Res.* 1993;73(1):71-78.

292. Beyer EC. Molecular cloning and developmental expression of two chick embryo gap junction proteins. *J Biol Chem.* 1990;265(24):14439-14443.

293. Akester AR. Intercalated discs, nexuses, sarcoplasmic reticulum and transitional cells in the heart of the adult domestic fowl (Gallus gallus domesticus). *J Anat.* 1981;133(Pt 2):161-179.

294. van Kempen MJ, Fromaget C, Gros D, Moorman AF, Lamers WH. Spatial distribution of connexin43, the major cardiac gap junction protein, in the developing and adult rat heart. *Circ Res.* 1991;68(6):1638-1651.

295. Veenstra RD. Developmental changes in regulation of embryonic chick heart gap junctions. *J Membr Biol.* 1991;119(3):253-265.

296. Marban E, Yamagishi T, Tomaselli GE. Structure and function of voltge gated sodium channels. .*J Physiol* 1998;508:647-657.

297. Wang Q, Shen, J., Li, Z., Timotyh, K., Vincent, G.M, Priori, S.G., Schwartz, P.J., Keating, M.T. Cardiac sodium channel mutations in patients with long QT syndrome, an inherited cardiac arrhythmia. *Hum Mol Genet.* 1995;4(9):1603-1607.

298. Abriel H. Cardiac sodium channel Nav1.5 and its associated proteins. *Arch Mal Coeur Vaiss.* 2007;100(9):787-793.

299. Lei M. SCN5a and sinoatrial node pacemaker function. *Cardiovasc Res.* 2007;74(3):356-365.

300. Nerbonne JM, Kass, R.S. Molecular physiology of cardic repolarization. *Physiol Rev.* 2005;85(4):1205-1253.

301. Laitinen-Forsblom PJ, Makynen, P., Makynen, H., Yli-Mayry, S., Virtanen,V., Kontula, K., Aalto-Setala, K. SCN5a mutation associated with cardiac conduction defect and atrial arrhythmias. *J Cardiovasc Electrophysiol.* 2006;17(5):480-485.

302. Allen HJ. Glycogen in the chick embryo. *Biological Bulletin.* 1919;36:63-U66.

303. Gossrau R. Histochemical and electromicroscopic studies on the conduction system of birds. *Verhandlungen der Anatomischen Gesellschaft.* 1967;62:49-56.

304. Hirako R. Fine structure of Purkinje fibers in the chick heart. *Archivum histologicum Japonicum Nippon soshikigaku kiroku.* 1966;27(1):485-499.

305. Kim Y, Yasuda M. The cardiac conducting system of the fowl. *Anatomia, histologia, embryologia.* 1979;8(2):138-150.

306. Yokochi K. *Jap J Med Sc V Path.* 1931;1:147.

307. Kantoch MJ. Supraventricular tachycardia in children. *Indian J Pediatr.* 2005;72(7):609-619.

308. Jackman WM, Nakagawa H, Heidbuchel H, Beckman K, McClelland J, Lazzara R. Three forms of atrioventricular nodal (junctional) reentrant tachycardia: differential diagnosis, electrophysiological characteristics and implications for anatomy of the reentrant circuit.. In: Zipes DP, Jalife, J., ed. *Cardiac Electrophysiology: From Cell to Bedside.* Vol second edition: WB Saunders; 1995:620-637.

309. Blaufox AD, Rhodes JF, Fishberger SB. Age related changes in dual AV nodal physiology. *PACE.* 2000;23(4 Pt 1):477-480.

310. Wellens HJ. Twenty-five years of insights into the mechanisms of supraventricular arrhythmias. *J Cardiovasc Electrophysiol.* 2003;14(9):1020-1025.

311. Boldt T, Eronen M, Andersson S. Long-term outcome in fetuses with cardiac arrhythmias. *Obstet Gynecol.* 2003;102(6):1372-1379.

312. Kolditz DP, Blom NA, Bokenkamp R, Schalij MJ. Low-energ radiofrequency catheter ablation as tretment for supraventricular tachycardia in a premature neonate. *Eur J Pediatr.* 2005;164(9):559-562.

313. Juneja R, Shah S, Naik N, Kothari SS, Saxena A, Talwar KK. Management of cardiomyopathy resulting from incessant supraventricular tachycardia in infants and children. *Indian Heart J.* 2002;54(2):176-180.

314. Vaughan Williams EM. A classification of antiarrhythmic actions reassessed after a decade of new drugs. *J Clin Pharmcol.* 1984;24(4):129-147.

315. Weindling SN, Saul JP, Walsh EP. Efficacy and risks of medical therapy for supraventricular tachycardia in neonates and infants. *Am Heart J.* 1996;131(1):66-72.

316. Kugler JD. Radiofrequency catheter ablation for supraventricular tachycardia. Should it be used in infants and small children? *Circulation.* 1994;90(1):639-641.

317. Rao PS, Gupta ML, Balaji S. Recent advances in pediatric cardiology--electrophysiology, transcatheter and surgical advances. *Indian J Pediatr.* 2003;70(7):557-564.

318. Haines DE. The biophysics of radiofrequency catheter ablation in the heart: the importance of temperature monitoring. *PACE.* 1993;16(3 Pt 2):586-591.

319. Vidaillet HJ, Pressley JC, Henke E, Harrell FE, German LD. Familial occurrence of accessory atrioventricular pathways (preexcitation syndrome). *N Engl J Med.* 1987;317(2):65-69.

320. Perry JC, Garson A. Supraventricular tachycardia due to Wolff-Parkinson-White syndrome in children: early disappearance and late recurrence. *J Am Coll Cardiol.* 1990;16(5):1215-1220.

321. Kugler JD, Danford DA. Management of infants, children, and adolescents with paroxysmal supraventricular tachycardia. *J Pediatr.* 1996;129(3):324-338.

322. Obel OA, Camm AJ. Accessory pathway reciprocating tachycardia. *Eur Heart J.* 1998;19 Suppl E:E13-24, E50-11.

323. Prystowsky EN, Heger JJ, Zipes DP. The Wolff-Parkinson-White syndrome--diagnosis and treatment. *Heart Lung.* 1981;10(3):465-474.

324. Guize L, Soria R, Chaouat JC, Chrétien JM, Houe D, Le Heuzey JY. Prevalence and course of Wolf-Parkinson-White syndrome in a population of 138,048 subjects. *Annales de médecine interne.* 1985;136(6):474-478.

325. Josephson ME, Miller JM. Atrioventricular nodal reentry: evidence supporting an intranodal location. *PACE.* 1993;16(3 Pt 2):599-614.

326. Goudevenos JA, Katsouras CS, Graekas G, Argiri O, Giogiakas V, Sideris DA. Ventricular pre-excitation in the general population: a study on the mode of presentation and clinical course. *Heart.* 2000;83(1):29-34.

327. Leitch JW, Klein GJ, Yee R, Murdock C. Prognostic value of electrophysiology testing in asymptomatic patients with Wolff-Parkinson-White pattern. *Circulation.* 1990;82(5):1718-1723.

328. Munger TM, Packer DL, Hammill SC, Feldman BJ, Bailey KR, Ballard DJ, Holmes DR, Gersh BJ. A population study of the natural history of Wolff-Parkinson-White syndrome in Olmsted County, Minnesota, 1953-1989. *Circulation.* 1993;87(3):866-873.

329. Brechenmacher C, Courtadon, M. Wolff-Parkinson-White syndrome caused by association of atrio-Hissian and Mahaim fibers. Comparison between the electrophysiology and histology. *Arch Mal Coeur Vaiss.* 1976;69(12):1275-1283.

330. James TN. De subitaneis mortibus IX. Type A Wolff-Parkinson-White syndrome. *Circulation.* 1974;50(6):1264-1280.

331. Rossi L. Anatomic variants of AV junction and surgery of supraventricular arrhythmias. *Circulation.* 1980;62(4):916-917.

332. Bauersfeld U, Pfammatter JP. Diagnosis and treatment of common pediatric supraventricular tachycardias. *Therapeutische Umschau Revue Thérapeutique.* 2001;58(2):94-98.

333. Deal BJ, Keane, J.F, Gillette, P.C., Garson, A Jr. Wolff-Parkinson-White syndrome and supraventricular tchycardia during infancy: management and follow-up. *J Am Coll Cardiol.* 1985;5(1):130-135.

334. Mantakas ME, McCue CM, Miller WW. Natural history of Wolff-Parkinson-White syndrome discovered in infancy. *Am J Cardiol.* 1978;41(6):1097-1103.

335. Gollob MH, Seger, J.J., Gollob, T.N., Tapscott, T., Gonzales, O, Bachiniski, L., Roberts, R. Novel PRKAG2 mutation responsible for the genetic syndrome of ventricular preexcitation and conduction system disease with childhood onset and absence of cardiac hypertrophy. *Circulation.* 2001;104(25):3030-3035.

336. MacRae CA, Ghaisas N, Kass S, Donnelly S, Basson CT, Watkins HC, Anan R, Thierfelder LH, McGarry K, Rowland E. Familial Hypertrophic cardiomyopathy with Wolff-Parkinson-White syndrome maps to a locus on chromosome 7q3. *J Clin Invest.* 1995;96(3):1216-1220.

337. Wolf CM, Arad, M., Ahnud, F., Sanbe, A., Bernstein, S.A., Tok, O., Konno, T., Morley, G., Robbins, J., Seidmn, J.G., Seidmn, C.E., Berul, C.I. Reversibility of PRKAG2 glycogen-storage cardiomyopathie and electrophysiological manifestations. *Circulation.* 2008;2008(117):2.

338. Arad M, Moskowitz IP, Patel VV, Ahmad F, Perez-Atayde AR, Sawyer DB, Walter M, Li GH, Burgon PG, Maguire CT, Stapleton D, Schmitt JP, Guo XX, Pizard A, Kupershmidt S, Roden DM, Berul CI, Seidman CE, Seidman JG. Transgenic mice overexpressing mutant PRKAG2 define the cause of Wolff-Parkinson-White syndrome in glycogen storage cardiomyopathy. *Circulation.* 2003;107(22):2850-2856.

339. Bulkley BH, Hutchins, G.M. Pompe's disease presenting as hypertrophic cardiomyopathie with Wolff-Parkinson-White syndrome. *Am Heart J.* 1978;96(2):246-252.

340. Yang Z, McMahon CJ, Smith LR, Bersola J, Adesina AM, Breinholt JP, Kearney DL, Dreyer WJ, Denfield SW, Price JF, Grenier M, Kertesz NJ, Clunie SK, Fernbach SD, Southern JF, Berger S, Towbin JA, Bowles KR, Bowles NE. Danon disease as an underrecognized cause of hypertrophic cardiomyopathy in children. *Circulation.* 2005;112(11):1612-1617.

341. Boineau JP, Moore EN. Evidence for propagation of activation across an accessory atrioventricular connection in types A and B pre-excitation. *Circulation.* 1970;41(3):375-397.

342. Gallagher JJ, Svenson RH, Sealy WC, Wallace AG. The Wolff-Parkinson-White syndrome and the preexcitation dysrhythmias. Medical and surgical management. *Med Clin North Am.* 1976;60(1):101-123.

343. Wellens HJ, Brugada P, Penn OC. The management of preexcitation syndromes. *JAMA.* 1987;257(17):2325-2333.

344. Bromberg BI, Lindsay BD, Cain ME, Cox JL. Impact of clinical history and electrophysiologic characterization of accessory pathways on management strategies to reduce sudden death among children with Wolff-Parkinson-White syndrome. *J Am Coll Cardiol.* 1996;27(3):690-695.

345. Dubin AM, Collins KK, Chiesa N, Hanisch D, Van Hare GF. Use of electrophysiologic testing to assess risk in children with Wolff-Parkinson-White syndrome. *Cardiol Young.* 2002;12(3):248-252.

346. Kugler JD, Danford DA, Houston KA, Felix G, Society PRARotPRARotPE. Pediatric radiofrequency catheter ablation registry success, fluoroscopy time, and complication rate for supraventricular tachycardia: comparison of early and recent eras. *J Cardiovasc Electrophysiol.* 2002;13(4):336-341.

347. Kirsh JA, Gross GJ, O'Connor S, Hamilton RM, Registry CIP. Transcatheter cryoablation of tachyarrhythmias in children: initial experience from an international registry. *J Am Coll Cardiol.* 2005;45(1):133-136.

348. Sporton SC, Earley MJ, Nathan AW, Schilling RJ. Electroanatomic versus fluoroscopic mapping for catheter ablation procedures: a prospective randomized study. *J Cardiovasc Electrophysiol.* 2004;15(3):310-315.

349. Van Hare GF, Dubin AM, Collins KK. Invasive electrophysiology in children: state of the art. *Journal Electrocardiol.* 2002;35 Suppl:165-174.

350. Flensted-Jensen E. Wolff-Parkinson-White syndrome. A long term follow-up. *Acta Med Scand.* 1969;186(1-2):65-74.

351. Klein GJ, Prystowsky EN, Yee R, Sharma AD, Laupacis A. Asymptomatic Wolff-Parkinson-White. Should we intervene? *Circulation.* 1989;80(6):1902-1905.

352. Klein GJ, Yee R, Sharma AD. Longitudinal electrophysiologic assessment of asymptomatic patients with the Wolff-Parkinson-White electrocardiographic pattern. *N Engl J Med.* 1989;320(19):1229-1233.

353. Timmermans C, Smeets JL, Rodriguez LM, Vrouchos G, van den Dool A, Wellens HJ. Aborted sudden death in the Wolff-Parkinson-White syndrome. *Am J Cardiol.* 1995;76(7):492-494.

354. Klein GJ, Bashore, T.M., Sellers, T.D., Pritchetti, E.L., Smith, W.M., Gallagher, J.J. Ventricular fibrillation in the Wolff-Parkison-White syndrome. *N Engl J Med.* 1979;301(20):1080-1085.

355. Basso C. Postmortem diagnosis in sudden cardiac death victems: macroscopic, microscopic and molecular findings. *Cardiovasc Res.* 2001;50(2):290-300.

356. Sidhu JS, Rajawat YS, Rami TG, Gollob MH, Wang Z, Yuan R, Marian AJ, DeMayo FJ, Weilbacher D, Taffet GE, Davies JK, Carling D, Khoury DS, Roberts R. Transgenic mouse model of ventricular preexcitation and atrioventricular reentrant tachycardia induced by an AMP-activated protein kinase loss-of-function mutation responsible for Wolff-Parkinson-White syndrome. *Circulation.* 2005;111(1):21-29.

357. Gaussin V. Offbeat mice. *Anat Rec.* 2004;280(2):1022-1026.

358. McGuire MA, Janse MJ, Ross DL. "AV nodal" reentry: Part II: AV nodal, AV junctional, or atrionodal reentry? *J Cardiovasc Electrophysiol.* 1993;4(5):573-586.

359. Casta A, Wolff GS, Mehta AV, Tamer D, Garcia OL, Pickoff AS, Ferrer PL, Sung RJ, Gelband H. Dual atrioventricular nodal pathways: a benign finding in arrhythmia-free children with heart disease. *Am J Cardiol.* 1980;46(6):1013-1018.

360. Sung RJ, Styperek JL. Electrophysiologic identification of dual atrioventricular nodal pathway conduction in patients with reciprocating tachycardia using anomalous bypass tracts. *Circulation.* 1979;60(7):1464-1476.

361. Mazgalev TN. The dual AV nodal pathways: are they dual and where are they? *J Cardiovasc Electrophysiol.* 1997;8(12):1408-1412.

362. Gonzalez MD, Contreras LJ, Cardona F, Klugewicz CJ, Conti JB, Curtis AB, Morey TE, Dennis DM. Demonstration of a left atrial input to the atrioventricular node in humans. *Circulation.* 2002;106(23):2930-2934.

363. Heidbuchel H, Jackman, W.M. Characterization of subforms of AV nodal reentrant tachycardia. *Europace.* 2004;6(4):316-329.

364. Blaufox AD, Saul JP. Influences on fast and slow pathway conduction in children: does the definition of dual atrioventricular node physiology need to be changed? *J Cardiovasc Electrophysiol.* 2002;13(3):210-211.

365. Jazayeri MR, Hempe SL, Sra JS, Dhala AA, Blanck Z, Deshpande SS, Avitall B, Krum DP, Gilbert CJ, Akhtar M. Selective transcatheter ablation of the fast and slow pathways using radiofrequency energy in patients with atrioventricular nodal reentrant tachycardia. *Circulation.* 1992;85(4):1318-1328.

366. Baker JH, Plumb VJ, Epstein AE, Kay GN. PR/RR interval ratio during rapid atrial pacing: a simple method for confirming the presence of slow AV nodal pathway conduction. *J Cardiovasc Electrophysiol.* 1996;7(4):287-294.

367. Epstein LM, Scheinman MM, Langberg JJ, Chilson D, Goldberg HR, Griffin JC. Percutaneous catheter modification of the atrioventricular node. A potential cure for atrioventricular nodal reentrant tachycardia. *Circulation.* 1989;80(4):757-768.

368. Haissaguerre M, Warin JF, Lemetayer P, Saoudi N, Guillem JP, Blanchot P. Closed-chest ablation of retrograde conduction in patients with atrioventricular nodal reentrant tachycardia. *N Engl J Med.* 1989;320(7):426-433.

369. Jackman WM, Beckman KJ, McClelland JH, Wang X, Friday KJ, Roman CA, Moulton KP, Twidale N, Hazlitt HA, Prior MI. Treatment of supraventricular tachycardia due to atrioventricular nodal reentry, by radiofrequency catheter ablation of slow-pathway conduction. *N Engl J Med.* 1992;327(5):313-318.

370. Langberg JJ. Radiofrequency catheter ablation of AV nodal reentry: the anterior approach. *PACE.* 1993;16(3 Pt 2):615-622.

371. Lee MA, Morady F, Kadish A, Schamp DJ, Chin MC, Scheinman MM, Griffin JC, Lesh MD, Pederson D, Goldberger J. Catheter modification of the atrioventricular junction with radiofrequency energy for control of atrioventricular nodal reentry tachycardia. *Circulation.* 1991;83(3):827-835.

PART I

DEVELOPMENT OF THE ANNULUS FIBROSIS AND ACCESSORY PATHWAY PERSISTENCE IN RELATION TO ARRHYTHMIA ETIOLOGY

Chapter 2

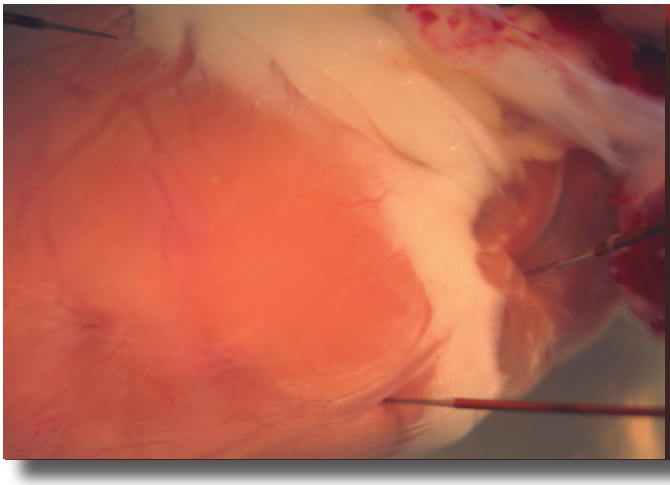

Denise P. Kolditz[1,2]
Maurits C.E.F. Wijffels[3]
Nico A. Blom[4]
Arnoud van der Laarse[1]
Roger R. Markwald[5]
Martin J. Schalij[1]
Adriana C. Gittenberger-de Groot[2]

[1]Department of Cardiology, Leiden University Medical Center, Leiden, The Netherlands;
[2]Department of Anatomy and Embryology, Leiden University Medical Center, Leiden, The Netherlands;
[3]Department of Cardiology, St. Antonius Hospital, Nieuwegein, The Netherlands
[4]Department of Pediatric Cardiology, Leiden University Medical Center, Leiden, The Netherlands;
[5]Department of Cell Biology and Anatomy, Medical University of South Carolina, Charleston, South Carolina

Persistence of Functional Atrioventricular Accessory Pathways in Post-Septated Embryonic Avian Hearts: Implications for Morphogenesis and Functional Maturation of the Cardiac Conduction System

Circulation 2007;115(1):17-26

Abstract

Background. During heart development, the ventricular activation sequence changes from a base-to-apex to an apex-to-base pattern. We investigated the possibility of impulse propagation through remnants of atrioventricular (AV) connections in quail hearts.

Methods and Results. In 86 hearts (group A, HH30-34, n=15; group B, HH35-44, n=65; group C, 5-6 months, n=6) electrodes were positioned on the left atrium (LA), right ventricular base (RVB), left ventricular base (LVB) and left ventricular apex (LVA). In group A, LVB activation preceded LVA activation in the majority of cases (60%; 9/15), while hearts in group B primarily demonstrated a LV apex-to-base activation pattern (72%; 47/65). Interestingly, in group B the RVB (17%; 11/65) or LVB (8%; 5/65) exhibited premature activation in 25% (16/65) of cases, while in 26% (17/65) the RVB or LVB was activated simultaneously with the LVA. Morphological analysis confirmed functional data by showing persistent muscular AV connections in embryonic hearts. Interestingly, all myocardial AV connections stained positive for periostin, a non-myocardial marker. Longitudinal analysis (HH35-44) demonstrated a decrease in both the number of hearts exhibiting premature base activation ($p=0.015$) as the number ($p=0.004$) and width ($p=0.179$) of accessory AV pathways with developmental stage in a similar time course. In the adult quail hearts, accessory myocardial AV-pathways were functionally and morphologically absent.

Conclusion. Thus, impulse propagation through persistent accessory AV connections remains possible at near-hatching stages (HH44) of development, which may provide a substrate for AV reentrant arrhythmias in perinatal life. Periostin positivity and absence of AV pathways in the adult heart, suggest that these connections eventually loose their myocardial phenotype, implicating ongoing AV-ring isolation peri- and postnatally.

Introduction

Atrioventricular (AV) reentrant tachycardias involve the presence of an accessory myocardial AV pathway bypassing the insulating annulus fibrosis and are one of the most common arrhythmias in humans.[1-3] In children, the first episode of this arrhythmia occurs prenatally or in the first months of life in approximately 60% of cases and appears to resolve spontaneously in two-thirds of cases before the age of one year.[4, 5] The natural course in foetuses or neonates is usually benign,[4] but a radiofrequency catheter ablation procedure may be necessary to control the arrhythmia.[6] Although a causal relationship between abnormal cardiogenesis and arrhythmogenesis has been hypothesized,[7] the underlying mechanisms responsible for the development of these accessory pathways (APs) are still not completely understood.

In the early tubular heart, the atrial myocardium is continuous with the ventricular myocardium and the blood is driven in a caudal to cranial direction by virtue of a slow peristaltic contraction pattern, originating from the primitive pacemaker in the caudal sinus venosus region[8, 9] and with the endocardial cushions serving as primitive valves.[10] Shortly thereafter, the emerging atrium and ventricle in the looped heart start to contract sequentially as a result of the development of alternating slow (sinoatrial region, atrioventricular junction and outflow tract) and fast (atrial and ventricular regions) conducting regions, while propagation of the depolarization wave keeps following the direction of the bloodstream.[11] Ultimately however, ventricular activation shifts from this immature base-to-apex sequence to a mature apex-to-base pattern.[12-19]

This transition in ventricular activation pattern reflects maturation of the His-Purkinje system (HPS) and coincides with completion of ventricular septation.[12, 17] Importantly, and almost simultaneously, the existing AV myocardial continuity, which is present all around the circumference of the AV junction in the looped embryonic heart, disappears due to formation of the fibrous annulus.[14] Although morphologically, remnants of these AV connections, bypassing the insulating AV groove, have been found in post-septated embryonic and/or adult chick,[20, 21] mouse,[22] and human[23-27] hearts, the electrophysiological properties have not been studied systematically. Recently, a conducting right-sided AV myocardial continuity was demonstrated in post-septated CCS-lacZ transgenic mice, providing a possible explanation for the occurrence of functional atrio-fascicular bypass tracts via the moderator band causing Mahaim tachycardias.[28] The developmental mechanisms underlying the occurrence, and in many cases

early and spontaneous disappearance of APs in foetuses and neonates,[4, 5] are however incompletely understood.

We hypothesized that accessory AV connections bypassing the insulating annulus fibrosis are embryonic remnants of myocardium that retain their conducting properties in post-natal life. By analyzing the ventricular activation sequence in embryonic and adult quail hearts with extracellular electrode recordings and by correlating these electrophysiological data with morphology, we could demonstrate that functional remnants of AV connections indeed remain present at late post-septational stages of embryonic heart development.

Materials and Methods

Experimental Preparations

Fertilized eggs of the Japanese quail (*Coturnix coturnix japonica*) were incubated at 37.5°C and 80% humidity. All animal experiments were in accordance with the institutional guidelines of the Leiden University Medical Center. After termination of incubation at the desired developmental stages (HH30-34, n=15; HH35-44, n=65) and staging according to Hamburger-Hamilton criteria,[29] the embryonic hearts were carefully isolated from the embryo after euthanization by decapitation. Additionally, 6 hearts were harvested from adult quails (5-6 months) after cervical dislocation.

The hearts were placed into a custom-built fluid-heated temperature-controlled tissue bath. Subsequently, the embryonic hearts were superfused (30±0.1°C) and the adult hearts Langendorff-perfused (65 mmHg, 37±0.1°C) with carboxygenated (95% O_2, 5% CO_2) Tyrode's solution: NaCl 130, KCl 4, KH_2PO_4 1.2, $MgSO_4$ 0.6, $NaHCO_3$ 20, $CaCl_2$ 1.5, glucose 10 (mmol/l) (pH 7.35).

Electrophysiological Recordings – Technical Features

Unipolar extracellular recordings were performed by consistently positioning 4 tungsten electrodes (tip: 1-2μm; impedance 0.5-1.0MΩ, WPI Inc., Berlin, Germany) on the left atrium (LA), right ventricular base (RVB), left ventricular base (LVB) and left ventricular apex (LVA)(**Figure 1**). Electrograms were recorded using a high-gain low-noise DC bio-amplifier system (Iso-DAM8A; WPI Inc., Berlin, Germany). The signals were band-pass- (300Hz-1kHz) and notch-filtered (50Hz) before being digitized at a sampling rate of ≥ 1kHz using a computerized recording system (Prucka Engineering Inc., Houston TX., USA). Pacing was performed with a stimulator (EP-3, EP MedSystems Inc., West-Berlin NJ, USA), providing monophasic stimuli (strength 5-10mA, width 1.0ms). The embryonic hearts were stimulated at the high right atrium (RA).

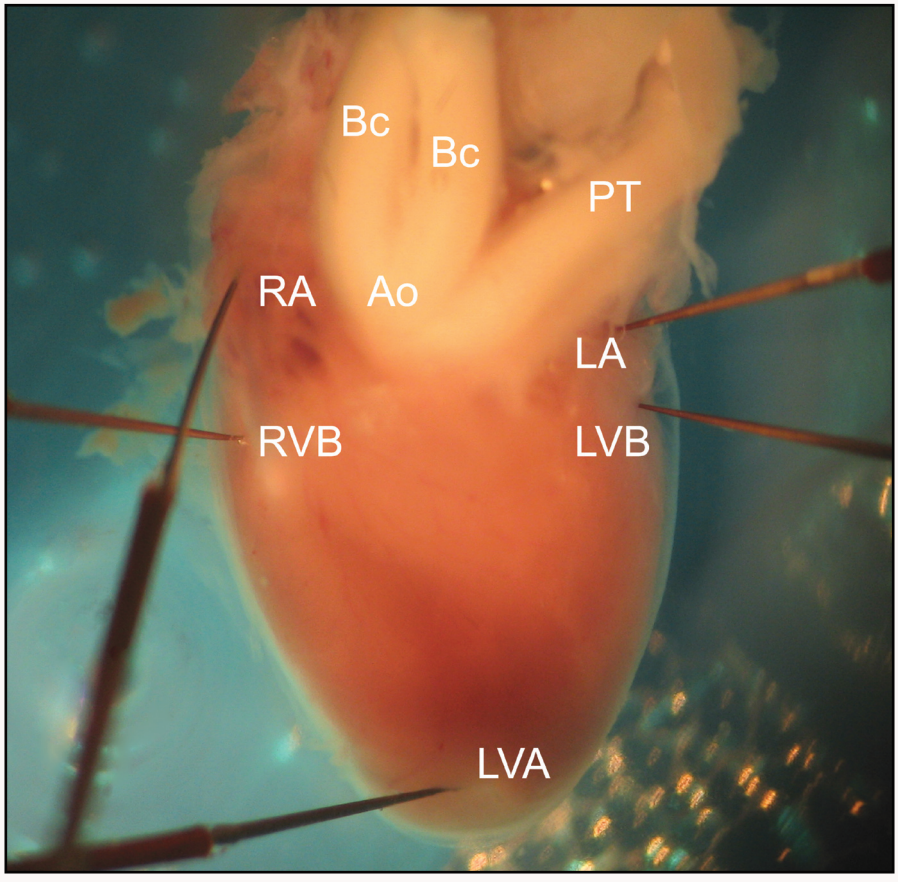

Figure 1. A representative HH43 embryonic heart showing recording electrode placement on the LA, RVB, LVB and LVA. A bipolar pacing electrode for pacing of the hearts was placed on the high RA. Ao=aorta, PT=pulmonary trunk, Bc=brachiocephalic artery, LA=left atrium, RA=right atrium, LVB=left ventricular base, RVB=right ventricular base, LVA=left ventricular apex

Electrophysiological Recording Protocol

The experimental preparations were allowed to equilibrate for 10 minutes before starting the recording protocol. Hearts were categorized in three groups: group A (HH30-34, n=15), group B (HH35-44, n=65) and group C (5-6 months, n=6). Embryonic hearts in group A, hearts in group B with a stable spontaneous HR of at least 60 bpm (group B_1) and hearts in group C were allowed to beat spontaneously, whereas hearts with a HR of <60 bpm (group B_2) were stimulated at a fixed CL of 500 ms.

In 15 hearts (HH38-41), after baseline recordings, 1 ml adenosine (0.3mg/ml) was superfused on the heart to a final concentration of 0.03mg/ml(0.11μM) in the tissue bath, to analyze transitions in ventricular activation sequence after slowing conducting through the AV node.

Statistical analysis

Heart rate and AV interval were compared between groups with a 2-tailed Student's t-test for normally distributed values; otherwise, the Mann-Whitney U test was used (AV interval group B_1). The symmetry of the distribution was determined by measuring the Skewness value. For comparison of categorical variables (ventricular activation patterns, AP-number, AP-width), the χ^2-test was performed. Results are presented as mean ± SD (range). A probability value of < 0.05 (2-tailed) was considered statistically significant. All analyses were performed with the Statistical Package for Social Studies version 11.0 (SPSS Inc, Chicago, Ill).

The online-only Data Supplement contains more information about methods (Definitions and Immunohistochemistry) used in this study.

The authors had full access to the data and take responsibility for its integrity. All authors have read and agree to the manuscript as written.

Results

Experimental Preparations

In 15 group A hearts (HH30-34), electrograms were recorded during stable heart rhythm of 143±30 bpm (AV interval 100±20ms). In 15 group B_1 hearts (HH35-44), the heart rate (HR) (91±36 bpm) and the AV interval (80±15ms) were not significantly different compared to group A (p=0.414 and p=0.415 respectively). During RA-pacing (120 bpm) in the remaining 50 hearts in group B_2 (HH35-44), the mean AV interval was 78±28ms (p=0.758, compared to group B_1). The 6 adult quail hearts showed a HR of 199±52 bpm and an AV interval of 80±7ms. **Table 1** summarizes the general (electrophysiological) characteristics of the quail hearts.

Left Ventricular Activation Sequence: Base-to-Apex or Apex-to-Base ?

Since initial studies mainly reported on LV-activation patterns,[12] we initially analyzed the relationship between LVA and LVB electrograms. Hearts in group A primarily showed base-to-apex LV-activation patterns (9/15; 60%), with LVB activation preceding LVA activation by 5±4 ms (**Table 2**).

In contrast, hearts in group B mainly demonstrated apex-to-base LV-activation patterns, with LVA activation preceding LVB activation by 4±3 ms in 47/65 hearts (72%)(**Table 2**). In group B, no differences in LV-activation patterns were observed between hearts beating spontaneously and hearts driven by RA-pacing (p=0.843). Representative examples of electrode recordings in an embryonic heart from group A (panel a) and an embryonic heart from group B_2 (panel b) are shown in **Figure 2**.

Group	Age (HH/mnths)	SR/paced	N	HR(bpm) *mean±SD (range)*	AV(ms) *mean±SD (range)*
A(n=15)	30	SR	5	140±33(100-184)	100±15(87-125)
	31	SR	5	142±41(94-180)	93±10(82-107)
	32	SR	1	175	115
	33	SR	2	140±11(132-147)	137±12(129-146)
	34	SR	2	141±6(137-145)	76±2(74-78)
subtotal			**15**	**143±30(94-184)**†	**100±20(74-146)**‡
B_1(n=15)	35	SR	1	76	87
	36	SR	2	170±5(167-174)	91±19(78-105)
	37	SR	2	76±21(61-90)	74±20(60-89)
	38	SR	4	76±12(63-92)	71±9(62-81)
	39	SR	3	94±17(77-112)	72±9(61-78)
	40	SR	3	77±13(63-90)	94±18(78-114)
subtotal			**15**	**91±36(41-174)**†	**80±15(60-114)***‡
B_2 (n=50)	35	paced	1	120	48
	36	paced	4	120	96±40(62-132)
	37	paced	2	120	88±4(85-91)
	38	paced	3	120	93±46(42-132)
	39	paced	16	120	71±24(47-140)
	40	paced	6	120	67±21(41-89)
	41	paced	5	120	96±33(57-140)
	42	paced	7	120	77±28(47-127)
	43	paced	4	120	87±24(67-120)
	44	paced	2	120	58±10(51-65)
subtotal			**50**	**120**	**78±28(41-140)***
C(n=6)	5.5 months	SR	6	199±52(134-251)	80±7(71-89)

Table 1. Developmental stages of the quail hearts from both group A, B and C, with corresponding HRs and AV-intervals. SR=sinus rhythm, HR=heart rate, AV=atrioventricular interval. * p=0.758 (Student's t-test), †p=0.414 (Student's t-test), ‡p=0.415 (Student's t-test).

	LV-activation sequence	N (%)	LVB first	RVB first	LVA first	LVB or RVB = LVA
group A	**base-to-apex**	9(60%)	6	3	-	-
	concurrent	5(33%)	-	-	-	5
	apex-to-base	1(7%)	-	-	-	1
	subtotal	15	6(40%)	3(20%)	-	6(40%)
group B	**base-to-apex**	7(11%)	5	2	-	-
	concurrent	11(17%)	-	2	-	9
	apex-to-base	47(72%)	-	7	32	8
	subtotal	65	5(8%)	11(17%)	32(49%)	17(26%)
group B_1	**base-to-apex**	1(7%)	1	-	-	-
	concurrent	3(20%)	-	-	-	3
	apex-to-base	11(73%)	-	-	9	2
	subtotal	15	1(7%)	-	9(60%)	5(33%)
group B_2	**base-to-apex**	6(12%)	4	1	-	1
	concurrent	8(16%)	-	-	-	8
	apex-to-base	36(72%)	-	7	23	6
	subtotal	50	4(8%)	8(16%)	23(46%)	15(30%)
Group C	**base-to-apex**	-	-	-	-	-
	concurrent	-	-	-	-	-
	apex-to-base	6(100%)	-	-	6(100%)	-

Table 2. LV-activation sequences in both group A, B and C, with corresponding locations of earliest ventricular activation. LVB=left ventricular base, RVB=right ventricular base, LVA=left ventricular apex

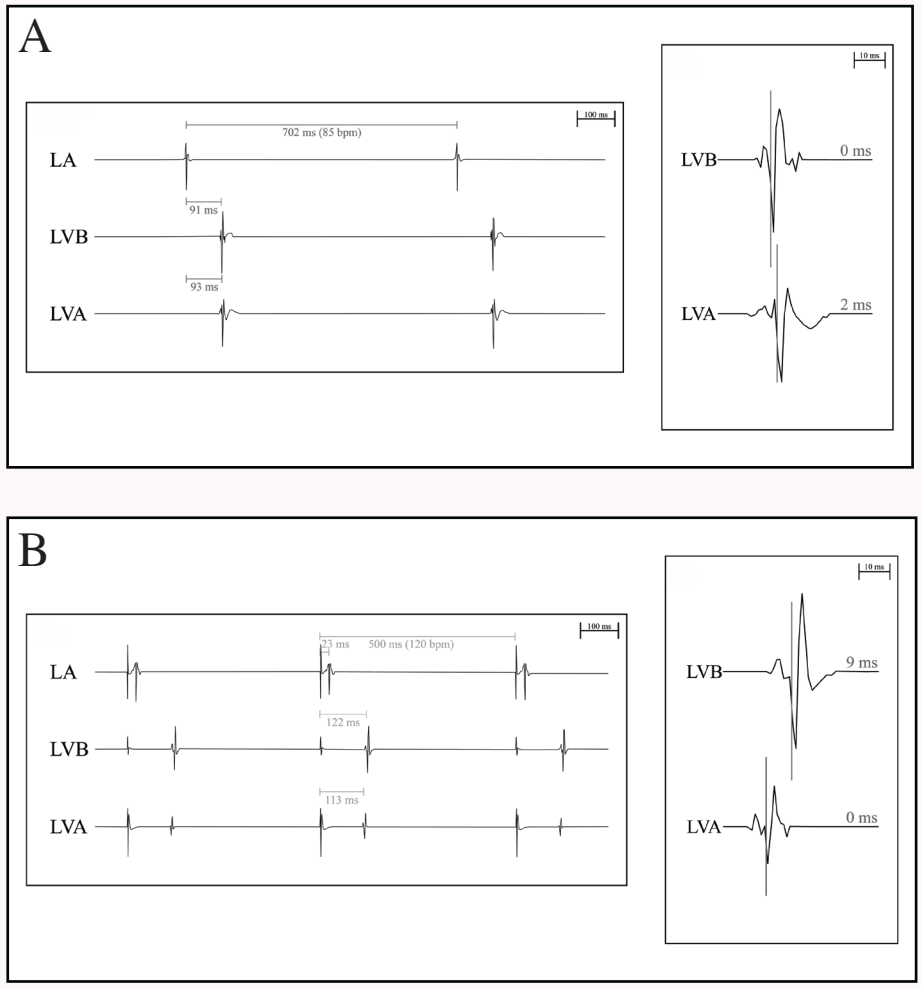

Figure 2. A. A representative example of electrograms recorded in a pre-septated quail heart at HH31 (HR 85 bpm, AV-interval 91ms), demonstrating a typical base-to-apex LV-activation pattern. As can be seen in the magnification, the LVB was activated 2ms earlier than the LVA. **B.** Electrograms recorded in a post-septated HH39 quail heart (HRpaced 120 bpm, AV-interval 113ms), representing a typical apex-to-base LV-activation pattern. The magnification shows that the LVA was activated 9ms prior to LVB activation. LA=left atrium, LVB=left ventricular base, LVA=left ventricular apex

Global (LV and RV) Activation Patterns

Analysis of the more global ventricular activation patterns, including RVB activation, revealed that quail hearts in group A demonstrated earliest ventricular activation at the LVB in 40% (n=6) of cases, while the RVB was the site of earliest ventricular activation in 20% (n=3) of cases (**Table 2**).

Interestingly, even at late developmental stages of embryonic development (HH35-44)(group B), the LVA was the true site of earliest activation in only 32/65(49%) hearts, while the RVB or LVB exhibited earliest ventricular activation in 11(17%) and 5(8%) cases respectively. In the remaining 17/65(26%) hearts concurrent activation of the LVA and RVB or LVB was observed (**Table 2**). Representative examples of electrogram recordings in embryonic hearts from group B, displaying early RVB and early LVB activation are shown in **Figure 3a** and **Figure 3b**, respectively.

In post-septated hearts (group B) with earliest ventricular activation of the LVB (n=5) or RVB (n=11), the AV intervals were 62±15ms and 74±31ms, respectively (p=0.540). Activation of the ventricular base occurred significantly faster in quails with a global base-to-apex pattern (69±26ms) of ventricular activation compared to quails with an apex-to-base pattern (83±22ms)(p=0.005), which suggests that slow conduction through the AV node was indeed bypassed in these hearts.

Additional longitudinal analysis demonstrated early activation of the ventricular base in 93%(14/15) of pre-septated HH30-34 hearts, while in 60%(23/38) of post-septated HH35-39 and in only 37%(10/27) of post-septated HH40-44 hearts the ventricular base was prematurely activated (p=0.015).

Ventricular Activation Patterns in the Adult Heart

In all adult quail hearts (n=6) in group C (HR 199±52, AV interval 80±7ms), the LVA was the location of earliest ventricular activation and was activated 5±4ms prior to the LVB or RVB. Surface ECG-recordings (n=4) did not reveal ventricular preexcitation: PR-intervals were not shortened (69±2ms, range 66-71ms) and showed an isoelectric segment and QRS-complexes did not show a delta-wave (31±2ms, 29-33ms). A representative example of extracellular- and surface ECG-recordings in an adult quail heart from group C is shown in **Figure 4**.

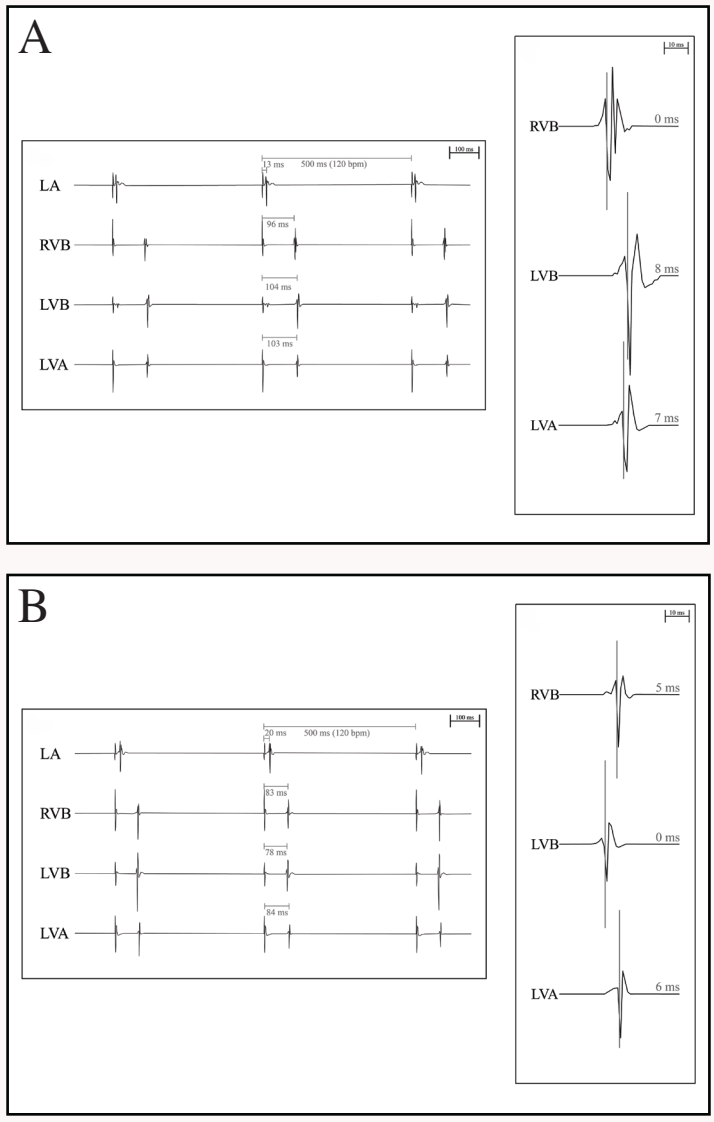

Figure 3. **A.** A representative example of electrograms recorded in a post-septated HH39 quail heart (HRpaced120 bpm, AV-interval 96ms), demonstrating an apex-to-base LV-activation pattern (LVA activation 1ms earlier than LVB activation), with premature RVB activation. The RVB was activated 7ms earlier than the LVA. **B.** Electrograms recorded in a post-septated HH42 quail heart (HRpaced120 bpm, AV-interval 78ms), representing a base-to-apex LV-activation pattern at this late developmental stage. The magnification shows that the LVB was activated 6 ms prior to LVA activation. The RVB was also activated prior (1 ms) to the LVA. LA=left atrium, RVB=right ventricular base, LVB=left ventricular base, LVA=left ventricular apex.

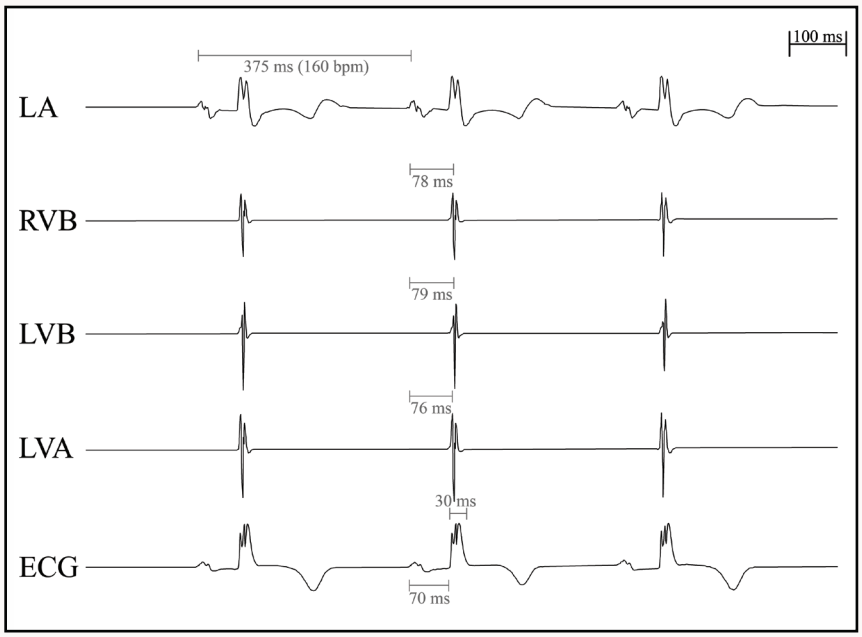

Figure 4. Extracellular and surface electrogram recordings in an adult quail heart (HR 160 bpm, AV interval 76ms, QRS 30ms, PR 70ms). The left ventricular apex (LVA) was the location of earliest ventricular activation.

Effect of Adenosine on Ventricular Activation

Adenosine was administrated in 15 (HH38-41) hearts from group B, which resulted in a rapid (1-2 minutes) and marked increase in AV interval from 67±18ms to 149±9ms ($p<0.001$) and concurrent changes in ventricular activation pattern ($p=0.022$). For instance, in 44% (4/9) of hearts with an apex-to-base global ventricular activation pattern (9/15,60%; AV interval 72±18ms) at baseline, the ventricular activation pattern switched to base-to-apex (RVB, n=2; LVB, n=1; AV interval 149±12 ms), while in 11% (1/9) of the cases a concurrent ventricular activation pattern was observed (AV interval 140ms). The ventricular activation sequence in hearts with a global base-to-apex pattern at baseline (5/15,33%; AV interval 61±15ms), remained unaltered, while the AV interval increased to 154±7ms. In the remaining heart (7%, AV interval 47ms) with a concurrent ventricular activation pattern (LVB and LVA activation simultaneously) at baseline, adenosine increased the AV interval to 149ms and the RVB was shown to be the location of earliest ventricular activation. Interestingly, in hearts with base-first activation, conduction through the AP also decreased markedly indicating intrinsic AV nodal conduction properties.

Immunohistochemical Correlations with Electrophysiological Data

In all 16 sectioned post-septated embryonic quail hearts (HH35-44), a MLC2a positive myocardial AV continuity was found at the right posteroseptal region. In all hearts, one or more, mostly right-sided additional AV continuities could be identified up until stage HH44. Left-sided continuities were frequently found in HH35-39 hearts (9/10,90%), while only 1/6 (17%) of HH40-44 hearts showed a left-sided continuity (**Table 3**). All APs could be followed easily from section to section. Interestingly, all MLC2a positive myocardial APs found in these embryonic post-septated hearts also stained positive for periostin, a non-myocardial marker. In **Figure 5A-H** representative examples of MLC2a and periostin staining in a HH36 and HH39 embryonic heart are given.

Embryo #	HH-stage	Location of AP	Cumulative (and individual) AP width in µm (AP-widths)	Global Activation Pattern
1	36	RAS+RMS+ RPS+LAS+LAL	120 (30,15,30,20,25)	RVB-first
2	37	RAS+RMS+RPS+RML+LPS	100 (25,15,30,15,15)	LVA-first
3	37	RMS+RPS+RPM+RML	135 (25,40,30,40)	RVB-first
4	38	RMS+RPS+RMP+LMS+LPL	140 (40,45,15,15,25)	LVA-first
5	38	RAS+RMS+RPS+RMP+LML	120 (20,25,30,20,25)	LVA-first
6	38	RMS+RPS+RPL+RMP+LPS	140 (35,30,40,20,15)	RVB+LVA concurrent
7	39	RAS+RMS+RPS+RMP+LML	115 (20,35,25,20,15)	LVA-first
8	39	RMS+RPS+RMP+LAS+LML	80 (15,30,15,10,10)	RVB+LVA concurrent
9	39	RAS+RPS+LMS+LML+LPS	115 (30,40,15,15,15)	LVB-first
10	39	RMS+RPS+RPM+LML	85 (25,35,15,10)	LVB-first
11	40	RAS+RPS	45 (15,30)	LVA-first
12	40	RMS+RPS+RMP	80 (25,35,20)	LVA-first
13	41	RMS+RPS	40 (15,25)	LVA-first
14	41	RMS+RPS	40 (20,20)	LVA-first
15	42	RMS+RPS+LPS	75 (20,45,10)	LVB-first
16	44	RMS+RPS	30 (10,20)	RVB-first

Table 3. Location of APs, cumulative and individual width and corresponding global activation patterns in the 16 morphologically analyzed embryonic quail hearts. AP=accessory pathway, RAS=right anteroseptal, RMS=right midseptal, RPS=right posteroseptal, RMP=right midposterior, RPL=right posterolateral, LAL=left anterolateral, LAS=left anteroseptal, LAL=left anterolateral, LMS = left midseptal, LPS=left posteroseptal, LPL=left posterolateral.

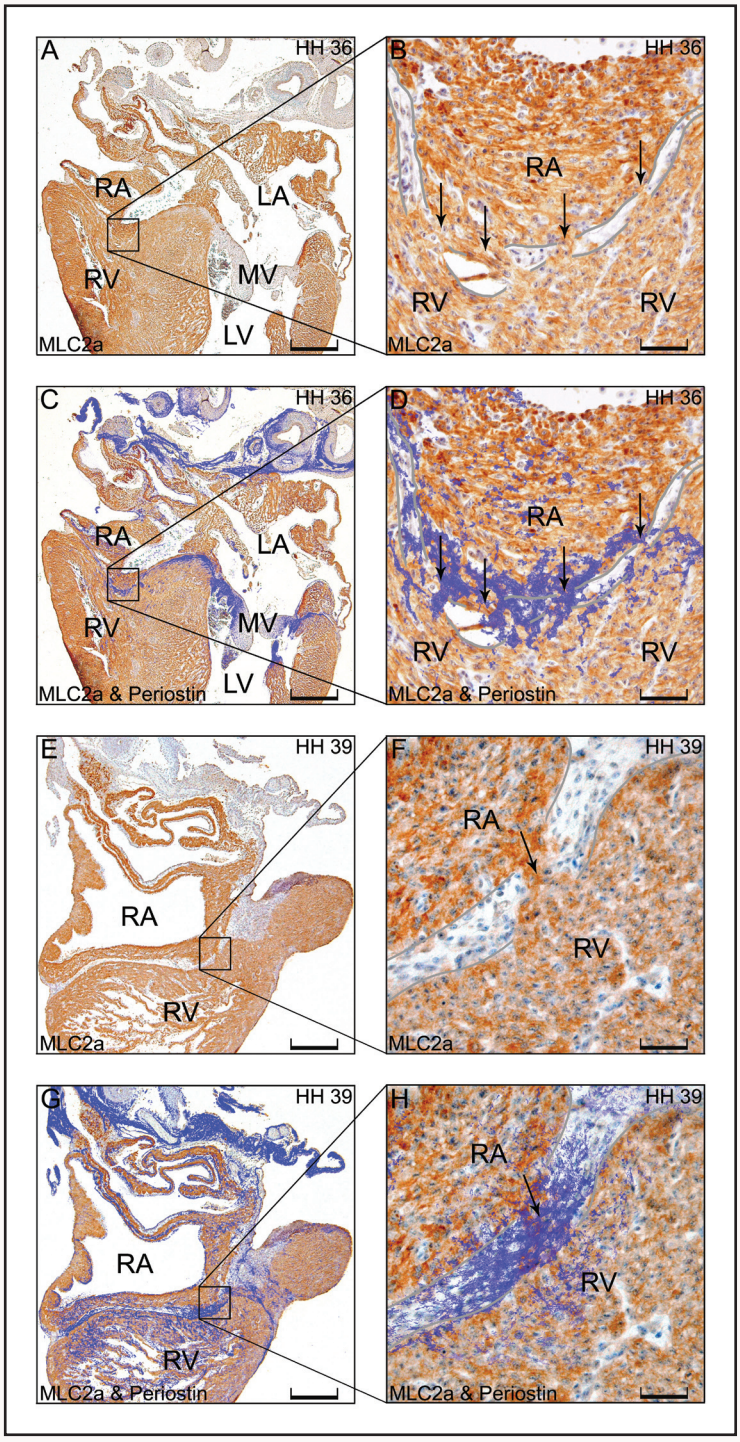
A
HH 36
RA
LA
RV
MV
LV
MLC2a
B
HH 36
RA
RV
RV
MLC2a
C
HH 36
RA
LA
RV
MV
LV
MLC2a & Periostin
D
HH 36
RA
RV
RV
MLC2a & Periostin
E
HH 39
RA
RV
MLC2a
F
HH 39
RA
RV
MLC2a
G
HH 39
RA
RV
MLC2a & Periostin
H
HH 39
RA
RV
MLC2a & Periostin

Figure 5. **A.** Morphological findings in a representative example of a post-septated HH36 quail heart, which demonstrated earliest ventricular activation at the RVB. Histologically, a broad region of AV-myocardial continuity was found in the RPS region of the MLC2a stained slides. Bar = 1000μm. **B.** Magnification of boxed area, in which these AV-myocardial continuities (arrows), are shown. Bar = 100μm. **C.** Periostin staining (blue) from adjacent section, superimposed on the MLC2a stained section, showing periostin expression in the AV-myocardial bridges. Bar = 1000μm. **D.** Magnification of boxed area. Bar = 100μm. **E.** Morphological findings in a representative example of a post-septated HH39 quail heart, which demonstrated concurrent activation of the RVB and LVA. Histologically, a small RPS AV-myocardial continuity was found in the MLC2a stained slides. Bar = 1000μm. **F.** Magnification of boxed area, in which this AP (arrow), is shown to course through the insulating annulus fibrosis. Bar = 100μm. **G.** Periostin staining (blue), showing marked periostin expression in the AP. Bar = 1000μm. **H.** Magnification of boxed area. Bar = 100μm.

Longitudinal analysis showed that with increasing developmental stage both the number ($p=0.004$) and width ($p=0.179$) of APs decreased. Whereas hearts at HH35-39 showed multiple broad APs in various locations, hearts at HH40-44 primarily harbored small AV continuities in the right posteroseptal and right midseptal region, while the adult heart demonstrated complete fibrous annular isolation.

Morphological findings could not be directly correlated with electrophysiological data: right- or left-sided APs were found both in embryonic hearts displaying earliest ventricular activation at the RVB or LVB as in hearts with a concurrent or apex-to-base global ventricular activation pattern (**Table 3**). Morphologically, the APs showed no discriminating features which could explain these different ventricular activation sequences.

Discussion

We analyzed ventricular activation patterns in embryonic and adult quail hearts using extracellular electrode recording techniques and correlated these activation patterns with the morphology of the insulating AV annulus. Key finding of this study is that although the LV-activation pattern in septated hearts changed from an immature base-to-apex to a mature apex-to-base pattern, premature activation of the RVB and LVB remained present in 51%(33/65) of post-septated hearts up to HH44 (hatching at HH45-46). This premature ventricular base activation can morphologically be explained, as shown in this study, by persisting accessory myocardial continuities between atrium and ventricle.

Transition of the Ventricular Activation Sequence Versus Persistent Early Activation of the Ventricular Base

While hearts at pre-septational stages of development (group A) primarily exhibited an immature base-to-apex pattern of LV-activation (9/15; 60%), hearts at post-septational stages of development (group $B_{1,2}$) demonstrated a mature apex-to-base LV-activation pattern in the vast majority of cases (47/65; 72%). This transition from an immature base-to-apex to a mature apex-to-base LV-activation pattern has been studied previously and is associated with maturation of the HPS.[12, 13, 15-19] Optical mapping studies indeed showed that this transition marks the emergence of mature 'apex-first' epicardial breakthrough near the termini of the bundle branches and demonstrated that right and left bundle branch apical breakthrough sites appear at HH29 and HH35 respectively,[15] which is consistent with the transition of the LV-activation sequence occurring at HH35 in this study. Different from previous studies, we observed that in post-septated hearts (HH35-44), the ventricular base could still be "prematurely" activated in a significant number of cases (33/65,51%). For instance, the RVB was activated prior to the LVA in 11(17%) cases and the LVB prior to the LVA in 5(8%) cases, while in another 17(26%) hearts the ventricular base and LVA were activated simultaneously. This simultaneous activation can, given the position of our recording electrodes (**Figure 1**), most likely be explained by simultaneous conduction over two different pathways, being the AVN/HPS on one hand and an AP on the other hand. Furthermore, in 44% (4/9) of hearts with an apex-to-base global ventricular activation pattern at baseline, the ventricular activation pattern switched to base-to-apex after administration of adenosine, indicating conduction through an AP.

Thus, in contrast to previous studies, our data show that despite maturation of the HPS and transition of the LV-activation sequence from base-to-apex to apex-to-base, premature and direct activation of the ventricular base remained present in 51% of post-septated hearts at baseline.

Early Activation of The Ventricular Base in Post-Septated Embryonic Hearts can be Explained by Persisting AV Continuities

In the present study, continuities between atrial and ventricular myocardium were found in the posteroseptal region of the tricuspid annulus in all 16 analyzed post-septated quail hearts. In addition, in several hearts one or more connections were found mostly at the right anteroseptal and midseptal regions, while left-sided pathways were less frequently encountered (**Table 3**).

The fact that left-sided APs were structurally uncommonly found in late post-septated embryonic hearts (HH40-44)(1/6,17%), might reflect a developmental time-difference in completion of left and right AV ring isolation, which agrees with a previous description that the left annulus fibrosis in the human adult heart is anatomically usually well formed and nearly always complete, in contrast to the poorly formed and at many sites deficient right annulus fibrosis.[23] Further supported by the demonstrated difference in AV interval between hearts with earliest ventricular activation at the RVB (74±31 ms) versus the LVB (62±15 ms)(p=0.540), it may be speculated that different developmental mechanisms can be anticipated to cause the appearance of right- and left-sided APs.

Normal Development of the Isolating AV ring: Possible Fate of Persisting AV Connections and Periostin Expression

In the looped embryonic heart, the AV junction constitutes one of the slow conducting regions of the heart responsible for the sequential contraction pattern at this developmental stage.[11, 30] The subsequent separation of the atria and ventricles is thought to be caused by the fusion of the epicardially located AV sulcus with the endocardially situated AV cushions at the ventricular site of the junction.[31] The processes underlying atrial and ventricular myocardium dissociation are however still incompletely understood and the tissues responsible for the formation of the annulus fibrosis have yet remained mainly unknown. Epicardium Derived Cells (EPDCs) migrating through the developing AV dissociated borderline have been followed in their differentiation and shown to

become fibroblasts of the fibrous heart skeleton.[32] During formation of the annulus fibrosis, the embryonic slow conducting AV junctional myocardium becomes incorporated in the definitive atrium.[31, 33, 34] With completion of this AV isolation, the primitive AV myocardial connections make way for conduction through the AVN/HPS, which eventually constitutes the only remaining conduction pathway of the adult heart.[35] Since the sulcus and cushion tissue fuse at the ventricular side of the AV junctional myocardium,[31, 33, 34] we postulate that the myocardium of the APs found in the post-septated quail hearts consists of primitive remnants of the slow conducting AV junctional myocardium in the looped heart. This is in ample agreement with the relatively slow conduction through these pathways as found in our current study compared to the higher conduction velocity through the AVN/HPS and the decrease in conduction velocity through the AP after administrating adenosine.

Interestingly, in the present study anatomical AV myocardial continuities were found *both* in embryonic hearts exhibiting base-first activation as in those with a concurrent or apex-first activation pattern. Based on morphological data, we were unable to find any discriminating factors that can explain why some of the morphologically demonstrated APs in retrospect gave rise to premature ventricular activation and others did not. We propose that inter-embryonic variance in conduction properties of the AV connections on one hand and of the AVN/HPS on the other hand can be held responsible for this observation. Poor cellular coupling, a slow upstroke of the action potential and perhaps "zig-zag conduction" or an unfavorable source-sink relationship at the ventricular insertion side may all contribute to the very slow conduction or even conduction block at the AP causing preferential activation via the AVN/HPS.[36-38] In précis, the presence of an AP is required to give rise to ventricular preexcitation, but their mere presence does however not assure the existence of a faster route for anterograde AV conduction. The high prevalence of functional APs in hearts at late post-septational stages however strengthens the hypothesis that APs causing AV reentrant tachycardias in neonates are remnants of primitive AV myocardium.

Periostin was originally isolated as an osteoblast-specific factor that functions as a cell adhesion molecule involved in osteoblast recruitment, attachment and spreading. Expression of periostin mRNA was later also found in the embryonic mouse and chicken heart in the endocardial cushions that ultimately divide the primitive heart tube in a four-chambered heart.[39, 40] Periostin is secreted during cushion mesenchym formation[41] and has been suggested to

induce myocardium to transform into mesenchym of a mixed phenotype, which can subsequently transdifferentiate into cells with a fibrous identity, while at late stages of development periostin may also serve to maintain the integrity of the fibrous tissues of the heart.[41, 42] At the boundary where myocardial cells directly face endocardial cushion tissue at the AV junction, periostin expression is enhanced and myocardial cells are replaced over time by dense fibrous periostin-positive tissue.[43] Periostin is also abundantly present in epicardium and EPDCs.

Based on our observations that 1) the functionality, number and width of persisting APs decreased with developmental stage, 2) the persistent APs all stained positive for periostin and 3) APs were functionally and structurally absent in the adult quail heart, we assume that periostin expression in persistent myocardial APs perinatally results in inhibition of the myocardial phenotype by transdifferentiation of these myocytes into fibrous tissue. This implicates that these AV connections will thus disappear within the first weeks to months after birth.

This postulated ongoing process of isolation of the AV ring postnatally provides a good etiological explanation for the clinical observation that AV reentrant tachycardias in human neonates spontaneously disappear before the age of 1 year in the majority of cases,[4, 5] which is further strengthened by the previously reported remarkable morphological transformations of the sinus node, AVN and bundle of His, which similarly commences about 1-2 weeks after birth.[44-46] Furthermore, local failure or a delay in this remodeling process until adolescence or adulthood, may explain the occurrence of reentrant tachycardias later in life.[46]

Limitations of the Study

It was the aim of this study to investigate whether AV conduction remains possible via remnants of AV connections in post-septated hearts despite the well known maturation of the HPS. Although we indeed showed that early activation of the ventricular base is present in a large number of post-septated hearts, which can be explained by the demonstrated persisting connections between atrial and ventricular myocardium, we did not demonstrate that the strands of tissue found by immunohistochemical staining were indeed the structures responsible for the recorded premature ventricular activation. For this, detailed mapping of impulse propagation via these connections and 1:1 correlation with morphology in all hearts will be necessary.

Furthermore, in order to meet the metabolic demands of the older embryonic hearts we performed our experiments, similar to others,[11] at subphysiological temperatures (30°C). Although this might have had an effect on our measurements (e.g. slower heart rates or longer conduction times), the recorded AV intervals, time-differences between apex and base activation and the developmental stage at which the transition in LV-activation sequence occurred, were comparable to previous studies.[12, 13, 15, 17, 18]

Conclusions

AV myocardial pathways bypassing the AVN remain present and functional in hearts at late post-septational stages of embryonic development and may provide a physiological substrate for AV reentrant tachycardias in peri- and postnatal life. However, since 1) the number of embryonic hearts with premature ventricular base activation decreased significantly with developmental stage, 2) a decrease in both AP-number and AP-width was observed in a similar time-course, 3) persistent APs stained positive for periostin and 4) APs were proven to be structurally and functionally absent in the adult heart, it is likely that these AV connections will disappear within the first weeks to months after birth. Further research should clarify the processes causing the disappearance or persistence of these APs more precisely.

Funding Sources

None

Disclosures

None

References

1. Ko JK, Deal BJ, Strasburger JF, Benson DW. Supraventricular tachycardia mechanisms and their age distribution in pediatric patients. *Am J Cardiol.* 1992;69(12):1028-1032.
2. Kolditz DP, Blom NA, Bökenkamp R, Bootsma M, Zeppenfeld K, Schalij MJ. Radiofrequency catheter ablation for treating children with cardiac arrhythmias: favourable results after a mean of 4 years. *Ned Tijdschr Geneeskd.* 2005;149(24):1339-1346.
3. Morady F. Catheter ablation of supraventricular arrhythmias: state of the art. *J Cardiovasc Electrophysiol.* 2004;15(1):124-139.
4. Bauersfeld U, Pfammatter JP, Jaeggi E. Treatment of supraventricular tachycardias in the new millennium--drugs or radiofrequency catheter ablation? *Eur J Pediatr.* 2001;160(1):1-9.
5. Weindling SN, Saul JP, Walsh EP. Efficacy and risks of medical therapy for supraventricular tachycardia in neonates and infants. *Am Heart J.* 1996;131(1):66-72.
6. Kolditz DP, Blom NA, Bökenkamp R, Schalij MJ. Low-energy radiofrequency catheter ablation as therapy for supraventricular tachycardia in a premature neonate. *Eur J Pediatr.* 2005;164(9):559-562.
7. Janse MK, Anderson RH, van Capelle FJ, Durrer D. A combined electrophysiological and anatomical study of the human fetal heart. *Am Heart J.* 1976;91(5):556-562.
8. Kamino K. Optical approaches to ontogeny of electrical activity and related functional organization during early heart development. *Physiol Rev.* 1991;71(1):53-91.
9. Patten BM. The initiation of contraction in th embryonic chick heart. *Am J Anat.* 1933;53(349-375).
10. Patten BM. Initiation and early changes in the character of the heart beat in vertebrate embryos. *Physiol Rev.* 1949;29(1):31-47.
11. de Jong F, Opthof T, Wilde AA, Janse MJ, Charles R, Lamers WH, Moorman AF. Persisting zones of slow impulse conduction in developing chicken hearts. *Circ Res.* 1992;71(2):240-250.
12. Chuck ET, Freeman DM, Watanabe M, Rosenbaum DS. Changing activation sequence in the embryonic chick heart. Implications for the development of the His-Purkinje system. *Circ Res.* 1997;81(4):470-476.

13. Chuck ET, Meyers K, France D, Creazzo TL, Morley GE. Transitions in ventricular activation revealed by two-dimensional optical mapping. *Anat Rec.* 2004;280(2):990-1000.

14. Moorman AF, Lamers WH. Molecular anatomy of the developing heart. *Trends Cardiovasc Med.* 1994;4:257-264.

15. Reckova M, Rosengarten C, deAlmeida A, Stanley CP, Wessels A, Gourdie RG, Thompson RP, Sedmera D. Hemodynamics is a key epigenetic factor in development of the cardiac conduction system. *Circ Res.* 2003;93(1):77-85.

16. Rothenberg F, Nikolski VP, Watanabe M, Efimov IR. Electrophysiology and anatomy of embryonic rabbit hearts before and after septation. *Am J Physiol Heart Circ Physiol.* 2005;288(1):H344-351.

17. Rothenberg F, Watanabe M, Eloff B, Rosenbaum D. Emerging patterns of cardiac conduction in the chick embryo: waveform analysis with photodiode array-based optical imaging. *Dev Dyn.* 2005;233(2):456-465.

18. Sedmera D, Reckova M, Bigelow MR, deAlmeida A, Stanley CP, Mikawa T, Gourdie RG, Thompson RP. Developmental transitions in electrical activation patterns in chick embryonic heart. *Anat Rec.* 2004;280(2):1001-1009.

19. Sedmera D, Reckova M, Rosengarten C, Torres MI, Gourdie RG, Thompson RP. Optical mapping of electrical activation in the developing heart. *Microsc Microanal.* 2005;11(3):209-215.

20. Davies F. The conducting system of the bird's heart. *J Anat.* 1930;64:129-146.

21. Lieberman M, P. The electrophysioloical Organization of the Embryonic Chick Heart. *J Gen Physiol.* 1965.

22. Rentschler S, Vaidya DM, Tamaddon H, Degenhardt K, Sassoon D, Morley GE, Jalife J, Fishman GI. Visualization and functional characterization of the developing murine cardiac conduction system. *Development.* 2001;128(10):1785-1792.

23. Becker AE, Anderson RH, Durrer D, Wellens HJ. The anatomical substrates of wolff-parkinson-white syndrome. A clinicopathologic correlation in seven patients. *Circulation.* 1978;57(5):870-879.

24. Klein GJ, Hackel DB, Gallagher JJ. Anatomic substrate of impaired antegrade conduction over an accessory atrioventricular pathway in the Wolff-Parkinson-White syndrome. *Circulation.* 1980;61(6):1249-1256.

25. Ohnell RF. Preexcitation, a cardiac abnormality. *Acta Med Scand.* 1944;152:1-167.

26. Peters NS, Rowland E, Bennett JG, Green CR, Anderson RH, Severs NJ. The Wolff-Parkinson-White syndrome: the cellular substrate for conduction in the accessory atrioventricular pathway. *Eur Heart J.* 1994;15(7):981-987.

27. Wood FC. Histologic demonstration of ccessory muscular connections between auricle and ventricle in a case of short P-R interval and prolonged QRS complex. *Am Heart J.* 1943;25:454-462.

28. Jongbloed MR, Wijffels MC, Schalij MJ, Blom NA, Poelmann RE, van der Laarse A, Mentink MM, Wang Z, Fishman GI, Gittenberger-de Groot AC. Development of the right ventricular inflow tract and moderator band: a possible morphological and functional explanation for Mahaim tachycardia. *Circ Res.* 2005;96(7):776-783.

29. Hamburger V, Hamilton HL. A series of normal stages in the development of the chick embryo. 1951. *Dev Dyn.* 1992;195(4):231-272.

30. Argüello C, Alanís J, Pantoja O, Valenzuela B. Electrophysiological and ultrastructural study of the atrioventricular canal during the development of the chick embryo. *J Mol Cell Cardiol.* 1986;18(5):499-510.

31. Wessels A, Markman MW, Vermeulen JL, Anderson RH, Moorman AF, Lamers WH. The development of the atrioventriclar junction in the human heart. *Circ Res.* 1996;78:110-117.

32. Gittenberger-de Groot AC, Vrancken Peeters MP, Mentink MM, Gourdie RG, Poelmann RE. Epicardium-derived cells contribute a novel population to the myocardial wall and the atrioventricular cushions. *Circ Res.* 1998;82(10):1043-1052.

33. Di Lisi R, Sandri C, Franco D, Ausoni S, Moorman AF, Schiaffino S. An atrioventricular canal domain defined by cardiac troponin I transgene expression in the embryonic myocardium. *Anat Embryol.* 2000;202(2):95-101.

34. Kim JS, Virágh S, Moorman AF, Anderson RH, Lamers WH. Development of the myocardium of the atrioventricular canal and the vestibular spine in the human heart. *Circ Res.* 2001;88(4):395-402.

35. Lev M, Lerner R. The theory of Kent; a histologic study of the normal atrioventricular communications of the human heart. *Circulation.* 1955;12(2):176-184.

36. Cranefield PF, Wit AL, Hoffman BF. Conduction of the cardiac impulse. 3. Characteristics of very slow conduction. *J Gen Physiol.* 1972;59(2):227-246.

37. de Bakker JM, van Capelle FJ, Janse MJ, Tasseron S, Vermeulen JT, de Jonge N, Lahpor JR. Slow conduction in the infarcted human heart. 'Zigzag' course of activation. *Circulation.* 1993;88(3):915-926.

38. Jalife J, Sicouri S, Delmar M, Michaels DC. Electrical uncoupling and impulse propagation in isolated sheep Purkinje fibers. *Am J Physiol.* 1989;257(1 Pt 2): H179-189.

39. Kruzynska-Frejtag A, Machnicki M, Rogers R, Markwald RR, Conway SJ. Periostin (an osteoblast-specific factor) is expressed within the embryonic mouse heart during valve formation. *Mech Dev.* 2001;103(1-2):183-188.

40. Norris RA, Kern CB, Wessels A, Moralez EI, Markwald RR, Mjaatvedt CH. Identification and detection of the periostin gene in cardiac development. *Anat Rec.* 2004;281(2):1227-1233.

41. Kern CB, Hoffman S, Moreno R, Damon BJ, Norris RA, Krug EL, Markwald RR, Mjaatvedt CH. Immunolocalization of chick periostin protein in the developing heart. *Anat Rec.* 2005;284(1):415-423.

42. Ji X, Chen D, Xu C, Harris SE, Mundy GR, Yoneda T. Patterns of gene expression associated with BMP-2-induced osteoblast and adipocyte differentiation of mesenchymal progenitor cell 3T3-F442A. *J Bone Miner Metab.* 2000;18(3):132-139.

43. Litvin J, Zhu S, Norris R, Markwald R. Periostin family of proteins: therapeutic targets for heart disease. *Anat Rec.* 2005;287(2):1205-1212.

44. James TN. Sudden death in babies: new observations in the heart. *Am J Cardiol.* 1968;22(4):479-506.

45. James TN. Cardiac conduction system: fetal and postnatal development. *Am J Cardiol.* 1970;25(2):213-226.

46. James TN. Normal and abnormal consequences of apoptosis in the human heart. From postnatal morphogenesis to paroxysmal arrhythmias. *Circulation.* 1994;90(1):556-573.

Clinical Perspective

The embryogenesis of the structures involved in AV conduction is as intriguing as it is unexplained. Nonetheless, knowledge of the anatomical substrates resulting in accessory pathway mediated tachycardia has progressed from being of purely scientific interest to being integral to the management of patients who suffer from them. Within a short time, the primary heart tube transforms into a four chambered heart. Whereas initially sequential activation is caused by slow conduction over the circumferential AV continuity, the AV ring becomes isolated in later stages and conduction runs through the AVN/His-Purkinje system (HPS). As a result, ventricular activation changes from an immature base-to-apex pattern in pre-septated hearts to a mature apex-to-base sequence in post-septated hearts. Abnormal development of the annulus fibrosis resulting in accessory pathways may cause AV reentrant arrhythmias. Because these arrhythmias frequently occur in fetuses and neonates, we hypothesized that during normal development, primitive AV connections bypassing the annulus fibrosis remain present even after development of the HPS. We indeed demonstrated that the annulus fibrosis in post-septated prenatal quail hearts is still far from complete, resulting in functional AV myocardial pathways. We speculate that AV ring isolation continues postnatally implicating disappearance of accessory AV connections within the first weeks after birth, which provides an etiological explanation for the clinical observation that AV reentrant tachycardias in human neonates spontaneously obliterate before the age of 1 year in the majority of cases. Local failure or a delay in this remodeling process of the isolating AV ring until adulthood may explain the occurrence of AV reentrant tachycardia, a prevalent adult arrhythmia, later in life.

Online Data Supplement

Materials and Methods

Experimental Preparations

Fertilized eggs of the Japanese quail (*Coturnix coturnix japonica*) were incubated blunt end up at 37.5°C and 80% humidity. All animal experiments were in accordance with the institutional guidelines of the Leiden University Medical Center. After termination of incubation at the desired developmental stages (HH 30-34, n = 15, group A; HH 35-44, n = 65, group B) and staging according to Hamburger-Hamilton criteria,[1] the embryonic hearts were carefully isolated from the embryo under a dissecting microscope (Wild Heerbrugg, M3, Switzerland) after euthanization by decapitation. Additionally, 6 hearts were harvested from adult quails (5-6 months) after cervical dislocation.

The hearts were placed into a custom-built fluid-heated temperature-controlled superfused tissue bath (epoxy). The bottom of the tissue bath was covered with agarose (Invitrogen™ Life Technologies) to allow fixation of the hearts with fine wires through non-cardiac tissue at the inflow and outflow sides of the heart. The embryonic hearts (30±0.1°C) were superfused and the adult hearts Langendorff-perfused (65mmHg, 37±0.1°C) with carboxygenated (95% O_2 and 5% CO_2) Tyrode's solution with the following composition (mmol/l): NaCl 130, KCl 4, KH_2PO_4 1.2, $MgSO_4$ 0.6, $NaHCO_3$ 20, $CaCl_2$ 1.5, glucose 10 (pH 7.35).

Electrophysiological Recordings – Technical Features

Unipolar extracellular recordings were performed by positioning 4 tungsten electrodes (tip diameter; 1-2 μm; impedance 0.5-1.0 MΩ, World Precision Instruments Inc., Berlin, Germany) on the surface of the hearts, using microscopic guided micromanipulators (Wild Heerbrugg, M7A, Switzerland). In all experiments, the electrodes were consistently positioned on the left atrium (LA), the right ventricular base (RVB), left ventricular base (LVB) and left ventricular apex (LVA), as shown in **Figure 1**. An Ag/AgCl electrode in the tissue bath served as reference electrode.

Electrograms were recorded using a high-gain low-noise DC bio-amplifier system (Iso-DAM8A; World Precision Instruments Inc., Berlin, Germany) with 4 isolated preamplifier modules with an input impedance of $>10^{12}$ Ω. The signals were band-pass- (300 Hz-1 kHz) and notch-filtered (50Hz) before being digitized at a sampling rate of ≥1 kHz using a computerized recording system (Prucka

Engineering Inc., Houston TX., USA) and stored on optical disks for offline analysis.

Pacing was performed with a stimulator (EP-3 clinical stimulator, EP MedSystems Inc., West-Berlin NJ, U.S.A.), providing monophasic stimuli (stimulus strength 5-10 mA, stimulus width 1.0 ms). The embryonic hearts were stimulated through a bipolar tungsten electrode (interelectrode distance 125 microns (World Precision Instruments Inc., Berlin, Germany)) mounted on a small custom-built carbon-fiber manipulator at the high right atrium (RA) with a cycle length (CL) of 500 ms (slightly shorter than the observed spontaneous sinus CL). Stable capture of the RA was judged by 1:1 left atrial electrical activity. Similarly, 1:1 atrioventricular conduction was objectified by a sequential and stable relationship between atrial and ventricular electrical activity. In all experiments, electrical activity was confirmed visually by mechanical activity (contraction) of the atria and ventricles.

Surface ECGs in adult quail hearts were recorded by placing 3 silver wire electrodes (0.5 mm) in a triangle in the petri-dish. The electrodes were glued in position and connected to one of the isolated preamplifier modules with an input impedance of $>10^{12}$ Ω of a high-gain low-noise DC bio-amplifier system (Iso-DAM8A; World Precision Instruments Inc., Berlin, Germany). The ECGs were digitally recorded as bipolar between two electrodes (Prucka Engineering Inc., Houston TX., USA) continuously during and simultaneously with extracellular electrogram recordings.

Electrophysiological Recording Protocol

As described above, recording electrodes were positioned on the LA, RVB, LVB and LVA in all experiments. The preparations were allowed to equilibrate for 10 minutes before start of the recording protocol.

Hearts were categorized in three groups: group A (HH30-34, n=15), group B (HH35-44, n=65) and group C (5-6 months, n=6). Embryonic hearts in group A, hearts in group B with a stable spontaneous HR of at least 60 bpm (group B_1) and hearts in group C were allowed to beat spontaneously, whereas hearts with a HR of <60 bpm (group B_2) were stimulated at a fixed CL of 500 ms.

Because of its negative dromotropic effects on the atrioventricular (AV) node,[2, 3] adenosine was used to analyze transitions in ventricular activation sequence after slowing atrioventricular conduction through the AVN. Since the onset of pharmacological sensitivity of embryonic chick hearts for the negative chronotropic effect of adenosine is reported to occur on embryonic day 7 (HH

stage 31) and does not exert its full effect until day 12 (HH stage 38),[3] we postulated that sensitivity for the full dromotropic effect would occur around the same developmental stage of embryonic development as the chronotropic effect does and therefore conducted these experiments in embryonic hearts of at least HH stage 38. Furthermore, we analyzed the effect of adenosine on ventricular activation sequence only in post-septated embryonic quail hearts driven by external pacing to exclude possible bias in our results as a result of the negative chronotropic effect of adenosine on the sinoatrial (SA) node.[2]

Adenosine was administered in 15 hearts (HH 38-41) by slowly adding 1 ml adenosine (0.3 mg/ml) on the embryonic quail heart in a petri-dish containing 10 ml Tyrode's solution to a final concentration of 0.03 mg/ml (0.11 μM).

The steepest negative deflection of the unipolar electrogram was taken as the local activation time. Local depolarization time was consequently calculated from each of the four digitized recorded electrograms using the sample-point average of 10 consecutive beats.

Definitions

The variability in measuring local depolarization time for 10 consecutive beats was associated with a mean standard deviation of 0.4 ms (range 0.2-0.9 ms). Therefore, a mean difference in local depolarization time between two recording electrodes of ≥ 1 ms was considered to be significant. As a consequence, the *left* ventricular activation sequence was denominated as 1) base-to-apex if the LVB depolarized ≥ 1 ms earlier than the LVA, 2) apex-to-base if the LVA depolarized ≥ 1 ms earlier than the LVB and 3) concurrent if the time difference between LVB and LVA activation was < 1 ms.

In all experiments, a stable 1:1 relation between atrial activation and ventricular activation was assured to be present. The time difference between LA activation and the location of earliest ventricular activation was denominated as the AV interval both in embryonic hearts beating in sinus rhythm as in hearts driven by RA-pacing. The number of different APs in each heart was denominated as the AP-number, while the cumulative width (in μm) of all the APs in each heart was denominated as the AP-width.

Immunohistochemistry

After completion of the electrophysiological recordings, the hearts were removed from the Tyrode's solution and fixated in a 4% paraformaldehyde solution for 24 hours, dehydrated and embedded in paraffin. Subsequently, 16 preparations

of post-septated quail hearts which displayed variable ventricular activation sequences (**Table 3**) and one adult quail heart were serially sectioned in the frontal plane at 5 μm and 7 μm respectively, and transferred to albumin/glycerin-coated objective slides.

After deparaffinization and rehydration, the adult sections were prepared for standard Haematoxylin-Eosin (HE) staining and the embryonic sections were treated with 0.3% H_2O_2 in phosphate buffered saline (PBS) for 20 minutes to smother endogenous peroxidase activity. Routine immunohistochemical staining was performed by overnight incubation with the primary antibody; rabbit primary antibodies against Myosin-Light-Chain 2 atrium (MLC2a)[4] diluted 1:5000 and against periostin[5, 6] diluted 1:200 in PBS with 0.05% Tween-20 and 1% Bovine Serum Albumin (BSA) (Sigma Aldrich, USA) in a humified chamber.

After rinsing in PBS and PBS-Tween, the sections were incubated with Goat-anti-Rabbit IgG labeled with biotin (GAR-Biotin) diluted 1:200 and Goat-serum diluted 1:66 in PSB-Tween for 40 minutes. Goat-serum was used to block aspecific binding of the secondary antibody. After rinsing in PBS and PBS-Tween, the sections were incubated with ABC-reagent, which consisted of reagent A diluted 1:100 and reagent B diluted 1:100 in PBS for the MLC2a sections and reagent A diluted 1:50 and reagent B diluted 1:50 in PBS for the periostin sections, in a humified chamber for 40 minutes. After rinsing with PBS, PBS-Tween and tris/maleate pH 7.6, the sections were incubated with 3,3'-diaminobenzidin (DAB) in a concentration of 400 mg/l with 4 droplets of H_2O_2 acting as a catalyzer, for 5 minutes. After incubation with DAB, the sections were rinsed with H_2O-demi and counterstained with 0.1% Heamatoxylin (Merck, Darmstadt, Germany) for 10 seconds. Finally, the sections were rinsed with tap water for 10 minutes, dehydrated and mounted in Entellan.

MLC2a is a protein, which is predominantly expressed in atrial myocardium and to a lesser extent in the ventricular myocardium and outflow tract of the heart. Anti-MLC2a is a polyclonal antibody raised in rabbit against mouse MLC2a.[4] This antibody was a gift from Dr. S.W. Kubalak (Charleston SC, USA). Probably due to a large homology of MLC2a in mice and avians, preliminary studies showed that this antibody could also be used in quails. Periostin is a member of the fasciclin gene family and acts as a cell adhesion protein that is expressed during cushion mesenchyme formation and throughout valvulogenesis and is thought to function in the organization of extracellular matrix molecules, providing cues necessary for attachment and spreading during the epithelial-to-mesenchymal transitions (EMT) of the endocardial epithelium.[5, 6] At post-

septational stages of avian heart development, periostin is predominantly found in the fibrous regions of the heart.[5] Anti-periostin is a polyclonal antibody raised in rabbit. This antibody was a gift from Prof. Dr. R.R. Markwald (Charleston, SC, USA).

Morphometric analysis of the AP-width (in μm) was performed by determining the number of frontally sectioned slides in which the AP could be followed multiplied by 5μm (slide thickness).

Statistical Analysis

Results are presented as means ± SD (range). χ^2-test, Student's t-test and Mann-Whitney's test were used to compare variables. P-values of < 0.05 were considered statistically significant.

The authors had full access to the data and take responsibility for its integrity. All authors have read and agree to the manuscript as written.

References

1. Hamburger V, Hamilton HL. A series of normal stages in the development of the chick embryo. 1951. *Dev Dyn.* 1992;195(4):231-272.
2. Belardinelli L, Lindern J, Berne RM. The cardiac effects of adenosine. *Prog Cardiovasc Dis.* 1989;32:73-79.
3. Blair TA, Parenti M, Murray TF. Development of pharmacological sensitivity to adenosine analogs in embryonic chick heart: role of A1 adenosine receptors and adenylyl cyclase inhibition. *Mol Pharmacol.* 1989;35:661-670.
4. Kubalak SW, Miller-Hance WC, O'Brien TX, Dyson E, Chien KR. Chamber specification of atrial myosin light chain-2 expression precedes septation during murine cardiogenesis. *J Biol Chem.* 1994;269(24):16961-16970.
5. Kern CB, Hoffman S, Moreno R, Damon BJ, Norris RA, Krug EL, Markwald RR, Mjaatvedt CH. Immunolocalization of chick periostin protein in the developing heart. *Anat Rec.* 2005;284(1):415-423.
6. Norris RA, Kern CB, Wessels A, Moralez EI, Markwald RR, Mjaatvedt CH. Identification and detection of the periostin gene in cardiac development. *Anat Rec.* 2004;281(2):1227-1233.

Chapter 3

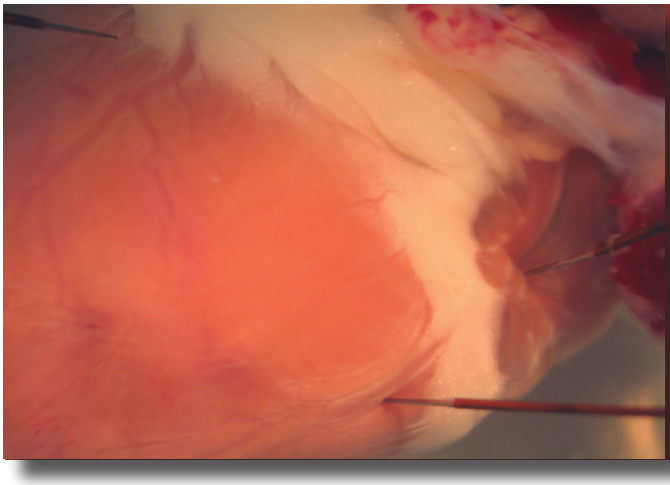

Denise P. Kolditz[1,2]
Maurits C.E.F. Wijffels[3]
Nico A. Blom[4]
Arnoud van der Laarse[1]
Nathan D. Hahurij[2,4]
Heleen Lie-Venema[2]
Roger R. Markwald[5]
Robert E. Poelmann[2]
Martin J. Schalij[1]
Adriana C. Gittenberger-de Groot[2]

[1]Department of Cardiology, Leiden University Medical Center, Leiden, The Netherlands;
[2]Department of Anatomy and Embryology, Leiden University Medical Center, Leiden, The Netherlands
[3]Department of Cardiology, St. Antonius Hospital, Nieuwegein, The Netherlands
[4]Department of Pediatric Cardiology, Leiden University Medical Center, Leiden, The Netherlands
[5]Department of Cell Biology and Anatomy, Medical University of South Carolina, Charleston, South Carolina

Epicardium-Derived-Cells (EPDCs) in Annulus Fibrosis Development and Persistence of Accessory Pathways

Circulation 2008;117(12):1508-1517

Abstract

Background. The developmental mechanisms underlying the persistence of myocardial accessory atrioventricular pathways (APs) bypassing the annulus fibrosis are mainly unknown. In this study, the role of Epicardium-Derived-Cells (EPDCs) in annulus fibrosis formation and the occurrence of APs were investigated.

Methods and Results. EPDC-migration was mechanically inhibited by *in-ovo* microsurgery in quail embryos. *In-ovo* electrocardiograms (ECGs) were recorded in wildtype (n=12) and EPDC-inhibited (n=12) hearts at Hamburger-Hamilton (HH) stages 38-42. Subsequently, in these EPDC-inhibited hearts (n=12) and in additional wildtype hearts (n=45) (HH38-42) *ex-ovo* extracellular electrograms were recorded. Electrophysiological data were correlated with differentiation markers for cardiomyocytes (MLC2a) and fibroblasts (periostin). *In-ovo* ECGs showed significantly shorter PR-intervals in EPDC-inhibited (45±10ms) compared to wildtype hearts (55±8ms, 95% C.I. 50-60 ms, p=0.030), while the QRS-durations were significantly longer in EPDC-inhibited hearts (29±14ms vs.19±2ms, 95% C.I 18-21 ms, p=0.011). Furthermore, *ex-ovo* extracellular electrograms (HH38-42) displayed base-first ventricular activation in 44%(20/45) of wildtype hearts, whereas in all EPDC-inhibited hearts (100%, 12/12) the ventricular base was activated first (p<0.001). Small, periostin and MLC2a-positive APs were found mainly in the posteroseptal region of both wildtype and EPDC-inhibited hearts. Interestingly, in all (n=10) EPDC-inhibited hearts, additional large periostin-negative and MLC2a-positive APs were found in the right and left lateral free wall coursing through marked isolation defects in the annulus fibrosis until the last stages of embryonic development.

Conclusions. EPDCs play an important role in annulus fibrosis formation. EPDC-outgrowth inhibition may result in marked defects in the fibrous annulus with persistence of large APs, resulting in ventricular preexcitation on ECG. These APs may provide a substrate for postnatally persistent reentrant arrhythmias.

Introduction

Accessory atrioventricular (AV) pathway mediated reentrant tachycardia (AVRT) is a common arrhythmia in humans.[1] It is well established that these accessory pathways (APs) consist of threads of abnormal cardiac musculature, crossing the fibrofatty AV grooves.[2] The AP in itself is however an enigma, since the etiological mechanisms underlying the appearance of these AV continuities remain as intriguing as they are unexplained.

It has long been thought that tissues of the endocardial AV cushions and epicardial AV grooves play a key role in the development of the electrically inert annulus fibrosis, thereby creating the isolating barrier between the atrial and ventricular tissues necessary for normal sequential activation of the heart.[3, 4] Recently, it was suggested that bone morphogenetic protein (BMP) signaling[5] and periostin induced AV junctional myocardial remodelling[6-8] play a critical role in configuration of the isolating annulus as well.

It is not uncommon that at birth annulus fibrosis formation is not completed and consequently APs can be found in embryonic wildtype quail hearts at near-hatching stages of embryonic development despite proper His-Purkinje-System (HPS) conduction and concurrent annulus fibrosis maturation.[6] These APs can persist for some time and provide the anatomical substrate for neonatal AVRTs, usually resolving spontaneously during the first year of life.[6, 9] The etiology of persistent AVRTs into childhood or adult life is however not fully understood, nor have the cell types and/or instructive signaling routes responsible for normal annulus fibrosis formation been fully elucidated.

Epicardium-Derived-Cells (EPDCs) migrating through the developing AV dissociated border may be crucial for proper annulus fibrosis formation, since the spatiotemporal expression of pro-collagen-I, a marker for collagen type-I synthesis, closely resembles the migratory patterns of EPDCs,[10-12] while abundant expression of periostin at the AV junction appears to be spatiotemporally co-localized with these cells.[8, 10] Moreover, periostin was recently found to co-localize and directly interact with collagen type-I in murine skin and heart valves.[13]

EPDCs originate from the proepicardium, which in avians initially develops as an outgrowth of the ventral wall of the intraembryonic splanchnopleural coelomic epithelium covering the sinus venosus.[14] After approximately 3 days of incubation (Hamburger-Hamilton (HH)[15] stage 16-18), the proepicardium transforms into a cauliflower-like cluster of vesicles - in avians generally referred to as the proepicardial organ (PEO)[16] - enabling proepicardial cells to migrate

over the myocardium to form the pericardium and epicardial monolayer.[14] A population of EPDCs is subsequently generated in the subepicardium resulting from epicardium-to-mesenchymal-transformation (EMT).[16, 17] Most EPDCs are generated in the intersegmented grooves,[10, 17-20] subsequently migrating through the continuous AV junctional myocardium to populate the endocardium-derived AV cushions.[10-12]

We hypothesize that EPDCs have an inductive role in annulus fibrosis formation, suggesting that postnatal APs may persist when EPDC-migration is inhibited. In wildtype and in *in-ovo* PEO-outgrowth inhibited quail embryos at postseptated stages of embryonic development, AV conduction was studied and correlated with annulus fibrosis morphology.

Methods

Experimental Preparations

Animal experiments were approved by the Committee on Animal Welfare of the Leiden University and conducted in compliance with the Guide for the Care and Use of Laboratory Animals (NIH Publication No.85-23, revised 1996). Fertilized eggs of the Japanese quail (*Coturnix coturnix japonica*, Leiden University) were incubated blunt end up at 37.5°C(80% humidity). Embryos were staged according to the Hamburger-Hamilton (HH) criteria.[15]

Outgrowth of the proepicardium was inhibited by performing *in-ovo* microsurgery, as described by Männer.[21] In short, on the third day of incubation (HH15-18), a small piece of eggshell membrane is inserted between the dorsal wall of the heart and the pericardial villi, cranially anchored in the sinu-atrial-sulcus and caudally constrained by the coelomic wall (**Figure 1**).

In-Ovo Electrocardiogram (ECG) Recordings

After termination of incubation at the desired developmental stages (HH38-42), a subset of quail eggs (EPDC-inhibition, n=12; wildtype, n=12) was prepared for *in-ovo* electrocardiogram (ECG) recording. The ECGs were digitally recorded (Prucka Engineering Inc., Houston TX., USA) continuously for 10-15 minutes in a small custom-built shielded incubator (37±0.1°C). *In-ovo* ECGs were evaluated by two independent observers.

After completion of ECG-recordings, euthanization by decapitation and subsequent staging, the embryonic hearts were isolated and prepared for *ex-ovo* extracellular electrogram recordings.

Ex-Ovo Extracellular Electrogram Recordings

Extracellular electrograms were recorded at HH38-42 in 45 wildtype and 12 EPDC-inhibited hearts during superfusion with oxygenated Tyrode solution, as previously described.[6] Definitions, immunohistochemistry, morphometry and statistical analysis are described in detail in the online-only Data Supplement. The authors had full access to the data and take responsibility for its integrity. All authors have read and agree to the manuscript as written.

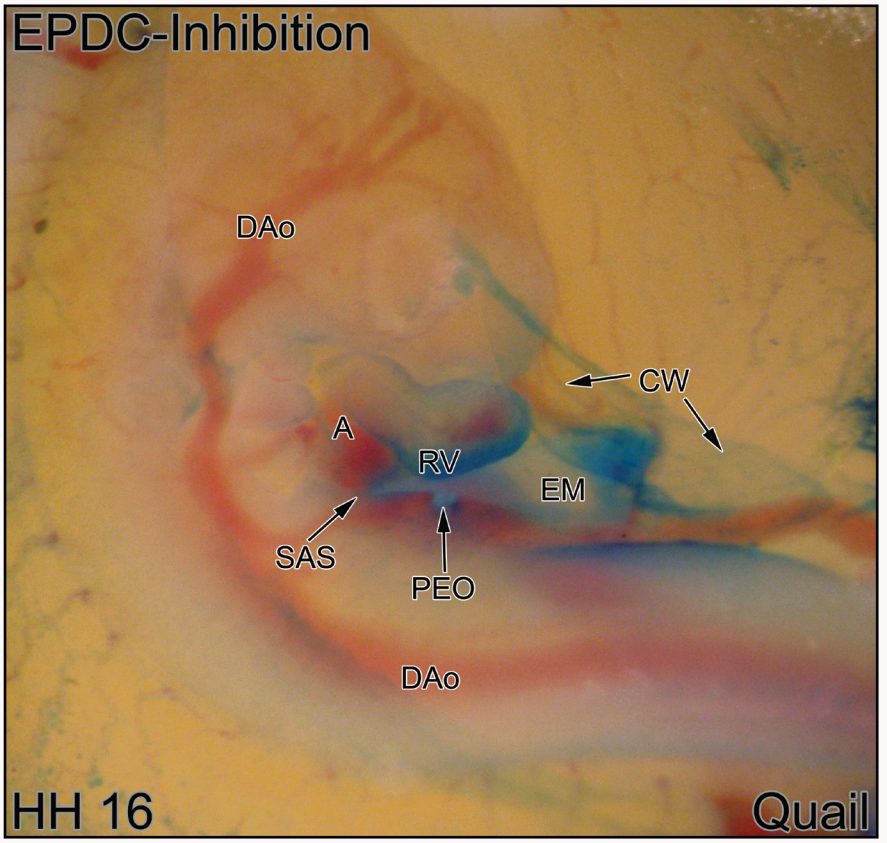

Figure 1. Representative example of the mechanical EPDC-inhibition technique in a HH16 quail embryo. A piece of eggshell membrane (EM) is placed between the right ventricle (RV) and the Pro-Epicardial-Organ (PEO). Nile blue staining was used to visualize transparent structures. SAS=Sinu-Atrial-Sulcus, CW=coelomic wall, DAo=dorsal aorta, A=atria.

Results

In-Ovo Electrocardiogram (ECG) Recordings

The heart rate (RR-interval) was similar in wildtype (n=12) and EPDC-inhibited (n=12) hearts (RR 246±29bpm vs. 252±39bpm,p=0.648). In 3/12 (25%) EPDC-inhibited hearts (group B_2) ECGs showed overt ventricular preexcitation reflected by: 1) short non-isoelectric PR-intervals, 2) initial slurring (delta-wave) and 3) resultant lengthening of the QRS-complexes. In these EPDC-inhibited hearts, the PR-interval during sinus rhythm was significantly shorter (33±12ms vs. 55±8ms,p=0.004), while the QRS-intervals were significantly longer (50±9ms vs.19±2ms,p=0.004) compared to wildtype hearts. EPDC-inhibited hearts in group B_1 (n=9) demonstrated slightly shortened PR-intervals (50±6ms vs. 55±8ms,p=0.165) and lengthened QRS-intervals (22±3ms vs. 19±2ms,p=0.064) compared to wildtype hearts. In EPDC-inhibited hearts the PR- and QRS-intervals were negatively correlated (Spearman's =ρ -0.314, p=0.320).

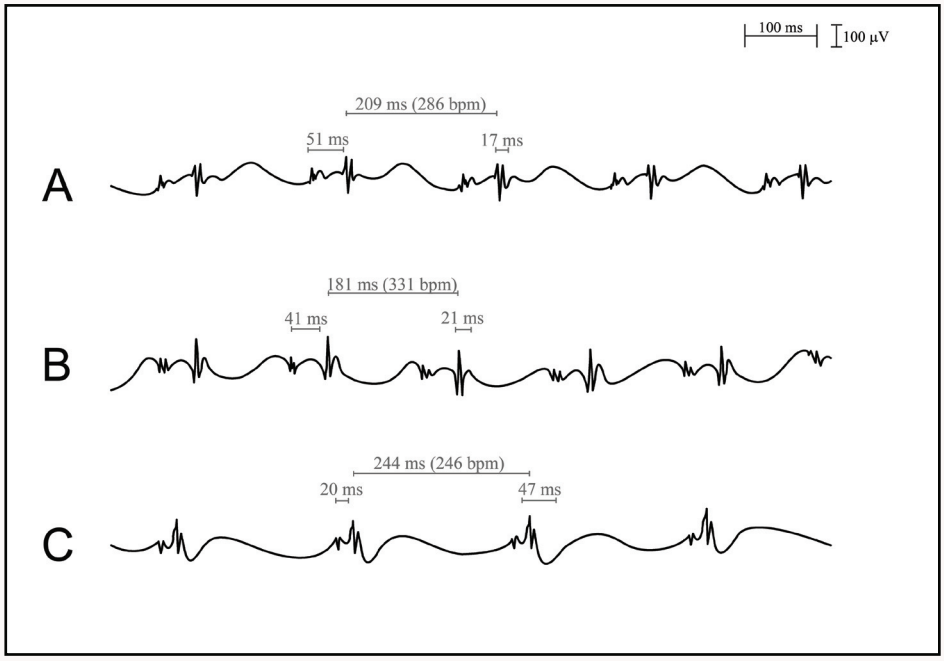

Figure 2. A. In-ovo ECG-recordings in a wildtype HH40 heart (group A). **B**. Recordings in an EPDC-inhibited HH40 heart (group B1) with a shortened PR-interval. **C**. Recordings in a HH41 EPDC-inhibited heart with overt preexcitation (group B2).

The ECG-evaluations of two independent observers were in agreement: P-values of 0.830 (PR), 0.344 (RR) and 0.187 (QRS) indicated no significant difference between the observers. Representative examples of *in-ovo* ECG-recordings in a wildtype HH40 heart (group A), an EPDC-inhibited HH40 heart (group B_1) and a HH41 EPDC-inhibited heart with overt preexcitation (group B_2) are shown in **Figures 2A, B** and **C**, respectively. **Table 1** summarizes the general electrophysiological (*in-ovo* and *ex-ovo*) characteristics of all analyzed quail hearts.

***In-Ovo* Electrocardiograms (ECGs)**

Group, HH-stage	n	RR(bpm)	PR(ms)	QRS(ms)
Group A (wildtype)	**12**	**246±29(210-287)***	**55±8(46-74)†§#*****	**19±2(17-26)‡§*******
HH38	3	214±4(210-217)	50±2(48-52)	18
HH40	1	271	46	19
HH41	4	255±27(222-287)	55±5(51-62)	18±1(17-19)
HH42	4	254±30(212-280)	61±10(50-74)	22±3(20-26)
Group B (EPDC-inhibition)	**12**	**252±39(212-333)***	**45±10(20-57)†||**	**29±14(15-60)‡||**
Group B_1	**9**	**257±43(213-333)**	**50±6(41-57)#**	**22±3(15-25)****
HH38	2	213	52±1(51-52)	21±4(18-23)
HH39	2	231±1(230-232)	51±9(44-57)	20±7(15-25)
HH40	2	308±35(283-333)	44±4(41-46)	23±3(21-25)
HH41	2	263±46(231-296)	50±6(46-54)	22
HH42	1	282	55	25
Group B_2 (overt preexcitation)	**3**	**238±23(212-257)**	**33±12(20-40)*****	**50±9(42-60) ******
HH40	1	256	39	42
HH41	2	229±24(212-246)	30±14(20-40)	54±9(47-60)

***Ex-Ovo* Electrograms**

Group, HH-stage	n	HR(bpm)	AV-interval(ms)	Premature V-base activation	
Group C (wildtype)	**45**	**111±17(63-120)*******	**79±26(41-140)********	**20/45(44%)**	**RVB(10),LVB(7), =(3)**
Group C_1 (sinus-rhythm)	**10**	**82±15(63-112)**	**78±15(63-111)*********	**3/10(33%)**	**RVB(1), =(2)**
HH38	4	76±12(63-92)	71±9(62-81)	0/4(0%)	
HH39	3	94±17(77-112)	72±9(61-78)	2/3(67%)	=(2)
HH40	3	77±13(63-90)	94±18(78-114)	1/3(33%)	RVB(1)
Group C_2 (Ω-rhythm)	**35**	**120**	**79±28(61-114)*********	**17/35(49%)**	**RVB(9),LVB(7), =(1)**
HH38	3	120	93±46(42-132)	3/3(100%)	RVB(2),LVB(1)
HH39	16	120	72±24(47-140)	11/16(69%)	RVB(6),LVB(4), =(1)
HH40	6	120	67±21(41-89)	1/6(17%)	LVB(1)
HH41	5	120	96±33(57-140)	0/5	
HH42	5	120	92±25(65-127)	2/5(40%)	RVB(1),LVB(1)

Table 1. Electrophysiological (In-Ovo and Ex-Ovo) Characteristics of Wild-type and EPDC-Inhibited Hearts. *p=0.648(Student t test);†p=0.030(Mann-Whitney U test);‡p= 0.011(Mann-Whitney U test);§Pearson's r=0.790,p=0.002;||Spearman's ρ=-0.314,p=0.320;#p=0.165(Mann, Whitney U test),**p=0.064(Mann-Whitney U test),***p=0.004(Mann-Whitney U test),****p=0.004(Mann-Whitney U test),*****p=0.693(Mann-Whitney U test),******p=0.033(Student t test);*******p=0.938(Student t test);********p=0.097(Student t test).

Ex-Ovo Extracellular Electrogram Recordings

The AV interval in EPDC-inhibited hearts was significantly shorter than the AV interval in wildtype hearts (62±12ms vs. 79±26ms,p=0.033), while the RR-interval did not differ (125±35bpm vs. 111±17bpm,p=0.693).

In line with previous data,[6] at these late stages of embryonic heart development, the ventricular base was activated prematurely in a considerable number of embryonic wildtype hearts (20/45,44%). In contrast, all EPDC-inhibited hearts (12/12,100%) showed earliest ventricular activation at the ventricular base. In the majority of hearts with premature ventricular base activation, the RVB was the location of first ventricular activation in both wildtype (RVB=10/20,50% vs. LVB=7/20,35%) and EPDC-inhibited hearts (RVB=9/12,75% vs. LVB=3/12,25%).

Interestingly, the interval between ventricular base and ventricular apex activation was significantly longer in EPDC-inhibited hearts (12±11ms) compared to wildtype hearts showing premature ventricular base activation (2±2ms,p<0.001). Representative examples of *ex-ovo* extracellular recordings in a wildtype HH40 heart (group C) are shown in **Figures 3A** and **3B** and recordings obtained in an EPDC-inhibited HH40 heart (group D) in **Figures 3C** and **3D**.

Morphology of the Annulus Fibrosis

Macroscopically, EPDC-inhibited embryos and their hearts were consistently smaller as compared to wildtype hearts. Furthermore, various known characteristics of the loss-of-PEO-function phenotype were observed to occur coincidently in these hearts: double-outlet-right-ventricle with ventricular-septal-defects (2/10), AV valve abnormalities (2/10), great artery abnormalities (1/10), coronary pathology (2/10) and myocardial hypoplasia (2/10) (**Table 2**).[10, 12, 19, 21-26] The central conduction axis of the EPDC-inhibited hearts did not show any histological abnormalities. In both wildtype (n=10) and EPDC-inhibited hearts (n=10), small MLC2a-positive APs with comparable volumes ($1.30 \cdot 10^6 \pm 0.40 \cdot 10^6$ μm^3 vs.$1.26 \cdot 10^6 \pm 0.52 \cdot 10^6$ μm^3,p=0.864) were found in mostly the postero- and midseptal region of all hearts.

In wildtype hearts, additional smaller ($0.38 \cdot 10^6 \pm 0.13 \cdot 10^6$ μm^3) APs were found in the right or left lateral wall of 6/10 hearts (**Table 2**). Interestingly however, in all EPDC-inhibited hearts multiple MLC2a-positive APs in both the right and left lateral free wall regions with larger volumes as compared to the small lateral APs in wildtype hearts were found ($3,14 \cdot 10^6 \pm 2,25 \cdot 10^6$ μm^3 vs. $0.38 \cdot 10^6 \pm 0.13 \cdot 10^6$ μm^3,p=0.001)(**Table 2**, **Figure 4A-T**, **Figure 5**).

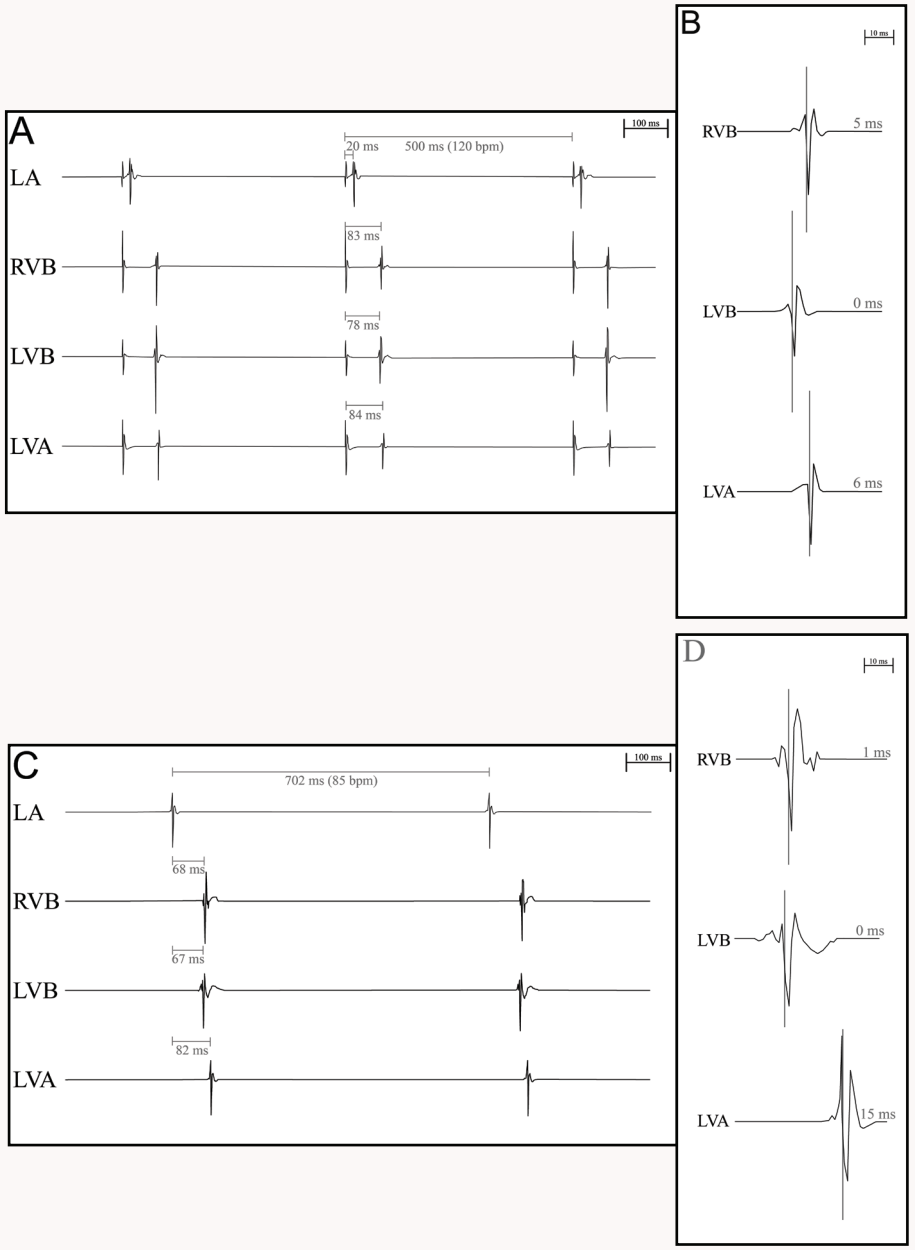

Figure 3. **A.** Ex-ovo extracellular electrograms recorded in a wildtype HH40 heart (group C) with premature LVB activation (AV-interval 78 ms). LA-interval (pacing artefact to LA activation) is 20 ms. **B.** Magnification showing LVB activation 6 ms before LVA activation. **C.** Recordings in an EPDC-inhibited HH40 heart (group D) demonstrating premature LVB activation (AV-interval 67 ms). **D.** Magnification showing LVB activation 15 ms before LVA activation.

Embryo #	HH-stage	Structural Abnormalities	AP-Location	Cumulative (and individual) AP-volumes in $\cdot 10^6$ µm^3	Ventricular Activation Pattern
Wildtype (Group A,n=10)†				1.67±0.69*	
1	38		S+LL+RL	2.44 (**1.46**+0.56+0.43)	LVA-first
2	38		S+LL+RL	2.15 (**1.29**+0.47+0.39)	LVA-first
3	39		S+LL+RL	2.79 (**2.10**+0.43+0.26)	LVA-first
4	39		S+LL	1.76 (**1.33**+0.43)	LVB-first
5	39		S+LL+RL	1.84 (**1.50**+0.17+0.17)	LVB-first
6	40		S	1.50	LVA-first
7	40		S+RL	1.72 (**1.24**+0.47)	LVA-first
8	41		S	0.77	LVA-first
9	41		S	0.69	LVA-first
10	42		S	1.07	RVB-first
EPDC-inhibited (Group B,n=10)†				6.90±3.26*	
Group B$_1$					
11	38	DORV+VSD+CA	S+LL+RL	10.85 (1.29+4.12+**5.45**)	RVB-first
12	38		S+LL+RL	3.22 (0.77+**1.29**+1.16)	RVB-first
13	38		S+LL	4.33 (1.97+**2.36**)	LVB-first
14	39	AVVA+GAA	S+LL+RL	8.19 (1.89+2.49+**3.82**)	LVB-first
15	39	DORV+VSD	S+LL+RL	7.20 (1.29+0.3+**5.62**)	RVB-first
16	40	MH+CA	S+LL+RL	6.13 (0.82+0.56+**4.76**)	RVB-first
17	41	MH	S+LL	2.36 (0.82+**1.54**)	LVB-first
Group B$_2$					
18	40		S+LL+RL	6.43 (0.52+1.12+**4.80**)	RVB-first
19	41	AVVA	S+LL+RL	12.95 (1.42+2.32+**9.22**)	RVB-first
20	41		S+LL+RL	7.33 (1.80+2.57+**2.96**)	RVB-first

Table 2. Structural Abnormalities, Locations of APs, Cumulative/Individual AP-Volumes, and Ventricular Activation Sequences in Wildtype and EPDC-Inhibited Hearts. *volume measurements according to the Cavalieri-method; †p<0.001 (Student t test); Bold=largest AP, RL=right lateral, LL=left lateral, S=septal, DORV=Double-Outlet-Right-Ventricle, VSD=Ventricular-Septal-Defect, CA=Coronary Abnormalities, AVVA=Atrio-Ventricular-Valve-Abnormalities, GAA=Great Artery Abnormalities, MH=myocardial hypoplasia.

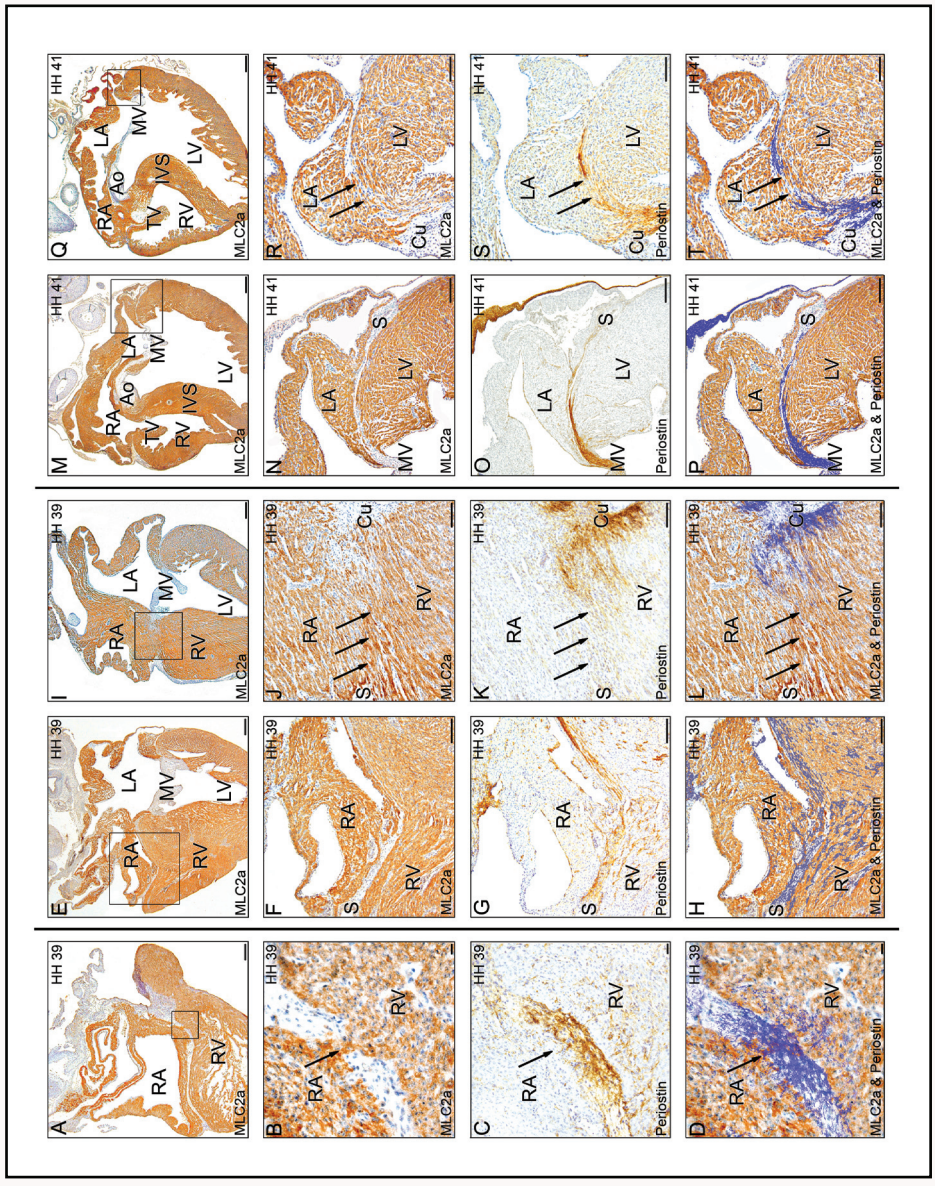
A
HH 39
RA
RV
MLC2a
B
HH 39
RA
RV
MLC2a
C
HH 39
RA
RV
Periostin
D
HH 39
RA
RV
MLC2a & Periostin
E
HH 39
RA
LA
MV
RV
LV
MLC2a
F
HH 39
RA
S
RV
MLC2a
G
HH 39
RA
S
RV
Periostin
H
HH 39
RA
S
RV
MLC2a & Periostin
I
HH 39
RA
LA
MV
RV
LV
MLC2a
J
HH 39
RA
S
Cu
RV
MLC2a
K
HH 39
RA
S
Cu
RV
Periostin
L
HH 39
RA
S
Cu
RV
MLC2a & Periostin
M
HH 41
RA
Ao
LA
MV
TV
RV
IVS
LV
MLC2a
N
HH 41
LA
S
MV
LV
MLC2a
O
HH 41
LA
MV
S
LV
Periostin
P
HH 41
LA
S
MV
LV
MLC2a & Periostin
Q
HH 41
RA
Ao
LA
MV
TV
IVS
RV
LV
MLC2a
R
HH 41
LA
Cu
LV
MLC2a
S
HH 41
LA
Cu
LV
Periostin
T
HH 41
LA
Cu
LV
MLC2a & Periostin

Figure 4. A-T. **A.** A small MLC2a-positive right posteroseptal AP in a HH39 wildtype heart. Bar=300µm. **B.** Magnification of boxed area. Bar=50µm. **C.** Periostin staining. Bar=50µm. **D.** Periostin staining (blue) from adjacent section, superimposed on the MLC2a-stained section, showing marked periostin expression in the myocardial AP. Bar=50µm. **E.** Right annulus fibrosis region of a HH39 wildtype heart. Bar=300µm. **F.** Magnification showing complete AV-isolation. Bar=2µm. **G.** Periostin-positivity of the fibrous annulus. Bar=2µm. **H.** Periostin-staining superimposed on MLC2a-staining. Bar=2µm. **I.** Right annulus fibrosis region of a HH39 EPDC-inhibited heart. Bar=300µm.**J.** Magnification showing a broad persistent MLC2a-positive AP in the right anterolateral AV-ring region. Bar=1µm. **K.** Periostin-staining. Bar=1µm. **L.** Periostin-staining superimposed on MLC2a-staining, showing periostin-negativity of the myocardial AP. Bar=1µm. **M.** Left annulus fibrosis region of a HH41 wildtype heart. Bar=300µm. **N.** Magnification showing complete AV-isolation. Bar=1µm. **O.** Periostin-positivity of the fibrous annulus. Bar=1µm. **P.** Periostin-staining superimposed on MLC2a-staining. Bar=1µm. **Q.** Left annulus fibrosis region of a HH41 EPDC-inhibited heart. Bar=300µm. **R.** Magnification showing a broad persistent MLC2a-positive AP in the left lateral AV-ring region. Bar=1µm. **S.** Periostin-staining. Bar=1µm. **T.** Periostin-staining superimposed on MLC2a-staining, showing periostin-negativity of the broad lateral AP. Bar=1µm. RA=right atrium, LA=left atrium, RV=right ventricle, LV=left ventricle, S=sulcus, Cu=cushion, TV=tricuspid valve, MV=mitral valve, IVS=interventricular septum, Ao=aorta.

As expected,[6] temporal analysis showed a decrease in AP-volume with increasing developmental stage in wildtype hearts (Pearson's r=-0.908,p=0.033). Maturation of the periostin-positive annulus fibrosis in EPDC-inhibited hearts however remained impeded as compared to wildtype hearts until near hatching stages of development.

Periostin Expression at the Isolating AV Ring

Periostin staining was found at the regions where EPDCs are known to be present, for example in the endocardial AV cushions, the atrial and ventricular subendocardium and at variable expression levels all around the circumference of the AV ring region in both wildtype and EPDC-inhibited hearts. In both wildtype and EPDC-inhibited hearts, periostin expression was slightly lower in the right AV ring region as compared to the left AV ring region.

The small, septal and MLC2a-positive APs in both wildtype and EPDC-inhibited hearts and the small lateral MLC2a-positive APs in wildtype hearts, stained positive for periostin. Periostin staining on the annulus fibrosis was however locally interrupted at locations where broad lateral APs crossed the annulus in EPDC-inhibited hearts. In **Figure 4A-T**, representative examples of MLC2a- and periostin-staining in the annulus fibrosis region of wildtype and EPDC-inhibited hearts at HH39 and HH41 are given.

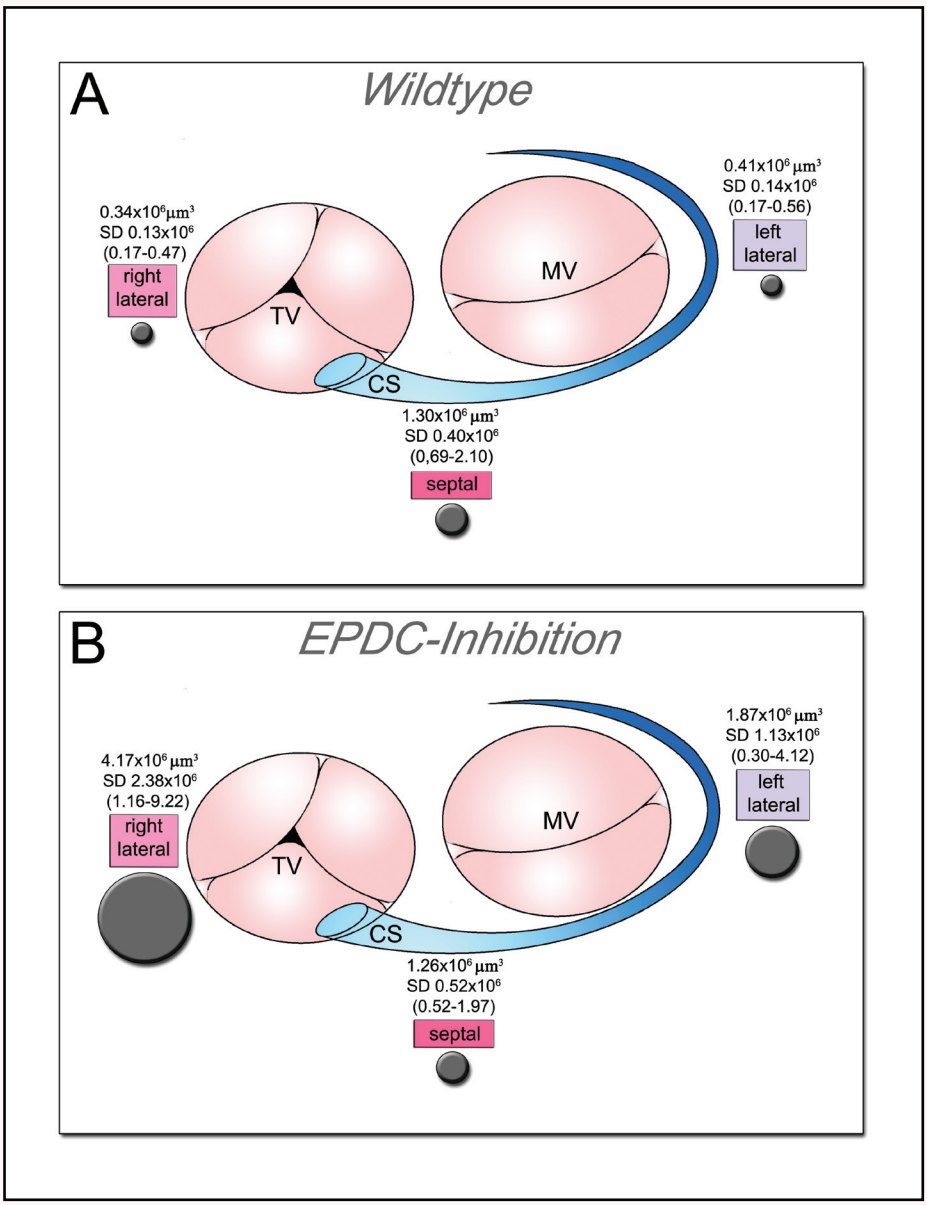

Figure 5. Schematic figure of mitral (MV) and tricuspid (TV) valve annuli in wildtype (A) and EPDC-inhibited (B) quail hearts with AP-locations and corresponding AP-volumes. CS=coronary sinus.

Comparison of Immunohistochemical and Electrophysiological Data

In line with our previous report,[6] AP-location in wildtype postseptated hearts could not be correlated directly with *ex-ovo* electrophysiological data: right- or left-sided APs were found both in hearts that displayed earliest ventricular activation at the RVB or LVB and in hearts with a concurrent or apex-to-base ventricular activation pattern.

In EPDC-inhibited hearts (n=10) however, right-sided APs corresponded with premature activation of the RVB and left-sided APs corresponded with premature activation of the LVB in 8/10 cases. In case of multiple APs, the location of earliest ventricular activation was found to correlate with the morphologically broadest AP present (**Table 2**). Moreover, conduction velocity along the AP (PR-interval) showed negative correlation with the AP-volume in EPDC-inhibited hearts (Pearson's r=-0.696,p=0.037). The observed additional structural defects in the EPDC-inhibited hearts did not correlate with the degree of ventricular preexcitation (*in-ovo* PR-interval) (Spearman's ρ=0.000). Interestingly, hearts in group B_2 demonstrated none to only mild additional structural abnormalities (**Table 2**).

Discussion

Key finding of this study is that EPDCs are essential for normal annulus fibrosis formation. Consequently, inhibition of EPDC-migration during cardiogenesis may result in marked defects in the isolating annulus fibrosis with persistence of broad accessory myocardial AV connections, resulting in ventricular preexcitation.

Embryonic Development of the Isolating Annulus Fibrosis: The Role of EPDCs at the AV Junction

During development of the electrically inert annulus fibrosis, the primitive slow conducting continuous AV junctional myocardium of the looped embryonic heart makes way for conduction through the AV node/HPS, which eventually constitutes the sole AV conducting pathway of the adult heart.[4, 27] It is well established that AV junctional myocardium is incorporated within the atrial myocardium by fusion of the endocardial AV cushions and the epicardial AV sulcus,[3, 4] while state of the art in literature postulates additional roles for bone-morphogenetic-protein (BMP) signaling and periostin in annulus fibrosis formation.[5-8] Interestingly, expression of periostin mRNA increases significantly in response to mechanically regulated BMP-signaling in mesenchymal cells in culture.[28]

Although the contribution of the multipotent EPDCs to the heart as 1) interstitial fibroblasts, as smooth muscle cells and fibroblasts of the coronary arteries and as mesenchymal cells in the developing AV cushions and 2) their role in formation of the compact and trabecular myocardium and in Purkinje fiber differentiation, has previously been shown to be indispensable,[10, 22-24, 29-31] the role of EPDCs in annulus fibrosis development has until now not been studied in detail.

Our present data show that in EPDC-inhibited hearts at late postseptated stages of development (HH38-42), large APs coursing through defects in the annulus fibrosis can be found in the right- and left-lateral free wall region, while as previously also described in wildtype postseptated quail hearts,[6] additional small APs can be found in mainly the posteroseptal regions.

After mechanical EPDC-inhibition (this study), epicardial outgrowth is delayed by inserting a piece of eggshell membrane to block the normal cell transfer.[11, 19, 21] Ultimately, regenerating PEO-cells growing around the eggshell membrane together with pericardial mesothelial cells originating from the pharyngeal arch area of the heart, form a compensatory epicardium and partially

rescue the normal phenotype, thereby yielding embryos with a delayed formation of PEO-derived tissues.[12, 16, 23, 26, 32] Normally, migration of subepicardial EPDCs through the continuous AV junctional myocardium to the endocardial cushions of the four chambered heart, starts from HH32 onwards.[10-12, 17, 18, 20] The impeded development of the AV sulcus in EPDC-inhibited hearts with consequent persistence of functional large APs at late postseptated developmental stages (HH38-42) thus strongly underlines the importance of EPDCs for the normal development of the annulus fibrosis. A schematic overview of the proposed role of EPDCs in normal annulus fibrosis formation is depicted in **Figure 6**.

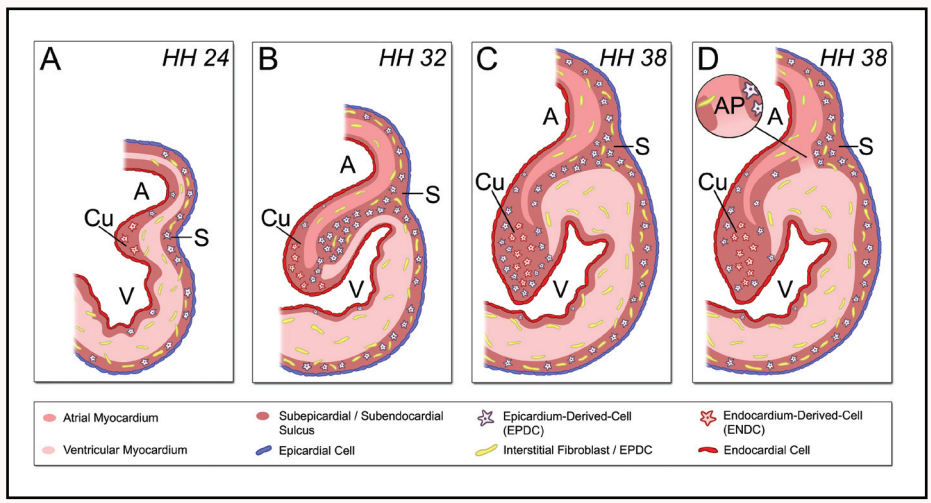

Figure 6. Annulus fibrosis formation and the role of EPDCs. A. Continuous AV-junctional myocardium in the looped embryonic heart. **B**. From HH32 onwards, subepicardial EPDCs in the AV-sulcus (S) migrate through the continuous AV-junctional myocardium to ultimately populate the endocardial AV-cushions (Cu). **C**. In the normal 4-chambered heart, EPDCs continue populating the AV-cushions and favour 2 positions: 1) myocardial/endocardial cushion interface, 2) subendocardially at the luminal face of the AV-cushions. **D.** Impeded development of the annulus fibrosis in EPDC-inhibited hearts results in subsequent persistence of large APs in the postseptated heart. A=atrium, V=ventricle, S=sulcus, Cu=cushion, AP=accessory pathway.

Periostin Expression in the Developing Annulus Fibrosis of Wildtype versus EPDC-Inhibited Postseptated Hearts: Relevance for EPDC-Functioning at the AV Junction

Periostin is a profibrogenic extracellular matrix protein secreted during cushion mesenchym formation and is strongly expressed in collagen-rich fibrous connective tissues subject to constant mechanical stress *in-vivo*.[7, 8, 33-39] It is thought that this fasciclin-I related protein is an inhibitor of the myocardial phenotype under both physiological as well as pathological conditions.[6, 30, 33, 35, 36, 40, 41] Moreover, periostin is likely also essential in maintaining the integrity of the fibrous heart skeleton of the mature heart.[36] Multiple cellular mechanisms regulated by periostin might support destabilization of the cardiomyocyte phenotype and the formation and maintainability of the fibrous scaffold, since periostin is known to bind to fibronectin, tenascin-C, collagen-V and periostin itself.[42]

The spatiotemporal colocalization of periostin and EPDCs at the AV junction of the developing heart substantiates its importance for EPDC-functioning.[8, 10] Interestingly, periostin was recently found to directly interact with collagen type-I,[13] while the migratory patterns of EPDCs in the AV sulcus were previously established to resemble the spatiotemporal expression of procollagen-I, a marker for collagen type-I synthesis.[10-12] The presence of periostin mRNA in the completely epicardium-derived subepicardial mesenchym further denotes the EPDC as an important player in the dynamic interplay between molecular cues and biomechanical determinants in the AV junctional myocardium.[7, 8, 10, 11]

We recently postulated that periostin expression in persistent small, and mostly posteroseptal located myocardial APs in wildtype postseptated quail hearts indicates their ultimate perinatal fate as fibrous tissue of the annulus fibrosis.[6] In the present study, periostin expression in the annulus fibrosis region of EPDC-inhibited postseptated quail hearts was found to be locally interrupted at sites where large myocardial APs in the lateral free wall region crossed the isolating annulus, further substantiating the importance of periostin in EPDC-functioning and annulus fibrosis formation. Interestingly, similar annulus fibrosis malformations occur in the periostin knockout mouse and in mice with a conditional deletion of the Alk3-gene and consequent downregulation of periostin in the AV region.[5, 30, 43, 44]

As shown in **Figure 4**, in both wildtype and EPDC-inhibited hearts, periostin expression was found in the endocardial AV cushions, one of the regions where EPDCs are normally known to be present.[10-12] Expression of periostin in the EPDC-deprived endocardial AV cushions of the EPDC-inhibited

heart, however indicates that periostin expression is not only dependent on the physical presence of EPDCs. Periostin expression can therefore be speculated to underlie the renowned,[3, 4] but still largely unknown role of the endocardial AV cushions in annulus fibrosis development, while the constant mechanical stress at the developing AV junction can also be postulated to induce expression of this profibrogenic protein.[34]

Annulus Fibrosis Development and Functional AP-Persistence

Normal formation of the epicardium is described to proceed from the point of attachment of the sinu-ventricular mesocardium - the dorsal atrial wall facing the sinus venosus - firstly to the dorsal parts of the atrial and the ventricular wall and subsequently to the ventral wall of the heart.[14, 17, 21] By the end of HH26, the myocardium of the looped embryonic heart is completely covered by epicardium,[14, 16] whereas cardiac septation and chamber formation have not been completed yet.[45, 46] Outgrowth of the right ventricular dorsal wall myocardium is one of the last processes in cardiogenesis and expands the right ventricular inflow tract and ultimately results in an inevitable shift of the right side of the AV canal, to become positioned above the right ventricle.[45, 46] Spatiotemporally, EPDC-population of the right posterior annulus fibrosis region can thus only be achieved after EPDC-migration through the expanding dorsal right ventricular wall, denoting temporal postnatal AP-persistence in the right posteroseptal region of embryonic wildtype quail hearts[6] as physiological perinatal remodeling of the AV junction.

Dyssynchrony in the delicate interplay between EPDCs and AV junctional cells, as shown in the EPDC-inhibited quail model, results in persistence of large lateral APs. While EPDCs derived from the compensatory epicardium ultimately do arrive at the epicardial AV sulcus of EPDC-inhibited hearts,[12, 32] these cells possibly encounter AV junctional cardiomyocytes already impermissive for EPDC-interaction and thus miss the appropriate time-window for their intended rescue of the normal cardiac phenotype. Persistent APs in wildtype versus EPDC-inhibited postseptated quail hearts also displayed divergent electrophysiological characteristics. In line with our previous report,[6] morphologically persistent APs in the wildtype heart, giving rise to premature ventricular activation can be found in a considerable number of cases. Inhibition of EPDC-migration however results in persistence of large APs with a relatively high conduction velocity (short *in-ovo* PR- and *ex-ovo* AV intervals), both not observed in any of the wildtype hearts, and premature ventricular base activation in all cases.

Moreover, overt ventricular preexcitation was observed in a subgroup of *in-ovo* ECGs in EPDC-inhibited hearts. Interestingly, these EPDC-inhibited hearts all demonstrated the 3 main clinical electrocardiographic features of ventricular preexcitation syndromes;[47, 48] 1) a short PR-interval, 2) initial slurring of the QRS-complex, known as the delta wave and 3) a resultant prolonged QRS-complex (**Figure 2**).

Clinical Significance

In children, the first episodes of AP-mediated AVRT occur before birth or in the first months of life in ~60% of cases and resolve spontaneously in most cases before the age of 1 year, while recurrence of tachycardia at the age of 8-10 years occurs in the remaining ~ 30%.[1, 9] Bolstered by the normal postnatal evolutionary process of anatomical moulding and shaping of the heart to facilitate adjustment to the increasing body mass and changes in vascular pressures, we previously postulated that under physiological circumstances persistent functional APs at near-hatching stages of avian development provide the anatomical substrate for spontaneously resolving neonatal AVRTs.[6]

However, any delay in EPDC-migration in the developing heart may result in imperfect annulus fibrosis development and consequently in AP-persistence. Clinically, most patients with persistent APs are not affected by additional cardiac pathology, although in some cases of ventricular preexcitation syndromes (e.g. Wolff-Parkinson-White syndrome) AP-persistence coincides with congenital cor vitia, for example Ebstein's anomaly.[9, 49] When EPDC-migration is blocked directly after PEO-formation, as in this study, multiple mild to severe congenital heart defects will occur.[10, 12, 22-24, 26] In humans, genetic alterations affecting EPDC-functioning during development and occurring after completing structural configuration of the heart, may result in postnatal AP-persistence in a structurally normal heart.[1, 48]

Limitations of the Study

Although we showed both functionally and morphologically that EPDCs are indispensable for proper annulus fibrosis formation, we were unable to demonstrate subsequent AP-persistence in hatched or adult EPDC-inhibited quail hearts.

Unfortunately, mechanical EPDC-inhibition yields embryos in which the degree of epicardial outgrowth inhibition is directly related to the severity of the cardiac abnormalities and thus to embryonic lethality.[10, 22, 23, 26] While the operated embryos surviving beyond HH38 were typically those only mildly affected by comorbidity, EPDC-inhibited quail embryos are relatively small and seem to lack sufficient reserve to survive postnatally. Interestingly, severe growth retardation, postnatal lethality and dwarfism in adult life have recently also been described in the periostin null mouse.[43, 44]

Conclusions

EPDCs appear to be essential for proper formation of the isolating annulus fibrosis. Inhibition of EPDC-migration during cardiogenesis may result in marked defects in the annulus fibrosis with persistence of broad APs, functionally resulting in ventricular preexcitation. While, under physiological conditions small septal APs in the wildtype heart remain temporarily functionally active,[6] broad lateral APs in the EPDC-inhibited heart might provide a pathological substrate for postnatally persistent APs and AVRTs into childhood or adult life.

Funding Sources

None

Disclosures

None

References

1. Morady F. Catheter ablation of supraventricular arrhythmias: state of the art. *PACE.* 2004;27(1):125-142.
2. Becker AE, Anderson RH, Durrer D, Wellens HJ. The anatomical substrates of wolff-parkinson-white syndrome. A clinicopathologic correlation in seven patients. *Circulation.* 1978;57(5):870-879.
3. Wenink AC, Gittenberger-de Groot AC, Brom AG. Developmental considerations of mitral valve anomalies. *Int J Cardiol.* 1986;11(1):85-101.
4. Wessels A, Markman MW, Vermeulen JL, Anderson RH, Moorman AF, Lamers WH. The development of the atrioventricular junction in the human heart. *Circ Res.* 1996;78(1):110-117.
5. Gaussin V, Morley GE, Cox L, Zwijsen A, Vance KM, Emile L, Tian Y, Liu J, Hong C, Myers D, Conway SJ, Depre C, Mishina Y, Behringer RR, Hanks MC, Schneider MD, Huylebroeck D, Fishman GI, Burch JB, Vatner SF. Alk3/Bmpr1a receptor is required for development of the atrioventricular canal into valves and annulus fibrosus. *Circ Res.* 2005;97(3):219-226.
6. Kolditz DP, Wijffels MC, Blom NA, van der Laarse A, Markwald RR, Schalij MJ, Gittenberger-de Groot AC. Persistence of functional atrioventricular accessory pathways in postseptated embryonic avian hearts: implications for morphogenesis and functional maturation of the cardiac conduction system. *Circulation.* 2007;115(1):17-26.
7. Kruzynska-Frejtag A, Machnicki M, Rogers R, Markwald RR, Conway SJ. Periostin (an osteoblast-specific factor) is expressed within the embryonic mouse heart during valve formation. *Mech Dev.* 2001;103(1-2):183-188.
8. Norris RA, Kern CB, Wessels A, Moralez EI, Markwald RR, Mjaatvedt CH. Identification and detection of the periostin gene in cardiac development. *Anat Rec.* 2004;281(2):1227-1233.
9. Bauersfeld U, Pfammatter JP, Jaeggi E. Treatment of supraventricular tachycardias in the new millennium--drugs or radiofrequency catheter ablation? *Eur J Pediatr.* 2001;160(1):1-9.
10. Gittenberger-de Groot AC, Vrancken Peeters MP, Mentink MM, Gourdie RG, Poelmann RE. Epicardium-derived cells contribute a novel population to the myocardial wall and the atrioventricular cushions. *Circ Res.* 1998;82(10):1043-1052.

11. Männer J. Does the subepicardial mesenchyme contribute myocardioblasts to the myocardium of the chick embryo heart? A quail-chick chimera study tracing the fate of the epicardial primordium. *Anat Rec.* 1999;255(2):212-226.

12. Pérez-Pomares JM, Phelps A, Sedmerova M, Carmona R, González-Iriarte M, Muñoz-Chápuli R, Wessels A. Experimental studies on the spatiotemporal expression of WT1 and RALDH2 in the embryonic avian heart: a model for the regulation of myocardial and valvuloseptal development by epicardially derived cells (EPDCs). *Dev Biol.* 2002;247(2):307-326.

13. Norris RA, Damon B, Mironov V, Kasyanov V, Ramamurthi A, Moreno-Rodriguez R, Trusk T, Potts JD, Goodwin RL, Davis J, Hoffman S, Wen X, Sugi Y, Kern CB, Mjaatvedt CH, Turner DK, Oka T, Conway SJ, Molkentin JD, Forgacs G, Markwald RR. Periostin regulates collagen fibrillogenesis and the biomechanical properties of connective tissues. *J Cell Biochem.* 2007;101(3):695-711.

14. Vrancken Peeters MP, Mentink MM, Poelmann RE, Gittenberger-de Groot AC. Cytokeratins as a marker for epicardial formation in the quail embryo. *Anat Embryol.* 1995;191(6):503-508.

15. Hamburger V, Hamilton HL. A series of normal stages in the development of the chick embryo. 1951. *Dev Dyn.* 1992;195(4):231-272.

16. Virágh S, Gittenberger-de Groot AC, Poelmann RE, Kálmán F. Early development of quail heart epicardium and associated vascular and glandular structures. *Anat Embryol.* 1993;188(4):381-393.

17. Muñoz-Chápuli R, Macías D, González-Iriarte M, Carmona R, Atencia G, Pérez-Pomares JM. The epicardium and epicardial-derived cells: multiple functions in cardiac development. *Revista española de cardiología.* 2002;55(10):1070-1082.

18. Cohen-Gould L, Mikawa T. The fate diversity of mesodermal cells within the heart field during chicken early embryogenesis. *Dev Biol.* 1996;177(1):265-273.

19. Poelmann RE, Gittenberger-de Groot AC, Mentink MM, Bökenkamp R, Hogers B. Development of the cardiac coronary vascular endothelium, studied with antiendothelial antibodies, in chicken-quail chimeras. *Circ Res.* 1993;73(3):559-568.

20. Wessels A, Pérez-Pomares JM. The epicardium and epicardially derived cells (EPDCs) as cardiac stem cells. *Anat Rec.* 2004;276(1):43-57.

21. Männer J. Experimental study on the formation of the epicardium in chick embryos. *Anat Embryol.* 1993;187(3):281-289.

22. Eralp I, Lie-Venema H, Bax NA, Wijffels MC, van der Laarse A, Deruiter MC, Bogers AJ, van den Akker NM, Gourdie RG, Schalij MJ, Poelmann RE, Gittenberger-de Groot AC. Epicardium-derived cells are important for correct development of the Purkinje fibers in the avian heart. *Anat Rec.* 2006;288(12):1272-1280.

23. Eralp I, Lie-Venema H, de Ruiter MC, van den Akker NM, Bogers AJ, Mentink MM, Poelmann RE, Gittenberger-de Groot AC. Coronary artery and orifice development is associated with proper timing of epicardial outgrowth and correlated Fas-ligand-associated apoptosis patterns. *Circ Res.* 2005;96(5):526-534.

24. Lie-Venema H, Gittenberger-de Groot AC, van Empel LJ, Boot MJ, Kerkdijk H, de Kant E, de Ruiter MC. Ets-1 and Ets-2 transcription factors are essential for normal coronary and myocardial development in chicken embryos. *Circ Res.* 2003;92(7):749-756.

25. Gundersen HJE. The efficiency of systematic sampling in stereology and its prediction. *J Microsc.* 1987;147:229-263.

26. Männer J, Schlueter J, Brand T. Experimental analyses of the function of the proepicardium using a new microsurgical procedure to induce loss-of-proepicardial-function in chick embryos. *Dev Dyn.* 2005;233(4):1454-1463.

27. Kim JS, Virágh S, Moorman AF, Anderson RH, Lamers WH. Development of the myocardium of the atrioventricular canal and the vestibular spine in the human heart. *Circ Res.* 2001;88(4):395-402.

28. Lindner V, Wang Q, Conley BA, Friesel RE, Vary CP. Vascular injury induces expression of periostin: implications for vascular cell differentiation and migration. *Arterioscler Thromb Vasc Biol.* 2005;25(1):77-83.

29. Mikawa T, Gourdie RG. Pericardial mesoderm generates a population of coronary smooth muscle cells migrating into the heart along with ingrowth of the epicardial organ. *Dev Biol.* 1996;174(2):221-232.

30. Visconti RP, Markwald RR. Recruitment of new cells into the postnatal heart: potential modification of phenotype by periostin. *Ann N Y Acad Sci.* 2006;1080:19-33.

31. Winter EM, Grauss RW, Hogers B, van Tuyn J, van der Geest R, Lie-Venema H, Steijn RV, Maas S, de Ruiter MC, de Vries AA, Steendijk P, Doevendans PA, van der Laarse A, Poelmann RE, Schalij MJ, Atsma DE, Gittenberger-de Groot AC. Preservation of left ventricular function and attenuation of remodeling after transplantation of human epicardium-derived cells into the infarcted mouse heart. *Circulation.* 2007;116(8):917-927.

32. Gittenberger-de Groot AC, Vrancken Peeters MP, Bergwerff M, Mentink MM, Poelmann RE. Epicardial outgrowth inhibition leads to compensatory mesothelial outflow tract collar and abnormal cardiac septation and coronary formation. *Circ Res.* 2000;87(11):969-971.

33. Butcher JT, Norris RA, Hoffman S, Mjaatvedt CH, Markwald RR. Periostin promotes atrioventricular mesenchyme matrix invasion and remodeling mediated by integrin signaling through Rho/PI 3-kinase. *Dev Biol.* 2007;302(1):256-266.

34. Iekushi K, Taniyama Y, Azuma J, Katsuragi N, Dosaka N, Sanada F, Koibuchi N, Nagao K, Ogihara T, Morishita R. Novel mechanisms of valsartan on the treatment of acute myocardial infarction through inhibition of the antiadhesion molecule periostin. *Hypertension.* 2007;49(6):1409-1414.

35. Katsuragi N, Morishita R, Nakamura N, Ochiai T, Taniyama Y, Hasegawa Y, Kawashima K, Kaneda Y, Ogihara T, Sugimura K. Periostin as a novel factor responsible for ventricular dilation. *Circulation.* 2004;110(13):1806-1813.

36. Kern CB, Hoffman S, Moreno R, Damon BJ, Norris RA, Krug EL, Markwald RR, Mjaatvedt CH. Immunolocalization of chick periostin protein in the developing heart. *Anat Rec.* 2005;284(1):415-423.

37. Lindsley A, Li W, Wang J, Maeda N, Rogers R, Conway SJ. Comparison of the four mouse fasciclin-containing genes expression patterns during valvuloseptal morphogenesis. *Gene Expr Patterns.* 2005;5(5):593-600.

38. Litvin J, Selim AH, Montgomery MO, Lehmann K, Rico MC, Devlin H, Bednarik DP, Safadi FF. Expression and function of periostin-isoforms in bone. *J Cell Biochem.* 2004;92(5):1044-1061.

39. Wilde J, Yokozeki M, Terai K, Kudo A, Moriyama K. The divergent expression of periostin mRNA in the periodontal ligament during experimental tooth movement. *Cell Tissue Res.* 2003;312(3):345-351.

40. Ji X, Chen D, Xu C, Harris SE, Mundy GR, Yoneda T. Patterns of gene expression associated with BMP-2-induced osteoblast and adipocyte differentiation of mesenchymal progenitor cell 3T3-F442A. *J Bone Miner Metab.* 2000;18(3):132-139.

41. Wang D, Oparil S, Feng JA, Li P, Perry G, Chen LB, Dai M, John SW, Chen YF. Effects of pressure overload on extracellular matrix expression in the heart of the atrial natriuretic peptide-null mouse. *Hypertension.* 2003;42(1):88-95.

42. Takayama G, Arima K, Kanaji T, Toda S, Tanaka H, Shoji S, McKenzie AN, Nagai H, Hotokebuchi T, Izuhara K. Periostin: a novel component of subepithelial fibrosis of bronchial asthma downstream of IL-4 and IL-13 signals. *J Allergy Clin Immunol.* 2006;118(1):98-104.

43. Oka T, Xu J, Kaiser RA, Melendez J, Hambleton M, Sargent MA, Lorts A, Brunskill EW, Dorn GW, Conway SJ, Aronow BJ, Robbins J, Molkentin JD. Genetic manipulation of periostin expression reveals a role in cardiac hypertrophy and ventricular remodeling. *Circ Res.* 2007;101(3):313-321.

44. Rios H, Koushik SV, Wang H, Wang J, Zhou HM, Lindsley A, Rogers R, Chen Z, Maeda M, Kruzynska-Frejtag A, Feng JQ, Conway SJ. periostin null mice exhibit dwarfism, incisor enamel defects, and an early-onset periodontal disease-like phenotype. *Mol Cell Biol.* 2005;25(24):11131-11144.

45. Gittenberger-de Groot AC, Bartelings MM, de Ruiter MC, Poelmann RE. Basics of cardiac development for the understanding of congenital heart malformations. *Pediatr Res.* 2005;57(2):169-176.

46. Jongbloed MR, Wijffels MC, Schalij MJ, Blom NA, Poelmann RE, van der Laarse A, Mentink MM, Wang Z, Fishman GI, Gittenberger-de Groot AC. Development of the right ventricular inflow tract and moderator band: a possible morphological and functional explanation for Mahaim tachycardia. *Circ Res.* 2005;96(7):776-783.

47. Willems JL, Robles de Medina EO, Bernard R, Coumel P, Fisch C, Krikler D, Mazur NA, Meijler FL, Mogensen L, Moret P. Criteria for intraventricular conduction disturbances and pre-excitation. World Health Organizational/ International Society and Federation for Cardiology Task Force Ad Hoc. *J Am Coll Cardiol.* 1985;5(6):1261-1275.

48. Wolff L, Parkinson J, White PD. Bundle-branch block with short P-R interval in healthy young people prone to paroxysmal tachycardia. 1930. *Ann Noninvasive Electrocardiol.* 2006;11(4):340-353.

49. Ho SY, Goltz D, McCarthy K, Cook AC, Connell MG, Smith A, Anderson RH. The atrioventricular junctions in Ebstein malformation. *Heart.* 2000;83(4):444-449.

Clinical Perspective

Atrio Ventricular Reentrant Tachycardia (AVRT) is a common arrhythmia in both children and adults. Although currently the vast majority of patients with AVRT are cured by standard ablative procedures, the etiological mechanisms underlying the appearance of accessory pathways still remain a subject of debate. During cardiogenesis, initial slow conduction over the circumferential myocardial AV continuity resulting in sequential activation of the pre-septated heart, is replaced by apex-to-base conduction through the specialized AV node/His-Purkinje System (HPS) in the septated heart. Concurrently, incorporation of the AV junctional myocardium in the lower atrial rim by fusion of the endocardial AV cushions and epicardial AV sulcus results in formation of the isolating annulus fibrosis. Migration of the multipotent Epicardium-Derived-Cells (EPDCs), through the continuous AV junctional myocardium to ultimately reach the endocardium-derived AV cushions, spatiotemporally correlates with annulus fibrosis formation. The AV junction has been postulated to be subjected to physiological perinatal remodeling, temporarily leaving functional small accessory pathways as anatomical substrates for spontaneously resolving neonatal AVRTs. Dyssynchrony in the delicate interplay between EPDCs and AV junctional cells, as shown in the EPDC-inhibited quail model in the present study, may result in marked defects in the isolating annulus fibrosis with the persistence of large accessory pathways functionally resulting in ventricular preexcitation. We speculate that absence of EPDCs or a delay in EPDC-migration results in the persistence of pathological substrates for postnatally persistent accessory pathways and AVRTs into childhood or adult life.

Online Data Supplement

Methods

Experimental Preparations

All animal experiments were approved by the Committee on Animal Welfare of the Leiden University Medical Center (LUMC), the Netherlands. Animal experiments were conducted in compliance with the Guide for the Care and Use of Laboratory Animals (NIH Publication No.85-23, revised 1996). Fertilized eggs of the Japanese quail (Coturnix coturnix japonica, Leiden University Medical Center, The Netherlands) were incubated blunt end up at 37.5°C and 80% humidity. Embryos were staged according to the Hamburger-Hamilton (HH) criteria.[1]

Complete-to-partial inhibition of outgrowth of the proepicardium was obtained by performing *in-ovo* microsurgery under stereomicroscopic control, as first described by Männer.[2] Nile-blue staining was used to visualize transparent structures. In short, on the 3rd day of incubation (HH15-18), a portion of the eggshell was removed to expose the embryo. Subsequently, the vitelline membrane was locally removed from the embryo by means of watchmaker forceps. Through the naturally existing body wall hiatus at HH15 or through a slit in the amniotic and pericardial membranes at HH16-18, the pericardial cavity of the embryo was reached. To prevent the attachment of the pericardial villi to the heart, a small rectangular piece of shell membrane was cut with iridectomy scissors and inserted between the dorsal wall of the heart and the pericardial villi, cranially anchored in the sinu-atrial sulcus and caudally constrained by the coelomic wall (**Figure 1**). After implantation of the shell membrane, the eggs were closed with Scotch Magic-tape (3M®, Maplewood, Minnesota, USA) and re-incubated.

In-Ovo Electrocardiogram (ECG) Recordings

After termination of incubation at the desired developmental stages (HH 38-42), a subset of the quail eggs (EPDC-inhibition, n=12; wildtype, n=12) was prepared for in-ovo electrocardiogram (ECG) recordings. The eggs were removed from the incubator, candled to determine the location of the embryo and marked for correct placement of the electrodes. Consequently, 3 AgCl wire electrodes (0.5 mm in diameter) were inserted into small holes in the eggshell: the first in front of the embryo, the second behind the embryo (both on the 'equator') and the third on the 'South Pole'(pointed bottom of the egg) (ground). The electrodes were

connected to an isolated preamplifier module with an input impedance of $>10^{12}$ Ω of a high-gain low-noise DC bio-amplifier system (Iso-DAM8A; World Precision Instruments Inc., Berlin, Germany).

Subsequently, the ECGs were digitally recorded as bipolar between the two 'equator' electrodes (Prucka Engineering Inc., Houston TX., USA) continuously for 10-15 minutes in a small custom-built shielded incubator (37±0.1ºC) to obtain steady state ECGs under near-physiological conditions. *In-ovo* ECGs were evaluated by two independent observers.

After completion of ECG recordings, euthanization by decapitation and staging, the embryonic hearts were carefully isolated and prepared for extracellular electrode recordings.

Ex-Ovo Extracellular Electrode Recordings – Technical Features & Recording Protocol

In total, extracellular electrode recordings were performed at HH38-42 in 45 wildtype (group A) and 12 EPDC-inhibited hearts (group B). The experimental preparations were placed in a custom-built, fluid-heated, temperature-controlled tissue bath and superfused with carbogenated (95% O_2 and 5% CO_2) Tyrode's solution (30±0.1°C) with the following composition (mmol/l): NaCl 130, KCl 4, KH_2PO_4 1.2, $MgSO_4$ 0.6, $NaHCO_3$ 20, $CaCl_2$ 1.5, glucose 10 (pH 7.35).

Unipolar extracellular electrogram recording and bipolar atrial pacing was subsequently performed, as previously described,[3] by consistently positioning 4 tungsten recording electrodes (tip:1-2µm; impedance 0.5-1.0MΩ, WPI Inc., Berlin, Germany) on the left atrium (LA), right ventricular base (RVB), left ventricular base (LVB) and left ventricular apex (LVA) and a bipolar pacing electrode on the high right atrium. A silver reference electrode was placed in the tissue bath.

In short, the experimental preparations were allowed to equilibrate for 10 minutes before starting the recording protocol. Embryonic hearts with a stable spontaneous HR of at least 60 bpm were allowed to beat spontaneously, whereas hearts with a HR of <60 bpm were stimulated at a fixed cycle length of 500 ms (120 bpm).

Definitions

In extracellular electrogram recording, a mean difference in local depolarization time between two recording electrodes of ≥1 ms was considered significant.[3] The left ventricular activation sequence was thus denominated as 1) base-to-apex if the ventricular base depolarized ≥1 ms earlier than LVA, 2) apex-to-base if the LVA depolarized ≥1 ms earlier than ventricular base and 3) concurrent if the time difference between ventricular base and LVA activation was <1 ms.

In all experiments, a stable 1:1 relation between atrial and ventricular activation was assured to be present. The time difference between LA activation and the location of earliest ventricular activation was denominated as the AV interval both in embryonic hearts beating in sinus rhythm as in hearts driven by RA-pacing.

Immunohistochemistry

After completion of the extracellular electrogram recordings, the hearts were removed from the Tyrode's solution and fixated in a 4% paraformaldehyde solution for 24 hours, dehydrated and embedded in paraffin. Subsequently, 10 EPDC-inhibited and 10 wildtype post-septated quail hearts were serially sectioned in the frontal plane at 5 μm, transferred to albumin/glycerin-coated objective slides and stained with anti-MLC2a and anti-periostin, as previously described.[3] Morphometry was performed by measurements of the total and individual AP volumes in each analyzed heart, according to the Cavalieri method.[4]

Statistical Analysis

The symmetry of the distribution was determined by determining the Skewness value. RR (*in-ovo*) and AV intervals (*ex-ovo*), heart rates (*ex-ovo*) and AP-volume were compared between groups using the 2-tailed Student *t* test for normally distributed values: otherwise, the Mann-Whitney *U* test was used (*ex-ovo* RR-intervals, *in-ovo* PR- and QRS-intervals). For comparison of categorical variables (ventricular activation sequence), the χ^2-test was applied. The Pearson correlation (r) coefficient was calculated, as a measure for the association between the AP-volume and the developmental stage and between the AP-volume and the AP-conduction velocity, while Spearman's correlation coefficient (ρ) was used as a measure for the association between the PR- and QRS-intervals in *in-ovo* ECGs and between the degree of ventricular preexcitation and additional structural heart defects.

The Paired-Samples *t* test was used to measure inter-observer agreement in evaluation of the *in-ovo* ECGs. Results are presented as means ± SD (range). A *P* value <0.05(2-tailed) was considered statistically significant. All analysis were performed using the Statistical Package for Social Studies version 12.0 (SPSS Inc, Chicago, Ill).

The authors had full access to the data and take responsibility for its integrity. All authors have read and agree to the manuscript as written.

References

1. Hamburger V, Hamilton HL. A series of normal stages in the development of the chick embryo. 1951. *Dev Dyn.* 1992;195(4):231-272.

2. Männer J. Experimental study on the formation of the epicardium in chick embryos. *Anat Embryol.* 1993;187(3):281-289.

3. Kolditz DP, Wijffels MC, Blom NA, van der Laarse A, Markwald RR, Schalij MJ, Gittenberger-de Groot AC. Persistence of functional atrioventricular accessory pathways in postseptated embryonic avian hearts: implications for morphogenesis and functional maturation of the cardiac conduction system. *Circulation.* 2007;115(1):17-26.

4. Gundersen HJE. The efficiency of systematic sampling in stereology and its prediction. *J Microsc.* 1987;147:229-263.

Editorial
Accessory Atrioventricular Pathways: Getting to the Origins

Siew Yen Ho[1]

[1]Department of Cardiac Morphology, National Heart & Lung Institute, Imperial College London and Royal Brompton Hospital, London, United Kingdom.

Circulation 2008;117(12):1502-1504

By definition, accessory atrioventricular pathways are aberrant muscle bundles that connect the atrium to a ventricle outside of the regular atrioventricular conduction system. Clinically, they may manifest as substrates for ventricular preexcitation. The first accessory pathway in a patient who suffered from Wolff-Parkinson-White syndrome was described in 1943 by Wood, Wolferth, and Geckler.[1] Shortly after, Öhnell created a reconstruction of an accessory pathway that very elegantly showed the close proximity of the pathway to the fibrous attachment of the mitral valve and its relationship with the sulcus coronarius (**Figure A**).[2] Subsequent histological studies have demonstrated unequivocally that these pathways are the anatomic substrates for the classical Wolff-Parkinson-White variety of preexcitation.

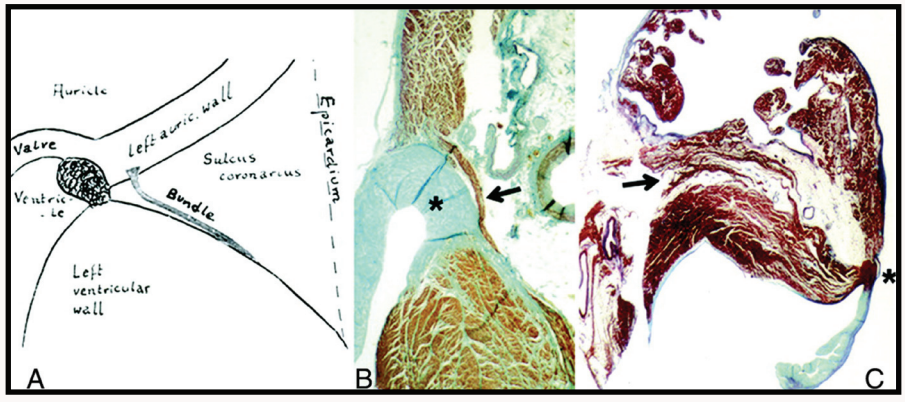

Figure. **A,**.Öhnell's depiction of an accessory bundle in the left atrioventricular groove. Reprinted with permission from Blackwell Publishing. **B.** Histological section stained with Masson's trichrome (fibrous tissue in green and myocardium in red) to show an accessory left-sided pathway (arrow) skirting the mitral annulus. **C.** Histological section showing a broad right-sided accessory pathway (arrow) that is formed by a myocardial pouch extending from the right atrial appendage to the ventricle and ultimately traced to a small right ventricular vein. This pathway is some distance from the fibrous annulus of the tricuspid valve. *Valvar annulus.

Accessory atrioventricular pathways are found most often in the parietal atrioventricular junctional areas, including the paraseptal areas. They breach the insulation provided by the fibrofatty tissues of the atrioventricular groove (sulcus tissue) and the hinge lines (fibrous annulus) of the valves. They are rarely found in the area of fibrous continuity between the aortic and mitral valves because in this area, there is usually a wide gap between the atrial myocardium and ventricular myocardium to accommodate the aortic outflow tract. On the left parietal side, the accessory pathways tend to pass close to the hinge line of the mitral valve (**Figure B**). In the right atrioventricular junction, the atrioventricular groove is much deeper than on the left side, and the accessory muscle bundles can cross at any depth. Cardiac surgeons have suggested that the deep groove may itself allow the atrial wall to fold over the ventricular wall, thereby producing atrial-ventricular myocardial continuity.[3] Most of the pathways identified through the use of microscopy have been working myocardium, with only a few reported to contain histologically specialized cells.[4] Whether comprising working myocardium or abnormal myocytes, these pathways have normal gap junctions with a pattern suggestive of working ventricular myocardium.[5] Morphologically, these threads of musculature are thicker at their atrial origins and they branch into finer strands at the ventricular insertions. They are up to 3 mm in width but may be 10 mm or more long.[2, 4, 6]

Other types of accessory atrioventricular pathways found in certain circumstances are well recognized. One of the 7 pathways in the study conducted by Becker and colleagues[4] was a specialized bundle that had its atrial insertion in a node of specialized tissues in the parietal margin of the tricuspid annulus, forming an atriofascicular tract.[7] Multiple pathways can occur in the setting of so-called Purkinje cell tumors, often with additional tumors within the ventricles. Another type of pathway related to coronary veins is usually manifested in the form of extensive myocardial cuffs around the veins crossing the atrioventricular junction or expanded as diverticulums into the ventricular mass. Others are related to the atrial appendages overlying ventricular masses (**Figure C**).

For several decades, accessory pathways have been avulsed successfully through surgery using conventional dissection or by cryothermy or radiofrequency ablation. In the past 2 decades, advancements in precision mapping and ablation of accessory pathways via the transcatheter route have made it possible for many patients to be cured. Although rare, sudden death may be the first presenting sign in patients with undiagnosed and/or asymptomatic preexcitation syndrome.

This is particularly worrisome for families with an affected child. The majority of cases have no clear familial involvement, but a small number of patients have affected relatives. Recently, the transcatheter procedure has been deemed safe and effective in experienced hands, but whether it should be used as a prophylactic measure against life-threatening events remains controversial.[8, 9] Clearly, there is a need to know more about how these pathways develop so as to guide further therapeutic strategies.

In the embryonic human heart, a ring of musculature at the atrioventricular canal provides myocardial continuity between developing atrial and ventricular myocardium in the early stages. This canal myocardium was shown initially to have slow conduction properties in the chick.[10] The canal myocardium is sandwiched by sulcus tissue on the outside and endocardial cushions on the inside. Kim and colleagues[11] showed that the bulk of the canal myocardium was incorporated into the vestibules making up the atrial walls leading toward the valvar orifices, but it did not contribute to ventricular myocardium. A small part of the canal myocardium becomes the atrioventricular node, and normally this is the only site of myocardial continuity, with the developing ventricular conduction bundles at completion of cardiac septation. In their earlier study, however, Wessels and colleagues[12] noted strands of myocardial continuity between atrial and ventricular tissues in all human fetal hearts and many normal neonatal hearts.

Pivotal to the understanding of accessory atrioventricular pathways is knowledge of how the insulating tissue plane at the sulcus and annulus came into being. Wessels and colleagues,[13] among others, offered the explanation that sulcus tissue joins with endocardial cushion tissues at the ventricular margin of the canal. According to this study,[13] the valvar leaflets were formed by cushion tissue, without contribution or real inward growth of sulcus tissue. Instead, the ventricular walls distal to the atrioventricular canal bulged like shoulders toward the atria. They suggested that accessory pathways resulted from incomplete fusion between sulcus and cushion tissues. It is not clear from their study, however, how myocardial discontinuity was effected so as to allow sulcus tissue to meet cushion tissue. In contrast, a simpler explanation was put forward by others who suggested that invagination of sulcus tissue like a wedge through the muscular canal wall was part of the process for development of valvar leaflets, with little contribution from the cushions.[14, 15] Be that as it may, there is consensus that the insulating tissues came from the epicardial side.

It was while studying the embryologic origins of the coronary vessels in chicken-quail chimeras that Gittenberger-de Groot and coworkers identified and traced the migration of a novel population of cells termed epicardial-derived cells (EPDCs) into the myocardial interstitium and endocardial cushions.[16] Observing a close relationship between EPDCs and cardiac fibroblasts, they suggested a potential role of migrating EPDCs in the formation of the insulating tissue plane between atrial and ventricular myocardium. This concept, based on exquisite experimental techniques, differs from their earlier work describing infolding of the epicardial tissues to form the core of the developing leaflets.[15] The latest article from this group[17] examines the role of EPDCs in formation of the insulating plane (annulus fibrosis) by comparing wild-type quail embryos with EPDC-inhibited embryos. In normal development, EPDCs migrate through the atrioventricular canal myocardium to populate the endocardial cushions.[16] By impeding EPDC migration, Gittenberger-de Groot et al observed persistence of broad bundles of accessory atrioventricular myocardial connections that resulted in ventricular preexcitation. In agreement with the previous findings of this group, the accessory bundles in wild-type embryos were smaller, and there was no correlation with ECG recordings.[17, 18] In the previous study,[18] the accessory bundles identified as myocardial on myosin light chain 2a positivity were noted to be broad and multiple and in various locations in young hearts (Hamburger-Hamilton stages 35–39), whereas in older embryos (Hamburger-Hamilton stages 40–44), the bundles were small and mainly located on the right side. By way of comparison, fibrous insulation was complete in the adult quail. Coincidentally, they observed that MLC2a-positive pathways were also stained with periostin, a fibroblast marker that has a role in regulating fibroblast-myocyte interaction.[19] In the present report,[17] the small pathways in both wild-type and EPDC-inhibited hearts stained positive for both MLC2a and periostin. Broad pathways were only found in EPDC-inhibited hearts, but these were associated with local interruption of periostin staining. An important observation of the present study[17] is the interplay between EPDCs, periostin, and accessory pathways. The investigators proposed the concept that impeded migration of EPDCs through the myocardium to the endocardial cushions delayed the development of the fibrous annulus. Although the study has given us a glimpse of pathways that are candidates for premature ventricular activation in the quail, the question of why some accessory pathways produce a functional effect, occasionally devastatingly so, whereas others do not, remains to be clarified.

In his monograph, Öhnell[2] considered that some may have been acquired, for instance after myocarditis, a view also put forward more recently by Basso and her colleagues.[6]

Developmentally, the work of Kolditz and colleagues would appear to support the notion that accessory pathways resulted from incomplete interruption of canal myocardium resulting from late arrival of EPDCs.[17] Although incomplete interruption due to sulcus tissue stopping short of the annulus can account for accessory atrioventricular pathways that pass close to the annulus, it is difficult to picture the same process being involved in pathways that are in peripheral locations or in other morphologies as described above. The conundrum of whether those develop later by growing through holes in the tissue plane remains. For those related to coronary veins, what causes the walls to become muscularized (or remain muscularized)? Do the multipotent EPDCs and periostin have a role in those, too? We await further insights into this intriguing area of study.

Sources of Funding

The Cardiac Morphology unit at the Royal Brompton Hospital receives funding support from the Royal Brompton and Harefield Hospital Charitable Fund.

Disclosures

None.

The opinions expressed in this article are not necessarily those of the editors or of the American Heart Association.

References

1. Wood FC, Wolferth, C.C., Geckeler, G.D. Histologic demonstration of accessory muscular connections betwen auricle and ventricle in a case of short P-R interval and prolonged QRS complex. *Am Heart J.* 1943;25:454-462.
2. Ohnell RF. Pre-excitation, cardiac abnormality, pathophysiological, pathoanatomical and clinical studies of excitatory spread phenomenon bearing upon the problem of the WPW (Wolff, Parkinson and White) electrocardiogram and paroxysmal tachycardia. *Acta Med Scand.* 1944;152:1-167.
3. Ferguson TBJ, Cox, J.L. Surgical management of the Wolff-Parkinson-White syndrome. In: Mandel WJ, ed. *Cardiac Arhythmias*. Philadelphia: J.B. Lippincott Co.; 1995:1154-1156.
4. Becker AE, Anderson RH, Durrer D, Wellens HJ. The anatomical substrates of wolff-parkinson-white syndrome. A clinicopathologic correlation in seven patients. *Circulation.* 1978;57(5):870-879.
5. Peters NS, Rowland E, Bennett JG, Green CR, Anderson RH, Severs NJ. The Wolff-Parkinson-White syndrome: the cellular substrate for conduction in the accessory atrioventricular pathway. *Eur Heart J.* 1994;15(7):981-987.
6. Basso C, Corrado D, Rossi L, Thiene G. Ventricular preexcitation in children and young adults: atrial myocarditis as a possible trigger of sudden death. *Circulation.* 2001;103(2):269-275.
7. Tchou P, Lehmann MH, Jazayeri M, Akhtar M. Atriofascicular connection or a nodoventricular Mahaim fiber? Electrophysiologic elucidation of the pathway and associated reentrant circuit. *Circulation.* 1988;77(4):837-848.
8. Pappone C, Manguso F, Santinelli R, Vicedomini G, Sala S, Paglino G, Mazzone P, Lang CC, Gulletta S, Augello G, Santinelli O, Santinelli V. Radiofrequency ablation in children with asymptomatic Wolff-Parkinson-White syndrome. *N Engl J Med.* 2004;351(12):1197-1205.
9. Wellens HJ. Catheter ablation for cardiac arrhythmias. *N Engl J Med.* 2004;351(12):1172-1174.
10. de Jong F, Opthof T, Wilde AA, Janse MJ, Charles R, Lamers WH, Moorman AF. Persisting zones of slow impulse conduction in developing chicken hearts. *Circ Res.* 1992;71(2):240-250.
11. Kim JS, Virágh S, Moorman AF, Anderson RH, Lamers WH. Development of the myocardium of the atrioventricular canal and the vestibular spine in the human heart. *Circ Res.* 2001;88(4):395-402.

12. Wessels A, Vermeulen JL, Verbeek FJ, Virágh S, Kálmán F, Lamers WH, Moorman AF. Spatial distribution of "tissue-specific" antigens in the developing human heart and skeletal muscle. III. An immunohistochemical analysis of the distribution of the neural tissue antigen G1N2 in the embryonic heart; implications for the development of the atrioventricular conduction system. *Anat Rec.* 1992;232(1):97-111.

13. Wessels A, Markman MW, Vermeulen JL, Anderson RH, Moorman AF, Lamers WH. The development of the atrioventricular junction in the human heart. *Circ Res.* 1996;78(1):110-117.

14. van Gils FA. The development of thehuman atrioventricular valves. *J Anat.* 1979;128:427-428.

15. Wenink AC, Gittenberger-de Groot AC. Embryology of the mitral valve. *Int J Cardiol.* 1986;11(1):75-84.

16. Gittenberger-de Groot AC, Vrancken Peeters MP, Mentink MM, Gourdie RG, Poelmann RE. Epicardium-derived cells contribute a novel population to the myocardial wall and the atrioventricular cushions. *Circ Res.* 1998;82(10):1043-1052.

17. Kolditz DP, Wijffels MC, Blom NA, van der Laarse A, Hahurij ND, Lie-Venema H, Markwald RR, Poelmann RE, Schalij MJ, Gittenberger-De Groot AC. Epicardium-Derived Cells in Development of Annulus Fibrosis and Persistence of Accessory Pathways. *Circulation.* 2008.

18. Kolditz DP, Wijffels MC, Blom NA, van der Laarse A, Markwald RR, Schalij MJ, Gittenberger-de Groot AC. Persistence of functional atrioventricular accessory pathways in postseptated embryonic avian hearts: implications for morphogenesis and functional maturation of the cardiac conduction system. *Circulation.* 2007;115(1):17-26.

19. Oka T, Xu J, Kaiser RA, Melendez J, Hambleton M, Sargent MA, Lorts A, Brunskill EW, Dorn GW, Conway SJ, Aronow BJ, Robbins J, Molkentin JD. Genetic manipulation of periostin expression reveals a role in cardiac hypertrophy and ventricular remodeling. *Circ Res.* 2007;101(3):313-321.

Chapter

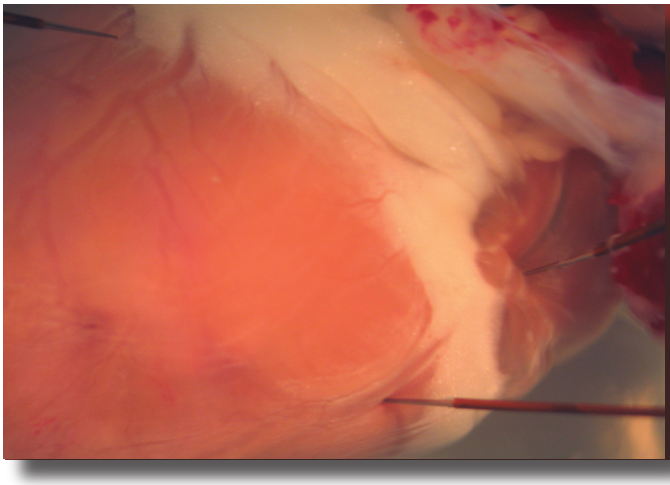

4

Nathan D. Hahurij[1,2]
Denise P. Kolditz[2,3]
Nico A. Blom[1]
Regina Bökemkamp[1]
Roger R. Markwald[4]
Martin J. Schalij[3]
Robert E. Poelmann[2]
Adriana C. Gittenberger-de Groot[2]

[1] Department of Pediatric Cardiology, Leiden University Medical Center, Leiden, The Netherlands;
[2] Department of Anatomy and Embryology, Leiden University Medical Center, Leiden, The Netherlands;
[3]Department of Cardiology, Leiden University Medical Center, Leiden, The Netherlands;
[4]Department of Cell Biology and Anatomy, Medical University of South Carolina, Charleston, South Carolina

Functional Accessory Atrioventricular Myocardial Pathways in Mouse Heart Development

Submitted

Abstract

Background. Atrioventricular reentry tachycardia (AVRT) requiring an accessory atrioventricular pathway (AP) is the most common type of arrhythmia in the perinatal period of development. The etiology of these arrhythmias is not fully understood as well as their capability to resolve spontaneously in the first year of life. The temporary presence of APs during annulus fibrosis development might be the cause of this specific type of arrhythmias.

Methods and Results. Electrophysiological recordings of ventricular activation patterns were studied in pre- and post-septated embryonic mouse hearts by placing unipolar electrodes on the right atrium, left ventricular apex and left and right ventricular base. The recordings revealed the presence of functional APs in early (13.5-15.5 dpc) and late (16.5-18.5 dpc) post-septated stages of mouse heart development. Immunohistochemical analysis with antibodies against MLC2a, Periostin, Nkx2.5 and Cx43 confirmed the presence of APs, which stained positive for MLC2a and Nkx2.5 and negative for Periostin and Cx43. Longitudinal analyses showed that the APs gradually decreased in number (P=0.003) and size (P=0.035) at subsequent stages of development (13.5-18.5 dpc). Expression of periostin was observed in the developing annulus fibrosis, adjacent to APs and other locations where formation of fibrous tissue is essential.

Conclusion. Functional APs are present during normal mouse heart development. These functional APs especially in late stages of cardiac development, can serve as a transient substrate for AVRTs in the perinatal period of development.

Introduction

In the fetus and newborn atrioventricular (AV) reentrant tachycardia (AVRT) is a relatively common tachyarrhythmia. Initial management of these tachycardias can be difficult but the natural course is benign and most children remain symptom free without medication after the age of one year.[1-3] AVRT requires the presence of an accessory atrioventricular myocardial pathway (AP) that crosses the annulus fibrosis. The factors contributing to the formation of APs are largely unknown. It has been hypothesized that the transient presence of APs during the normal formation of the isolating annulus fibrosis could serve as substrate for AVRT in the perinatal period, explaining its self-limiting character. In hearts of normal human fetuses and newborns the presence of APs clearly have been identified, but there are no data on conducting properties of these physiological APs in humans.[4, 5]

Proper development of the annulus fibrosis plays a key role in the separation of atrial and ventricular myocardium in the AV canal.[6] Formation of this isolating structure encompasses interactions between several molecular pathways, which have not yet been identified completely. Periostin, primarily described as osteoblast-specific factor 2[7] is highly expressed in collagen rich-fibrous connective tissue in the developing heart, which is subjected to high mechanical stress.[8, 9] Recently it has been shown that periostin directly regulates collagen I fibrillogenesis[9] and that it is also capable to induce proliferation of already differentiated cardiomyocytes in injured hearts.[10] The inductive role of periostin on both cardiomyocytes and fibrous tissue seems to be of special interest in the formation of the annulus fibrosis, where atrial and ventricular myocardium need to be separated by the formation of fibrous tissue.[11, 12]

The annulus fibrosis separates the atrial and ventricular myocardium in two separate myocardial compartments, which are connected via the AV conduction axis comprising the AVN and the bundle of His.[13] At early embryonic stages before ventricular septation has been completed and the development of the annulus fibrosis has started, atrial and ventricular myocardium are continuous in the primitive AV canal, which establishes a ventricular base-to-apex activation pattern. At later stages, ventricular conduction transforms into the mature apex-to-base activation. The switch from base-to-apex in apex-to-base activation is suggested to be closely related to the completion of ventricular septation and the separation of atrial and ventricular myocardium by the developing annulus fibrosis.[14, 15] Nevertheless, contemporary electrophysiological

studies in embryonic mouse hearts have shown that before completion of ventricular septation a mature apex-to-base activation is already present, suggesting that the AV conduction axis is functional far before ventricular septation has finished.[16, 17]

Studies in avian demonstrated that antegrade conducting APs are present at late post-septated stages of heart development, which gradually diminished during fetal development.[15] In mammalian hearts APs have also been described,[17, 18] however the description of these APs mainly focused on the electrophysiological properties of the primitive AV canal myocardium in pre-septated hearts[17] and neither late stages of fetal heart development nor the exact course of APs at the developing annulus fibrosis were studied.

The current study for the first time describes the presence of "functional" APs in early and late post-septated stages of mouse heart development. Furthermore we show that periostin is highly expressed in the developing annulus fibrosis at locations where separation of atrial and ventricular myocardium is mandatory.

Methods

Animals and Preparation of Hearts

All animal experiments were approved by the local medical ethical committee. To obtain the embryonic hearts two separate wildtype mouse strains were used, C57Bl6/Jico and CD1. If a vaginal plug was observed one day after breeding this embryonic stage was considered to be 0.5 day past conception (dpc). Embryos of subsequent stages were used, ranging from 11.5 dpc to 18.5 dpc (n=48). After cervical dislocation of the pregnant mouse, an incision was made in the mid-abdominal region followed by the extraction of the two laterally located uterus horns. The complete uterus was placed in Petri dish filled with Tyrode's solution containing (mmol/L) 130 NaCl, 4 KCL, 1,2 KH_2PO_4, 0,6 $MgSO_4 \cdot 7H_2O$, 20 $NaHCO_3$, 1,5 $CaCL_2 \cdot 2H_2O$ and 10 glucose at 37^0 Celsius. Subsequently in Tyrode's solution of 0^0 Celsius one-by-one the embryonic hearts were dissected. After isolation of the heart, excessive lung tissue was carefully removed and the hearts were further processed for electrophysiological recordings.

Electrophysiologic Recordings - Experimental Setup

Embryonic hearts were attached with fine wires through extra-cardiac tissue in a fluid heated, temperature controlled (Physitemp instruments Inc, Clifton NJ, USA) Petri dish of 35.5-37^0 Celsius onto a layer of agarose gel (Roche Diagnostics GmbH, Mannheim, Germany). During the equilibration period of 3 minutes and the subsequent electrophysiological recordings the hearts were constantly super-perfused with Carbogenated (95% O_2 and 5% CO_2) Tyrode's solution of 37^0 Celsius.

For electrophysiological extracellular recordings 4 unipolar tungsten electrodes (tip: 1 to 2 μm; impedance 0.9 to 1.0 MΩ; WPI Inc, Sarasota FL, USA) were placed on the right atrium (RA), right ventricular base (RVB), left ventricular base (LVB) and left ventricular apex (LVA) using microscopic guided micromanipulators (Wild Heerbrugg, M7A, Switzerland) (**Figure 1**).
Furthermore, an Ag/AgCl electrode in the Petri dish served as reference electrode. The complete experimental setting was located in a Faraday cage to prevent the recordings from exterior electrophysiological disturbances.
All electrograms were recorded with a high-gain, low-noise, direct current bioamplifier system (Iso-DAM8A; WPI Inc) with 4 isolated preamplifier modules with an output impedance of $>10^{12}$ Ω. The signals were band-pass (300 Hz to 1

kHz) and notch filtered (50 Hz) before being digitized at a sample rate of 1≥ kHz with a computerized recording system (Prucka Engineering Inc, Houston, Tex) and stored on optical disks for offline analysis.

Electrophysiological recordings of all cardiac developmental stages (12.5-18.5 dpc) were performed under stable sinus rhythm after a 3-minute calibration period. On the unipolar electrograms the steepest negative deflection was considered to be the local activation time. The local depolarization time of each electrode (RA, RVB, LVB and LVA) was calculated by the average of 10 consecutive beats. Subsequently, the global ventricular activation of each heart could be determined: base-to-apex if the RVB or LVB depolarized 1≥ms prior to the LVA; apex-to-base if the LVA depolarized 1≥ms prior to the RVB or LVB; concurrent if the depolarization time between the LVA and LVB or RVB was <1ms. Furthermore, the basal cycle length/HR of each heart was calculated by the average of 10 consecutive beats.

After EP recording the hearts were fixed in 4% paraformaldehyde (PFA) for immunohistochemical processing.

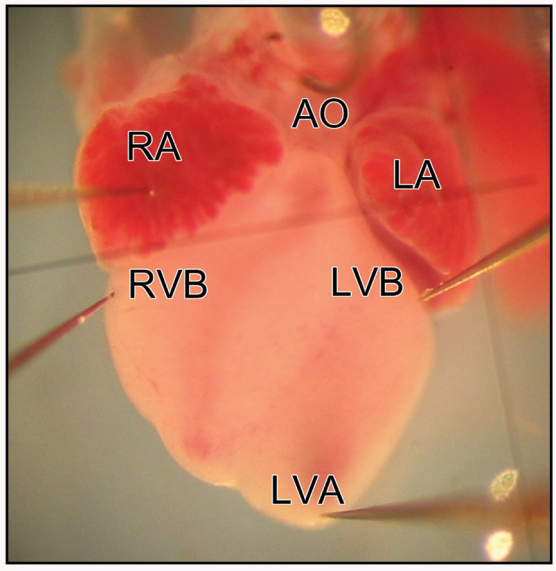

Figure 1. Positioning of the unipolar electrodes for electrophysiological recordings in a postseptated mouse heart. Electrophysiological measurements were performed under constant perfusion with carbogenated Tyrode's solution at 37 degrees C. Four Tungsten electrodes were placed on the epicardial surface of the embryonic hearts, at the right atrium (RA), right ventricular base (RVB), left ventricular base (LVB) and the left ventricular apex (LVA). All electrophysiological recordings were performed under stable heart rates after a 3 minute calibration period of the hearts. AO indicates Aorta.

Immunohistochemistry and Immunofluoresence

Standard immunohistochemistry was performed with antibodies specifically against atrial myosin light chain 2 (MLC2a, gift from S.W. Kubalak), Periostin (gift from R.R. Markwald) and Connexin 43 (Cx43, Sigma, C6219). In addition, immunofluorescent double staining procedures were performed with a combination of periostin and the NK2 transcription factor related locus 5 (Nkx2.5, Santa Cruz Biotechnology, sc-8697) specific antibodies. For details concerning the exact staining procedures, we refer to the online data supplement.

Morphology and Statistical Analysis

All hearts were carefully studied for the presence of accessory myocardial AV connections using an Olympus BH-2 lighting microscope. Accessory AV myocardial connections were classified based on their specific location at the developing annulus fibrosis. Furthermore the AP-width was calculated by counting the number of subsequent MLC2a stained sections through which a single accessory connection could be followed and multiplied by 25 μm (distance between subsequent MLC2a stained sections).

Statistical analysis of the HR and AV conduction time was performed with a students-*t*-test if values were equally distributed (Skewness is |-1|) otherwise a Mann-Whitney *U* test was performed. Analyses of AP-number and AP-width were performed with a univariate analyses of variance (unianova). A P value of < 0.05 (2-tailed) was considered to be significant. The SPSS 15.0 software package (SPSS Inc, Chicago, Ill) was used for all analyses.

Results

Electrophysiological Recordings

Pre-Septated Hearts (11.5-13.5 dpc; n=6)

After a 3-minute calibration period of the hearts in the experimental chamber, electrophysiological recordings were performed under stable HRs. The mean recorded HR in pre-septated hearts was 94±24 bpm with a mean AV interval of 84±13ms. Comparable to previous studies,[16,17] most pre-septated hearts (n=4; 67%) at these stages already showed a LVA activation prior to RVB or LVB activation, indicating that the AV conduction axis is functional before ventricular septation has been completed. In 33% (n=2) of hearts concurrent ventricular apex and base activation patterns were observed (**Table 1**).

Group,age,(n)	HR,BPM,mean±SD (range)	AV-interval,ms,mean±SD (range)	Ventricular Activation pattern		n (%)
Pre-septated	94±24 (66-135)	83±13 (64-105)	LVA>LVB/RVB		4 (67)
11,5-13,5dpc (n=6)			LVB>LVA		-
			RVB>LVA		-
			Concurrent		2 (33)
				LVA=LVB	-
				LVA=RVB	2 (33)
				LVA=LVB=RVB	-
Early Post-septated	115±41 (67-246)	80±17 (44-112)	LVA>LVB/RVB		11 (38)
13,5-15,5dpc (n=29)			LVB>LVA		2 (7)
			RVB>LVA		2 (7)
			Concurrent		14 (48)
				LVA=LVB	12 (41)
				LVA=RVB	2 (7)
				LVA=LVB=RVB	-
Late Post-septated	95±27 (63-146)	81±18 (56-110)	LVA>LVB/RVB		6 (46)
16,5-18,5dpc (n=13)			LVB>LVA		4 (31)
			RVB>LVA		1 (8)
			Concurrent		2 (15)
				LVA=LVB	2 (15)
				LVA=RVB	-
				LVA=LVB=RVB	-

Table 1. Summary of ventricular activation patterns in pre-, early post- and late post-septated hearts.

Early Post-Septated Hearts (13.5-15.5 dpc; n=29)

In early post-septated hearts (n=29) a mean HR of 115±41 bpm was recorded with a mean AV interval of 80±17ms. Interestingly, only 38% (n=11) of early post-septated hearts showed an apex-to-base ventricular activation pattern, the largest group showed base-to-apex and concurrent ventricular activation patterns (n=18; 62%). A concurrent apex and base activation was recorded in the majority of early post-septated hearts (n=14; 48%). More detailed analyses of the concurrent activated hearts showed that in most of these hearts (n=12; 41%) concurrent activation occurred between the LVB and LVA. In two hearts (7 %) the RVB was activated prior to the LVA and also in two hearts (7%) the LVB was activated prior to LVA (**Table 1**). Statistical analyses of the AV conduction time showed no significant differences (*P*=ns) between the mean AV conduction time in apex-to-base (78±12ms; n=11) and the base-to-apex and concurrent (81±20ms; n=14) activated hearts.

Late Post-Septated Hearts (16.5-18.5 dpc; n=13)

The mean HR recorded in these hearts was 95±27 bpm with a mean AV interval of 81±18ms. Even at late post-septated developmental stages a mature apex-to-base activation pattern was observed in only 46% (n=6) of the hearts. In a relatively large group of hearts activation of the LVB prior to the LVA was recorded (31%; n=4). Concurrent apex and base activation was observed in 15% (n=2), by which concurrent activation only occurred between the LVB and LVA. Furthermore, activation of the RVB prior to the LVA was observed in one heart (8%) (**Table 1**). Analysis of the mean AV conduction time showed no significant difference (*P*=ns) in apex-to-base (80±22ms; n=6) and base-to-apex and concurrent (82±16ms; n=7) activated hearts. Examples of the unipolar-electrophysiological recordings of apex-to-base, base-to-apex and concurrent activated hearts are shown in **Figures 2-4**.

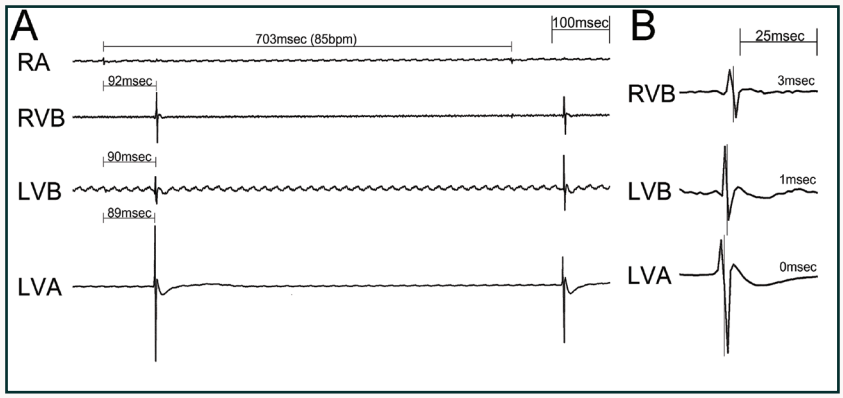

Figure 2. Representative electrophysiological recording of an Apex-to-Base activated heart. (A) shows a recording of an early post-septated embryonic heart of 13.5dpc with a cycle length of 703ms (85bpm). First activation of the left ventriclar apex (LVA) occurs 89ms after activation of the right atrium (RA) followed by the activation of the left and right ventricular base, (LVB; 90ms) and (RVB; 92ms) respectively. (B) magnification of the ventricular activation patterns, clearly showing that the point of the steepest negative deflection at the LVA precedes 1ms prior to LVB and 3ms prior to RVB activation, thereby creating an apex-to-base activation of the ventricles.

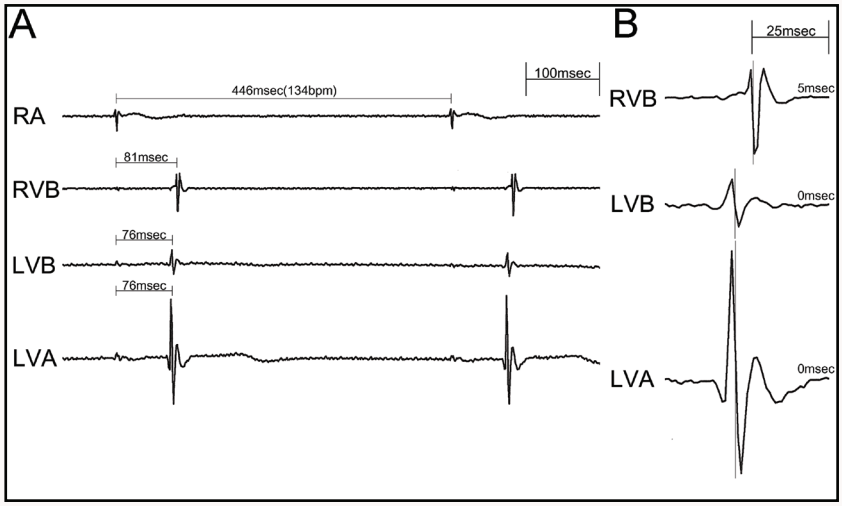

Figure 3. Representative electrophysiological recording of a concurrent Apex and Base activated heart. (A) Shows a recording of an early post-septated heart of 15.5dpc with a cycle length of 446ms (134bpm). 76ms after activation of the right atrium (RA), the first ventricular activation was observed both at the left ventricular apex (LVA) and left ventricular base (LVB). Subsequently the right ventricular base (RVB) was activated after 81ms. (B) Magnification of the ventricular activation patterns, showing that the steepest negative deflection of the RVB is 5ms next to that of the LVA and LVB, which are activated at the same time point. Therefore this heart showed a concurrent LVA and LVB activation.

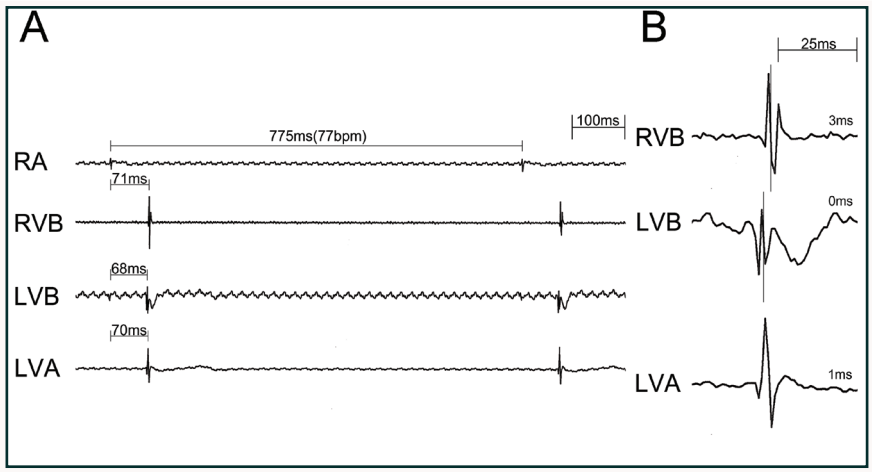

Figure 4. representative electrophysiological recording of a Base-to-Apex activated heart. (A) shows a recording of a late post-septated embryonic heart of 16.5dpc with a cycle length of 775ms (77bpm). 68ms after activation of the right atrium (RA) the first ventricular activation was observed at the left ventriclar base (LVB). Subsequently the left ventricular apex (LVA) and right ventricular base (RVB) were activated at 70ms and 71ms respectively. (B) magnification of the ventricular activation patterns, clearly showing that the point of the steepest negative deflection at the LVB precedes 2ms prior to LVA and 3ms prior to RVB activation, thereby creating an base-to-apex activation of the ventricles.

Morphological Substrates for Arrhythmias

In all pre-septated hearts (n=6) the MLC2a stained sections showed a myocardial continuity between the atria and ventricles in the region of the primitive AV canal. At several locations in the left and right AV ring separation of the atrial and ventricular myocardium by the developing annulus fibrosis was already observed (**Figure 5 A, B, E**). The primitive ventricular septum was already present at 11.5 dpc and ventricular septation was completed between 13.5-14.5 dpc. At these stages expression of Cx43 was present in the working myocardium of both atria and ventricles (**Figure 5 C**), whereas Cx43 expression was absent in the myocardium of the complete AV canal (**Figure 5 C and E**). At the dorsal side of the heart a broad myocardial continuity between the atria and ventricles was observed, the AV conduction axis comprising the AVN and the bundle of His (data not shown).

In all early post-septated hearts (13.5-15.5 dpc; n=29) APs were found around both the mitral and tricuspid orifice of the AV canal. Some of the APs consisted of a single strand of myocardium whereas others comprised broad myocardial continuities. At these stages the APs, similar to the complete AV

junctional myocardium, were negative for Cx43 (**Figure 5 G, H**). Expression of Cx43 was still clearly present in the working myocardium of the atria and ventricles. At early post-septated stages APs were mostly located around the mitral orifice (63%; *P*=0.000), and analyses of the AP-width also showed a larger mean total AP-width around the mitral orifice (*P*=0.000) (**Table 2**). Interestingly, in almost all early post-septated hearts (24/29) a broad Cx43 negative AP was present at the anterolateral position of the left AV junction connecting the left atrial myocardium with the left ventricular myocardium along its free wall (**Figure 5 F-H**).

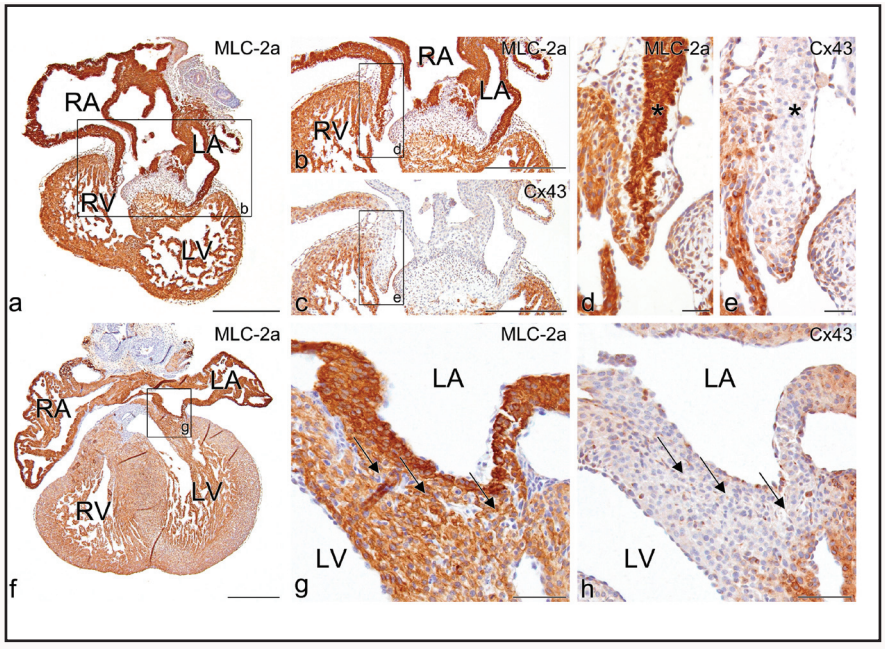

Figure 5. MLC2a and **Cx43 expression in the AV junction in pre- and post-septated hearts. A.** Represents a frontal section of a pre-septated heart of 12.5dpc stained with MLC-2a. In the AV junction area. **B**. Magnification of boxed area in (**A**), the expression of connnexin43 (Cx43) was absent ((**C**) consecutive section of (**A**)). Expression of Cx43 was clearly present in both the working myocardium of the atria and ventricles (**C**). **D**. and **E**., magnifications of boxed areas in (**B**) and (**C**) respectively, shows a detail of the myocardium of the right AV junction which is positive for MLC-2a (asterisk in (**D**)) and negative for Cx43 (asterisk in (E)). **F.** Shows a frontal section of a 15.5dpc heart stained with MLC-2a. **G**. magnification of the boxed area in (**F**) shows the location of the large antero-lateral AP which was observed in 37 of the 42 post-septated hearts which were investigated. Arrows in (**G**) indicate the exact location of the myocardial connections between the atria and ventricles. The myocardium of the AV junction, which includes these connections is negative for Cx43 (arrows in (**H**)). RA indicates right atrium; RV=right ventricle; LA=left atrium; LV=left ventricle. Scalebar A-C and F=300µm; D, E=30 µm; G, H=60µm.

In all late post-septated hearts (16.5-18.5 dpc; n=13) APs were still observed around the mitral and tricuspid orifice. The expressions pattern of Cx43 was similar as compared to earlier stages and all APs were still Cx43 negative (data not shown). Whereas the mean total AP width at these stages was largest at the mitral orifice (*P*=0.028), no differences were found between the mean number of APs at the mitral and tricuspid orifice (*P*=ns). Compared to earlier stages the mean number of APs per heart around the mitral orifice had decreased significantly (*P*=0.000), whereas no significant decrease was observed at the tricuspid orifice (*P*=0.136) (**Table 2**). Furthermore, the anterolateral AP at the left AV junction was present in all hearts (13/13).

Longitudinal analyses of AP-number and AP-width in all post-septated hearts of subsequent developmental stages (13.5-18.5 dpc; n=42) showed a significant decrease both in mean number of APs (*P*=0.003) (**Figure 6**) and mean total AP-width (*P*=0.035). Furthermore, differences were observed in the rate by which APs disappeared around the mitral and tricuspid orifice. Although the majority of APs were located around the mitral orifice, a higher rate of AP disappearance of these left sided APs was observed (*P*=0.015).

	Early post-septated 13,5-15,5dpc (n=29)	Late post-septated 16,5-18,5dpc (n=13)	Statistics (early vs late)
Mean number of APs	8,1	5,2	P=0,003
Mean number left sided APs	5,1	3,1	P=0,000
Mean number right sided APs	3,0	2,1	P=ns
Statistics mean AP number (left vs right)	P=0,000	P=ns	-
Mean width (μm) of APs	347	214	P=0,035
Mean width (μm) left sided APs	238	138	P=0,000
Mean width (μm) right sided APs	109	76	P=ns
Statistics mean AP width (μm; left vs right)	P=0,000	P=0,028	-

Table 2. Summary of the morphological analyses of APs in early and late post-septated hearts. For statistical analysis an Unianova was used, a P of <0.05 was considered to be significant.

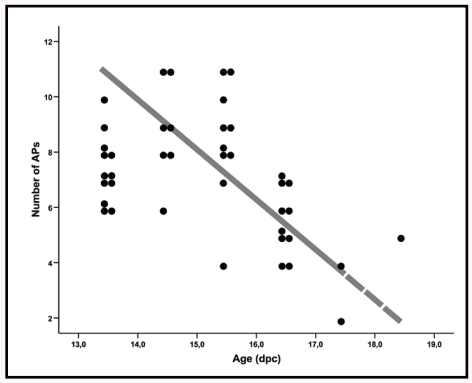

Figure 6. The course of APs in post-septated mouse hearts. The graph schematically represents the course of APs around both the developing tricuspid and mitral valve orifice in post-septated mouse hearts (n=42). Each heart is represented by a black circle which indicates the total number of APs in each heart (Y-axis), at subsequent developmental stages (X-axis). The gray line indicates the hypothesized course of persistent APs at the developing annulus fibrosus.

Periostin Expression in Relation to Annulus Fibrosis Development and APs

Immunohistochemical analysis showed that cardiac expression of periostin was present in all embryonic and fetal stages, which were investigated (11.5-18.5 dpc). Expression of periostin was limited to specific cardiac structures i.e. the epicardium, the endothelial lining of the atrial and ventricular trabeculae, the subendocardial region of both outflow and AV cushions and the interstitial fibroblasts which were flanked by working myocardium in the atria and ventricles. At later stages (>14.5 dpc) strong expression was also observed in the AV cushion derived AV valves including their tension apparatus and in the endothelial lining of the developing coronary vessels. Remarkable absence of periostin was observed in parts of the AV conduction axis, especially in the AVN (data not shown). Periostin expression was clearly present in the developing annulus fibrosis. Strongest expression was observed at the immediate border between the developing annulus fibrosis and myocardium of the AV canal (**Figure 7 A-C, G-I**). Furthermore, high expression of periostin seemed to overlie the MLC2a positive APs around both the mitral and tricuspid orifice (**Figure 7 I**).

Immunofluorescent double stained sections with periostin and Nkx2.5 were used for detailed studies on periostin expression in the developing annulus fibrosis in relation to the AP cardiomyocytes (**Figure 7 D-F, J-L**). At all stages

of development periostin was strongly expressed in fibroblasts bordering AP cardiomyocytes (11.5-18.5 dpc), however no periostin expression could be demonstrated in the Nkx2.5 positive cardiomyocytes themselves (**Figure 7 F, L**). It appears that periostin was predominantly expressed in fibroblasts flanking cardiomyocytes suggesting an inductive role in the process of isolation by the developing annulus fibrosis.

At early post-septated stages low expression of periostin was observed in almost all hearts at the anterior side of the left AV junction, which corresponds to the location of the left anterolateral APs. These broad APs were positive for the myocardial markers MLC2a and Nkx2.5 and negative for periostin. (**Figure 7 A-F**). At later post-septated stages, expression of periostin increased at these specific areas (**Figure 7 G-L**).

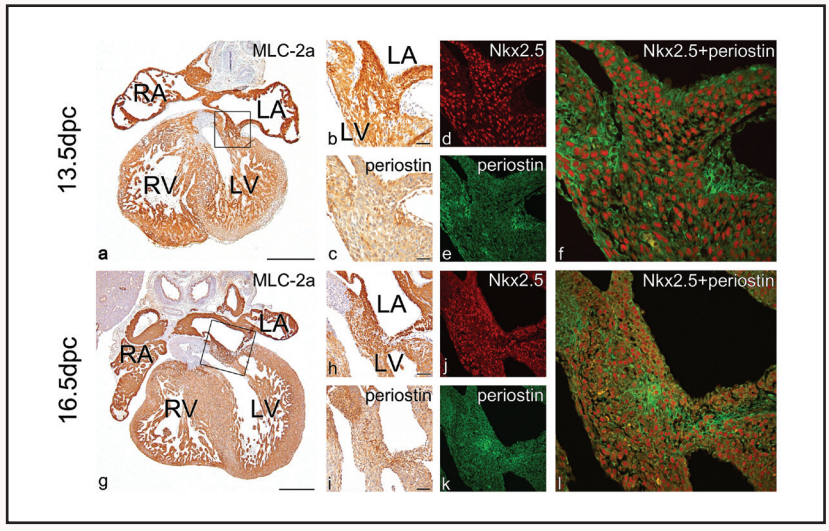

Figure 7. Nkx2.5 and periostin double expression in the developing annulus fibrosus and persistent APs. A. frontal section of an early post-septated heart of 13.5dpc stained with MLC-2a. The boxed area in (**A**) shows a left sided antero-lateral accessory myocardial pathway (AP) magnified in (**B**). Expression of periostin was observed next to the MLC-2a positive AP ((**C**) consecutive of (**A**)). An immunofluorescent (IF) double stained section shows that this AP ((**F**) consecutive section of (**A**)) was positive for Nkx2.5 (**D**) and negative for periostin (**E**). **G**. Frontal section of almost the same area in (**A**) of a late post-septated heart of 16.5dpc stained with MLC-2a. **H**. Magnification of the boxed area in (G), showing an MLC-2a positive AP which also is positive for periostin ((**I**) consecutive section of (**G**)). Compared to early post-septated stages (**F**), this AP ((**L**) IF consecutive section of (**A**)) is comprised of an intermingling network of Nkx2.5 positive cardiomyocytes (**J**) and periostin positive fibroblasts (**L**). RA indicates right atrium; RV=right ventricle; LA=left atrium; LV=left ventricle. Scalebars A, G=300µm; B-E=30 µm; H-I=60µm.

Discussion

AVRT is a relatively common tachyarrhythmia in the fetus and neonate that appears to resolve in the majority of cases during the first year of life.[1, 2] It has been suggested that APs involved in these tachycardias are remnant myocardial AV connections that disappear during the ongoing development of the isolating annulus fibrosis before and after birth.[4, 15] Although the presence of APs has been demonstrated during normal cardiac development in human fetuses and neonates, their conducting properties as well as their causative role in AVRT remains unknown.[4, 5, 19, 20]

It has been demonstrated that cardiac development is not finished by the time of birth and that cardiac maturation is an ongoing process extending into the first year of life.[19, 21, 22] Shortly after formation of the primary heart tube derived from two cardiogenic primordia, the future atrial and ventricular part of the heart develop with complete myocardial continuity at the primitive AV canal. Even in this primary heart tube before the formation of the specialized AV conduction axis, fast and slow conducting myocardial areas can already be discriminated. The primitive AV canal is composed of slow conducting Cx43 negative myocardium,[23] thereby separating the fast Cx43 positive atrial and ventricular myocardium, which will cause the heart to contract in a peristaltic manner.[24]

Eventually the AV conduction axis will develop, which coincides with the formation of the isolating annulus fibrosis between atria and ventricles in the region of the Cx43 negative AV canal myocardium. The development of this isolating structure is regulated through a complex of several developmental processes, in which bone morphogenetic protein (BMP) signaling,[13, 25] periostin an osteoblast specific factor[8, 15] and epicardium derived cells entering the heart at the AV sulcus play a key role.[11, 12, 15, 26, 27] Annulus fibrosis formation is not a process strictly limited to the embryonic stages of development, since contemporary studies have shown that the formation of the fibrous structures of the heart, including the annulus fibrosis and AV valves, extends into early postnatal development.[21, 22]

In the current study we have shown that the development of the annulus fibrosis occurs in the area of the Cx43 negative AV canal myocardium. During formation of this isolating structure we demonstrated the presence of antegrade conducting APs in normal mouse heart development. These APs significantly decreased in number and size at subsequent developmental stages, but remained

present even at late post-septated stages of heart development (**Figure 6**). Modern electrophysiological animal studies demonstrated the conducting properties of primitive AV canal myocardium[17] and the incidental presence of APs, which have been related to the etiology of Mahaim tachycardias in early developing mouse hearts.[18] The presence and course of functional APs as described in the present study have not been reported during mammalian heart development before.

A recent study of normal quail heart development also demonstrated antegrade conducting APs decreasing in number and size at subsequent developmental stages.[15] In quail the majority of APs were located at the posteroseptal aspect of the developing tricuspid orifice whereas in mouse hearts the APs were mainly located around the anterolateral aspect of the developing mitral orifice especially at later developmental stages.

Several factors may underlie the preferential location of persistent APs at the developing annulus fibrosis and the differences observed between mouse and avian. As a result of the physiological delay of right ventricular inflow tract formation, the isolation of this part of the annulus fibrosis in general is delayed as compared to the left side,[18] which might explain the high incidence of right posteroseptal APs in quail.[15] This however may only explain the APs present around the tricuspid orifice and not the high frequency of left anterolateral APs as observed in developing mouse hearts. Interestingly, recent studies on the development of the cardiac conduction system (CCS) by means of CCS-*lacZ* expression in mouse hearts, designated bundles of CCS-*lacZ* expressing cardiomyocytes at the same left anterolateral position at the developing AV junction. These β-galactosidase positive myocardial bundles, which are not a part of the developing CCS, could be traced in some hearts until postnatal stages of development and have been related to Wolff-Parkinson-White (WPW) pre-excitation syndrome.[16]

AP Location in Relation to Arrhythmias

The current study showed the presence of APs around the mitral as well as the tricuspid valve orifice at early and late post-septated stages of development. Like others, a direct one-to-one relation between morphologically observed APs and their ability to conduct could not be made.[15] However, differences were found between APs around the mitral and tricuspid valve orifice. At early post-septated stages a significant majority of APs were observed around the mitral orifice. In late post-septated hearts no significant differences were observed, although absolute AP numbers showed that the majority of APs were still

located at the left side. In addition, the total AP-width both in early and late post-septated hearts was largest around the mitral valve orifice. Interestingly, the electrophysiological recordings showed that in the majority of early and late post-septated hearts, base-to-apex activation occurred at the LVB. Furthermore, in most concurrent apex and base activated hearts activation arose between the LVA and LVB. Therefore, it seems most likely that premature base activation in post-septated hearts occurs more often via the large and broad APs situated around the mitral valve orifice.

Interestingly, we have recently reported,[4] like several others in the past on the presence of similar APs in developing human hearts.[5, 19, 20] In these hearts APs were observed around both the developing mitral and tricuspid valve orifice. Even in newborns APs were present with similar characteristics as observed in embryos and fetuses.[20] Although these APs have been related to clinically observed arrhythmias, their true functionality had never been established. In fetuses and infants APs involved in AVRT are found around both the tricuspid and more frequently around the mitral valve orifice,[28] which seems to be equivalent to the high frequency of temporary conducting APs at the developing mitral valve orifice as observed in the current study. However, we have to notice that we only measured antegrade conduction of the APs, which could serve as substrate for AVRTs and that neither retrogradely conducting APs nor sustained arrhythmias were recorded.

Periostin Expression in Relation to Annulus Fibrosis Formation and Persistent APs

Periostin is a member of the fasciclin gene family and acts as an adhesion molecule through binding of cell surface integrins.[29] In mouse heart development periostin expression can be detected as from 9.5 dpc in low levels in the developing AV cushions and cardiac expression levels slightly decrease along development.[8, 30] Like others we also observed that periostin expression was mainly present in those parts of the developing heart, which are known to be subjected to high rates of mechanical stress.[9] Furthermore we showed that expression of periostin was clearly present in the developing annulus fibrosis,[4, 15] specifically at locations were separation of atrial and ventricular myocardium is needed. At these regions periostin might induce formation of the isolating fibrous tissue, since it can directly regulate collagen-I fibrillogenesis.[9]

The broad Cx43 negative anterolateral left sided APs which most probably have an imperative role in the large group of early LVB and concurrent activated hearts were predominantly periostin negative in early post-septated stages of development. At later stages periostin expression increased at the location of left anterolateral APs, suggesting an active process of isolation at that specific area of the AV junction. Therefore we postulate that periostin has an important role in the isolation of the AV junction by the stimulation of fibrous tissue formation thereby separating the atrial and ventricular myocardium, which subsequently will lead to regression of temporary APs for conduction.

The exact signaling pathway by which periostin is regulated remains unknown, although it has been shown that periostin is upregulated by several growth factors including BMPs.[31] Transforming Growth Factor-Beta (TGF-β)[7] and Platelet Derived Growth Factors (PDGFs),[32] which are highly expressed in the developing AV region. In addition, state of the art studies performed in avian showed that Epicardium Derived Cells (EPDCs) play a key role in periostin regulation underlying proper annulus fibrosis development. Inhibition of the epicardial outgrowth at early embryonic stages of development, resulted in a disturbed annulus fibrosis development, which coincided with a high frequency of antegrade conducting APs staining negative for periostin.[11, 12]

The etiology of APs has not yet been clarified. In the majority of patients with WPW syndrome there is no familial involvement. APs are also associated with congenital heart disease specifically with abnormal development of the tricuspid valve like in Morbus Ebstein.[33] A minority of cases is inherited as a single gene disorder or occurs as part of a syndrome with a strong genetic basis.[34, 35] In humans *LAMP2*, *PRKAG2* gene mutations have been identified to be involved in familial WPW syndrome associated with cardiac hypertrophy.[36, 37] Animal studies have shown that mutations in the *Alk3* gene result in Cx43 positive APs due to disrupted formation of the annulus fibrosis.[13] In the present study we demonstrate that antegrade conducting APs remain present until late fetal stages of normal mouse heart development. These APs are Cx43 negative and appear to be remnants of the primitive AV myocardium. The presence of these APs may act as transient substrate for AVRT and may explain the spontaneous resolution of these arrhythmias in the fetal and neonatal period.

Study Limitations

All electrophysiological recordings were performed at a basal heart rate of a spontaneously beating mouse heart under sub-physiological circumstances, which of course influences the heart rate. For all electrophysiological recordings four unipolar electrodes were used. The authors are aware of the fact that with this small number of electrodes a direct one-to-one relation cannot be made between a morphologically discriminated AP and the electrophysiological measurements. As a consequence, the positioning of the electrodes together with the relatively small size of these embryonic mouse hearts might therefore explain that no differences were observed in AV conduction time between apex-to-base, base-to-apex and concurrent activated hearts.

Funding Sources

The presented work was supported by the Gisela Thier Foundation (Nathan D. Hahurij).

Conflict of Interest Disclosures

None.

References

1. Bauersfeld U, Pfammatter JP, Jaeggi E. Treatment of supraventricular tachycardias in the new millennium--drugs or radiofrequency catheter ablation? *Eur J Pediatr.* 2001;160(1):1-9.
2. Ko JK, Deal BJ, Strasburger JF, Benson DW. Supraventricular tachycardia mechanisms and their age distribution in pediatric patients. *Am J Cardiol.* 1992;69(12):1028-1032.
3. Naheed ZJ, Strasburger JF, Deal BJ, Benson DW, Gidding SS. Fetal tachycardia: mechanisms and predictors of hydrops fetalis. *J Am Coll Cardiol.* 1996;27(7):1736-1740.
4. Hahurij ND, Gittenberger-De Groot AC, Kolditz DP, Bökenkamp R, Schalij MJ, Poelmann RE, Blom NA. Accessory atrioventricular myocardial connections in the developing human heart: relevance for perinatal supraventricular tachycardias. *Circulation.* 2008;117(22):2850-2858.
5. Robb JS, Kaylor CT, Turman WG. A study of specialized heart tissue at various stages of development of the human fetal heart. *Am J Med* 2007;5:324-336.
6. Wessels A, Markman MW, Vermeulen JL, Anderson RH, Moorman AF, Lamers WH. The development of the atrioventricular junction in the human heart. *Circulation Research.* 1996;78(1):110-117.
7. Horiuchi K, Amizuka N, Takeshita S, Takamatsu H, Katsuura M, Ozawa H, Toyama Y, Bonewald LF, Kudo A. Identification and characterization of a novel protein, periostin, with restricted expression to periosteum and periodontal ligament and increased expression by transforming growth factor beta. *J Bone Miner Res.* 1999;14(7):1239-1249.
8. Kruzynska-Frejtag A, Machnicki M, Rogers R, Markwald RR, Conway SJ. Periostin (an osteoblast-specific factor) is expressed within the embryonic mouse heart during valve formation. *Mech Dev.* 2001;103(1-2):183-188.
9. Norris RA, Damon B, Mironov V, Kasyanov V, Ramamurthi A, Moreno-Rodriguez R, Trusk T, Potts JD, Goodwin RL, Davis J, Hoffman S, Wen X, Sugi Y, Kern CB, Mjaatvedt CH, Turner DK, Oka T, Conway SJ, Molkentin JD, Forgacs G, Markwald RR. Periostin regulates collagen fibrillogenesis and the biomechanical properties of connective tissues. *J Cell Biochem.* 2007;101(3):695-711.
10. Kühn B, del Monte F, Hajjar RJ, Chang YS, Lebeche D, Arab S, Keating MT. Periostin induces proliferation of differentiated cardiomyocytes and promotes cardiac repair. *Nat Med.* 2007;13(8):962-969.

11. Kolditz DP, Wijffels MC, Blom NA, van der Laarse A, Hahurij ND, Lie-Venema H, Markwald RR, Poelmann RE, Schalij MJ, Gittenberger-De Groot AC. Epicardium-Derived Cells in Development of Annulus Fibrosis and Persistence of Accessory Pathways. *Circulation.* 2008;117(12):1508-1517.

12. Lie-Venema H, Eralp I, Markwald RR, van den Akker NM, Wijffels MC, Kolditz DP, van der Laarse A, Schalij MJ, Poelmann RE, Bogers AJ, Gittenberger-De Groot AC. Periostin expression by epicardium-derived cells is involved in the development of the atrioventricular valves and fibrous heart skeleton. *Differentiation.* 2008;76(7):809-819.

13. Gaussin V, Morley GE, Cox L, Zwijsen A, Vance KM, Emile L, Tian Y, Liu J, Hong C, Myers D, Conway SJ, Depre C, Mishina Y, Behringer RR, Hanks MC, Schneider MD, Huylebroeck D, Fishman GI, Burch JB, Vatner SF. Alk3/Bmpr1a receptor is required for development of the atrioventricular canal into valves and annulus fibrosus. *Circ Res.* 2005;97(3):219-226.

14. Chuck ET, Freeman DM, Watanabe M, Rosenbaum DS. Changing activation sequence in the embryonic chick heart. Implications for the development of the His-Purkinje system. *Circ Res.* 1997;81(4):470-476.

15. Kolditz DP, Wijffels MC, Blom NA, van der Laarse A, Markwald RR, Schalij MJ, Gittenberger-de Groot AC. Persistence of functional atrioventricular accessory pathways in postseptated embryonic avian hearts: implications for morphogenesis and functional maturation of the cardiac conduction system. *Circulation.* 2007;115(1):17-26.

16. Rentschler S, Vaidya DM, Tamaddon H, Degenhardt K, Sassoon D, Morley GE, Jalife J, Fishman GI. Visualization and functional characterization of the developing murine cardiac conduction system. *Development.* 2001;128(10):1785-1792.

17. Valderrábano M, Chen F, Dave AS, Lamp ST, Klitzner TS, Weiss JN. Atrioventricular ring reentry in embryonic mouse hearts. *Circulation.* 2006;114(6):543-549.

18. Jongbloed MR, Wijffels MC, Schalij MJ, Blom NA, Poelmann RE, van der Laarse A, Mentink MM, Wang Z, Fishman GI, Gittenberger-de Groot AC. Development of the right ventricular inflow tract and moderator band: a possible morphological and functional explanation for Mahaim tachycardia. *Circ Res.* 2005;96(7):776-783.

19. James TN. Normal and abnormal consequences of apoptosis in the human heart. From postnatal morphogenesis to paroxysmal arrhythmias. *Circulation.* 1994;90(1):556-573.

20. Truex RC, Bishof JK, Hoffman EL. Accessory atrioventricular muscle bundles of the developing human heart. *Anat Rec.* 1958;131(1):45-59.

21. Kruithof BP, Krawitz SA, Gaussin V. Atrioventricular valve development during late embryonic and postnatal stages involves condensation and extracellular matrix remodeling. *Dev Biol.* 2007;302(1):208-217.

22. Visconti RP, Markwald RR. Recruitment of new cells into the postnatal heart: potential modification of phenotype by periostin. *Ann N Y Acad Sci.* 2006;1080:19-33.

23. Delorme B, Dahl E, Jarry-Guichard T, Marics I, Briand JP, Willecke K, Gros D, Théveniau-Ruissy M. Developmental regulation of connexin 40 gene expression in mouse heart correlates with the differentiation of the conduction system. *Dev Dyn.* 1995;204(4):358-371.

24. de Jong F, Opthof T, Wilde AA, Janse MJ, Charles R, Lamers WH, Moorman AF. Persisting zones of slow impulse conduction in developing chicken hearts. *Circ Res.* 1992;71(2):240-250.

25. Okagawa H, Markwald RR, Sugi Y. Functional BMP receptor in endocardial cells is required in atrioventricular cushion mesenchymal cell formation in chick. *Dev Biol.* 2007;306(1):179-192.

26. Eralp I, Lie-Venema H, Bax NA, Wijffels MC, van der Laarse A, Deruiter MC, Bogers AJ, van den Akker NM, Gourdie RG, Schalij MJ, Poelmann RE, Gittenberger-de Groot AC. Epicardium-derived cells are important for correct development of the Purkinje fibers in the avian heart. *Anat Rec.* 2006;288(12):1272-1280.

27. Gittenberger-de Groot AC, Vrancken Peeters MP, Mentink MM, Gourdie RG, Poelmann RE. Epicardium-derived cells contribute a novel population to the myocardial wall and the atrioventricular cushions. *Circ Res.* 1998;82(10):1043-1052.

28. Strasburger JF, Cheulkar B, Wichman HJ. Perinatal arrhythmias: diagnosis and management. *Clinics in perinatology.* 2007;34(4):627-652, vii-viii.

29. Norris RA, Kern CB, Wessels A, Moralez EI, Markwald RR, Mjaatvedt CH. Identification and detection of the periostin gene in cardiac development. *Anat Rec.* 2004;281(2):1227-1233.

30. Lindsley A, Li W, Wang J, Maeda N, Rogers R, Conway SJ. Comparison of the four mouse fasciclin-containing genes expression patterns during valvuloseptal morphogenesis. *Gene Expr Patterns.* 2005;5(5):593-600.

31. Inai K, Norris RA, Hoffman S, Markwald RR, Sugi Y. BMP-2 induces cell migration and periostin expression during atrioventricular valvulogenesis. *Dev Biol.* 2008;315(2):383-396.

32. Lindner V, Wang Q, Conley BA, Friesel RE, Vary CP. Vascular injury induces expression of periostin: implications for vascular cell differentiation and migration. *Arterioscler Thromb Vasc Biol.* 2005;25(1):77-83.

33. Smith WM, Gallagher JJ, Kerr CR, Sealy WC, Kasell JH, Benson DW, Reiter MJ, Sterba R, Grant AO. The electrophysiologic basis and management of symptomatic recurrent tachycardia in patients with Ebstein's anomaly of the tricuspid valve. *Am J Cardiol.* 1982;49(5):1223-1234.

34. Roberts DE, Hersh LT, Scher AM. Influence of cardiac fiber orientation on wavefront voltage, conduction velocity, and tissue resistivity in the dog. *Circ Res.* 1979;44(5):701-712.

35. Vidaillet HJ, Pressley JC, Henke E, Harrell FE, German LD. Familial occurrence of accessory atrioventricular pathways (preexcitation syndrome). *N Engl J Med.* 1987;317(2):65-69.

36. Arad M, Moskowitz IP, Patel VV, Ahmad F, Perez-Atayde AR, Sawyer DB, Walter M, Li GH, Burgon PG, Maguire CT, Stapleton D, Schmitt JP, Guo XX, Pizard A, Kupershmidt S, Roden DM, Berul CI, Seidman CE, Seidman JG. Transgenic mice overexpressing mutant PRKAG2 define the cause of Wolff-Parkinson-White syndrome in glycogen storage cardiomyopathy. *Circulation.* 2003;107(22):2850-2856.

37. Gollob MH, Green MS, Tang AS, Gollob T, Karibe A, Ali Hassan AS, Ahmad F, Lozado R, Shah G, Fananapazir L, Bachinski LL, Roberts R, Hassan AS. Identification of a gene responsible for familial Wolff-Parkinson-White syndrome. *N Engl J Med.* 2001;344(24):1823-1831.

Online Data Supplement

Methods

Immunohistochemistry

Immunohistochemical experiments were performed using the following antibodies against: atrial myosin light chain 2 (MLC2a, gift from S.W. Kubalak), periostin (Gift from R.R. Markwald) and Connexin 43 (Cx43, Sigma, C6219). After fixation in 4% PFA, the hearts were dehydrated and embedded in paraffin. The embedded hearts were 5 μm sectioned and mounted 1 to 5 onto protein/glycerin coated slides, so 5 different staining procedures could be performed on one embryo. After dehydration of the slides, inhibition of the endogenous peroxidase was performed for MLC2a with a solution of 0.3% H_2O_2 in PBS for 20 min. For periostin and Cx43 antigen retrieval was performed in 0.01M Citric buffer of Ph 6.0 at 97°C for 12 minutes, followed by inhibition of the endogenous peroxidase in a solution of 0.3% H_2O_2 in PBS for 20 min. Overnight incubation with the primary antibodies was performed: 1/2000 anti-MLC2a, 1/1000 anti-periostin and 1/200 anti-Cx43. The primary antibodies were dissolved in PBS-Tween-20 with 1% Bovine Serum Albumin (BSA, Sigma Aldrich, USA). The slides were rinsed between subsequent incubation steps: PBS (2x) and PBS-Tween-20 (1x). A 40 min incubation with secondary antibodies was performed, for MLC2a, periostin and Cx43: 1/200 goat-anti-rabbit-biotin (Vector Laboratories, USA, BA-100) and 1/66 goat serum (Vector Laboratories, USA, S1000) in PBS-Tween-20. Thereafter a 40 minute incubation with ABC-reagent (Vector-Laboratories, USA, PK 6100) was performed. For visualization, all slides were incubated with 400 μg/ml 3-3'di-aminobenzidin tetrahydrochloride (DAB, Sigma-Aldrich Chemie, USA, D5637) dissolved in Tris-maleate buffer pH7.6 to which 20 μl H_2O_2 was added for 10 min. 0.1% Haematoxilin (Merck, Darmstad, Germany) was used to counter stain the slides: MLC2a and Cx43 10 sec and periostin 5 sec, followed by rinsing with tap water for 10 minutes. Finally, the slides were dehydrated and mounted with Entellan (Merck, Darmstadt, Germany).

Immunofluoresence

An immunofluorescent double staining was performed with antibodies specifically against periostin and NK2 transcription factor related locus 5 (Nkx2.5, Santa Cruz Biotechnology, sc-8697). Preparation of sections was executed as described above. Overnight incubation with the primary antibodies was performed 1/2000

Nkx2.5 in combination with 1/250 periostin. Thereafter, a 60 minute incubation with the secondary antibody (1/200 horse-anti-goat-biotin and 1/66 horse serum) in combination with 1/50 donkey-anti-rabbit-FITC (Santa Cruz Biotechnology, sc-2090) was performed, followed by another 60 minute incubation with 1/200 Avidine-TRITC (Vector Laboratories, USA, A-2002). A 5 minute incubation with 4',6-diamidine-2-phenylidole-dihydrochloride (DAPI, Molecular probes, D3571) was executed to counter stain the slides. Finally the slides were mounted with Prolong Gold (Molecular probes, P36930).

Chapter 5

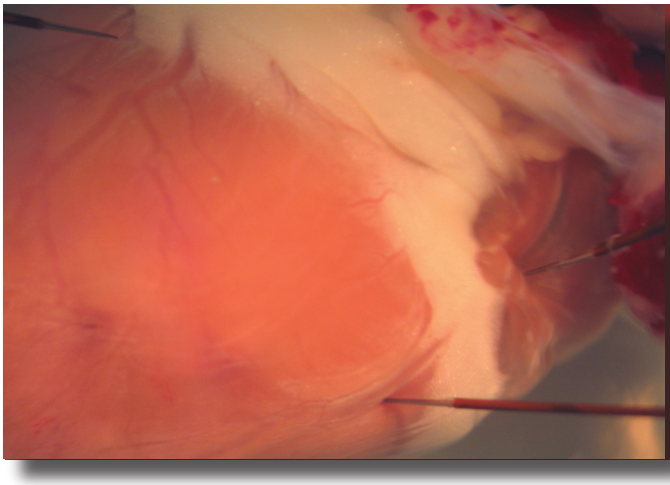

Nathan D. Hahurij[1,2]
Adriana C. Gittenberger-De Groot [2]
Denise P. Kolditz[2,3]
Regina Bökenkamp[1]
Martin J. Schalij[3]
Robert E. Poelmann[2]
Nico A. Blom[1]

[1]Department of Pediatric Cardiology, Leiden University Medical Center, Leiden, The Netherlands
[2]Department of Anatomy and Embryology, Leiden University Medical Center, Leiden, The Netherlands
[3]Department of Cardiology, Leiden University Medical Center, Leiden, The Netherlands

Accessory Atrioventricular Myocardial Connections in the Developing Human Heart: Relevance for Perinatal Supraventricular Tachycardias

Circulation 2008;117(22):2850-2858

Abstract

Background. Fetal and neonatal atrioventricular reentrant tachycardias (AVRTs) can be life threatening but resolve in most cases during the first year of life. Transient presence of accessory atrioventricular (AV) myocardial connections during annulus fibrosis development may explain this phenomenon.

Methods and Results. 45 human embryonic, fetal and neonatal sectioned hearts (4 to 36 weeks of development) were studied immunohistochemically. Accessory myocardial AV connections were quantified and categorized according to their specific location and 3-D AMIRA reconstructions were made. Between 4 and 6 weeks of development: atrial and ventricular myocardium was continuous at the primitive AV canal. At 6-10 weeks: numerous accessory myocardial AV connections were identified at the left (45%), right (35%) and septal (20%) region of the AV junction. Most right sided accessory connections comprised distinct myocardial strands, left sided connections consisted of larger myocardial continuities. At 10-20 weeks: all accessory AV connections comprised discrete myocardial strands and gradually decreased in number. The majority of accessory connections were located at the right AV junction (67%), predominantly at the lateral aspect (45%). At the left AV junction 17% and at the septal region 16% of the accessory connections were observed. 3-D reconstructions of the developing AV nodal area at these stages demonstrated multiple AV nodal related accessory connections. From 20 weeks until birth and in neonatal hearts no more accessory myocardial AV connections were observed.

Conclusions. Isolation of the AV junction is a gradual and ongoing process and particularly right lateral accessory myocardial AV connections are commonly found at later stages of normal human cardiac development. These transitory accessory connections may act as substrate for AVRTs in fetuses or neonates.

Introduction

Atrioventricular reentrant tachycardia (AVRT) requiring the presence of an accessory atrioventricular (AV) myocardial pathway (AP) is the most common type of supraventricular tachycardia (SVT) in both the foetus and newborn.[1,2] AVRT is a potentially life threatening problem in this young age group and these tachycardias are sometimes difficult to control with antiarrhythmic drug therapy.[3-5] However, most tachycardias spontaneously resolve within the first months of life and more than 60% of patients require no antiarrhythmic drug therapy and remain free of symptoms after the age of one year.[2, 3]

This self-limiting character of most perinatal AVRTs suggests that the majority of the accessory AV pathways involved eventually disappear after birth, furthermore a discontinuation of tachycardia initiating events may also explain the disappearance of these type of arrhythmias. It is unknown whether APs involved in perinatal AVRT have a different etiology as compared to APs involved in AVRT presenting later in life. We hypothesize that self-limiting perinatal AVRT can be explained by the transitory presence of accessory myocardial connections during the normal process of isolation of the AV junction in cardiac development.

Shortly after the formation of the primary heart tube, the heart is subjected to extensive remodeling processes.[6] Previous studies have shown that around the seventh week of human development, the separation process of the atrial and ventricular myocardium at the primitive AV canal has started. As from the twelfth week of development atrial and ventricular myocardium are separated by a layer of fibrous tissue, the annulus fibrosis, in which the AV conduction axis comprises the only myocardial continuity.[7] Recently, electrophysiological studies in avian[8] and mouse models[9, 10] have shown that up to late stages of cardiac development multiple accessory AV myocardial connections were present. These accessory connections demonstrated retrograde[10] and antegrade AV conduction and gradually decreased in number at subsequent developmental stages.[8] In addition, an electrophysiological study in mice demonstrated the onset of AVRT at early stages of development.[10]

In this study we investigated the presence and the specific locations of accessory AV myocardial pathways in relation to the process of formation of the annulus fibrosis during the different stages of normal heart development in humans.

Methods

Hearts

The human embryonic, fetal and neonatal hearts (n=45) were obtained from the collection of the Department of Anatomy and Embryology of the Leiden University Medical Center, The Netherlands. The study was approved by the local Medical Ethical Committee. Only specimens with a normal karyotype and structural normal hearts were included for this study. All hearts were already sectioned either in transverse, frontal or sagittal plain and immunohistochemically stained with different myocardial (HHF-35, DAKO, Glostrup, Denmark; Myosin, α-MHC and β-MHC kindly supplied by A.F.M. Moorman) and fibrous tissue (Fibronectin, A245, DAKO, Glostrup, Denmark ; CollagenVI, Southern Biotechnology, Birmingham, AL ; Laminin, PU078, BioGenex, San Remon, USA) markers. Furthermore, histological stained sections were used: Haematoxylin eosin (HE), Resorcin-fuchsin-iron haematoxylin-picric acid-thiazin red (modified Verhoeff-Van Gieson stain) and Azan. A detailed description of staining protocols can be found in previous publications.[11, 12] According to pregnancy duration and Crown-Rump-Length (CRL) all embryos, fetuses and neonates were separated into 4 groups of subsequent gestational stages of development: Group 1: 4 weeks / CRL5mm - 6 weeks / CRL11mm (n=2); Group 2: 6 weeks / CRL11mm - 10 weeks / CRL 40 mm (n=7); Group 3: 10 weeks / CRL 40mm - 20 weeks / CRL164-170mm (n=27); Group 4: 20 weeks / CRL164-170 -birth- neonates (n=9).

The hearts were carefully studied section by section for the presence of accessory AV myocardial connections at the left, right and septal area of the AV junction using an Olympus BH-2 light microscope. An accessory myocardial AV connection was defined as an uninterrupted strand of myocardium, which crosses the annulus fibrosis in addition to the AV conduction axis in post-septated hearts.

All accessory myocardial AV connections in the embryonic or fetal hearts were categorized based on their specific location in the AV junction. The accessory myocardial connections related to the developing AV node (AVN) were described separately.

Immunohistochemistry

Additional immunohistochemical experiments were performed using MLC2a and periostin specific antibodies as additional myocardial and fibrous tissue markers respectively. All embryonic hearts were fixed in 4% paraformaldehyde (PFA), after dehydration they were embedded in paraffin. The embedded hearts were 5 µm sectioned and mounted 1 to 6 onto protein/glycerin-coated slides, so 6 different staining procedures could be performed on one embryo. After dehydration of the slides, inhibition of the endogenous peroxidase was performed for MLC2a with a solution of 0.3% H_2O_2 in PBS for 20 min. For periostin antigen retrieval was performed in 0.01M Citric buffer of Ph 6.0 at 97°C for 12 minutes, followed by inhibition of the endogenous peroxidase in a solution of 0.3% H_2O_2 in PBS for 20 min. Overnight incubation with the primary antibody was performed with the following antibodies: 1/2000 anti-atrial myosin light chain 2 (MLC2a, gift from S.W. Kubalak) and 1/1000 anti-periostin (gift from R.R. Markwald). The primary antibodies were dissolved in PBS-Tween-20 with 1% Bovine Serum Albumin (BSA, Sigma Aldrich, USA). The slides were rinsed between subsequent incubation steps: PBS (2x) and PBS-Tween-20 (1x). For both MLC2a and periostin, a 40 min incubation with the secondary antibodies was performed using 1/200 goat-anti-rabbit-biotin (Vector Laboratories, USA, BA-100) and 1/66 goat serum (Vector Laboratories, USA, S1000) in PBS-Tween-20. Thereafter a 40 minute incubation with ABC-reagent (Vector-Laboratories, USA, PK 6100) was performed. For visualisation, all slides were incubated with 400 µg/ml 3-3'di-aminobenzidin tetrahydrochloride (DAB, Sigma-Aldrich Chemie, USA, D5637) dissolved in Tris-maleate buffer pH7.6 to which 20 µl H_2O_2 was added for 10 min. 0.1% Haematoxylin (Merck, Darmstad, Germany) was used to counter stain the slides: MLC2a 10 sec and periostin 5 sec, followed by rinsing with tap water for 10 minutes. Finally, the slides were dehydrated and mounted with Entellan (Merck, Darmstadt, Germany).

AMIRA reconstruction

Reconstructions were made of the developing AVN region, as described earlier,[9] using the AMIRA software package (Template Graphics Software, San Diego, USA).

The authors had full access to and take responsibility for the integrity of the data. All authors have read and agree to the manuscript as written.

Results

Morphology of the Developing Annulus Fibrosis

4 weeks / CRL 5 mm – 6 weeks / CRL 11 mm (n=2)

At 4 weeks (CRL 5mm) of development the heart tube had looped and the common atrium was completely positioned above the primitive left ventricle. Large endocardial cushions were observed in the region of the common outflow tract and at the anterosuperior and posteroinferior luminal side of the primitive AV canal. At this stage, the atrial and ventricular myocardium was continuous at the region of the primitive AV junction. At 5 weeks (CRL 7 mm) the formation of the right ventricle had started and the future left and right ventricle were clearly discernible. In the AV canal region the myocardium of the primitive atria and the ventricles was continuous (data not shown).

6 weeks / CRL 11 mm – 10 weeks / CRL 40 mm (n=7)

Between 6-7 weeks, the AV cushions had fused and the future tricuspid and mitral valve orifice of the AV junction became visible. Almost all atrial and ventricular myocardium was still continuous at the AV junction. Around the seventh week of development ventricular septation was nearly completed, thereby separating the left and right blood streams. The separation of atrial and ventricular myocardium had clearly commenced at the right dorsal aspect of the embryonic heart and to a lesser extent at the left dorsal side. At 7 to 8 weeks, ventricular septation was completed and formation of the partially AV cushion derived tricuspid valves at the right and mitral valve at the left AV junction had started. At the end of the ninth week AV cushion tissue was no longer observed, and well shaped mitral and tricuspid valves were present at the AV junction. At this stage, the atrial and ventricular myocardium was almost completely separated by the fibrous tissue of the developing annulus fibrosis. At the dorsal side of the fetal heart a distinct AV myocardial continuity was observed which corresponded to the developing AV conduction axis, comprising the developing AVN and the bundle of His. Between 6 and 10 weeks of development, many parts of the AV junction showed an incomplete isolation at the annulus fibrosis (**Figure 1A-C**). Accessory AV myocardial connections were found both at the left (45%), right (35%) and septal (20%) region of the AV junction (**Figure 1D**). Most of the accessory myocardial connections were identified as broad accessory AV myocardial continuities. At the dorsal aspect of the right AV junction accessory connections consisted of small single myocardial strands.

At the right AV junction, the so-called right AV ring (RAVR) bundle could easily be distinguished from the atrial myocardium as a separate structure. The RAVR bundle, considered to be part of the embryonic AV conduction system, formed a ring of myocardium around the tricuspid annulus at the atrial side (**Figure 2 A-C**).[13]

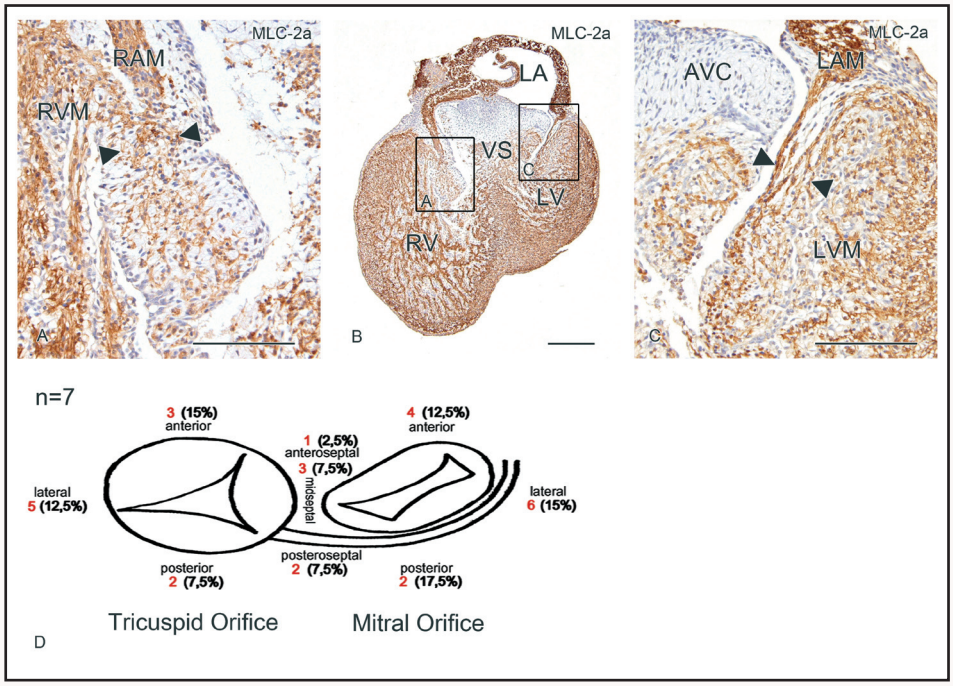

Figure 1. Separation of atrial and ventricular myocardium at 6 to 10 weeks of development. In early post-septated hearts large myocardial continuities between atrial and ventricular myocardium were observed at the right AV junction ((**A**) magnification of boxed area in (**B**)) and left AV junction ((**C**) magnification of boxed area in (**B**)), as shown in these frontal sections of an MLC-2a stained embryonic heart of 7 weeks of development (**B**). The region between the arrowheads in (**A**) and (**C**) show the myocardial continuity at the left and right lateral AV junction. (**D**) Between 6 and 10 weeks of development 7 hearts were studied, the red numbers indicate the total number of hearts in which accessory myocardial AV continuities were observed at a specific location at the tricuspid and mitral orifice of the developing AV junction. The percentages represent the total amount of accessory myocardial AV continuities at a specific location, compared to the total number of accessory myocardial AV continuities at the entire AV junction. VS indicates ventricular septum; LA=left atrium; LV=left ventricle; LAM=left atrial myocardium; LVM=left ventricular myocardium; RV=right ventricle; RAM=right atrial myocardium; RVM=right ventricular myocardium. Scale bars: A, C=150 µm; B=300 µm.

Interestingly, the majority of the right-sided accessory myocardial AV connections (65%) were located subendocardially and made contact with the RAVR bundle. In all examined hearts the isolating tissue between the RAVR bundle and the ventricular myocardium was not as extensive as at other locations at the AV junction. Frequently, only a single layer of fibrous tissue was observed between the RAVR bundle and the ventricular myocardium.

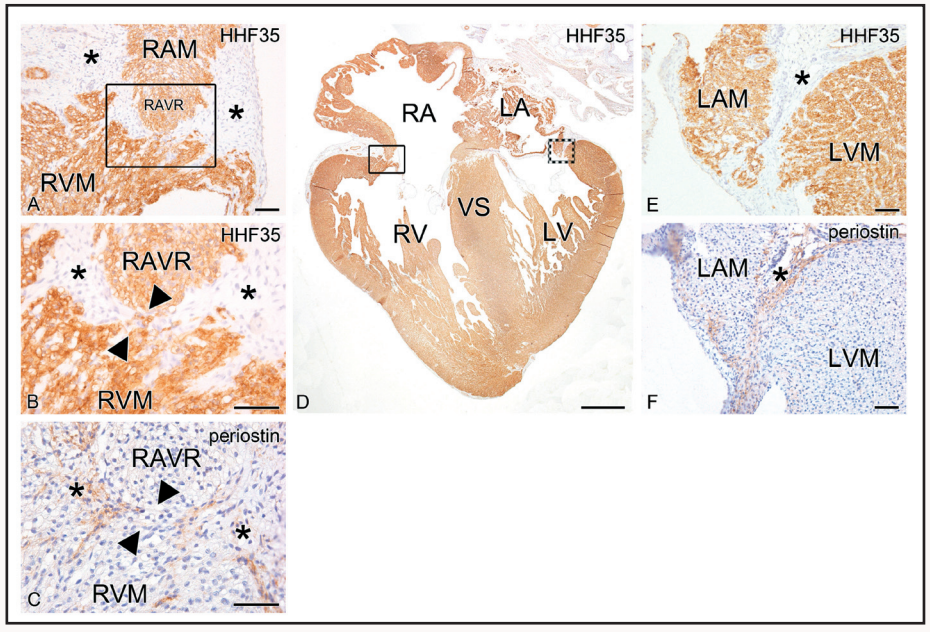

Figure 2. Separation of atrial and ventricular myocardium at eleven weeks of development. The right AV junction ((**A**) magnification of boxed area in (**D**)) of an eleven week old fetal heart frontally sectioned (**D**). Atrial and ventricular myocardium is separated by a layer of periostin positive fibrous annulus fibrosis tissue (asterisk in (**A**), (**B**) and (**C**)). HHF-35 positive accessory AV myocardial connections (region between arrowheads in (**B**), magnification of boxed area in (**A**)), negative for periostin ((**C**) adjacent section of (**B**)), were present between the right atrioventricular ring (RAVR) bundle and the right ventricular myocardium (RVM). **E**. Magnification of dotted box in (**D**) shows that the left atrial myocardium (LAM) and left ventricular myocardium (LVM) are separated by a thick layer of periostin positive ((**F**) adjacent section of (**E**)) fibrous annulus fibrosis tissue (asterisk in (**E**) and (**F**)). RA indicates right atrium; RV=right ventricle; LA=left atrium; LV=left ventricle; VS=ventricular septum. Scale bars: D=1 mm; all others 60 µm.

10 weeks / CRL 40 mm - 20 weeks / CRL 164-170 mm (n=27)

Between 10 (CRL 40 mm) and 20 weeks (CRL 164-170 mm) of development the annulus fibrosis and valve formation had progressed further and cardiac development was mainly dominated by growth. At the left AV junction, the annulus fibrosis had become a firm structure with a thick layer of fibrous tissue isolating the left atrial and ventricular myocardium (**Figure 2 D-F**). The developing AVN was positioned in the right posteroseptal region and was continuous with the bundle of His traversing the annulus fibrosis behind the aorta. At the right AV junction the annulus fibrosis was more fragile and accessory myocardial AV connections were frequently found especially adjacent to the RAVR bundle (**Figure 2 A-D**), which could still be observed in most hearts up to 20 weeks.

Between 10 and 20 weeks broad accessory AV myocardial continuities as seen at earlier embryonic stages, could no longer be detected. However, up to 20 weeks of development numerous accessory myocardial AV connections were identified (**Figure 3 A-E**). At these stages, all accessory myocardial AV connections only consisted of single strands of myocardium crossing the annulus fibrosis (**Figure 3 C-E**). As expected, the majority of accessory myocardial AV connections were now located at the right AV junction (67%) and only 17% were located at the left AV junction. Furthermore, 16% of accessory myocardial AV connections were observed at the midseptal and anteroseptal region of the AV junction (**Figure 3 F**). Right-sided connections (45%) were located subendocardially at the lateral aspect of the right AV junction, mostly related to the RAVR bundle (**Figure 3 C,E**).

20 weeks / CRL 164-170 mm – birth - neonatal stages (n=9)

The annulus fibrosis of 5 fetal and 4 neonatal hearts was examined completely. In both fetal and neonatal hearts no accessory myocardial AV connections were observed at the left, right and septal area of the AV junction (data not shown).

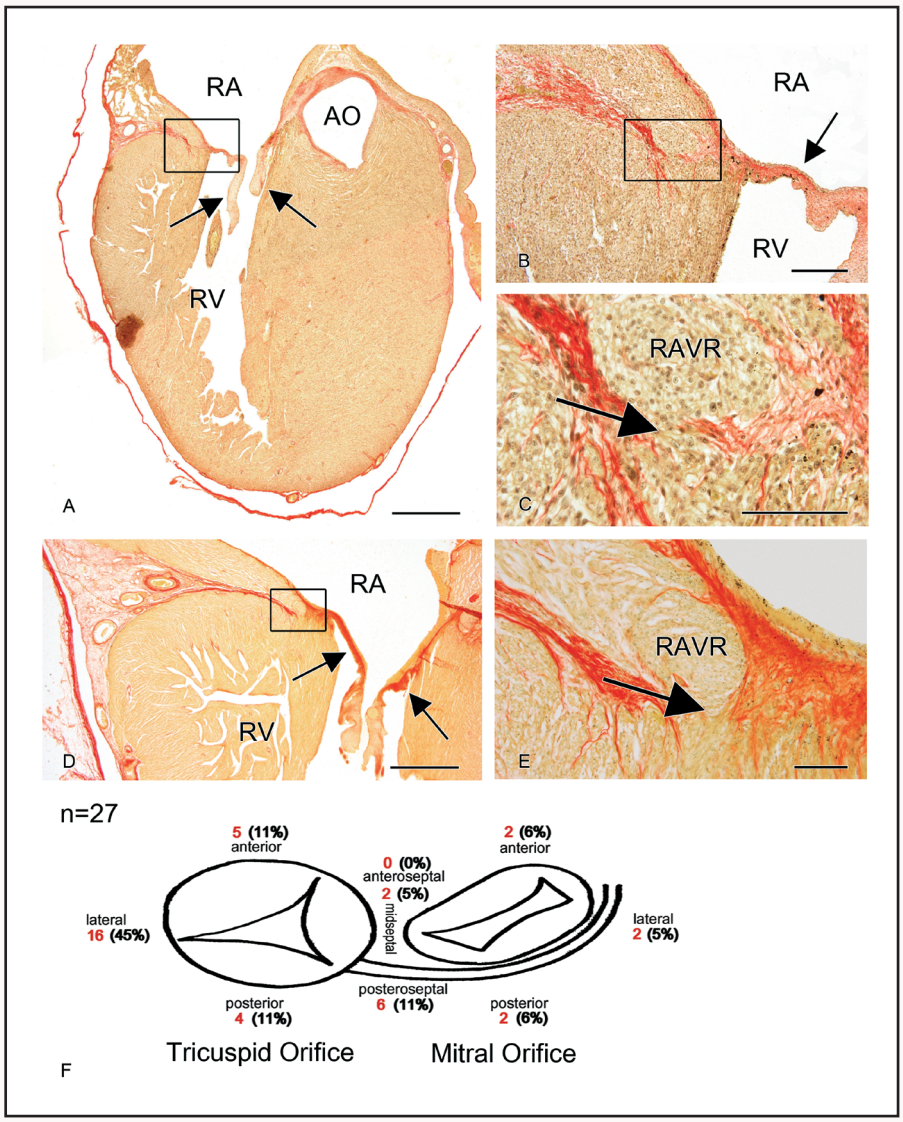
RA
AO
RV
A
RA
RV
B
RAVR
C
RA
RV
D
RAVR
E
n=27
5 (11%)
anterior
0 (0%)
anteroseptal
2 (5%)
midseptal
2 (6%)
anterior
lateral
16 (45%)
lateral
2 (5%)
posterior
4 (11%)
posteroseptal
6 (11%)
posterior
2 (6%)
Tricuspid Orifice
Mitral Orifice
F

Figure 3. (left) **Separation of atrial and ventricular myocardium at 10 to 20 weeks of development.** Between 10 and 20 weeks of development several accessory myocardial AV connections bypassing the AV conduction axis were present. **A**. Modified Verhoeff-Van Gieson stain stained frontal section of a 15,3 week fetal heart in which myocardium is stained yellow-brown and fibrous tissue is stained red. **B**. Represents the boxed area in (**A**) showing a detail of the annulus fibrosis of the right AV junction which is in continuity with the base of the tricuspid valve (arrows in **A** and **B**). **C**. Detail of the boxed area in (**B**), showing the right atrioventricular ring (RAVR) bundle which is in continuity with the ventricular myocardium, thereby creating an accessory myocardial AV connection (arrow in (**C**)). **D**. Shows a frontal section of the right AV junction of a fetal heart of 19,6 weeks of development. The arrows indicate the tricuspid valve in continuity with the fibrous tissue of the annulus fibrosis (red). **E**. Represents the magnification of the boxed area in (**D**) showing an accessory myocardial AV connection in contact with the RAVR bundle (arrow in (**E**)). Between 10 and 20 weeks of development 27 fetal hearts were investigated for the presence of accessory myocardial AV connections at the developing AV junction (**F**). The red numbers indicate the total number of hearts in which accessory myocardial AV connections were present at a specific location at the AV junction. The percentages represent the amount of accessory myocardial AV connections at a specific location at the AV junction compared to the total number of accessory myocardial AV connections at the entire AV junction. RA indicates right atrium; RV=right ventricle; AO=aorta. Scale bars: A, D 1mm; B=200 μm; C, E=100 μm.

Accessory Connections Related to the Developing AVN

The developing AVN and bundle of His were examined during different stages of fetal heart development. The cardiomyocytes of the AVN were large pale and rounded cells and could be well distinguished from the adjacent atrial working myocardium (data not shown). From 10 weeks onward the developing AVN remained positioned anterior to the coronary sinus ostium to the mid-atrial septum, immediately adjacent to the tricuspid annulus (**Figure 4 A**). Shortly after completion of ventricular septation, the bundle of His was a prominent structure crossing the annulus fibrosis in the midseptal region continuing at the ventricular side divided into a left and right bundle branch. Along fetal heart development the bundle of His was better isolated and could be easily identified from the surrounding structures. During subsequent stages of development until birth, numerous small strands of cardiomyocytes originating from the AVN region, penetrated the annulus fibrosis. These accessory AV nodal extensions of large pale rounded cardiomyocytes connected to the ventricular septal myocardium but had no relationship with the penetrating bundle of His (**Figure 4 A, B**). Sections and a three dimensional reconstruction of the AVN region and AV nodal accessory connections of a 14,2 week fetal heart are shown in **Figure 4**.

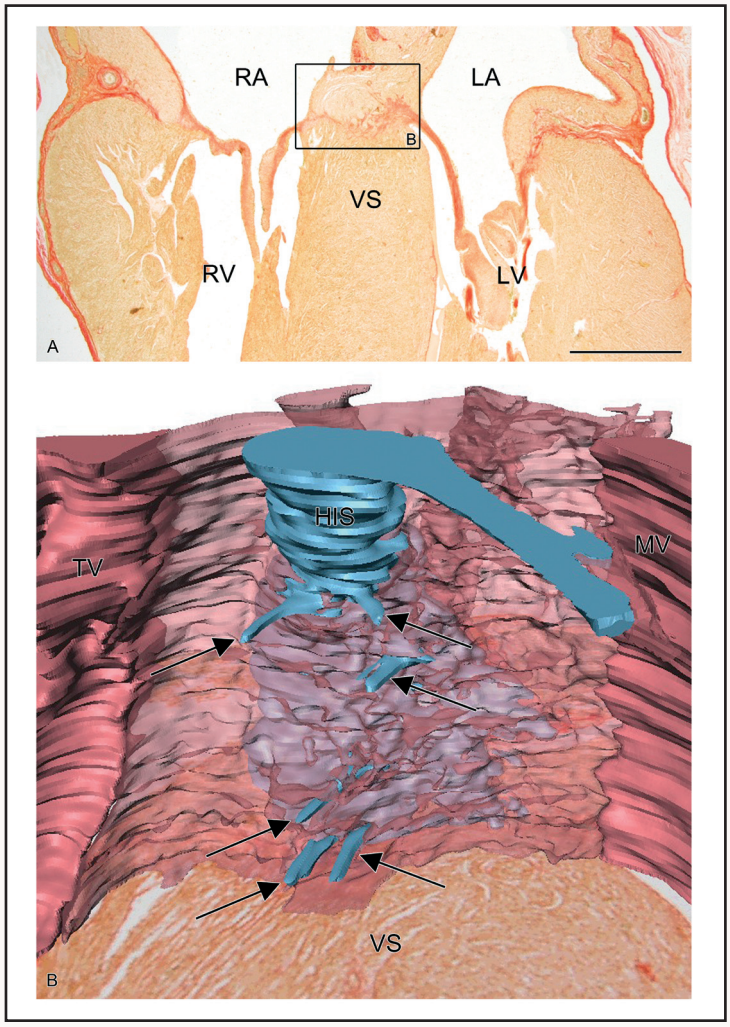

Figure 4. Accessory atrioventricular connections related to the developing atrioventricular node (AVN). A. Shows a modified Verhoeff-Van Gieson stain stained transverse section of a 14,2 week fetal heart. The boxed area in (**A**) shows the AVN region of which a 3-D reconstruction is shown in (**B**). During subsequent stages of development until birth multiple accessory myocardial connections related to the AVN were observed. (**B**) The 3-D reconstruction visualizes a frontal view of these so-called nodoventricular connections penetrating the annulus fibrosis (red transparent) and connecting the AVN with the ventricular septal (VS) myocardium. For display purpose the nodoventricular connections have been elongated, which are indicated by the arrows in (**B**). RA indicates right atrium; LA=left atrium; RV=right ventricle; LV=left ventricle. In the 3-D reconstruction, red indicates base of mitral valve (MV) and tricuspid valve (TV); blue, myocardium of the atrioventricular conduction axis, including the bundle of His (HIS). Scale bar: A=1 mm

Discussion

SVTs affect about 0.1% of fetuses and newborns. In most cases the substrate for arrhythmia is an abnormal electrical conduction through an accessory AV myocardial pathway causing a circus movement between atria and ventricles.[1] However, the majority of children presenting with AVRT in the fetal or neonatal period has no recurrences after the age of one year and show disappearance of ventricular preexcitation and non-inducibility of AVRT by transesophageal electrophysiological studies in approximately one third of the patients.[14, 15] This self-limiting character of most AVRTs in fetuses and newborns is an intriguing clinical phenomenon, but the mechanism has not yet been elucidated. AVRT in this age group has been speculated to originate from the transient presence of conducting APs during the normal process of maturation of the annulus fibrosis.[8, 16] The development of this isolating structure involves several processes in which the endocardial cushions lining the luminal side of the primitive AV canal together with the inward migration of the epicardially located AV sulcus tissue have an important role.[17-19] Recently, it has been shown in more detail that a combination of bone-morphogenetic-protein (BMP) signalling,[20, 21] periostin an osteoblast–specific factor[22] and epicardial derived cells which enter the heart at the AV sulcus play a key role in this process.[23, 24]

The etiology of APs has not been elucidated. The majority of APs conduct antegradely as seen in patients with Wolff-Parkinson-White (WPW) syndrome (OMIM #194200; incidence in general population 1,5 per 1000 persons),[25] the prevalence of WPW syndrome in children under 13 years of age is lower (0.07%).[26] In adults, twenty-five percent of APs involved in AVRT are concealed indicating that they only have retrograde conducting properties.[27] In infants, the percentage of concealed APs is higher, approximately 60%.[28] In the majority of cases of WPW syndrome there is no familial involvement. However, significant minority of cases are inherited as a single gene disorder or occur as part of a syndrome with a strong genetic basis.[25, 29, 30] Recently *PRKAG2* gene missense mutations have been identified to be involved in familial WPW syndrome often associated with cardiac hypertrophy.[29] Animal studies have shown that mutations in the *Alk3* gene result in a disrupt formation of the annulus fibrosis causing ventricular preexcitation via posterior paraseptal bypass tracts.[20] The differences in location and specific electrophysiological properties of APs as well as their association with structural heart disease like hypertrophic cardiomyopathy and congenital heart disease indicate that not all APs share the same etiological pathway.

Previous studies have demonstrated the presence of accessory myocardial AV connections between atrial and ventricular myocardium during normal embryological and fetal heart development in humans[16, 31, 32] and other mammals.[9, 10] However, the present study for the first time systematically describes the presence and the specific locations of gradually disappearing accessory AV myocardial connections crossing the developing annulus fibrosis in human embryonic, fetal and neonatal hearts. We demonstrate that atrial and ventricular myocardium was continuous at the primitive AV canal at early stages of development. First separation of atrial and ventricular myocardium by the developing annulus fibrosis was observed at the right dorsal AV junction around 7 weeks of development and myocardial continuity persisted longer near the left junction. Total separation of atrial and ventricular myocardium was completed around ten to eleven weeks, which corresponds to other studies regarding the formation of the annulus fibrosis in developing human hearts.[7] However, numerous accessory AV myocardial connections can be identified up to the end of the second trimester of pregnancy. Comparable to other studies,[16] these accessory AV myocardial connections were observed at the subendocardial aspect of both the right and left lateral AV junction of the heart. In the second and third trimester the left AV ring becomes firmly isolated by a thick layer of fibrous tissue followed by isolation of the right AV ring.

Especially the isolation of the right AV ring is weak and frequently consists only of very thin layers of fibrous tissue. Up to 20 weeks of gestation small AV myocardial strands remain present near the lateral side of the tricuspid valve that are mainly located subendocardially. The high frequency of these right sided accessory myocardial AV connections and the weak isolation of especially this part of the AV junction might be associated with the normal developmental process of the right ventricular inflow tract. In early stages of heart development, as observed in the current study, the common atrium is completely positioned above the left ventricle. Formation of the right ventricular inflow tract starts with a groove, which is embedded in the myocardium of the primary fold. As a result of the expansion and outgrowth of this myocardial groove the right ventricular inflow tract will be formed, which eventually establishes the right part of the AV junction.[9] Therefore, the formation of the right ventricular inflow tract might result in a weaker isolation and a high frequency of accessory myocardial AV connections, since this part of the AV junction develops subsequent to the already existent left AV junction. The right sided AV myocardial connections frequently are located in close relationship with the RAVR bundle.[13] This semicircular

structure forms part of the temporary embryological specialized AV conduction system and is continuous with the AVN posteriorly. In the fetus it can be identified as a ring of node-like cells in the right atrium just above the tricuspid valve that obliterates later on.[13, 33, 34] These accessory myocardial AV connections seem to correspond to the presumed multiple AV nodes and pathways as originally reported by Kent and reviewed by Anderson (1996).[35] The relationship of right sided accessory myocardial AV connections with the RAVR bundle could explain the decremental properties as seen in some of the right sided APs.[36]

Within the developing AVN small myocardial extensions can be identified that cross the annulus fibrosis and connect the developing AVN with the ventricular septal myocardium. These AV nodal extensions remain present until birth. The presence of the so-called nodoventricular connections in fetal and neonatal hearts has been reported earlier and this phenomenon has been described as fetal dispersion of the AVN.[37] In the first months after birth extensive remodeling of the fibrous heart skeleton including the AVN area takes place,[31, 38] in which the AVN becomes a more solid structure.[39] AV nodal extensions appear to be a common finding in neonatal hearts, although it has been associated with sudden infant death syndrome in the past.[40] In theory, nodoventricular pathways could provide the substrate for SVT, but to our knowledge this rare form of reentrant tachycardia has not been documented in the perinatal period.

Recently, the temporary presence of functional accessory myocardial AV connections has been demonstrated by electrophysiological studies in avian hearts up to late stages of fetal development. These connections appeared to have antegrade conducting properties, which was demonstrated by unipolar electrogram recordings showing premature left and right ventricular base activation in post-septated hearts.[8] Furthermore, studies performed in mammals[9, 10] showed that in normal mouse embryos conducting accessory AV pathways are present during cardiac development that can actually create the substrate for reentrant tachycardias. Some of these pathways even appeared to have decremental properties as observed in the Mahaim preexcitation syndrome.[9] In normal human fetuses the conducting properties of transient accessory AV connections, depending on factors such as intercellular coupling remain to be elucidated as well as their capability to establish a pathway for AVRT. However, these accessory myocardial AV connections in human fetuses and their specific locations show strong similarities with the conducting accessory myocardial AV connections as demonstrated in avians and mice.[8-10]

APs in adult patients with AVRT are mostly found around the mitral valve orifice and approximately 60% are located in the left ventricular free wall.[27] In the pediatric age group the incidence of APs around the tricuspid annulus appears to be higher.[41] APs around the tricuspid valve are usually located at the subendocardial aspect of the heart, whereas left sided APs can also have a more epicardial course in the AV sulcus. This implicates that the persistence of subendocardially located accessory myocardial AV connections as demonstrated in normal fetuses could only partly explain the pathogenesis of APs in patients with AVRT. However the delayed disappearance of fetal APs as reported in the current study offers a good explanation for the onset and disappearance of fetal and neonatal AVRT. One-third of the fetuses and neonates with AVRT have WPW syndrome showing ventricular pre-excitation on the postnatal electrocardiogram, the others have concealed APs with only retrograde conduction.[42] Although late recurrences of tachycardia after 8 to 10 years have been reported in neonates with WPW syndrome, the majority of these children remains free of symptoms during life.[43] Recently it has been reported that the group of neonates with concealed APs has an even better prognosis and more than 80% remain asymptomatic after the first year, without recurrences later in life.[42] In the present study we have demonstrated that accessory myocardial AV connections remain present up to late stages of fetal heart development, which indicates that the process of isolation of the AV junction is a continuous process not finished by the time of birth. The temporary presence of these accessory myocardial AV connections could serve as substrate for perinatal AVRT.

Study Limitations

The current study demonstrated the presence of accessory AV connections in normal heart development. However, none of the hearts investigated were from fetuses or neonates with known episodes of SVT. Therefore, it cannot be determined whether the accessory connections served as functional substrate for AP mediated SVT.

Funding sources

The presented work was supported by the Gisela Thier Foundation (Nathan D. Hahurij)

Disclosures

None

References

1. Bauersfeld U, Pfammatter JP, Jaeggi E. Treatment of supraventricular tachycardias in the new millennium--drugs or radiofrequency catheter ablation? *Eur J Pediatr.* 2001;160(1):1-9.
2. Ko JK, Deal BJ, Strasburger JF, Benson DW. Supraventricular tachycardia mechanisms and their age distribution in pediatric patients. *Am J Cardiol.* 1992;69(12):1028-1032.
3. Naheed ZJ, Strasburger JF, Deal BJ, Benson DW, Gidding SS. Fetal tachycardia: mechanisms and predictors of hydrops fetalis. *J Am Coll Cardiol.* 1996;27(7):1736-1740.
4. Simpson JM, Sharland GK. Fetal tachycardias: management and outcome of 127 consecutive cases. *Heart.* 1998;79(6):576-581.
5. Weindling SN, Saul JP, Walsh EP. Efficacy and risks of medical therapy for supraventricular tachycardia in neonates and infants. *Am Heart J.* 1996;131(1):66-72.
6. Gittenberger-de Groot AC, Bartelings MM, Deruiter MC, Poelmann RE. Basics of cardiac development for the understanding of congenital heart malformations. *Pediatr Res.* 2005;57(2):169-176.
7. Wessels A, Markman MW, Vermeulen JL, Anderson RH, Moorman AF, Lamers WH. The development of the atrioventricular junction in the human heart. *Circ Res.* 1996;78(1):110-117.
8. Kolditz DP, Wijffels MC, Blom NA, van der Laarse A, Markwald RR, Schalij MJ, Gittenberger-de Groot AC. Persistence of functional atrioventricular accessory pathways in postseptated embryonic avian hearts: implications for morphogenesis and functional maturation of the cardiac conduction system. *Circulation.* 2007;115(1):17-26.
9. Jongbloed MR, Wijffels MC, Schalij MJ, Blom NA, Poelmann RE, van der Laarse A, Mentink MM, Wang Z, Fishman GI, Gittenberger-de Groot AC. Development of the right ventricular inflow tract and moderator band: a possible morphological and functional explanation for Mahaim tachycardia. *Circ Res.* 2005;96(7):776-783.
10. Valderrábano M, Chen F, Dave AS, Lamp ST, Klitzner TS, Weiss JN. Atrioventricular ring reentry in embryonic mouse hearts. *Circulation.* 2006;114(6):543-549.

11. Gittenberger-de Groot AC, Blom NM, Aoyama N, Sucov H, Wenink AC, Poelmann RE. The role of neural crest and epicardium-derived cells in conduction system formation. *Novartis Found Symp.* 2003;250:125-134; discussion 134-141, 276-129.

12. Oosthoek PW, Wenink AC, Vrolijk BC, Wisse LJ, de Ruiter MC, Poelmann RE, Gittenberger-de Groot AC. Development of the atrioventricular valve tension apparatus in the human heart. *Anat Embryol.* 1998;198(4):317-329.

13. Blom NA, Gittenberger-de Groot AC, de Ruiter MC, Poelmann RE, Mentink MM, Ottenkamp J. Development of the cardiac conduction tissue in human embryos using HNK-1 antigen expression: possible relevance for understanding of abnormal atrial automaticity. *Circulation.* 1999;99(6):800-806.

14. Benson DW, Dunnigan A, Benditt DG. Follow-up evaluation of infant paroxysmal atrial tachycardia: transesophageal study. *Circulation.* 1987;75(3):542-549.

15. Deal BJ, Keane JF, Gillette PC, Garson A. Wolff-Parkinson-White syndrome and supraventricular tachycardia during infancy: management and follow-up. *J Am Coll Cardiol.* 1985;5(1):130-135.

16. Truex RC, Bishof JK, Hoffman EL. Accessory atrioventricular muscle bundles of the developing human heart. *Anat Rec.* 1958;131(1):45-59.

17. Rothenberg F, Efimov IR, Watanabe M. Functional imaging of the embryonic pacemaking and cardiac conduction system over the past 150 years: technologies to overcome the challenges. *Anat Rec.* 2004;280(2):980-989.

18. Wenink AC, Gittenberger-de Groot AC. The role of atrioventricular endocardial cushions in the septation of the heart. *Int J Cardiol.* 1985;8(1):25-44.

19. Wenink AC, Gittenberger-de Groot AC. Embryology of the mitral valve. *Int J Cardiol.* 1986;11(1):75-84.

20. Gaussin V, Morley GE, Cox L, Zwijsen A, Vance KM, Emile L, Tian Y, Liu J, Hong C, Myers D, Conway SJ, Depre C, Mishina Y, Behringer RR, Hanks MC, Schneider MD, Huylebroeck D, Fishman GI, Burch JB, Vatner SF. Alk3/Bmpr1a receptor is required for development of the atrioventricular canal into valves and annulus fibrosus. *Circ Res.* 2005;97(3):219-226.

21. Okagawa H, Markwald RR, Sugi Y. Functional BMP receptor in endocardial cells is required in atrioventricular cushion mesenchymal cell formation in chick. *Dev Biol.* 2007;306(1):179-192.

22. Kruzynska-Frejtag A, Machnicki M, Rogers R, Markwald RR, Conway SJ. Periostin (an osteoblast-specific factor) is expressed within the embryonic mouse heart during valve formation. *Mech Dev.* 2001;103(1-2):183-188.

23. Eralp I, Lie-Venema H, Bax NA, Wijffels MC, van der Laarse A, de Ruiter MC, Bogers AJ, van den Akker NM, Gourdie RG, Schalij MJ, Poelmann RE, Gittenberger-de Groot AC. Epicardium-derived cells are important for correct development of the Purkinje fibers in the avian heart. *Anat Rec.* 2006;288(12):1272-1280.

24. Gittenberger-de Groot AC, Vrancken Peeters MP, Mentink MM, Gourdie RG, Poelmann RE. Epicardium-derived cells contribute a novel population to the myocardial wall and the atrioventricular cushions. *Circ Res.* 1998;82(10):1043-1052.

25. Vidaillet HJ, Pressley JC, Henke E, Harrell FE, German LD. Familial occurrence of accessory atrioventricular pathways (preexcitation syndrome). *N Engl J Med.* 1987;317(2):65-69.

26. Sano S, Komori S, Amano T, Kohno I, Ishihara T, Sawanobori T, Ijiri H, Tamura K. Prevalence of ventricular preexcitation in Japanese schoolchildren. *Heart.* 1998;79(4):374-378.

27. Kuck KH, Schlüter M. Junctional tachycardia and the role of catheter ablation. *Lancet.* 1993;341(8857):1386-1391.

28. Benson DW, Dunnigan A, Benditt DG, Pritzker MR, Thompson TR. Transesophageal study of infant supraventricular tachycardia: electrophysiologic characteristics. *Am J Cardiol.* 1983;52(8):1002-1006.

29. Gollob MH, Green MS, Tang AS, Gollob T, Karibe A, Ali Hassan AS, Ahmad F, Lozado R, Shah G, Fananapazir L, Bachinski LL, Roberts R, Hassan AS. Identification of a gene responsible for familial Wolff-Parkinson-White syndrome. *N Engl J Med.* 2001;344(24):1823-1831.

30. Roberts R. Genomics and cardiac arrhythmias. *J Am Coll Cardiol.* 2006;47(1):9-21.

31. James TN. Normal and abnormal consequences of apoptosis in the human heart. From postnatal morphogenesis to paroxysmal arrhythmias. *Circulation.* 1994;90(1):556-573.

32. Robb JS, Kaylor CT, Turman WG. A study of specialized heart tissue at various stages of development of the human fetal heart. *Am J Med* 2007;5:324-336.

33. Virágh S, Challice CE. The development of the conduction system in the mouse embryo heart. II. Histogenesis of the atrioventricular node and bundle. *Dev Biol.* 1977;56(2):397-411.

34. Wessels A, Vermeulen JL, Verbeek FJ, Virágh S, Kálmán F, Lamers WH, Moorman AF. Spatial distribution of "tissue-specific" antigens in the developing human heart and skeletal muscle. III. An immunohistochemical analysis of the distribution of the neural tissue antigen G1N2 in the embryonic heart; implications for the development of the atrioventricular conduction system. *Anat Rec.* 1992;232(1):97-111.

35. Anderson RH, Ho SY, Gillette PC, Becker AE. Mahaim, Kent and abnormal atrioventricular conduction. *Cardiovasc Res.* 1996;31(4):480-491.

36. Haïssaguerre M, Cauchemez B, Marcus F, Le Métayer P, Lauribe P, Poquet F, Gencel L, Clémenty J. Characteristics of the ventricular insertion sites of accessory pathways with anterograde decremental conduction properties. *Circulation.* 1995;91(4):1077-1085.

37. James TN, Marshall TK. XVIII. Persistent fetal dispersion of the atrioventricular node and His bundle within the central fibrous body. *Circulation.* 1976;53(6):1026-1034.

38. Visconti RP, Markwald RR. Recruitment of new cells into the postnatal heart: potential modification of phenotype by periostin. *Ann N Y Acad Sci.* 2006;1080:19-33.

39. James TN. Cardiac conduction system: fetal and postnatal development. *Am J Cardiol.* 1970;25(2):213-226.

40. James TN. Sudden death in babies: new observations in the heart. *Am J Cardiol.* 1968;22(4):479-506.

41. Morady F. Catheter ablation of supraventricular arrhythmias: state of the art. *PACE.* 2004;27(1):125-142.

42. Tortoriello TA, Snyder CS, Smith EO, Fenrich AL, Friedman RA, Kertesz NJ. Frequency of recurrence among infants with supraventricular tachycardia and comparison of recurrence rates among those with and without preexcitation and among those with and without response to digoxin and/or propranolol therapy. *Am J Cardiol.* 2003;92(9):1045-1049.

43. Perry JC, Garson A. Supraventricular tachycardia due to Wolff-Parkinson-White syndrome in children: early disappearance and late recurrence. *J Am Coll Cardiol.* 1990;16(5):1215-1220.

Clinical Perspective

Atrioventricular reentrant tachycardias presenting in fetal or neonatal life can be life threatening but also tend to resolve in the majority of patients in the first year of life. The etiology of accessory pathway mediated tachycardias in the perinatal period has not been elucidated. In early embryonic development the atrial and ventricular myocardium are continuous in the primitive atrioventricular canal. The AV conduction axis will then develop, which coincides with separation of the atrial and ventricular myocardium by formation of the annulus fibrosis. Annulus fibrosis development involves several processes in which the endocardial AV cushions lining the luminal side of the primitive AV canal together with the inward migration of the epicardially located AV sulcus tissue have an important role. In post-septated human hearts we demonstrated the presence of numerous accessory AV myocardial connections around both the mitral and tricuspid annulus during normal cardiac development. At the end of the second trimester the connections gradually decreased in number and size, and were located mostly around the tricuspid annulus. The persistence of fetal AV connections may serve as substrate for AV reentrant tachycardia in the fetus and newborn. The self limiting character of most of these tachycardias could be explained by loss of the substrate due to the ongoing development of the annulus fibrosis, a process not completely finished by the time of birth.

PART II

DEVELOPMENT OF THE ATRIOVENTRICULAR NODE (AVN) IN RELATION TO ARRHYTHMIA ETIOLOGY

Chapter 6

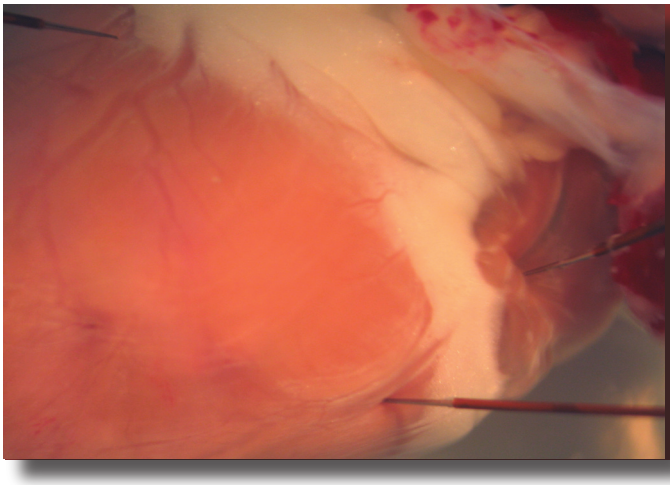

Denise P. Kolditz[1,2]
Adriana C. Gittenberger-de Groot[2]
Martin J. Schalij[1]

[1]Department of Cardiology, Leiden University Medical Center, Leiden, The Netherlands
[2]Department of Anatomy and Embryology, Leiden University Medical Center, Leiden, The Netherlands

Development of the Atrioventricular Conduction Axis in Relation to Cardiac Arrhythmia Etiology

Submitted

Abstract

While the ontogenic development of the AV nodal region has, since the first detailed report on the specialized AV node (AVN) in the monumental monograph of Sunao Tawara in 1906, been studied for over a 100 years now, the anatomical boundaries and developmental origin of the AVN still remain a subject of debate. Clinically, the vast majority (>90%) of patients with AVNRT are cured by radiofrequency (RF) catheter ablation procedures targeting the slow pathway of the AVN, while the anatomical boundaries of the electrophysiologically distinct slow (α) and fast (β) AV nodal pathways as substrates for AVNRT have still remained a conundrum in this confusing field. In this review, an overview of historical and contemporary knowledge on the anatomy of the AVN and its atrial inputs is given. Furthermore, structural AV nodal development and the cellular electrophysiology of the developing AV junction in relation to the adult AVN and the concept of AV nodal conduction dichotomy are discussed.

Atrioventricular (AV) Nodal Reentrant Tachycardia (AVNRT) is the most common mechanism of supraventricular tachycardia (SVT) in adults (>80%),[1] yet it accounts for a comparatively small number of cases of SVTs in pediatric patients (5-16%).[2] Although currently the vast majority (>90%) of patients with AVNRT are cured by radiofrequency catheter ablation procedures,[3] it is still unknown whether the areas that appear 'specialized' to and are targeted by the electrophysiologist indeed show distinctive morphological characteristics, neither has the developmental origin of the AV Node (AVN) been clarified. In view of the persisting discrepancies in literature and the rekindled interest in the developmental morphology of the AVN, the purpose of this article is to review the developmental anatomy, physiology and ontogeny of the AV specialized tissues in relation to AV nodal arrhythmia etiology.

The Anatomical Location of the Adult AVN

The architecture of the AV conduction axis was first described in 1906 by Sunao Tawara, who stated that this axis was the only myocardial structure that crossed the insulating plane of the annulus fibrosis at the AV junction.[4] In the normal mature heart, the atrial components of the AV conduction axis are contained within the triangle of Koch.[5] The triangular area of Koch occupies the atrial component of the muscular AV septum and is delimited by three anatomical landmarks: 1) superiorly by the tendon of Todaro (the fibrous commissure of the flap guarding the openings of the inferior caval vein and the coronary sinus) positioned in the center of the myocardialized spina vestibulum, 2) inferiorly by the attachment of the septal leaflet of the tricuspid valve and 3) at the base by the mouth of the coronary sinus (CS). The apex of the triangle of Koch overlies the membranous component of the AV septum and lies at the center of the short axis of the heart.[5, 6] Within the triangle of Koch, between the mouth of the CS and the hinge of the septal leaflet of the tricuspid valve, the septal isthmus can be found, which is thought to carry the histologically undefined slow pathway into the AVN.[7, 8] The AVN itself lies only a few millimeters anterior to the CS ostium, directly adjacent to the central fibrous body (CFB) of the heart and directly beneath the right atrial septal endocardium and above the septal attachment of the tricuspid valve, where it rests on the CFB, which forms the anchor for the septal portion of the mural leaflet of the mitral valve. The atrial margin of the AVN is apposed to the myocardialized vestibular spine, containing the tendon of Todaro, while the ventricular margin of the AVN is continuous with the bundle of His (**Figure 1**).[9, 10]

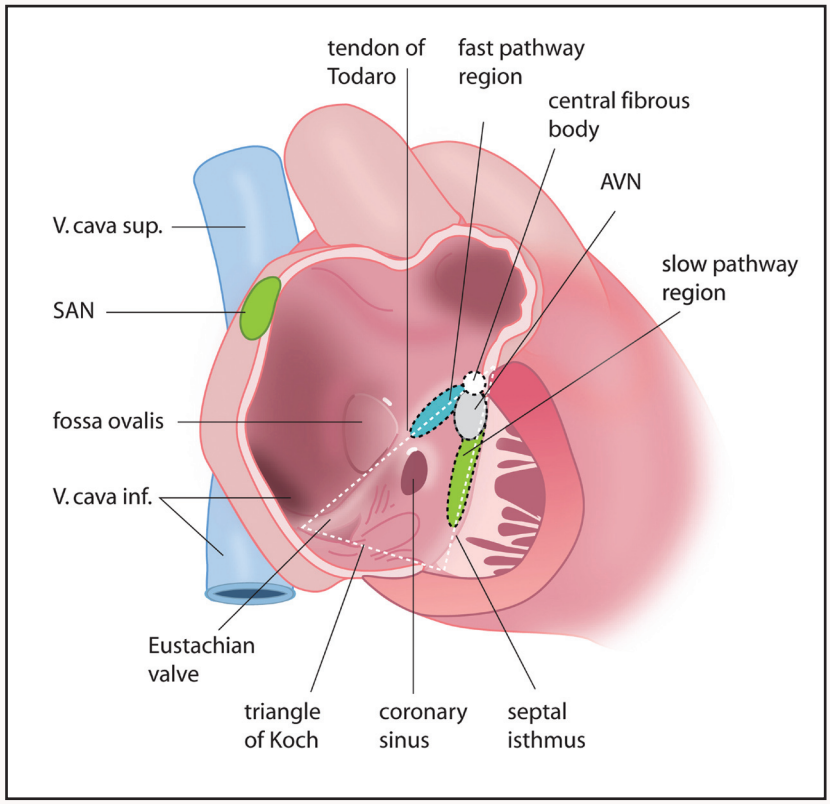

Figure 1. Schematic representation of the AVN in the triangle of Koch. The triangular area of Koch (white dotted lines) is delimited by three anatomical landmarks: 1) superiorly by the tendon of Todaro, 2) inferiorly by the attachment of the septal leaflet of the tricuspid valve and 3) at the base by the mouth of the coronary sinus (CS). The apex of the triangle of Koch overlies the membranous component of the AV septum and lies at the center of the short axis of the heart. Within the triangle of Koch, between the mouth of the CS and the hinge of the septal leaflet of the tricuspid valve, the septal isthmus can be found, which is thought to carry the slow pathway into the AVN. The adult AVN (grey) is positioned a few millimeters anterior to the CS ostium, directly adjacent to the central fibrous body (CFB) of the heart and directly beneath the right atrial septal endocardium and above the septal attachment of the tricuspid valve, where it rests on the central fibrous body, which forms the anchor for the septal portion of the mural leaflet of the mitral valve. The atrial margin of the AVN is apposed to the myocardialized vestibular spine, containing the tendon of Todaro, while the ventricular margin of the AVN is continuous with the bundle of His. The slow pathway of the AVN (green) is a myocardial inferior extension of the compact part of the AVN running rightwards over the septal isthmus towards the tricuspid valve annulus. The fast pathway of the AVN (blue) starts anterosuperiorly in the interatrial septum. Both the slow and fast pathway converge onto the AVN at sites known as the posterior and anterior nodal inputs, respectively.

The AVN Relative to its Atrial Inputs in Koch's Triangle

The compact AVN itself only occupies a small area of the triangle of Koch and is composed of a half-oval of distinctive interweaving cells, while the larger area of the triangle of Koch is occupied by transitional cells, which interpose between the nodal cells and atrial myocytes.[9] Transitional cells are intermediate in their morphology between nodal cells and ordinary atrial musculature, are not insulated by fibrous tissue and their arrangement varies markedly form heart to heart.[9, 11, 12]

When traced inferiorly, the compact part of the AVN gives rise to two myocardial inferior nodal extensions: a large inferior nodal extension (INE) running rightwards towards the tricuspid valve annulus and a smaller INE running leftwards towards the mitral valve annulus.[11] The myocardial right-sided INE of the compact AVN runs through the vestibule of the tricuspid valve over the septal isthmus to the subthebesian sinus. While morphologically the larger right-sided INE has been recognized as the anatomical correlate of the electrophysiologically distinct slow pathway of the AVN,[7] clinicopathologic studies in the human heart targeted for slow pathway ablation only demonstrated lesions in the normal working myocardium distant from the INE and compact AVN.[8] The fast pathway of the AVN allegedly starts anterosuperiorly in the interatrial septum. Both the slow and fast pathway converge onto the AVN at sites known as the posterior and anterior nodal inputs, respectively.[13, 14] In addition to the fast and slow AVN pathways multiple other anatomic pathways composed of atrial myocytes enter the AVN.[6]

Classically, the adult AV junction can be subdivided into three anatomically distinct cell types correlating to different cellular electrophysiologic features: AN (Atrio-Nodal, transitional cell), N (Nodal, mid-Nodal cell) and NH (Nodal-His, lower bundle cells).[15-17] Similarly, 3 types of cardiomyocytes have recently been visualized by distinct expression levels of Nav1.5 (the most prominent sodium α-subunit in the heart generating the I_{Na} current initiating the action potential of the normal and cardiac conduction system (CCS myocardium) in the AV junction of the adult rat heart.[18]

The Sino-Atrial-Node (SAN) and the Internodal Pathways

In the adult heart, the SAN is located in the crista terminalis (representing the internal fusion-line of the sinus venosus and the primitive atrium) near the superior caval entrance into the right atrium.[19, 20] During mammalian development, the first morphological signs of the developing SAN are present

at Carnegie stage 15 (~5 weeks of human development, avians ~HH stage 18, mouse ~E 11.5)[21] in the anterior wall of the right common cardinal vein, which will ultimately give rise to the superior caval vein.[22] While all adult heart muscle cells retain the capacity to rhythmically beat without an external stimulus, the cells of the SAN are those with the most rapid intrinsic rate of excitation (the dominant pacemaking rate).[23]

Within the right atrium three internodal tracts for preferential interatrial conduction have been demonstrated between the SAN and AVN: 1) the anterior bundle running through the septum spurium (SS),[26] which connects to *Bachmann's bundle*[24-25] running in a retroaortic position connecting the right atrium to the left atrium, 2) the posterior bundle running through the right venous valve (RVV)[27] partly corresponding to the posterior bundle or *Thorel's bundle*[27] localized along the crista terminalis and 3) the posterior bundle running through the left venous valve (LVV)[26] partly corresponding to the middle bundle or *Wenckebach's bundle*.[24-28] Considerable controversy and debate has however surrounded the mostly semantic discussion on the existence of these internodal tracts in the atrium between the SAN and AVN, which were initially postulated to be specialized and insulated.[24, 27, 28] Currently, it is well established that preferential conduction, through the ultrastructural and electrophysiological heterogenic atrial myocardium between the cardiac nodes (SAN and AVN), highly depends on the nonuniform anisotropic arrangement of the normal working myocardial fibers giving rise to the internodal pathways, instead of on the existence of truly specialized and insulated atrial internodal tracts.[29] These internodal atrial tracts are made up in part of transitional cells, which interpose between the working atrial myocardium and the unequivocally histologically specialized compact AVN.[11]While these internodal tracts can be differentiated based on histological, immunohistochemical and molecular characteristics,[24-28, 30-32] the exact functional correlate of these anatomical tracts still remains unclear. Interestingly, elegant experimental studies in dogs, in which elevated levels of potassium (to depolarize the atrial tissues) were used to render the atrial myocardium inexcitable, have revealed that the electrical impulse is normally conducted through distinct internodal tracts between the SAN and AVN, relatively insensitive to potassium levels.[33, 34] Additionally, optical mapping studies have demonstrated a non-radial spread of intra-atrial conduction in the rat in a pattern corresponding to the anterior and posterior internodal pathways,[35] while three bundles with unique conduction properties were demonstrated to run between the SAN and AVN in the adult dog heart.[36]

Anatomical Recognition of the Adult versus Embryonic CCS Tissues

Histologically, in the adult heart the cardiomyocytes of the CCS share some characteristics with embryonic normal working cardiomyocytes: they are small compared to the cardiomyocytes of the surrounding adult working myocardium and have poorly organized actin and myosin filaments and a scantily developed sarcoplasmatic reticulum. By applying the criteria established by Monckeberg and Aschoff in 1910, using the AV conduction axis as the paradigm, discrete specialized conduction tracts in the postnatal heart: 1) are histologically distinct, 2) can be followed from section to section and 3) are insulated from the adjacent working myocardium by fibrous tissue.[37] While these criteria permit adequate recognition of the components of the CCS in the postnatal human heart, in the early embryonic heart the individual cells of the CCS can hardly be distinguished from the surrounding myocardium by unique histological features, while their separate arrangement and topography can in some cases be helpful.[22, 38, 39] A multitude of transgenes, such as minK-LacZ,[32] and Engrailed2-lacZ/CCS-LacZ[31, 40] has however been consistently proposed to properly reflect the arrangement of the developing CCS.

Moreover, each subcomponent of the CCS expresses a distinct set of discriminating ion channels,[41, 42] channel-associated proteins,[43] connexins,[44-46] cytoskeletal components[47, 48] and transcriptional regulators,[49, 50] useful for immunohistological recognition. Additionally, important known signaling and transcription factors implicated in the induction, maturation and patterning of the CCS including endothelin (ET),[51-56] neuregulin,[57, 58] Notch,[57] Wnt,[59] Msx,[60] Nkx,[61-64] Hop,[65] Id-2,[66] Tbx, podoplanin[67] and GATA gene families[68-71] can also be of help. State-of-the-art studies focusing on the transcription factors involved in cardiogenesis have made evident that myocardial differentiation to CCS cells cannot be dependent on a single gene, but should be considered as a multifactorial process in which many of different gene families must contribute.

A Century of Theories on the Developmental Origin of the AVN

In the debate of the 20th century, controversy concerning the ontogenic development of the AVN has led to a multitude of proposals for its origin. While these competing theories based on observations in different species and complicated by the use of variable terminology for identification and non-specific staining, failed to provide a definitive resolution on this subject, these studies provide essential tools in our further understanding of the structure-function correlation in the developing and adult AVN region. Morphological studies in the embryonic calf, mouse and human heart suggested that the AVN is solely derived as a remnant of the musculature of the AV canal,[72-75] further substantiated by functional studies in the developing chick heart demonstrating decremental impulse conduction across the early embryonic AV junction.[76-78] Conversely, extensive morphological studies in various animal and human hearts suggested that the AVN is an actively growing supraventricular structure budding off at a proliferating part of the posterior AV canal myocardium.[73, 79-82]

Early morphological studies in the developing chick and human heart, furthermore suggested that the AVN develops as a left-sided counterpart of the SAN in the left sinus horn and is moved to its adult location by development of the body of the left atrium and incorporation of the sinus venosus into the atria.[83, 84] Subsequently, in the human embryo two cellularly distinct collections of tissue were identified in the AVN region ultimately becoming more closely related and enclosing an intermediate block of specialized tissue and suggested to derive from both the left sinus horn myocardium and the AV canal musculature.[15]

The concept of dual AVN primordia was further advocated by identification of dual primordia in the posterior wall of the common atrium in the developing human and ferret heart.[85-87] In the human heart, these two (left and right) distinct AVN primordia could be identified from the fourth week of gestation in humans in the posterior atrial wall in the region of the posterior mesocardium, while postnatally these two components appeared as one fused structure.[87] Quite similarly, later studies in the developing rat and human heart identified dual AVN primordia reported to be positioned anteriorly in the myocardium along the upper right portion of the superior endocardial cushion and posteriorly in the base of the septum secundum.[88, 89] This concept was extended by morphological studies in the developing human embryo, demonstrating the presence of a prominent medioposterior AVN primordium (continuous with the bundle of His) and a smaller medioanterior AVN primordium (continuous with the retroaortic ring), minutely apposing during cardiac development.[30]

Another concept on AVN development was based on the classical ring theory, according to which the CCS is derived from a set of myocardial rings of specialized myocardium positioned between the primitive segments of the heart: 1) the sinoatrial (SA) ring between the sinus venosus and atrium, 2) the AV ring between the atrium and ventricle, 3) the bulboventricular ring or primary ring or fold between the bulbus and ventricle and 4) the truncobulbar or ventriculo-arterial ring between the outflow tract and ventricle.[10, 15, 28, 90-92] During development, parts of these rings loose their specialized character and the remaining parts are identified as putative elements of the mature CCS (**Figure 2**).[15, 28, 31, 64]

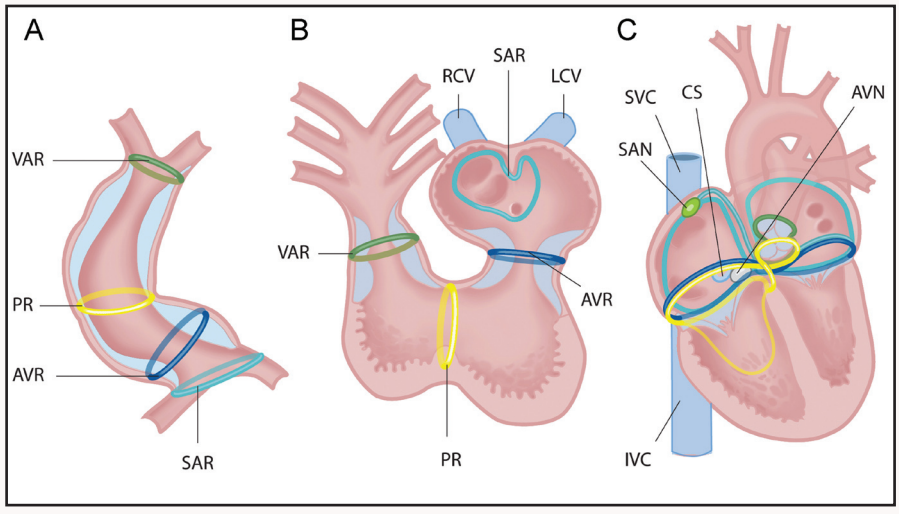

Figure 2. Schematic representation of the spatiotemporal relation of the myocardial rings of specialized tissue in cardiogenesis. During cardiogenesis the tubular heart undergoes dextral looping, which transforms the heart in a C-shape (**A**) and later in a S-shape (**B**) and finally in a four chambered heart (**C**). In the embryonic heart, the transitional zones or rings dividing the different putative chambers of the heart can be recognized, being the sinu-atrial transition (SAR), the atrioventricular ring (AVR), the primary ring (PR) and the ventriculo-arterial transition (VAR). The SAR seems to contribute to both the sinoatrial node (SAN) and atrioventricular node (AVN), while the AVN seems to receive a contribution from both the SAR, AVR and PR. RCV=right cardinal vein, LCV=left cardinal vein,CS=coronary sinus, SVC=superior vena cava, IVC=inferior vena cava.

Initially, the SA ring was thought to contribute to formation of the SAN, the SA ring and the AV ring were thought to both contribute to the AVN and the primary ring was thought to give rise to the His bundle and bundle branches,[28] while a single ring origin in the primary ring or fold has also been suggested.[93] Later on, contemporary marker studies could again confirm the important contribution of the SA ring to the developing SAN and AVN by HNK-1 expression patterns in the developing human embryo and analysis of CCS-LacZ and MinK-LacZ expression in the mouse embryo identified the SA ring, AV ring and primary ring as important contributors to CCS development.[26,30-32]

Contemporary Views on AVN Development

While currently insight into the molecular and genetic underpinnings of the specification and formation of the CCS is still growing, contemporary marker studies demonstrating expression patterns of multiple signaling and transcription factors implicated in the induction, maturation and patterning of the cardiac conduction system (CCS) – e.g. Nkx2.5, Shox-2, podoplanin, Id-2, HNK-1, Leu-7, PSA-NCAM, CCS-LacZ and minK-LacZ[30-32, 64, 66, 67, 94-96] - have re-established the hypothesized[83, 84] link between the myocardium of the sinus venosus (SV) (derived from the second heart field)[67] and the developing CCS.

Additionally, bone morphogenetic protein (BMP) – a multifunctional signaling molecule expressed throughout development in a multitude of tissues - has been shown to be required in the myocardium of the AV canal to assure proper structural development and function of the annulus fibrosis and the AVN itself.[97] Interestingly, BMP signaling seems to stimulate expression of periostin,[98] a profibrogenic extracellular matrix protein implicated in the formation of the annulus fibrosis and essential in maintaining the integrity of the fibrous heart skeleton of the mature heart.[99-101] While the T-box transcription factors Tbx2, Tbx3 and Tbx5 have also been shown to be essential molecular components for proper formation of the AV conduction axis as a whole,[68] their specific role in formation of the AVN itself remains unclear. In the developing heart, Tbx2, Tbx3 and Tbx5 are variably expressed in the developing SAN, AVN, internodal myocardium, His bundle and the bundle branches.[70, 71, 102] Studies aimed at identifying targets important for molecular specification of the CCS have identified Tbx3 as a critical factor in formation of the SAN[103] and molecular specification of the AV bundle and bundle branches.[68] Tbx2 is regulated by Hesr1 and Hesr2 (transcriptional repressors of the Hes-related gene family) expression and is required to repress chamber differentiation in the AV canal myocardium and seems important for

formation of the boundaries between the atrial and ventricular myocardium.[104, 105] Furthermore, dominant mutations in the Tbx5 gene are known to cause congenital heart defects and conduction system abnormalities (resembling Holt-Oram syndrome) in the adult human and mouse heart.[69, 106, 107]

The role of Nkx2.5 – one of the earliest markers of cardiac progenitor cells[108] - in normal differentiation and function of the CCS, has also been extensively substantiated in both animal models and humans.[62, 63] Since Nkx2.5 mRNA is transiently upregulated during formation of conduction fibers relative to the surrounding myocardium in embryonic chick, mouse and human hearts, a role in the development of the CCS seems highly plausible.[64] Additionally, in line with the demonstrated myocardial heterogeneity in the AV conduction system,[109] Nkx2.5 negative myocardial areas, additionally visualized by podoplanin,[67] Tbx18,[110] RhoA and Isl-1 positivity[111] and Nav1.5 and Cx43 negativity[112] (see also **Chapter 7**, *this Thesis*) and postulated to contribute to the developing CCS, have recently also been identified. While mutations in the human Nkx2.5 gene mapped to chromosome 5q35[113] have been shown to give rise to structural heart malformations - including ventricular septal defects, tetralogy of Fallot, ventricular hypertrophy, pulmonary atresia and subvalvular aortic stenosis – and AV conduction delays localized in the AVN,[63] the precise role of Nkx2.5 in the AVN remains unclear. Animal studies have however shown that the Nkx2.5 null mutant embryos completely lack the primordium of the developing AVN, while embryos with Nkx2.5 haploinsufficiency demonstrate an AVN with half the normal number of cells.[61]

Another recently discovered transcription gene, Id-2, which is a member of the Id family of transcriptional repressors, has been shown to have a conduction-system-specific expression pattern, which is dependent on its cooperatively expressed upstream targets Nkx2.5 and Tbx5 in specification of the ventricular conduction system.[66] Expression of Id-2 is also evident in the developing AV sulcus and AV cushions,[114] while its potential role in specification of the AVN has not been investigated.

Cellular Electrophysiology of the Developing AV Junction in Relation to the Function of the Adult AVN

In the early primary heart tube consisting solely of the common ventricle, a primitive electrocardiogram (ECG) can already be recorded showing a sinusoidal curve dropping below and above the isoelectric line, reflecting the linear, caudocephalic and isotropic impulse conduction with constant low velocity

of the primitive myocardium.[115-119] As the developing heart transforms from a tubular to a looped morphology, the pattern and speed of ventricular activation also undergo their first changes. The pattern of universally slow propagation along the primitive tubular heart develops heterogeneities in conduction properties in the different cardiac segments.[120, 121] As cardiac looping proceeds, a slowly conducting AV canal is forming separating the synchronous activation of the atrial and ventricular segments,[116, 122, 123] while action potentials in the atrial and ventricular working myocardium with a fast rising phase and high amplitude characteristic of fast voltage-gated sodium channels are concordantly emerging.[124, 125]

As a consequence, the emerging atrium and ventricle in the embryonic looped heart start displaying fast conduction, while the myocardium of the AV junction is now characterized by relatively slow conduction, which is thought to result from a lack of fast sodium channels and a relative lack of the gap junctional protein connexin-43.[76, 78, 118, 126] In the looped embryonic heart, an adult type electrocardiogram including a P-wave reflecting atrial activation, an AV delay caused by relatively slow conduction in the embryonic AV junctional myocardium and a QRS complex reflecting fast ventricular activation, can already be recorded in animal models in the absence of a structurally recognizable AVN.[117, 127-129]

Furthermore, the cellular electrophysiology of the embryonic AV junctional tissue is also already quite similar to the adult nodal tissue:[130] it responds to adenosine with a reduction in action potential amplitude and dV/dt_{max}.[14] Histologically, like the adult SAN and adult AVN but unlike the working myocardium, the developing AV junctional tissue displays a relative lack of connexin-43.[126] Myocytes at the AV junction preferentially express connexin-45,[131] a low conductance gap junction channel that is also expressed in the SAN as well as in the AVN of the mature heart.[44]

Besides maintaining an AV conduction delay (decremental conduction) essential for efficient hemodynamic functioning,[132, 133] the adult AVN is also responsible for 1) gathering the incoming signals from the SAN (probably through the internodal pathways, as described above), 2) directing the electrical impulse to the His bundle, 3) automaticity and generation of an escape rhythm and 4) responding to the autonomic nervous system and humoral signals.[132, 134, 135]

While propagation of the electrical impulse from the AVN to the adjacent bundle of His seems relatively simple, physical contact between the node and bundle is brought about by a complex developmental remodeling process in which the muscular interventricular septum (IVS) fuses with the right tubercle

of the dorsal endocardial cushion (future right basal portion of the interatrial septum) facilitating the continuity between the AV bundle and AVN.[129] The ontogenic origin of the bundle of His is equally indistinct compared to the origin of the AVN. Various studies have provided puzzling proof for simultaneous[74, 75] or independent[28, 90-92] AVN and His bundle development, consecutive AVN and His bundle development[73, 79, 80, 136] and consecutive His bundle and AVN development.[137-139]

Traditionally, the leading pacemaker site responsible for automaticity in the AV junction was thought to be located in the compact AVN or nodal-His regions.[140] Contemporary studies however demonstrated that automaticity in the AVN in case of e.g. SAN dysfunction with ectopic pacemaking, is most often initiated in the region of the INE or slow pathway of the rabbit AVN,[141-143] a cellular population which has been postulated to originate from the early pacemaking left sinus horn primordial AVN tissues of the developing embryo.[111, 112] (see also **Chapter 7,** *this thesis*). Moreover, during RF ablation of the slow pathway in case of AVNRT, the emergence of an accelerated junctional rhythm (AJR), which has been suggested to result from enhanced automaticity of the AV Nodal or perinodal tissues in response to thermal effects,[144] is frequently observed and used as a guide for successful application.[144, 145] Interestingly, in animal studies a heat sensitive area of nodal type cells was observed inferiorly to the compact AVN.[146]

The autonomic control of the AV junction and AVN has been the subject of numerous studies. In the rat AV junction, the distribution of sympathetic and parasympathetic neurons has been elaborately documented.[147] Functionally, autonomic modulation of AV junctional conduction has also been extensively studied.[148, 149] The AV junctional pacemaker can be autonomically modulated to increase its rate to levels similar to the SAN,[142] comparable to the AJR observed after slow pathway ablation for treatment of AVNRT.[144-146]

AV Nodal Conduction Dichotomy

Clinically, interest in the structure of the AVN mainly focuses on the anatomical basis for the reentry circuit in AVNRT which has still remained poorly defined. The agreed-upon substrate for AVNRT, electrophysiologically defined by the response to atrial extrastimulation, with a 50-millisecond increase or greater in AVN conduction time (A2H2) in response to a 10-millisecond decrease in atrial coupling interval (A1A2), implies involvement of functionally separate and anatomically discrete dual AVN pathways (dual AV nodal physiology).[150, 151]

Many essential elements of AV nodal reentry were already described in the first known functional experiments on the AV connections of the heart of the electric ray in 1913 by Mines.[152] Important terms in AV nodal reentry were subsequently introduced by Scherf and Schookhoff in 1926 (longitudinal dissociation) and by Rosenblueth in 1958 (echo), further established by Schuilenburgin 1968.[153, 154,155]

The true concept of dual AV nodal conduction was first demonstrated in the late 1950s and 1960s by microelelectrode recordings in dog and rabbit hearts by Moe and colleagues.[156] Evidence linking AV nodal conduction dichotomy and AVNRT in humans was subsequently found in the late 1960s and early 1970s[157, 158] and established in 1981 by the demonstration of distinct atrial exits during retrograde conduction through the fast (region of the anterior septum) and slow (region of the CS) AV nodal pathways.[159] Functionally, the two pathways have distinct conduction velocities and refractory periods, although their precise anatomic boundaries are unknown. The fast pathway conducts rapidly and has a relatively long refractory period in the antegrade direction, while the slow pathway conducts relatively slowly and has a shorter antegrade refractory period than the fast pathway.[160]

The polemic in dual AV nodal pathways has however concentrated on confinement of the slow and fast pathway to the AVN itself or the presence of an upper common pathway in the adjacent atrial tissues to complete the reentry circuit. In dual AV nodal physiology, the retrograde atrial exit of the fast pathway in the anterior approaches to the AVN is found at the lower septal right atrium and the exit of the slow AV nodal pathway in the posterior approaches to the AVN is located in or near the coronary sinus ostium,[159] while an origin well outside the specialized area of the triangle of Koch has also been postulated.[6]

Experimentally, evidence in favor of an intra AV nodal reentry circuit was found in vivo in various animal models[161, 162] while evidence for the participation of adjacent extra-nodal tissues was also provided.[163-166] Clinically, the concept of intra AV nodal reentry was advocated by its proponents,[167] while placement of multiple lesions in the slow pathway region around the AVN to cure AVNRT without altering AV nodal conduction however eventually eroded support for this view.[3, 160, 168-171] The currently largely accepted anatomic understanding of the AVN, in which the INEs as well as the transitional cells are part of the AVN,[172] largely resolves this debate. Needless to say, precise knowledge of the exact anatomical substrates for normal and abnormal conduction would aid refinement of the placement of the lesion lines when treating AV nodal arrhythmias.

The Presence of Dual AVN Pathways as Substrates for AVNRT: Physiology versus Pathophysiology ?

AV Nodal Reentrant Tachycardia (AVNRT) demonstrates an age related incidence disparity, with increasing incidence with age.[2, 173, 174] Although AVNRT is the most common mechanism of supraventricular tachycardia (SVT) in adults (>80%),[1] it only accounts for a comparatively small number of SVT cases in pediatric patients (5-16%),[2] eventually becoming the most common form of SVT around adolescence.[175] Later on in life, both the incidence of AVNRT and the functional presence of dual AV nodal pathways however progressively decreases again.[176] Mechanistically, these apparent age-differences in AVNRT incidence initially seem to reflect maturational histological and electrophysiological changes in the AVN region, while at the end of life in the setting of coronary artery disease or hypertension a natural degeneration of the AV conduction axis seems more likely.[173, 176]

Structurally, the compact AVN and its transitional zone have been shown to undergo gradual structural and geometric changes until the age of 20 years, including a widening of the transitional zone, a progressive increase in fibrofatty tissue and an increase in the right inferior nodal extension (INE) (slow pathway) of the AVN.[177] Electrophysiologically, in comparison to adolescents, pediatric AVNRT patients demonstrate a significantly shorter fast pathway effective refractory period (ERP), slow pathway ERP and AVNRT cycle length, gradually lengthening with increasing age.[175]

Interestingly, in the pediatric AVNRT population the prevalence of dual AV nodal physiology is reported to be equal in comparison to pediatric controls.[178] The presence of dual AV nodal pathways in patients without AVNRT increases with age,[173] which was also demonstrated in experimental studies on maturational differences of AV nodal physiology in mice.[179] Moreover, ventriculoatrial (VA) conduction through the AVN is possible in 40% to 90% of normal adults[180] and 61% of normal children.[173]

Although it has been fully established that the ability to generate AVNRT implies the presence of dual anatomically distinct AV nodal pathways, in some cases the two pathways cannot be demonstrated with typical criteria in electrophysiological (EP) studies, as was illustrated in a report of 159 children with AVNRT in which in only 62% percent of children a clear dual AV nodal physiology could be demonstrated.[181] In adult AVNRT patients however, dual AV nodal physiology can normally be demonstrated in 82-100% of cases.[157, 180] The inability to elicit dual AV nodal pathways by programmed electrical stimulation

might reflect the relative infrequency of AVNRT in the pediatric age group[173] and has been suggested to be caused by a age-related difference in response to autonomic input, while the current concept of dual AV nodal pathways might also simply be inadequate to explain this mechanism.[151]

Furthermore, AVNRT displays a striking 2:1 predominance of women.[182-184] Experimental studies have shown direct hormonal effects on the expression and function of cardiac ion channels,[185] while clinically the frequency and duration of tachycardia was found to be positively correlated with progesterone levels and inversely correlated with β-estradiol levels.[186] Since gender-related differences in AV nodal ERP persist after major changes in hormonal status after menopause,[187] an additional role for the autonomic nervous system seems plausible. While large studies concerning gender-related differences in normal AVN function do not exist, intrinsic changes in the electrophysiology of the SAN and AVN have been reported in long-term physical training.[188]

Based on the clinical data at hand, dual AV nodal pathways are probably present in all structurally normal hearts with and without reported episodes of AVNRT.[134, 189] While large studies on the inducibility of echoes or repetitive reentry in normal hearts of arrhythmia free patients unfortunately do not exist, both historical and contemporary developmental data on AVN development seems largely in favor of the suggestion that the presence of functional longitudinal dissociation in AV conduction should be considered normal physiology of the AVN. The question however still remains, why and when some people develop AVNRT and other do not.

Conclusions

While the electrophysiological substrates for AVNRT are well known, the anatomical correlates forming the reentry circuit have still remained incompletely understood. Similarly, the physiology of the adult AVN has also still remained puzzling, since the structural boundaries of the AVN itself and its developmental origin are largely unknown. Although recent marker studies have provided some clues to the origin of the AVN,[67, 110-112] further studies examining the ontogeny of the individual parts of the AVN are essential in unraveling the (patho)physiological structure-function relations of the adult AVN region. In an era where increasingly sophisticated strategies to unambiguously identify cells of the CCS and determine their pattern of gene expression and function continue to evolve,[190, 191] progress in our theoretical understanding of the mechanisms governing physiological AV nodal functioning will provide a benchmark to successfully interpret the electrophysiological observations in AVNRT.

References

1. Jackman WM, Nakagawa H, Heidbuchel H, Beckman K, McClelland J, Lazzara R. Three forms of atrioventricular nodal (junctional) reentrant tachycardia: differential diagnosis, electrophysiological characteristics and implications for anatomy of the reentrant circuit.In: Zipes DP, Jalife, J., ed. *Cardiac Electrophysiology: From Cell to Bedside*. Vol second edition: WB Saunders; 1995:620-637.

2. Ko JK, Deal BJ, Strasburger JF, Benson DW. Supraventricular tachycardia mechanisms and their age distribution in pediatric patients. *Am J Cardiol*. 1992;69(12):1028-1032.

3. Jackman WM, Beckman KJ, McClelland JH, Wang X, Friday KJ, Roman CA, Moulton KP, Twidale N, Hazlitt HA, Prior MI. Treatment of supraventricular tachycardia due to atrioventricular nodal reentry, by radiofrequency catheter ablation of slow-pathway conduction. *N Engl J Med*. 1992;327(5):313-318.

4. Tawara S. Das reizleitungssystem des saugetierherzens. Eine anatomisch-histologische studie uber das atrioventrikularbundel und die Purkinjeschen faden. Verslag von Gustav Fischer; 1906.

5. Koch W. Weiter mitteilungen uber der sinusknoten der herzens. *Verh Deutch Pathol Gesell*. 1909;7:13-20.

6. Janse MJ, Anderson RH, McGuire MA, Ho SY. "AV nodal" reentry: Part I: "AV nodal" reentry revisited. *J Cardiovasc Electrophysiol*. 1993;4(5):561-572.

7. Inoue S, Becker AE. Posterior extensions of the human compact atrioventricular node: a neglected anatomic feature of potential clinical significance. *Circulation*. 1998;97(2):188-193.

8. Sanchez-Quintana D, Davies DW, Ho SY, Oslizlok P, Anderson RH. Architecture of the atrial musculature in and around the triangle of Koch: its potential relevance to atrioventricular nodal reentry. *J Cardiovasc Electrophysiol*. 1997;8(12):1396-1407.

9. Anderson RH, Becker AE, Brechenmacher C, Davies MJ, Rossi L. The human atrioventricular junctional area. A morphological study of the A-V node and bundle. *Eur J Cardiol*. 1975;3(1):11-25.

10. Anderson RH, Janse MJ, van Capelle FJ, Billette J, Becker AE, Durrer D. A combined morphological and electrophysiological study of the atrioventricular node of the rabbit heart. *Circ Res*. 1974;35(6):909-922.

11. Anderson RH, Ho SY, Becker AE. Anatomic boundaries between the atrioventricular node and the atrioventricular bundle. *J Cardiovasc Electrophysiol.* 1998;9(2):225-228.

12. Ho SY, Kilpatrick L, Kanai T, Germroth PG, Thompson RP, Anderson RH. The architecture of the atrioventricular conduction axis in dog compared to man: its significance to ablation of the atrioventricular nodal approaches. *J Cardiovasc Electrophysiol.* 1995;6(1):26-39.

13. Mazgalev TN. The dual AV nodal pathways: are they dual and where are they? *J Cardiovasc Electrophysiol.* 1997;8(12):1408-1412.

14. McGuire MA, de Bakker JM, Vermeulen JT, Moorman AF, Loh P, Thibault B, Vermeulen JL, Becker AE, Janse MJ. Atrioventricular junctional tissue. Discrepancy between histological and electrophysiological characteristics. *Circulation.* 1996;94(3):571-577.

15. Anderson RH, Taylor IM. Development of atrioventricular specialized tissue in human heart. *Br Heart J.* 1972;34(12):1205-1214.

16. Billette J. Atrioventricular nodal activation during periodic premature stimulation of the atrium. *Am J Physiol.* 1987;252(1 Pt 2):H163-177.

17. Paes de Carvalho A, de Almeida, D.F. Spread of activity through the atrioventricular node. *Circ Res.* 1960;8:801-809.

18. Yoo S, Dobrzynski H, Fedorov VV, Xu SZ, Yamanushi TT, Jones SA, Yamamoto M, Nikolski VP, Efimov IR, Boyett MR. Localization of Na+ channel isoforms at the atrioventricular junction and atrioventricular node in the rat. *Circulation.* 2006;114(13):1360-1371.

19. Moorman AF, Christoffels VM, Anderson RH. Anatomic substrates for cardiac conduction. *Heart Rhythm.* 2005;2(8):875-886.

20. Moorman AF, Soufan AT, Hagoort J, de Boer PA, Christoffels VM. Development of the building plan of the heart. *Ann N Y Acad Sci.* 2004;1015:171-181.

21. Moorman AF, de Jong F, Denyn MM, Lamers WH. Development of the cardiac conduction system. *Circ Res.* 1998;82(6):629-644.

22. Virágh S, Challice CE. The development of the conduction system in the mouse embryo heart. *Dev Biol.* 1980;80(1):28-45.

23. Mikawa T, Hurtado R. Development of the cardiac conduction system. *Semin Cell Dev Biol.* 2007;18(1):90-100.

24. James TN. The connecting pathways between the sinus node and A-V node and between the right and the left atrium in the human heart. *Am Heart J.* 1963;66:498-508.

25. James TN. The internodal pathways of the human heart. *Progr Cardiovasc Dis.* 2001;43(6):495-535.

26. Jongbloed MR, Wijffels MC, Schalij MJ, Blom NA, Poelmann RE, van der Laarse A, Mentink MM, Wang Z, Fishman GI, Gittenberger-de Groot AC. Development of the right ventricular inflow tract and moderator band: a possible morphological and functional explanation for Mahaim tachycardia. *Circ Res.* 2005;96(7):776-783.

27. Thorel C. Vorlaufige mitteilung uber eine besondere muskelverbindung zwischen der cava superior und dem Hisschen Bundel. *Munch Med Wochschr.* 1909;56.

28. Wenink AC. Development of atrio-ventricular conduction pathways. *Bulletin de l'Association des anatomistes.* 1976;60(170):623-629.

29. Spach MS, Kootsey JM. The nature of electrical propagation in cardiac muscle. *Am J Physiol.* 1983;244(1):H3-22.

30. Blom NA, Gittenberger-de Groot AC, DeRuiter MC, Poelmann RE, Mentink MM, Ottenkamp J. Development of the cardiac conduction tissue in human embryos using HNK-1 antigen expression: possible relevance for understanding of abnormal atrial automaticity. *Circulation.* 1999;99(6):800-806.

31. Jongbloed MR, Schalij MJ, Poelmann RE, Blom NA, Fekkes ML, Wang Z, Fishman GI, Gittenberger-de Groot AC. Embryonic conduction tissue: a spatial correlation with adult arrhythmogenic areas. *J Cardiovasc Electrophysiol.* 2004;15(3):349-355.

32. Kondo RP, Anderson RH, Kupershmidt S, Roden DM, Evans SM. Development of the cardiac conduction system as delineated by minK-lacZ. *J Cardiovasc Electrophysiol.* 2003;14(4):383-391.

33. Vassale M, Greenspan K., Jomain S., Hoffman BF. Effects of potassium on automaticity and conduction of canine hearts. *Am J Physiol.* 1964;207.

34. Wagner ML, Lazzara, R., Weiss, R.M., Hoffman, B.F. Specialized conducting fibers in the interatrial band. *Circ Res.* 1966;18.

35. Sakai T, Hirota A, Momose-Sato Y, Sato K, Kamino K. Optical mapping of conduction patterns of normal and tachycardia-like excitations in the rat atrium. *Jpn J Physiol.* 1997;47(2):179-188.

36. Racker DK. Sinoventricular transmission in 10 mM K+ by canine atrioventricular nodal inputs. Superior atrionodal bundle and proximal atrioventricular bundle. *Circulation.* 1991;83(5):1738-1753.

37. Monckebreg JG. Beitrage zur normalen und pathologischen anatomie des herzens. *Verh Disch Pathol Ges.* 1910;14:64-71.

38. Virágh S, Porte A. The fine structure of the conducting system of the monkey heart (Macaca mulatta). I. The sino-atrial node and the internodal connections. *Zeitschrift für Zellforschung und Mikroskopische Anatomie.* 1973;145(2):191-211.

39. Virágh SZ, Porte A. On the impulse conducting system of the monkey heart (Macaca mulatta). II. The atrio-ventricular node and bundle. *Zeitschrift für Zellforschung und Mikroskopische Anatomie.* 1973;145(3):363-388.

40. Rentschler S, Morley GE, Fishman GI. Patterning of the mouse conduction system. *Novartis Found Symp.* 2003;250:194-205; discussion 205-199, 276-199.

41. Callewaert G, Vereecke J, Carmeliet E. Existence of a calcium-dependent potassium channel in the membrane of cow cardiac Purkinje cells. *Pflugers Arch.* 1986;406(4):424-426.

42. Kaupp UB, Seifert R. Molecular diversity of pacemaker ion channels. *Annu Rev Physiol.* 2001;63:235-257.

43. Kupershmidt S, Yang T, Anderson ME, Wessels A, Niswender KD, Magnuson MA, Roden DM. Replacement by homologous recombination of the minK gene with lacZ reveals restriction of minK expression to the mouse cardiac conduction system. *Circ Res.* 1999;84(2):146-152.

44. Coppen SR, Kodama I, Boyett MR, Dobrzynski H, Takagishi Y, Honjo H, Yeh HI, Severs NJ. Connexin45, a major connexin of the rabbit sinoatrial node, is co-expressed with connexin43 in a restricted zone at the nodal-crista terminalis border. *J Histochem Cytochem.* 1999;47(7):907-918.

45. Gourdie RG, Cheng G, Thompson RP, Mikawa T. Retroviral cell lineage analysis in the developing chick heart. *Methods Mol Biol.* 2000;135:297-304.

46. Gros DB, Jongsma HJ. Connexins in mammalian heart function. *Bioessays.* 1996;18(9):719-730.

47. Welikson RE, Fischman DA. The C-terminal IgI domains of myosin-binding proteins C and H (MyBP-C and MyBP-H) are both necessary and sufficient for the intracellular crosslinking of sarcomeric myosin in transfected non-muscle cells. *J Cell Sci.* 2002;115(Pt 17):3517-3526.

48. Alyonycheva T, Cohen-Gould L, Siewert C, Fischman DA, Mikawa T. Skeletal muscle-specific myosin binding protein-H is expressed in Purkinje fibers of the cardiac conduction system. *Circ Res.* 1997;80(5):665-672.

49. Davis DL, Edwards AV, Juraszek AL, Phelps A, Wessels A, Burch JB. A GATA-6 gene heart-region-specific enhancer provides a novel means to mark and probe a discrete component of the mouse cardiac conduction system. *Mech Dev.* 2001;108(1-2):105-119.

50. Pennisi DJ, Rentschler S, Gourdie RG, Fishman GI, Mikawa T. Induction and patterning of the cardiac conduction system. *Int J Dev Biol.* 2002;46(6):765-775.

51. Gassanov N, Er F, Zagidullin N, Hoppe UC. Endothelin induces differentiation of ANP-EGFP expressing embryonic stem cells towards a pacemaker phenotype. *FASEB J.* 2004;18(14):1710-1712.

52. Gourdie RG, Wei Y, Kim D, Klatt SC, Mikawa T. Endothelin-induced conversion of embryonic heart muscle cells into impulse-conducting Purkinje fibers. *Proc Natl Acad Sci USA.* 1998;95(12):6815-6818.

53. Hall CE, Hurtado R, Hewett KW, Shulimovich M, Poma CP, Reckova M, Justus C, Pennisi DJ, Tobita K, Sedmera D, Gourdie RG, Mikawa T. Hemodynamic-dependent patterning of endothelin converting enzyme 1 expression and differentiation of impulse-conducting Purkinje fibers in the embryonic heart. *Development.* 2004;131(3):581-592.

54. Kanzawa N, Poma CP, Takebayashi-Suzuki K, Diaz KG, Layliev J, Mikawa T. Competency of embryonic cardiomyocytes to undergo Purkinje fiber differentiation is regulated by endothelin receptor expression. *Development.* 2002;129(13):3185-3194.

55. Patel R, Kos L. Endothelin-1 and Neuregulin-1 convert embryonic cardiomyocytes into cells of the conduction system in the mouse. *Dev Dyn.* 2005;233(1):20-28.

56. Takebayashi-Suzuki K, Yanagisawa M, Gourdie RG, Kanzawa N, Mikawa T. In vivo induction of cardiac Purkinje fiber differentiation by coexpression of preproendothelin-1 and endothelin converting enzyme-1. *Development.* 2000;127(16):3523-3532.

57. Milan DJ, Giokas AC, Serluca FC, Peterson RT, MacRae CA. Notch1b and neuregulin are required for specification of central cardiac conduction tissue. *Development.* 2006;133(6):1125-1132.

58. Rentschler S, Morley GE, Fishman GI. Molecular and functional maturation of the murine cardiac conduction system. *Cold Spring Harb Symp Quant Biol.* 2002;67:353-361.

59. Bond J, Sedmera D, Jourdan J, Zhang Y, Eisenberg CA, Eisenberg LM, Gourdie RG. Wnt11 and Wnt7a are up-regulated in association with differentiation of cardiac conduction cells in vitro and in vivo. *Dev Dyn.* 2003;227(4):536-543.

60. Chan-Thomas PS, Thompson RP, Robert B, Yacoub MH, Barton PJ. Expression of homeobox genes Msx-1 (Hox-7) and Msx-2 (Hox-8) during cardiac development in the chick. *Dev Dyn.* 1993;197(3):203-216.

61. Jay PY, Harris BS, Maguire CT, Buerger A, Wakimoto H, Tanaka M, Kupershmidt S, Roden DM, Schultheiss TM, O'Brien TX, Gourdie RG, Berul CI, Izumo S. Nkx2-5 mutation causes anatomic hypoplasia of the cardiac conduction system. *J Clin Invest.* 2004;113(8):1130-1137.

62. Pashmforoush M, Lu JT, Chen H, Amand TS, Kondo R, Pradervand S, Evans SM, Clark B, Feramisco JR, Giles W, Ho SY, Benson DW, Silberbach M, Shou W, Chien KR. Nkx2-5 pathways and congenital heart disease; loss of ventricular myocyte lineage specification leads to progressive cardiomyopathy and complete heart block. *Cell.* 2004;117(3):373-386.

63. Schott JJ, Benson DW, Basson CT, Pease W, Silberbach GM, Moak JP, Maron BJ, Seidman CE, Seidman JG. Congenital heart disease caused by mutations in the transcription factor NKX2-5. *Science.* 1998;281(5373):108-111.

64. Thomas PS, Kasahara H, Edmonson AM, Izumo S, Yacoub MH, Barton PJ, Gourdie RG. Elevated expression of Nkx-2.5 in developing myocardial conduction cells. *Anat Rec.* 2001;263(3):307-313.

65. Ismat FA, Zhang M, Kook H, Huang B, Zhou R, Ferrari VA, Epstein JA, Patel VV. Homeobox protein Hop functions in the adult cardiac conduction system. *Circ Res.* 2005;96(8):898-903.

66. Moskowitz IP, Kim JB, Moore ML, Wolf CM, Peterson MA, Shendure J, Nobrega MA, Yokota Y, Berul C, Izumo S, Seidman JG, Seidman CE. A molecular pathway including Id2, Tbx5, and Nkx2-5 required for cardiac conduction system development. *Cell.* 2007;129(7):1365-1376.

67. Gittenberger-de Groot AC, Mahtab EA, Hahurij ND, Wisse LJ, Deruiter MC, Wijffels MC, Poelmann RE. Nkx2.5-negative myocardium of the posterior heart field and its correlation with podoplanin expression in cells from the developing cardiac pacemaking and conduction system. *Anat Rec.* 2007;290(1):115-122.

68. Bakker ML, Boukens BJ, Mommersteeg MT, Brons JF, Wakker V, Moorman AF, Christoffels VM. Transcription factor Tbx3 is required for the specification of the atrioventricular conduction system. *Circ Res.* 2008;102(11):1340-1349.

69. Bruneau BG, Logan M, Davis N, Levi T, Tabin CJ, Seidman JG, Seidman CE. Chamber-specific cardiac expression of Tbx5 and heart defects in Holt-Oram syndrome. *Dev Biol.* 1999;211(1):100-108.

70. Christoffels VM, Burch JB, Moorman AF. Architectural plan for the heart: early patterning and delineation of the chambers and the nodes. *Trends Cardiovasc Med.* 2004;14(8):301-307.

71. Moskowitz IP, Pizard A, Patel VV, Bruneau BG, Kim JB, Kupershmidt S, Roden D, Berul CI, Seidman CE, Seidman JG. The T-Box transcription factor Tbx5 is required for the patterning and maturation of the murine cardiac conduction system. *Development.* 2004;131(16):4107-4116.

72. Mall FP. On the development of the human heart. *Am J Anat.* 1912;13:249-298.

73. Shaner RF. The development of the atrioventricular node, bundle of His and sinoatrial node in the calf, with a description of a third embryonic node-like structure. *Anat Rec.* 1929;44:85-99.

74. Viragh S, Challice, C.E. The development of the conduction system in the mouse embryo heart. I. The first embryonic A-V conduction pathway. *Dev Biol.* 1977;56:382-396.

75. Virágh S, Challice CE. The development of the conduction system in the mouse embryo heart. II. Histogenesis of the atrioventricular node and bundle. *Dev Biol.* 1977;56(2):397-411.

76. Argüello C, Alanís J, Pantoja O, Valenzuela B. Electrophysiological and ultrastructural study of the atrioventricular canal during the development of the chick embryo. *J Mol Cell Cardiol.* 1986;18(5):499-510.

77. Lieberman M, Paes de Carvalho, A. The spread of excitation in the embryonic chick heart. *J Gen Physiol.* 1965;49:365-379.

78. Patten BM. Initiation and early changes in the character of the heart beat in vertebrate embryos. *Physiol Rev.* 1949;29(1):31-47.

79. Retzer R. The anatomy of the conduction system in the mammalian heart. *Bull Johns Hopkins Hosp.* 1908;19:208-215.

80. Tandler J. The development of the human heart. In: Kiebel F, Mall, F.P., ed. *Manual of human embryology.* Vol 2. Mexico: J.B. Lippincott; 1912.

81. Wahlin B. Das reizleitungssystem unde die nerven des saugetierherzens. *Stockholm.* 1935;125.

82. Walls EW. An investigation into the regenerative capacity of mammalian heart muscle. *J Anat.* 1949;83(Pt. 1):66.

83. James TN. Cardiac conduction system: fetal and postnatal development. *Am J Cardiol.* 1970;25(2):213-226.

84. Patten BM. The development of the sinoventricular conduction system. *Medical Bulletin* 1956;22(1):1-21.

85. Marino TA, Severdia J. The early development of the AV node and bundle in the ferret heart. *Am J Anat.* 1983;167(3):299-312.

86. Marino TA, Truex RC, Marino DR. The development of the atrioventricular node and bundle in the ferret heart. *Am J Anat.* 1979;154(2):135-150.

87. Truex RC, Marino TA, Marino DR. Observations on the development of the human atrioventricular node and bundle. *Anat Rec.* 1978;192(3):337-350.

88. Aoyama N, Tamaki H, Kikawada R, Yamashina S. Development of the conduction system in the rat heart as determined by Leu-7 (HNK-1) immunohistochemistry and computer graphics reconstruction. *Lab Invest.* 1995;72(3):355-366.

89. Ikeda T, Iwasaki K, Shimokawa I, Sakai H, Ito H, Matsuo T. Leu-7 immunoreactivity in human and rat embryonic hearts, with special reference to the development of the conduction tissue. *Anat Embryol.* 1990;182(6):553-562.

90. Anderson RH, Becker AE, Wilkinson JL, Gerlis LM. Morphogenesis of univentricular hearts. *Br Heart J.* 1976;38(6):558-572.

91. Anderson RH, Wenick AC, Losekoot TG, Becker AE. Congenitally complete heart block. Developmental aspects. *Circulation.* 1977;56(1):90-101.

92. Benninghof A. Uber die beziehungen des reitzleitungssystem und der papillarmuskeln zu der konturfasern des herzschlauches. *Anatomischer Anzeicher* 1923;57:185-208.

93. Wessels A, Vermeulen JL, Verbeek FJ, Virágh S, Kálmán F, Lamers WH, Moorman AF. Spatial distribution of "tissue-specific" antigens in the developing human heart and skeletal muscle. III. An immunohistochemical analysis of the distribution of the neural tissue antigen G1N2 in the embryonic heart; implications for the development of the atrioventricular conduction system. *Anat Rec.* 1992;232(1):97-111.

94. Blaschke RJ, Hahurij ND, Kuijper S, Just S, Wisse LJ, Deissler K, Maxelon T, Anastassiadis K, Spitzer J, Hardt SE, Schöler H, Feitsma H, Rottbauer W, Blum M, Meijlink F, Rappold G, Gittenberger-de Groot AC. Targeted mutation reveals essential functions of the homeodomain transcription factor Shox2 in sinoatrial and pacemaking development. *Circulation.* 2007;115(14):1830-1838.

95. de Ruiter MC, Gittenberger-de Groot AC, Wenink AC, Poelmann RE, Mentink MM. In normal development pulmonary veins are connected to the sinus venosus segment in the left atrium. *Anat Rec.* 1995;243(1):84-92.

96. Watanabe M, Timm M, Fallah-Najmabadi H. Cardiac expression of polysialylated NCAM in the chicken embryo: correlation with the ventricular conduction system. *Dev Dyn.* 1992;194(2):128-141.

97. Stroud DM, Gaussin V, Burch JB, Yu C, Mishina Y, Schneider MD, Fishman GI, Morley GE. Abnormal conduction and morphology in the atrioventricular node of mice with atrioventricular canal targeted deletion of Alk3/Bmpr1a receptor. *Circulation.* 2007;116(22):2535-2543.

98. Lindner V, Wang Q, Conley BA, Friesel RE, Vary CP. Vascular injury induces expression of periostin: implications for vascular cell differentiation and migration. *Arterioscler Thromb Vasc Biol.* 2005;25(1):77-83.

99. Kern CB, Hoffman S, Moreno R, Damon BJ, Norris RA, Krug EL, Markwald RR, Mjaatvedt CH. Immunolocalization of chick periostin protein in the developing heart. *Anat Rec.* 2005;284(1):415-423.

100. Kolditz DP, Wijffels MC, Blom NA, van der Laarse A, Hahurij ND, Lie-Venema H, Markwald RR, Poelmann RE, Schalij MJ, Gittenberger-De Groot AC. Epicardium-Derived Cells in Development of Annulus Fibrosis and Persistence of Accessory Pathways. *Circulation.* 2008.

101. Kolditz DP, Wijffels MC, Blom NA, van der Laarse A, Markwald RR, Schalij MJ, Gittenberger-de Groot AC. Persistence of functional atrioventricular accessory pathways in postseptated embryonic avian hearts: implications for morphogenesis and functional maturation of the cardiac conduction system. *Circulation.* 2007;115(1):17-26.

102. Hoogaars WM, Tessari A, Moorman AF, de Boer PA, Hagoort J, Soufan AT, Campione M, Christoffels VM. The transcriptional repressor Tbx3 delineates the developing central conduction system of the heart. *Cardiovasc Res.* 2004;62(3):489-499.

103. Mommersteeg MT, Hoogaars WM, Prall OW, de Gier-de Vries C, Wiese C, Clout DE, Papaioannou VE, Brown NA, Harvey RP, Moorman AF, Christoffels VM. Molecular pathway for the localized formation of the sinoatrial node. *Circ Res.* 2007;100:354-362

104. Harrelson Z, Kelly RG, Goldin SN, Gibson-Brown JJ, Bollag RJ, Silver LM, Papaioannou VE. Tbx2 is essential for patterning the atrioventricular canal and for morphogenesis of the outflow tract during heart development. *Development.* 2004;131(20):5041-5052.

105. Kokubo H, Tomita-Miyagawa S, Hamada Y, Saga Y. Hesr1 and Hesr2 regulate atrioventricular boundary formation in the developing heart through the repression of Tbx2. *Development.* 2007;134(4):747-755.

106. Basson CT, Cowley GS, Solomon SD, Weissman B, Poznanski AK, Traill TA, Seidman JG, Seidman CE. The clinical and genetic spectrum of the Holt-Oram syndrome (heart-hand syndrome). *N Engl J Med.* 1994;330(13):885-891.

107. Li QY, Newbury-Ecob RA, Terrett JA, Wilson DI, Curtis AR, Yi CH, Gebuhr T, Bullen PJ, Robson SC, Strachan T, Bonnet D, Lyonnet S, Young ID, Raeburn JA, Buckler AJ, Law DJ, Brook JD. Holt-Oram syndrome is caused by mutations in TBX5, a member of the Brachyury (T) gene family. *Nat Genet.* 1997;15(1):21-29.

108. Harvey RP. NK-2 homeobox genes and heart development. *Dev Biol.* 1996;178(2):203-216.

109. Kitajima S, Miyagawa-Tomita S, Inoue T, Kanno J, Saga Y. Mesp1-nonexpressing cells contribute to the ventricular cardiac conduction system. *Dev Dyn.* 2006;235(2):395-402.

110. Christoffels VM, Mommersteeg MT, Trowe MO, Prall OW, de Gier-de Vries C, Soufan AT, Bussen M, Schuster-Gossler K, Harvey RP, Moorman AF, Kispert A. Formation of the venous pole of the heart from an Nkx2-5-negative precursor population requires Tbx18. *Circ Res.* 2006;98(12):1555-1563.

111. Vicente-Steijn R, Kolditz DP, Mahtab EAF, Bax NAM, van der Graaf LM, Schalij MJ, Poelmann RE, Gittenberger-de Groot AC, Jongbloed MRM. Pacemaker activity in the developing chick heart and correlation with the expression of RhoA in the developing cardiac conduction system. *Unpublished results*: Leiden University Medical Center; 2008.

112. Kolditz DP, Vicente-Steijn R, Pijnappels DA, Jongbloed MRM., Poelmann RE, Schalij MJ, Gittenberger-de Groot AC. Development of the atrioventricular node from heterogeneous primordia: implications for the anatomical correlate of the slow-pathway. *Unpublished results*: Leiden University Medical Center; 2008.

113. Turbay D, Wechsler SB, Blanchard KM, Izumo S. Molecular cloning, chromosomal mapping, and characterization of the human cardiac-specific homeobox gene hCsx. *Mol Med.* 1996;2(1):86-96.

114. Martinsen BJ, Frasier AJ, Baker CV, Lohr JL. Cardiac neural crest ablation alters Id2 gene expression in the developing heart. *Dev Biol.* 2004;272(1):176-190.

115. Bogue JY, Mendez R. The relation between the mechanical and electrical response of the frog's heart. *J Physiol* 1930;69(3):316-330.

116. Hoff EC, Kramer, T.C., Dubois, D., Patten, B.M. The development of the electrocardiogram of the embryonic heart. *Am Heart J.* 1939;17:471-488.

117. Paff GH, Boucek RJ, Harrell TC. Observations on the development of the electrocardiogram. *Anat Rec.* 1968;160(3):575-582.

118. Patten BM. The initiation of contraction in the embronic chick heart. *Am J Anat.* 1933;53(3):349-375.

119. Seidl W, Schulze M, Steding G, Kluth D. A few remarks on the physiology of the chick embryo heart (Gallus gallus). *Folia morphologica.* 1981;29(3):237-242.

120. de Jong F, Opthof T, Wilde AA, Janse MJ, Charles R, Lamers WH, Moorman AF. Persisting zones of slow impulse conduction in developing chicken hearts. *Circ Res.* 1992;71(2):240-250.

121. Lieberman M, Paes de Carvalho A. Effect of locally applied acetylcholine on the embryonic cardiac action potential. *Experientia.* 1967;23(7):539-540.

122. Gourdie RG, Harris BS, Bond J, Justus C, Hewett KW, O'Brien TX, Thompson RP, Sedmera D. Development of the cardiac pacemaking and conduction system. *Birth Defects Res C Embryo Today.* 2003;69(1):46-57.

123. Robb JS. The elemental character of embryonic electrocardiograms. *Am J Physiol.* 1929;90:496.

124. Galper JB, Smith TW. Properties of muscarinic acetylcholine receptors in heart cell cultures. *Proc Natl Acad Sci USA.* 1978;75(12):5831-5835.

125. Sperelakis N, Pappano AJ. Physiology and pharmacology of developing heart cells. *Pharmacol Ther.* 1983;22(1):1-39.

126. Oosthoek PW, Virágh S, Mayen AE, van Kempen MJ, Lamers WH, Moorman AF. Immunohistochemical delineation of the conduction system. I: The sinoatrial node. *Circ Res.* 1993;73(3):473-481.

127. Boucek RJ, Murphy WP, Paff GH. Electrical and mechanical properties of chick embryo heart chambers. *Circ Res.* 1959;7:787-793.

128. Paff GH, Boucek RJ, KLOPFENSTEIN HS. Exeprimental heart-block in the chick embryo *Anat Rec.* 1964;149:217-223.

129. Van Mierop LH. Location of pacemaker in chick embryo heart at the time of initiation of heartbeat. *Am J Physiol.* 1967;212(2):407-415.

130. Clemo HF, Belardinelli L. Effect of adenosine on atrioventricular conduction. I: Site and characterization of adenosine action in the guinea pig atrioventricular node. *Circ Res.* 1986;59(4):427-436.

131. Alcoléa S, Théveniau-Ruissy M, Jarry-Guichard T, Marics I, Tzouanacou E, Chauvin JP, Briand JP, Moorman AF, Lamers WH, Gros DB. Downregulation of connexin 45 gene products during mouse heart development. *Circ Res.* 1999;84(12):1365-1379.

132. Meijler FL, Janse MJ. Morphology and electrophysiology of the mammalian atrioventricular node. *Physiol Rev.* 1988;68(2):608-647.

133. Zipes DP, Mendez C, Moe GK. Evidence for summation and voltage dependency in rabbit atrioventricular nodal fibers. *Circ Res.* 1973;32(2):170-177.

134. Zipes DP, Mendez C, Moe GK. Evidence for summation and voltage dependancy in rabbit atrioventricular nodal fibers. *Circ Res.* 1973;32:170-177.

135. Josephson ME. *Clinical Cardiac Electrophysiology*. 2nd. ed: Williams&Wilkins; 1992:181-224.

136. Walls EW. The development of the specialized conducting tissue of the human heart. *J Anat.* 1947;81(Pt 1):93-110.116.

137. Field EJ. The development of the conducting system in the heart of sheep. *Br Heart J.* 1951;13(2):129-147.

138. Muir AR. The development of the ventricular part of the conducting tissue in the heart of the sheep. *J Anat.* 1954;88(3):381-391.

139. Navaratnam V. Development of the nerve supply to the human heart. *Br Heart J.* 1965;27(5):640-650.

140. Watanabe Y, Dreifus LS. Sites of impulse formation within the atrioventricular junction of the rabbit. *Circ Res.* 1968;22(6):717-727.

141. Dobrzynski H, Nikolski VP, Sambelashvili AT, Greener ID, Yamamoto M, Boyett MR, Efimov IR. Site of origin and molecular substrate of atrioventricular junctional rhythm in the rabbit heart. *Circ Res.* 2003;93(11):1102-1110.

142. Hucker WJ, Sharma V, Nikolski VP, Efimov IR. Atrioventricular conduction with and without AV nodal delay: two pathways to the bundle of His in the rabbit heart. *Am J Physiol Heart Circ Physiol.* 2007;293(2):H1122-1130.

143. Li J, Greener ID, Inada S, Nikolski VP, Yamamoto M, Hancox JC, Zhang H, Billeter R, Efimov IR, Dobrzynski H, Boyett MR. Computer three-dimensional reconstruction of the atrioventricular node. *Circ Res.* 2008;102(8):975-985.

144. Matsushita T, Chun S, Sung RJ. Influence of isoproterenol on the accelerated junctional rhythm observed during radiofrequency catheter ablation of atrioventricular nodal slow pathway conduction. *Am Heart J.* 2001;142(4):664-668.

145. Thakur RK, Klein GJ, Yee R, Stites HW. Junctional tachycardia: a useful marker during radiofrequency ablation for atrioventricular node reentrant tachycardia. *J Am Coll Cardiol.* 1993;22(6):1706-1710.

146. Thibault B, de Bakker JM, Hocini M, Loh P, Wittkampf FH, Janse MJ. Origin of heat-induced accelerated junctional rhythm. *J Cardiovasc Electrophysiol.* 1998;9(6):631-641.

147. Petrecca K, Shrier A. Spatial distribution of nerve processes and beta-adrenoreceptors in the rat atrioventricular node. *J Anat.* 1998;192 (Pt 4):517-528.

148. Schauerte P, Mischke K, Plisiene J, Waldmann M, Zarse M, Stellbrink C, Schimpf T, Knackstedt C, Sinha A, Hanrath P. Catheter stimulation of cardiac parasympathetic nerves in humans: a novel approach to the cardiac autonomic nervous system. *Circulation.* 2001;104(20):2430-2435.

149. Mazgalev TN, Ho SY, Anderson RH. Anatomic-electrophysiological correlations concerning the pathways for atrioventricular conduction. *Circulation.* 2001;103(22):2660-2667.

150. Blaufox AD, Saul JP. Influences on fast and slow pathway conduction in children: does the definition of dual atrioventricular node physiology need to be changed? *J Cardiovasc Electrophysiol.* 2002;13(3):210-211.

151. Van Hare GF. Developmental aspects of atrioventricular node reentry tachycardia. *J Electrocardiol.* 2008.

152. Mines GR. On functional analysis by the action of electrolytes. *J Physiol* 1913;46(3):188-235.

153. Rosenblueth A. Ventricular echoes. *Am J Physiol.* 1958;195(1):53-60.

154. Scherf D, Schookhoof, C. Reizleitungsstorungen im Bundel. *Mitteilung Wien Arch Inn Med.* 1926;11(425).

155. Schuilenburg RM, Durrer D. Atrial echo beats in the human heart elecited by induced atrial premature beats. *Circulation.* 1968;37(5):680-693.

156. Moe GK, Preston JB, Burlington H. Physiologic evidence for a dual A-V transmission system. *Circ Res.* 1956;4(4):357-375.

157. Denes P, Wu D, Dhingra RC, Chuquimia R, Rosen KM. Demonstration of dual A-V nodal pathways in patients with paroxysmal supraventricular tachycardia. *Circulation.* 1973;48(3):549-555.

158. Rosen KM, Mehta A, Miller RA. Demonstration of dual atrioventricular nodal pathways in man. *Am J Cardiol.* 1974;33(2):291-294.

159. Sung RJ, Waxman HL, Saksena S, Juma Z. Sequence of retrograde atrial activation in patients with dual atrioventricular nodal pathways. *Circulation.* 1981;64(5):1059-1067.

160. McGuire MA, Janse MJ, Ross DL. "AV nodal" reentry: Part II: AV nodal, AV junctional, or atrionodal reentry? *J Cardiovasc Electrophysiol.* 1993;4(5):573-586.

161. Janse MJ, van Capelle FJ, Freud GE, Durrer D. Circus movement within the AV node as a basis for supraventricular tachycardia as shown by multiple microelectrode recording in the isolated rabbit heart. *Circ Res.* 1971;28(4):403-414.

162. Wallace AG, Mignone RJ. Physiologic evidence concerning the re-entry hypothesis for ectopic beats. *Am Heart J.* 1966;72(1):60-70.

163. Iinuma H, Dreifus LS, Mazgalev T, Price R, Michelson EL. Role of the perinodal region in atrioventricular nodal reentry: evidence in an isolated rabbit heart preparation. *J Am Coll Cardiol.* 1983;2(3):465-473.

164. Mazgalev T, Dreifus LS, Bianchi J, Michelson EL. The mechanism of AV junctional reentry: role of the atrionodal junction. *Anat Rec.* 1981;201(1):179-188.

165. Mendez C, Han J, Garciadejalon PD. Some characteristics of ventricular echoes. *Circ Res.* 1965;16:562-581.

166. Wit AL, Hoffman BF, Cranefield PF. Slow conduction, reentry, and the mechanism of ventricular arrhythmias in myocardial infarction. *Bulletin of the New York Academy of Medicine.* 1971;47(10):1233-1234.

167. Josephson ME, Miller JM. Atrioventricular nodal reentry: evidence supporting an intranodal location. *PACE.* 1993;16(3 Pt 2):599-614.

168. Cox JL, Holman WL, Cain ME. Cryosurgical treatment of atrioventricular node reentrant tachycardia. *Circulation.* 1987;76(6):1329-1336.

169. Guiraudon GM, Klein GJ, van Hemel N, Guiraudon CM, Yee R, Vermeulen FE. Anatomically guided surgery to the AV node. AV nodal skeletonization: experience in 46 patients with AV nodal reentrant tachycardia. *Eur J of Cardio Thorac Surg.* 1990;4(9):461-464; discussion 464-465.

170. Haissaguerre M, Gaita F, Fischer B, Commenges D, Montserrat P, d'Ivernois C, Lemetayer P, Warin JF. Elimination of atrioventricular nodal reentrant tachycardia using discrete slow potentials to guide application of radiofrequency energy. *Circulation.* 1992;85(6):2162-2175.

171. Ross DL, Johnson DC, Denniss AR, Cooper MJ, Richards DA, Uther JB. Curative surgery for atrioventricular junctional ("AV nodal") reentrant tachycardia. *J Am Coll Cardiol.* 1985;6(6):1383-1392.

172. Medkour D, Becker AE, Khalife K, Billette J. Anatomic and functional characteristics of a slow posterior AV nodal pathway: role in dual-pathway physiology and reentry. *Circulation.* 1998;98(2):164-174.

173. Cohen MI, Wieand TS, Rhodes LA, Vetter VL. Electrophysiologic properties of the atrioventricular node in pediatric patients. *J Am Coll Cardiol.* 1997;29(2):403-407.

174. Lin MH, Young ML, Wu JM, Wolff GS. Developmental changes of atrioventricular nodal recovery properties. *Am J Cardiol.* 1997;80(9):1178-1182.

175. Blaufox AD, Rhodes JF, Fishberger SB. Age related changes in dual AV nodal physiology. *PACE.* 2000;23(4 Pt 1):477-480.

176. D'Este D, Bertaglia E, Zanocco A, Reimers B, Pascotto P. Electrophysiological properties of the atrioventricular node and ageing: evidence of a lower incidence of dual nodal pathways in the elderly. *Europace* 2001;3(3):216-220.

177. Waki K, Kim JS, Becker AE. Morphology of the human atrioventricular node is age dependent: a feature of potential clinical significance. *J Cardiovasc Electrophysiol.* 2000;11(10):1144-1151.

178. Blurton DJ, Dubin AM, Chiesa NA, Van Hare GF, Collins KK. Characterizing dual atrioventricular nodal physiology in pediatric patients with atrioventricular nodal reentrant tachycardia. *J Cardiovasc Electrophysiol.* 2006;17(6):638-644.

179. Maguire CT, Bevilacqua LM, Wakimoto H, Gehrmann J, Berul CI. Maturational atrioventricular nodal physiology in the mouse. *J Cardiovasc Electrophysiol.* 2000;11(5):557-564.

180. Goldreyer BN, Bigger JT. Site of reentry in paroxysmal supraventricular tachycardia in man. *Circulation.* 1971;43(1):15-26.

181. Van Hare GF, Chiesa NA, Campbell RM, Kanter RJ, Cecchin F, Society PE. Atrioventricular nodal reentrant tachycardia in children: effect of slow pathway ablation on fast pathway function. *J Cardiovasc Electrophysiol.* 2002;13(3):203-209.

182. Chen SA, Lee SH, Wu TJ, Chiang CE, Cheng CC, Tai CT, Chiou CW, Ueng KC, Wen ZC, Chang MS. Initial onset of accessory pathway-mediated and atrioventricular node reentrant tachycardia after age 65: clinical features, electrophysiologic characteristics, and possible facilitating factors. *J Am Geriatr Soc.* 1995;43(12):1370-1377.

183. Kalusche D, Ott P, Arentz T, Stockinger J, Betz P, Roskamm H. AV nodal re-entry tachycardia in elderly patients: clinical presentation and results of radiofrequency catheter ablation therapy. *Coron Artery Dis.* 1998;9(6):359-363.

184. Rodriguez LM, de Chillou C, Schläpfer J, Metzger J, Baiyan X, van den Dool A, Smeets JL, Wellens HJ. Age at onset and gender of patients with different types of supraventricular tachycardias. *Am J Cardiol.* 1992;70(13):1213-1215.

185. Saba S, Zhu W, Aronovitz MJ, Estes NA, Wang PJ, Mendelsohn ME, Karas RH. Effects of estrogen on cardiac electrophysiology in female mice. *J Cardiovasc Electrophysiol.* 2002;13(3):276-280.

186. Rosano GM, Leonardo F, Sarrel PM, Beale CM, De Luca F, Collins P. Cyclical variation in paroxysmal supraventricular tachycardia in women. *Lancet.* 1996;347(9004):786-788.

187. Liuba I, Jönsson A, Säfström K, Walfridsson H. Gender-related differences in patients with atrioventricular nodal reentry tachycardia. *Am J Cardiol.* 2006;97(3):384-388.

188. Stein RA, Goldsmith R. Cardiovascular exercise and wellness. Exercise training for cardiac rehabilitation patients: meeting the challenges of the millennium. *Prev Cardiol.* 2002;3(2):59-62.

189. Casta A, Wolff GS, Mehta AV, Tamer D, Garcia OL, Pickoff AS, Ferrer PL, Sung RJ, Gelband H. Dual atrioventricular nodal pathways: a benign finding in arrhythmia-free children with heart disease. *Am J Cardiol.* 1980;46(6):1013-1018.

190. Berul CI. Electrophysiological phenotyping in genetically engineered mice. *Physiol Genomics.* 2003;13(3):207-216.

191. Rentschler S, Vaidya DM, Tamaddon H, Degenhardt K, Sassoon D, Morley GE, Jalife J, Fishman GI. Visualization and functional characterization of the developing murine cardiac conduction system. *Development.* 2001;128(10):1785-1792.

Chapter 7

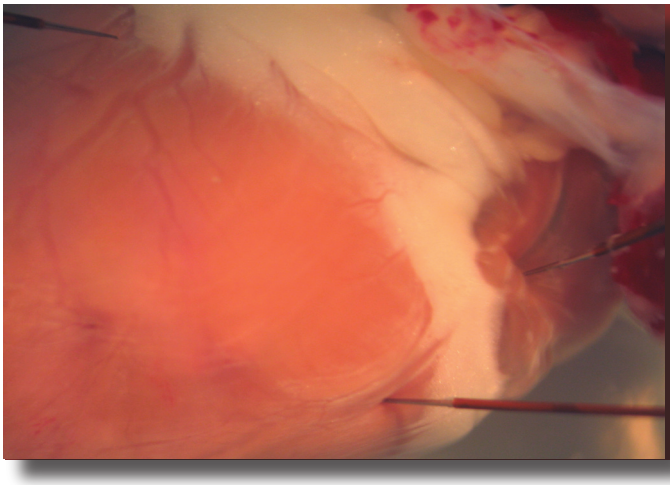

Denise P. Kolditz[1,2]
Rebecca Vicente-Steijn[1,2]
Daniel A. Pijnappels[1]
Monique R.M. Jongbloed[1,2]
Robert E. Poelmann[2]
Martin J. Schalij[1]
Adriana C. Gittenberger-de Groot[2]

[1]Department of Cardiology, Leiden University Medical Center, Leiden, The Netherlands
[2]Department of Anatomy and Embryology, Leiden University Medical Center, Leiden, The Netherlands

Development of the Atrioventricular Node from Heterogeneous Primordia: Implications for the Anatomical Correlate of the Slow Pathway

Submitted

Abstract

Background. While the electrophysiological substrate causing atrioventricular (AV) nodal reentrant tachycardia (AVNRT) is well known, the anatomical boundaries and developmental origin of the AV node (AVN) remains a subject of debate. We hypothesized that the myocardium surrounding the proximal part of the left cardinal vein (LCV) contributes to the developing AVN region.

Methods and Results. Isolated embryonic hearts of the Japanese quail (HH19-36, n=28) and white leghorn chick (HH19-36, n=36) were stained with Periodic-Acid-Schiff (PAS), anti-MLC2a, anti-Nkx2.5, anti-Nav1.5 and anti-Cx43. Morphology of the developing AVN was correlated to spatiotemporal changes in atrial activation sequences (HH20-30, n=96). At HH19, a MLC2a positive and Nkx2.5 negative region, expressing low levels of glycogen, Cx43 and Nav1.5, was distinguished surrounding the proximal part of the left cardinal vein (LCV) entering the sinus venosus (SV). An identical Nkx2.5 negative structure was found around HH22 surrounding the right cardinal vein (RCV) (sinoatrial node region). Around HH29-31, the LCV was transposed to the right to eventually become the coronary sinus (CS), while the myocardium surrounding the proximal LCV became positioned around the CS-ostium (AVN region). While in the majority of hearts right atrial (RA) activation preceded left atrial (LA) activation, dominant pacemaking originating in the LA could still be found until late developmental stages (until HH30).

Conclusions. The LCV tissues provide an important functional contribution to the AVN Anlagen. Based on the spatial relation of the embryonic LCV tissues and the adult AVN region, we furthermore postulate that the LCV myocardium contributes to formation of the slow pathway region of the AVN.

Introduction

Atrioventricular (AV) nodal reentrant tachycardia (AVNRT) is the most common (> 80%) supraventricular tachycardia (SVT) in adults,[1] yet it accounts for less than 5% of SVT cases in infants and toddlers and for only 13-16% of SVTs in children and adolescents.[2] Although currently the vast majority (>90%) of patients with AVNRT are cured by radiofrequency (RF) catheter ablation procedures targeting the slow (α) pathway of the AVN,[3] the anatomical boundaries of the electrophysiologically distinct slow (α) and fast (β) AVN pathways as substrates for AVNRT have still remained a conundrum in this confusing field.

Moreover, the ontogenic development of the AVN region has, since the first detailed report on the specialized AVN in the monumental monograph of Sunao Tawara in 1906, been studied for over a 100 years now.[4] In the earliest literature on AVN development, an ontogenic origin in the musculature of the AV ring myocardium, either as a remnant[5] or as a new supraventricular growth structure,[6] has most consistently been reported. Furthermore, the myocardium of the common atrium[7] and of the left sinus horn has also long been suggested to provide a candidate precursor population for the adult AVN,[8, 9] while an origin in the four myocardial rings of specialized tissue has been extensively debated as well.[10-15]

Later on, several morphological studies in the embryonic human, calf, ferret and rat heart identified two distinct collections of tissue in the developing AVN region,[7, 15] which were suggested to fuse or oppose at the final stages of cardiac septation enclosing an intermediate block of specialized conducting tissue.[10] In the debate of the 20th century, these competing theories based on observations in different species complicated by the use of variable terminology for identification and non-specific staining, have still failed to provide a definitive resolution on this subject.

Contemporary marker studies demonstrating expression patterns of multiple signaling and transcription factors implicated in the induction, maturation and patterning of the cardiac conduction system (CCS)–e.g. Nkx 2.5, Shox-2, podoplanin, Id-2, HNK-1, Leu-7, PSA-NCAM, CCS-LacZ and minK-LacZ[13-21]-have linked the myocardium of the sinus venosus (SV) (derived from the second heart field) to the developing CCS. In this study we aimed to combine previously established concepts on AVN development with new experiments to obtain more insight into the structure-function relationships of the developing AVN region in relation to arrhythmia etiology. We hypothesized that the

proximal part of the myocardial LCV tissues (the structural counterpart of the sinoatrial nodal primordial tissues surrounding the RCV) provides an important contribution to the developing AVN region. By analyzing spatiotemporal changes in atrial activation sequences in the embryonic avian heart and by correlating the electrophysiological data with morphology, we provide a new concept of AVN development in which the (heterogeneous) AVN is derived from both the AV ring myocardium, primary ring myocardium and the sinoatrial (SA) ring myocardium and receives an additional contribution from a population of cells originating from the LCV myocardium.

Methods

Experimental Preparations

All animal experiments were approved by the Committee on Animal Welfare of the Leiden University Medical Center (LUMC),Leiden, the Netherlands. Animal experiments were conducted in compliance with the Guide for the Care and Use of Laboratory Animals (NIH Publication No.85-23, revised 1996). Fertilized eggs of the Japanese quail (*Coturnix coturnix japonica*, Leiden University Medical Center, The Netherlands) and white leghorn chick (*Gallus domesticus*) were incubated blunt end up at 37.5°C and 80% humidity and staged according to the Hamburger-Hamilton(HH) criteria.[22]

Ex-Ovo Extracellular Electrogram Recordings

Extracellular electrograms were recorded at HH20-30 in wildtype embryonic chick (n=63) and quail (n=33) hearts (group A, HH20-30, n=37;group B, HH24-27, n=38;group C, HH28-30, n=21). The experimental preparations were positioned in a custom-built, fluid-heated, temperature-controlled tissue bath and superfused with carbogenated (95% O_2 and 5% CO_2) Tyrode's solution (30±0.1°C) with the following composition (mmol/l): NaCl 130, KCl 4, KH_2PO_4 1.2, $MgSO_4$ 0.6, $NaHCO_3$ 20, $CaCl_2$ 1.5, glucose 10(pH 7.35).

Unipolar extracellular electrograms were subsequently recorded, as previously described,[23] by positioning 3 tungsten recording electrodes (tip:1-2 μm; impedance 0.5-1.0MΩ,WPI Inc., Berlin, Germany) on respectively the left atrium (LA), right atrium (RA) and left ventricular apex (LVA)(**Figure 1**). A reference electrode was placed in the tissue bath.

The experimental preparations were allowed to equilibrate for 10 minutes before starting the recording protocol. Recordings in embryonic hearts with a spontaneous heart rate (HR) of < 60bpm were considered non-physiological and excluded from the present study.

Definitions, immunohistochemistry and statistical analysis are described in detail in the online-only data supplement. The authors had full access to and take responsibility for the integrity of the data. All authors have read and agree to the manuscript as written.

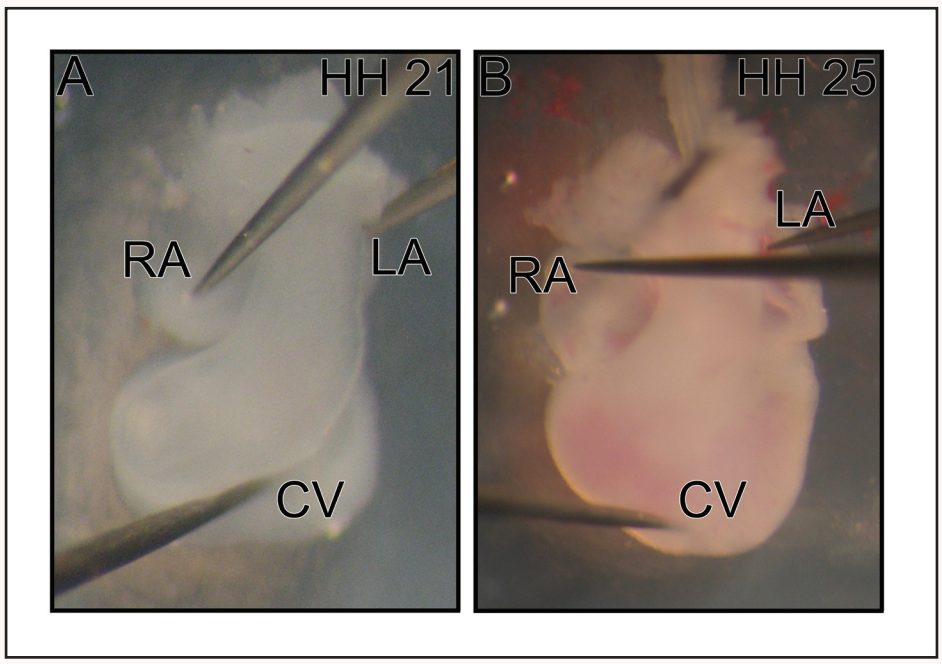

Figure 1. A representative HH21 and HH25 chick heart showing recording electrode placement on the LA, RA, and LVA. OFT=outflow tract,LA=left atrium,RA=right atrium,CV=common ventricle.

Results

Ex-Ovo Electrogram Recordings

In 63 chicken and 33 quail hearts (HH20-30) *ex-ovo* local electrocardiograms were recorded during stable sinus rhythm of 171±52bpm(AV interval 88±17ms) and 170±42bpm(AV interval 82±12ms), respectively. Since the mean HR and AV intervals were similar in chicken and quail hearts (p=0.339 and p=0.074, respectively), these data are used interchangeably. In line with our previous data,[23] these pre-septated avian hearts all demonstrated a base-to-apex ventricular activation pattern.

Spatiotemporal Changes in Atrial Activation Sequences During Cardiogenesis

Extracellular electrogram recordings demonstrated a high level of variability in atrial activation sequences at consecutive developmental stages. While in the majority (54%; 20/37) of hearts in group A (HH20-23, n=37) RA activation preceded LA activation, a relatively large number (35%; 13/37) of hearts demonstrated dominant pacemaker potentials originating in the high LA, indicating a left-sided dominant pacemaker (**Figure 2**).

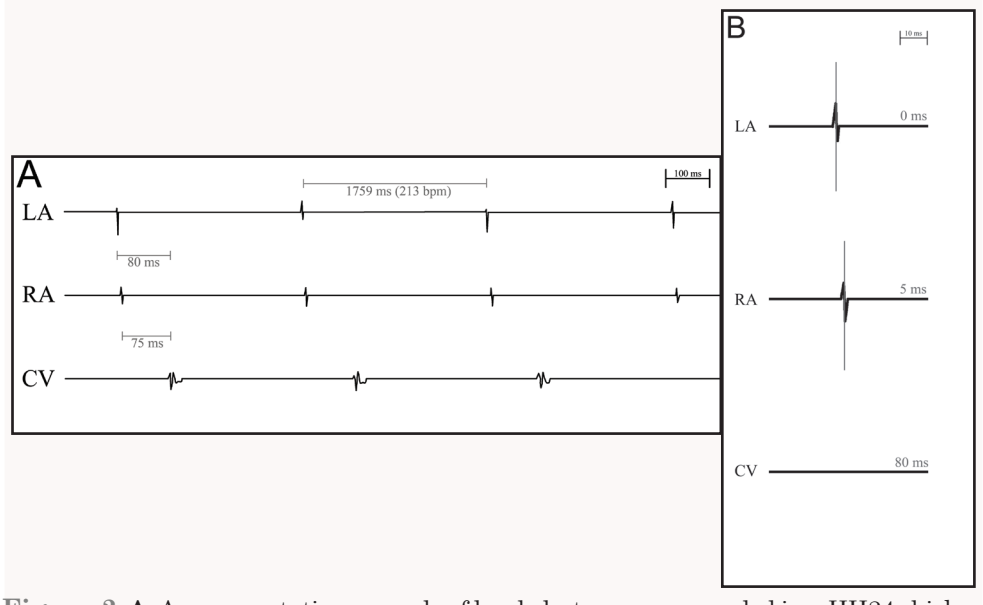

Figure 2. **A.** A representative example of local electrograms recorded in a HH24 chicken heart, demonstrating pacemaking dominance in the LA. **B.** Magnification.

Left atrial activation preceding RA activation, was also still found in 21% (8/38) of group B hearts (HH24-27, n=38), while in only 5% (1/21) of the hearts in group C (HH28-30, n=21) earliest atrial activation was found in the LA. Additionally, concurrent activation (time difference <1ms) of the RA and LA was found in 11% (4/37) of heart in group A, 19% (7/38) of hearts in group B and 14% (3/21) of hearts in group C. There was no difference (p=0.412) in AV interval in embryonic hearts with a left-sided pacemaker (n=22; 84±10 ms) versus hearts with a right-sided pacemaker (n=60; 82±12ms)(**Table 1**).

Developmental Stage,HH	n	HR,bpm,mean±SD(range)	AV-interval,ms, mean±SD (range)	LA	RA	LA=RA
Group A	37	162±38(77-228)	79±8(68-105)	13(35%)	20(54%)	4(11%)
HH20	6	164±50(77-222)	80±9(69-93)	1	5	0
HH21	11	155±36(105-209)	80±10(68-105)	3	7	1
HH22	11	156±38(110-210)	78±7(68-86)	3	6	2
HH23	9	177±32(135-228)	80±8(68-88)	6	2	1
Group B	38	169±36(84-238)	83±11(60-107)	8(21%)	23(61%)	7(18%)
HH24	10	176±35(106-238)	81±8(69-91)	1	6	3
HH25	7	164±26(115-198)	83±13(69-100)	1	4	2
HH26	12	176±35(99-211)	83±11(64-105)	4	7	1
HH27	9	155±47(84-221)	86±15(60-107)	2	6	1
Group C	21	190±54(128-297)	87±15(66-122)	1(5%)	17(81%)	3(14%)
HH28	4	167±17(146-186)	88±11(72-98)	1	2	1
HH29	8	163±30(128-204)	86±16(67-112)	0	6	2
HH30	9	225±64(144-297)	86±16(66-122)	0	9	0
Total	96	171±42(77-297)	83±11(60-122)	22(23%)	60(62%)	14(15%)

Table 1. Developmental stages of avian hearts form groups A, B and C, with corresponding HRs,AV-intervals and atrial activation sequences.

Immunohistochemical Analysis of the Developing CCS

HH19-25 (~3-5 days of incubation)

Structurally, at HH19 the linear heart tube was still in the midst of its looping phase and the common atrium and AV ring were positioned above the primitive left ventricle (LV), while the outflow tract was situated above the primitive right ventricle (RV). The interatrial septum (IAS) was still forming, while formation of the primitive interventricular septum (IVS) was just initiated. The S-shaped heart tube consisted of several segments: the bilateral sinus horns (the myocardial parts of the cardinal veins (CV)) draining caudodorsally into the developing sinus venosus (SV), the common atrium and the ventricular inlet and outlet segment. These segments were divided by so-called transitional zones (described below), which will be brought together in the inner curvature of the heart by the ongoing looping process.[14, 15]

At HH19, the common atrium, AV ring and primitive ventricle showed expression of MLC2a, nuclear localized Nkx2.5, Nav1.5 and Cx43 and were characterized by a high glycogen content (PAS staining). Interestingly, a distinct MLC2a positive but Nkx2.5 negative region could be distinguished surrounding the proximal myocardial part of the left cardinal vein (LCV)(**Figure 3,4**). Around HH22, an identical structure was found in the anterolateral wall of the proximal right cardinal vein (RCV)(the future sinoatrial node (SAN) region)(**Figure 3,4**).

These bilateral myocardial CV regions were further characterized by a relatively low level of Nav1.5 (**Figure 3E,F&K,L**) and Cx43 (**Figure 4E&J**) expression and a relatively low level of glycogen (**Figure 3D&J, 4D&I**) compared to the staining pattern in the neighboring common atrial and primitive ventricular myocardium. In the RCV region, Nav1.5 expression was primarily located in the circular periphery, while the central parts of these tissues demonstrated lower expression levels of Nav1.5 (**Figure 3E,F&K,L**).

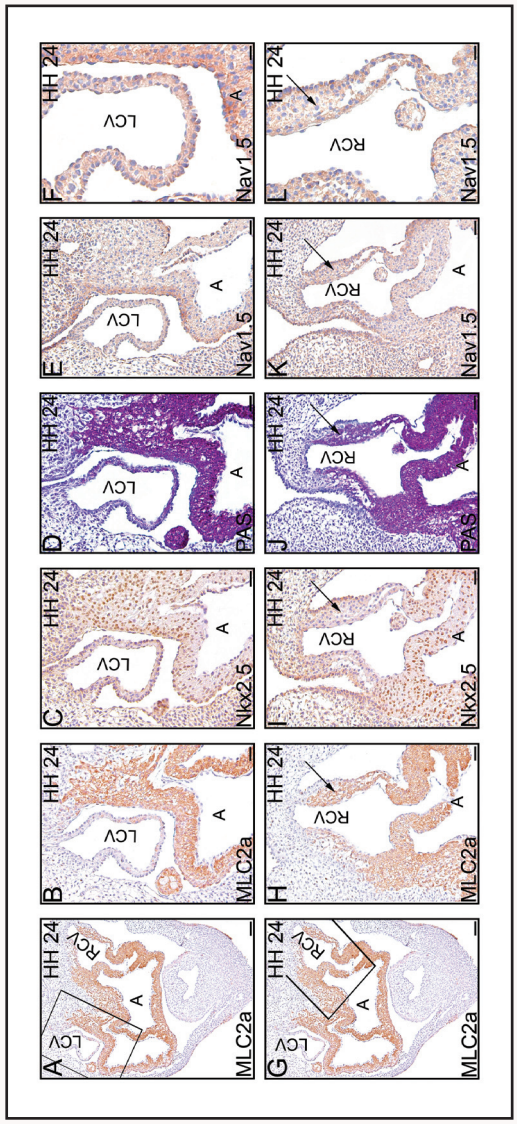

Figure 3. Morphological findings in a representative HH24 quail heart. A. Dorsal view of frontal MLC2a section at the LCV level. Bar=600µm. **B.** Magnification of the LCV region. Bar=50µm. **C.** Nkx2.5 staining in the LCV. Bar=50µm. **D.** PAS staining in the LSH. Bar=50µm. **E.** Nav1.5. staining in the LCV.Bar=50µm. **F.** Magnification of Nav1.5 staining in the LCV region. Bar=30µm. **G.**Dorsal view of frontal MLC2a section at the SAN level (arrow). Bar=600µm. **H.** Magnification of the SAN region. Bar=50µm. **I.** Nkx2.5 staining in the SAN. Bar=50µm. **J.** PAS staining in the SAN. Bar=50µm. **K.** Nav1.5 staining in the SAN.Bar=50µm. **L.** Magnification of Nav1.5 staining in the SAN region.Bar=30µm. LCV=left cardinal vein,RCV=right cardinal vein,A=atrium.

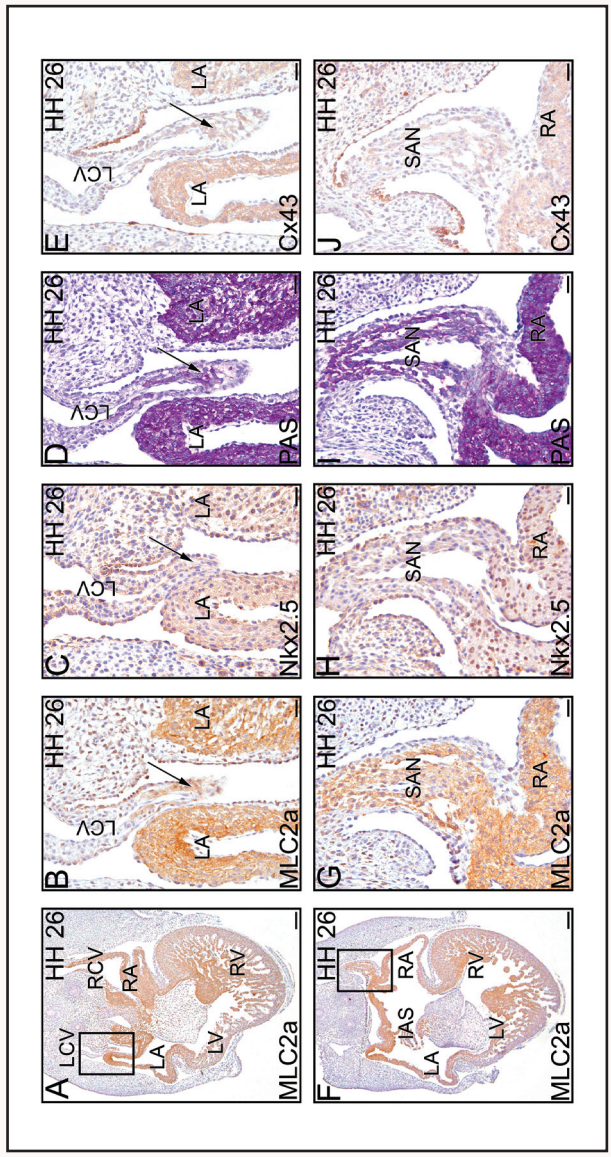

Figure 4. Morphological findings in a representative HH26 quail heart. A. Dorsal view of frontal MLC2a section at the LCV level. Bar=600μm. **B**. Magnification of the LCV. Bar=50μm. **C.** Nkx2.5 staining in the LCV. Bar=50μm. **D**. PAS staining in the LCV. Bar=50μm. **E.** Cx43 staining in the LCV.Bar=50μm. **F** .Dorsal view of frontal MLC2a section of the SAN level. Bar=600μm. **G.** Magnification of the SAN. Bar=50μm.**H.** Nkx2.5 staining in the SAN. Bar=50 μm. **I.** PAS staining in the SAN. Bar=50μm. **J**. Cx43 staining in the SAN.Bar=50μm. LCV=left cardinal vein,RCV=right cardinal vein,LA=left atrium, RA=right atrium,LV=left ventricle,RV=right ventricle,SAN=sinoatrial node.

HH26–30(~5-7 days of incubation)

Around HH26, the now septated RA and LA became positioned above the RV and LV, respectively and the external shape of a four chambered heart became visible, while the IVS had still not fused. From around HH28 onwards, outgrowth of the RA myocardium was initiated and the still mainly left-sided SV and LCV were transposed to the right to become submerged in the RA (**Figure 5,6**), running through the dorsal mesocardium and myocardialized spina vestibulum to the base of the IAS to become the CS at the crux of the heart (adult AVN region). Around HH29 the developing IVS started to approach the AV cushions and formation of the compact myocardium became evident (*data not shown*).

At this stage, the SAN and the LCV tissues were still Nkx2.5 negative and the Cx43, Nav1.5 and glycogen expression levels were still relatively low (**Figure 5**). Connexin43 expression was now primarily present in the atrial and ventricular myocardium with a predisposition for the endomyocardial trabecular surface, while expression in the AV ring was slightly less intense compared to the surrounding myocardium.

HH31–36 (~7–10 days of incubation)

From HH31 onwards, Nkx2.5 expression became more nonuniformely and nuclear localized Nkx2.5 expression was clearly higher in the atrial myocardium versus ventricular myocardium, while even more intense Nkx2.5 staining was present in the AV ring, the IVS and on the endomyocardial surface of the ventricular trabeculae (**Figure 7**). Around HH32, formation of the isolating annulus fibrosis was initiated with incorporation of the Nkx2.5 positive AV ring myocardium in the lower atrial rim. By the end of HH33 ventricular septation was completed (*data not shown*).

A
HH 33
LCV
LA
RCV
RA
LV
RV
MLC2a
B
HH 33
SAN
RCV
A
MLC2a
C
HH 33
SAN
RCV
A
Nkx2.5
D
HH 33
SAN
RCV
A
PAS
E
HH 33
SAN
RCV
A
Nav1.5
F
HH 33
SAN
RCV
A
Cx43
G
HH 33
LCV
LA
RA
LV
RV
MLC2a
H
HH 33
LCV
LA
LV
MLC2a
I
HH 33
LCV
LA
LV
Nkx2.5
J
HH 33
LCV
LA
PAS
K
HH 33
LCV
LV
Nav1.5
L
HH 33
LCV
LV
Cx43

Figure 5. (page 271) **Ventral view of frontal section of the rightward migrated LCV submerged in the RA to become the CS in a HH33 quail heart, in which the Nkx2.5 nuclear negative myocardial tissue is stretched from the LCV through the dorsal mesocardium and spina vestibulum to the crux of the heart (AVN region)**. **A**.Dorsal view of frontal MLC2a section at the level of the SAN.Bar=600µm. **B.** Magnification.Bar= 50µm. **C.** Adjacent Nkx2.5 section, demonstrating nuclear Nkx2.5 negativity in the SAN.Bar= 50µm. **D.** Adjacent PAS section:relatively low levels of glycogen in the SAN. Bar= 50µm. **E.** Adjacent Nav1.5 section:relatively low levels of Nav1.5 in the SAN.Bar= 50µm.**F.** Adjacent Cx43 section: relatively low levels in the SAN.Bar= 50µm. **G.** Ventral view of frontal MLC2a section at the level of the LCV and SV entering the RA.Bar=600µm. **H.** Magnification.Bar= 50µm. **I.** Adjacent Nkx2.5 section, demonstrating Nkx2.5 nuclear negativity in the LCV tissues.Bar= 50µm. **J.** Adjacent PAS section:relatively low glycogen levels in the LCV and SV tissues. **K.** Adjacent Nav1.5 section:relatively low Nav1.5 levels in the LCV tissues.Bar= 50µm. **L.** Adjacent Cx43 section:relatively low Cx43 levels in the LCV tissues. Bar=50 µm. LCV=left cardinal vein,RCV=right cardinal vein,LA=left atrium, RA=right atrium,LV=left ventricle,RV=right ventricle,SAN=sinoatrial node.

Immunohistochemical Expression Patterns in the Transitional Zones (Figure 7, on page 275)

At HH30, a band of intense Nkx2.5 positive staining cells encircling the outflow tract (ventriculo-arterial ring) was found (A-C). The atrial myocardium demonstrated a heterogeneous expression pattern for Nkx2.5, while distinct atrial regions and the IAS (corresponding to the SA-ring tissues) stained intensely positive for Nkx2.5 (D-F). From HH30 onwards, the region of the AVN was characterized by a heterogeneous population of Nkx2.5 positive and negative cells (G-I), while the His bundle and bundle branches could easily be identified by low levels of glycogen and a heterogeneous expression of Nkx2.5 compared to the surrounding myocardium(J-O). Around HH32, an additional band of Nkx2.5 positive cells could clearly be identified surrounding the AV ring myocardium (I&L).

Immunohistochemical Correlations with Electrophysiological Data

Morphological findings largely correlated to electrophysiology. Until HH27 the LCV tissues were positioned caudodorsally to the LA and functionally a left-sided dominant pacemaker was still found in a considerable number of cases (21%). Impulse initiation in the LA could however no longer be found after HH28, perfectly correlating to the morphological observation that around HH29-30 the LCV was already submerged in the RA to become the CS.

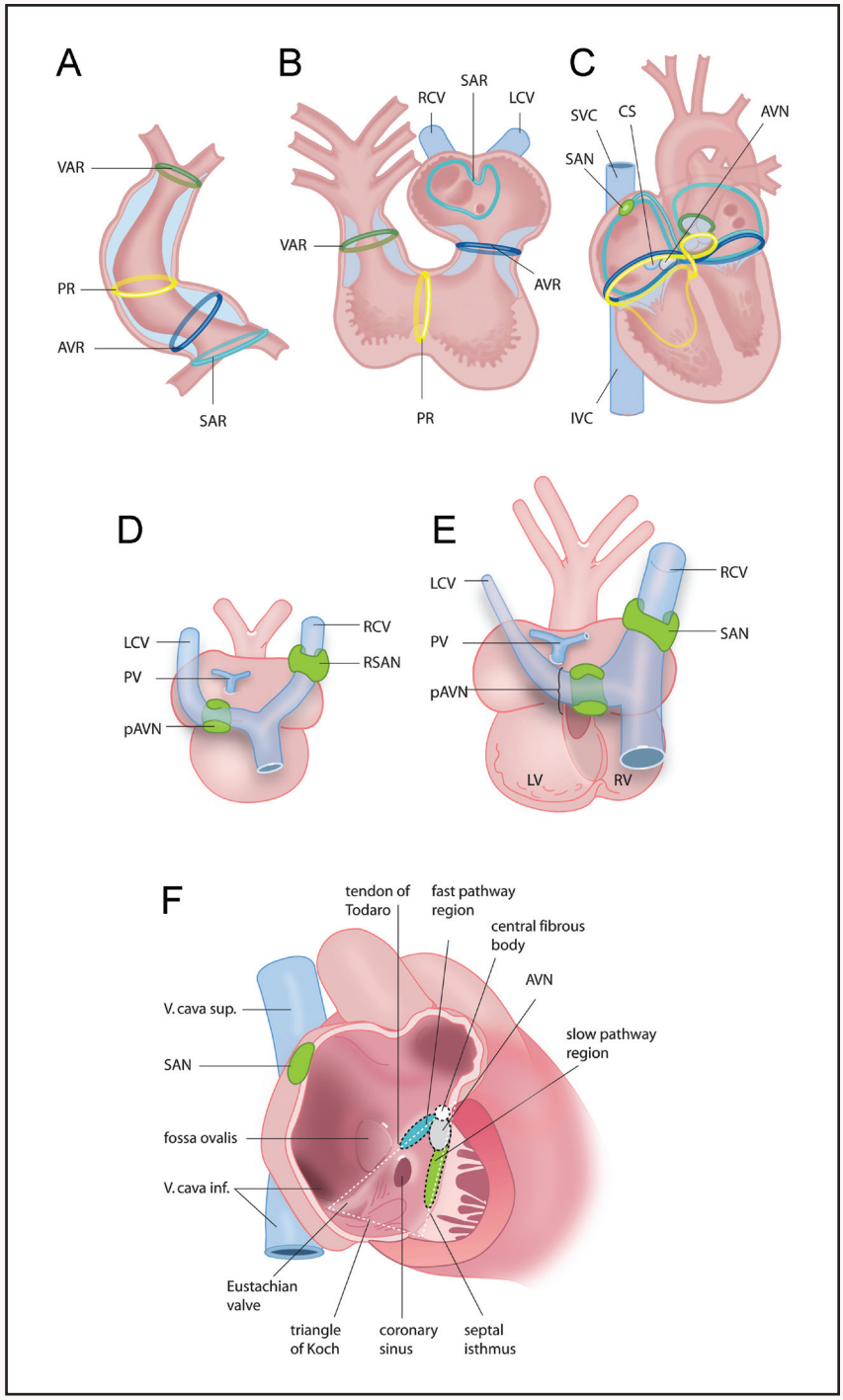
A
VAR
PR
AVR
SAR
B
RCV
SAR
LCV
VAR
AVR
PR
C
SVC
CS
AVN
SAN
IVC
D
LCV
PV
pAVN
RCV
RSAN
E
LCV
PV
pAVN
RCV
SAN
LV
RV
F
tendon of Todaro
fast pathway region
central fibrous body
AVN
slow pathway region
V. cava sup.
SAN
fossa ovalis
V. cava inf.
Eustachian valve
triangle of Koch
coronary sinus
septal isthmus

Figure 6. (above on page 273) **Schematic representation of the postulated ontogeny of the AVN. A.** During cardiogenesis the tubular heart undergoes dextral looping, which transforms the heart in a C-shape (**A**) and later in a S-shape (**B**) and finally in a four chambered heart (**C**). In the embryonic heart, the transitional zones or rings dividing the different putative chambers of the heart can be recognized, being the sinu-atrial transition (SAR), the atrioventricular ring (AVR), the primary ring (PR) and the ventriculo-arterial transition (VAR). The SAR seems to contribute to both the sinoatrial node (SAN) (green) and atrioventricular node (AVN) (green), while the AVN additionally receives a contribution from both the AVR and PR. **D**. Dorsal view of the developing avian heart around HH stage 24. A distinct MLC2a positive but Nkx2.5 negative myocardial region surrounds the proximal left cardinal vein (primordial AVN, pAVN) and right cardinal vein (right sinoatrial node, RSAN) (green). **E.** Dorsal view of the developing avian heart around HH stage 30. The distinct myocardial region surrounding the left cardinal vein (LCV) is now transposed to the right and submerged in the right atrium remaining positioned around the LCV, which is now developing into the coronary sinus (CS) at the crux of the heart in the region of the slow pathway of the AVN. The distinct myocardial tissue surrounding the right cardinal vein (RCV) remains positioned around the proximal part of the RCV (future superior vena cava) and becomes the SAN. **F.** Schematic representation of the triangle of Koch summarizing the different postulated contributions to the AVN. In green the distinct LCV tissues are positioned in the slow pathway region of the AVN and the SAN derived from the distinct RCV tissues is positioned in the upper right atrium surrounding the superior vena cava (SVC), in light blue part of the SAR tissues are positioned in the fast pathway region of the AVN, in grey the compact part of the AVN derived from the AVR and PR is depicted.

Figure 7. (right, page 275) **Expression patterns in the transitional zones of the quail heart. A.** Dorsal view of frontal section of a HH30 heart, demonstrating part of the Nkx2.5 positive truncobulbar ring surrounding the outflow tract.Bar=600µm. **B.** Magnification of the OFT region.Bar=200 µm. **C.** Adjacent section demonstrating low levels of PAS staining in the specialized ring tissues. Bar=200µm **D.** Frontal section of a HH26 heart demonstrating Nkx2.5 heterogeneity in the atrial myocardium (asterisks) and intense Nkx2.5 staining in the IAS (arrow).Bar=600µm. **E.** Magnification of the IAS. Bar=200µm. **F.** Magnification at the level of the intensely positive Nkx2.5 AV-ring tissues. Bar=200µm. **G.**Frontal MLC2a stained section at the AVN region of a HH30 quail heart. Bar=600µm. **H**. Magnification.Bar=50µm. **I.** Magnification demonstrating heterogeneous Nkx2.5 expression in the AVN region.Bar=50µm. **J.** MLC2a stained frontal section at the IVS level of a HH30 quail heart.Bar=600µm. **K.** Magnification of Nkx2.5 expression in the AVJ, His bundle and bundle branches. Bar=200µm. **L.** Magnification of the Nkx2.5 positive His bundle and bundle branches. Bar=50µm. **M.** PAS staining in a frontal section of a HH34 heart.Bar=200µm.**N.** Magnification demonstrating low glycogen levels in the His bundle (part of the CCS). Bar=30µm. **O.** Magnification of adjacent MLC2a stained section. Bar=30µm. LA=left atrium, RA=right atrium,LV=left ventricle,RV=right ventricle,Pu=pulmonalis,Ao=aorta, IAS=interatrial septum,IVS=interventricular septum,MV=mitral valve,TV=tricuspid valve,HIS=bundle of His,BBs=bundle branches,LBB=left bundle branch.

A
HH 30
RA
LA
Pu
Ao
LV
RV
Nkx2.5
B
HH 26
IAS
LA
RA
CV
Nkx2.5
C
HH 30
RA
TV
LA
MV
LV
RV
MLC2a
D
HH 30
RA
LA
LV
RV
MLC2a
E
HH 34
HIS
MV
LBB
RV
LV
PAS
F
HH 30
RA
Pu
Ao
RV
Nkx2.5
G
HH 26
*
*
IAS
RA
LA
Nkx2.5
H
HH 30
A
IVS
MLC2a
I
HH 30
RA
LV
HIS
RV
Nkx2.5
J
HH 34
HIS
PAS
K
HH 30
RA
Pu
Ao
RV
PAS
L
HH 26
LA
LV
Nkx2.5
M
HH 30
A
IVS
Nkx2.5
N
HH 30
HIS
BBs
LV
RV
Nkx2.5
O
HH 34
HIS
MLC2a

Discussion

Spatiotemporal changes in atrial activation sequences in the embryonic avian heart were correlated to developmental morphology to obtain more insight into the structure-function relationships of the developing AVN region in relation to the development of potential arrhythmogenic substrates. A key finding of the present study is that the proximal myocardial tissues of the left cardinal vein (LCV) provide an important contribution to the developing AVN.

Transitions in Atrial Activation Sequence Correlated to Developmental Morphology: Fate of the Cardinal Vein Myocardium

While in the early embryonic chick heart each cell inherently possesses pacemaker activity, only some time after the beginning of circulation the sinus venosus (SV) is added to the caudal end of the heart tube (HH12) and becomes the prevailing pacemaker. While the dominant pacemaking impulse initially originates from a pacemaking area in the LCV entering the SV,[8, 24, 25] it is well established that the myocardium surrounding the anterolateral wall of the proximal RCV harbors the primordium of the definitive SAN, whereas the vein itself becomes the right superior caval vein.[26, 27]

In line with early functional reports,[8] the temporal presence of bilateral pacemakers in the SV of the early developing heart could also be confirmed in the present study. Extracellular electrograms demonstrated pacemaker dominance in the RA in the vast majority of hearts, while initiation of the electrical impulse could still be found in the LA in a substantial number of hearts (21%) until late stages of cardiogenesis (HH30). Similarly, persistent LA dominance in ~10% of HH16-36 chick hearts was recently found in another avian study, while comparable atrial activation patterns have also been shown in the embryonic mammalian heart.[28] Furthermore, simultaneous activation (<1 ms) of the RA and LA was demonstrated in 15%(14/96) of HH20-30 hearts in the present study, possibly indicating nearly simultaneously firing bilateral pacemakers or rapid interatrial conduction through Bachmanns bundle, as was elegantly shown to become functionally active in avians between HH17 and 24.[28]

Structural correlation demonstrated that both the myocardial avian SAN primordium in the RCV and its left-sided counterpart in the LCV were characterized by low levels of glycogen expression, while the surrounding myocardium demonstrated a high glycogen content, in line with previous reports

in avians.[29] In contrast to mammalian glycogen expression, low levels of glycogen were reported in the specialized CCS tissues of the avian heart, implicating the LCV tissues as an important contributor to the CCS.[30, 31]

Furthermore, both primordia were identified by the expression of low levels of Nav1.5 (the most prominent sodium α-subunit in the heart generating the I_{Na} current initiating the action potential of the normal and CCS myocardium) and Cx43 (the principle connexin of the working myocardium), but failed to express the homeobox transcription factor Nkx2.5. The latter is perfectly in line with previous expression studies describing Nkx2.5 expression in the developing mouse SV.[17, 19, 26, 27] While the observed expression gradient of Nav1.5 and Cx43 in the avian SAN seems comparable to expression patterns described in the developing mammalian SAN, [32, 33] the expression pattern of Nav1.5, whose functional contribution to the activity of pacemaker cells has profoundly been rekindled in recent developmental studies,[34] has never been described in avian cardiogenesis before. Interestingly however, experimental studies in adult rats identified 3 types of cardiomyocytes in the AVN region expressing distinct and relatively low levels of Nav1.5 as compared to the surrounding atrial myocardium.[35]It is tempting to speculate that the distinct tissues surrounding the proximal LSH expressing relatively low levels of Nav1.5, described in the present study, might provide one of these cellular populations to the adult AVN.

Although based on the present data, a direct structure-function correlation cannot be made, the demonstrated bilateral morphologically distinct Nkx2.5 negative myocardial regions at the terminal portion of the RCV and LCV, expressing low levels of Cx43, Nav1.5 and glycogen, could structurally indeed represent the areas responsible for the demonstrated impulse initiation in the RA or LA, respectively. With ongoing development, the terminal portion of the LCV entering the SV becomes the CS attaching the RA to the cardiac venous system at the base of the IAS at the crux of the heart, while the remaining portion of the LCV is atrophied and recognizable as the oblique vein of Marshall in the adult human heart.[36] Due to these positional changes, the early Nkx2.5 negative myocardium surrounding the proximal LCV is transposed through the myocardialized spina vestibulum, along the base of the IAS to the crux of the heart surrounding the CS (the position of the adult AVN), in line with the recently described podoplanin expression pattern at the venous pole of the developing mouse heart.[19] Interestingly, abundant LacZ expression (indicating the presence of CCS tissue) in the myocardium surrounding the CS orifice has previously

been demonstrated in the CCS-LacZ mouse,[14] perfectly in line with the ultimate position of the morphologically distinct primordial AVN tissues derived from the LCV myocardium described in the present study. This would implicate that both the SAN and AVN (partly) derive from symmetrically distinct myocardial tissues with identical expression patterns for Nav1.5, Cx43, Nkx2.5 and MLC2a, surrounding the lumina of the developing early RCV and LCV respectively.

While a SV contribution to the developing AVN was already first suggested more than 50 years ago[8, 9] and several contemporary marker studies, including HNK1 and Leu7[15, 20] and transgenic reporter studies for CCS-LacZ and MinK,[13, 14] have linked the SV myocardium to the developing CCS, a LCV contribution to the developing AVN region has, to our best knowledge, been extensively suggested but both structurally and functionally not been studied systematically.

The Role of the Myocardial Specialized Ring Tissues in AVN Development

According to the classical ring theory,[11, 14, 15] the CCS is derived from four separate rings of specialized myocardium positioned between the primitive segments of the heart:1) the SA-ring between the SV and atrium, 2) the AV ring between the atrium and ventricle, 3) the bulboventricular ring or primary ring or fold between the bulbus and ventricle and 4) the truncobulbar or ventriculo-arterial ring between the outflow tract and ventricle. During development, parts of these rings loose their specialized character and the remaining parts are identified as putative parts of the mature CCS.[10, 11, 14, 15]

The contribution of the AV ring myocardium to the adult AVN has been well established.[6, 37] In avians, by 42 hours of development (~HH11) as cardiac looping proceeds, the AV ring myocardium is characterized by relatively low levels of Cx43, as also described in the present study, and starts displaying slow conduction responsible for an AV conduction delay, already giving rise to an adult type electrocardiogram.[38-40] During formation of the isolating annulus fibrosis,[23] the AV ring myocardium is sequestered as an atrial structure, forming the smooth walled atrial vestibules, leaving a small part of the slow conducting AV ring myocardium in-situ contributing to the developing AVN.[41] Interestingly, in the present study from ~HH31 onwards, the myocardium of the AV ring was found to express relatively high levels of Nkx2.5 possibly indentifying the precursors population of the Nkx2.5 positive cells in the future heterogeneous AVN.

Initially both the AV ring tissues and SA ring were demonstrated to contribute to the developing AVN,[11] while a single ring origin of the AVN in the primary ring or fold has also been suggested.[42] Later on, the important contribution of the SA ring to the developing AVN could again be established by HNK-1 expression patterns in the human embryo and analysis of CCS-LacZ and minK-LacZ expression in the mouse embryo.[13-15] The SA ring tissues furthermore provide a direct connection between the SAN and AVN and give rise to the 3 internodal pathways,[14, 15, 43] since both the anterior internodal pathway through the septum spurium and the two posterior internodal pathways in the region of the left and right venous valves are continuous with the AV ring.[14, 15] Since these pathways do not seem to satisfy the criteria set for adult specialized conduction tissue,[44] controversy has persisted about the existence and definition of these specialized fast conducting tissues in the atria.[43] In the present study however, from HH30 onwards distinct Nkx2.5 positive strands of myocardial cells were identified in the common atrial myocardial wall and IAS, again establishing parts of the SA-ring. Additionally, parts of the AV ring, primary ring and ventriculo-arterial ring could also be identified by Nkx2.5 staining (**Figure 7**). While transient elevated Nkx2.5 expression levels in the developing His bundle, bundle branches and Purkinje fibers were recently shown in chick cardiogenesis,[16] the myocardial specialized ring tissues have to our best knowledge, never been identified in the avian embryo by Nkx2.5 expression before.

Clinical Significance

Spatially, the ultimate location of the distinct LCV tissues described in the present study correlates to the location of the slow pathway of the adult human AVN located in the septal isthmus[45] which corresponds to the extensively described inferior nodal extension (INE) of the AVN[46] and often seems to follow the proximal part of the anterior margin of the CS.[45] Similar to the adult rabbit INE of the AVN,[46] relatively low expression levels of Nav1.5 and Cx43 were demonstrated in the AVN primordial LCV tissues running along the slow pathway region of the AVN in the present study, which might provide a morphological substrate for slow conduction in this region. Furthermore, during ectopic pacemaking in the AVN in case of SAN dysfunction, the action potential is first initiated in the region of the INE of the AVN.[46] While in the present study, the tissues of the developing LCV were indeed shown to be functionally capable of pacemaking, expression of proteins implicated in generating a pacemaking current was not analyzed. The rabbit INE of the adult AVN has however been shown to display

abundant expression of hyperpolarization activated cyclic nucleotide-gated potassium channel 4 (HCN4)[46] – the major isoform responsible for pacemaking If current – while the embryonic sinus horn tissues of the developing mouse heart were recently also demonstrated to express HCN4.[26]

Clinically, the remnant of the LCV in the CS region is known as the ligament of Marshall (LOM) and has been recognized as a potential source of ectopic activity deflagrating atrial tachyarrhythmias and atrial fibrillation amendable for RF ablation.[47] Based on the structural and functional data demonstrated in the present study, we postulate that rapid firing and slow conduction in the LOM region could very well be caused by functional remnants of early pacemaking cells of the LCV.

Proposed Concept of AVN Development

Based on the present data and previously established concepts,[11,14,15,19] we propose that the adult AVN is formed from heterogeneous AVN primordia. As previously demonstrated and partly re-established in the present study, both the AV ring, primary ring and SA ring contribute to the developing AVN forming at their junction [11, 13-15] Furthermore, as demonstrated in the present study an additional atrial contribution to the slow pathway region of the AVN is provided by the early morphologically distinct proximal part of the LCV myocardium, ultimately stretched to the crux of the heart surrounding the CS orifice. We furthermore speculate that the tissues of the SA ring might contribute to formation of the fast-pathway region anterosuperior to the compact AVN, while the remnants of the AV ring and primary ring myocardium might contribute to the compact part of the AVN (**Figure 7**).

In this concept, we postulate that the Nkx2.5 negative LCV primordial AVN tissues surrounding the CS orifice join the AVN primordial Nkx2.5 positive tissues (the remnants of the AV ring, primary ring and SA ring tissue) already brought together at the crux of the heart, together constructing a heterogeneous AVN. It remains to be determined whether ultimate positioning of the early proximal LCV myocardium around the CS orifice in the AVN region is simply the result of the physiological remodeling process of the RA and SV or might result from outgrowth of the left atrium and left mitral valve orifice.

Study Limitations

The aim of the present study was to correlate changes in atrial activation sequences to the morphology of the developing AVN. Due to technical limitations we recorded local electrograms in the common atria while the pacemaking tissues were morphologically found in the dorsally adjoining CV myocardium. Similarly, electrical mapping of the human adult atrium identifies the first activated region of the working atrial myocardium rather than the distinct actual pacemaker site.[48]

Conclusions

The tissues of the LCV myocardium provide an important functional contribution to the AVN Anlagen. We furthermore propose a new concept of AVN development in which the adult AVN is postulated to derive from heterogeneous AVN primordia: the remnants of the AV ring myocardium, PR myocardium and the SA ring myocardium and the LCV primordium contributing to the slow pathway region of the AVN.

References

1. Jackman WM, Heidbuchel H, Beckman K, McClelland J, Lazzara R. Three forms of atrioventricular nodal (junctional) reentrant tachycardia: differential diagnosis, electrophysiological characteristics and implications for anatomy of the reentrant circuit. In: Zipes DP, Jalife, J., ed. *Cardiac electrophysiology: from cell to bedside.* second ed: W.B. Saunders; 1995:620-637.

2. Blaufox AD, Rhodes JF, Fishberger SB. Age related changes in dual AV nodal physiology. *PACE.* 2000;23(4 Pt 1):477-480.

3. Jackman WM, Beckman KJ, McClelland JH, Wang X, Friday KJ, Roman CA, Moulton KP, Twidale N, Hazlitt HA, Prior MI. Treatment of supraventricular tachycardia due to atrioventricular nodal reentry, by radiofrequency catheter ablation of slow-pathway conduction. *N Engl J Med.* 1992;327(5):313-318.

4. Tawara S. Das reizleitungssystem des saugetierherzens. Eine anatomisch-histologische studie uber das atrioventrikularbundel und die Purkinjeschen faden.: Verslag von Gustav Fischer; 1906.

5. Keith A, Flack M. The Form and Nature of the Muscular Connections between the Primary Divisions of the Vertebrate Heart. *J Anat Physiol.* 1907;41(Pt 3):172-189.

6. Retzer. The anatomy of the conduction system in the mammalian heart. *Bull Johns Hopkins Hosp.* 1908;19:208-215.

7. Truex RC, Marino TA, Marino DR. Observations on the development of the human atrioventricular node and bundle. *Anat Rec.* 1978;192(3):337-350.

8. Patten BM. The development of the sinoventricular conduction system. *Medical Bulletin* 1956;22(1):1-21.

9. James TN. Cardiac conduction system: fetal and postnatal development. *Am J Cardiol.* 1970;25(2):213-226.

10. Anderson RH, Taylor IM. Development of atrioventricular specialized tissue in human heart. *Br Heart J.* 1972;34(12):1205-1214.

11. Wenink AC. Development of atrio-ventricular conduction pathways. *Bulletin de l'Association des anatomistes.* 1976;60(170):623-629.

12. Wessels A, Vermeulen JL, Verbeek FJ, Virágh S, Kálmán F, Lamers WH, Moorman AF. Spatial distribution of "tissue-specific" antigens in the developing human heart and skeletal muscle. III. An immunohistochemical analysis of the distribution of the neural tissue antigen G1N2 in the embryonic heart; implications for the development of the atrioventricular conduction system. *Anat Rec.* 1992;232(1):97-111.

13. Kondo RP, Anderson RH, Kupershmidt S, Roden DM, Evans SM. Development of the cardiac conduction system as delineated by minK-lacZ. *J Cardiovasc Electrophysiol.* 2003;14(4):383-391.

14. Jongbloed MR, Schalij MJ, Poelmann RE, Blom NA, Fekkes ML, Wang Z, Fishman GI, Gittenberger-de Groot AC. Embryonic conduction tissue: a spatial correlation with adult arrhythmogenic areas. *J Cardiovasc Electrophysiol.* 2004;15(3):349-355.

15. Blom NA, Gittenberger-de Groot AC, de Ruiter MC, Poelmann RE, Mentink MM, Ottenkamp J. Development of the cardiac conduction tissue in human embryos using HNK-1 antigen expression: possible relevance for understanding of abnormal atrial automaticity. *Circulation.* 1999;99(6):800-806.

16. Thomas PS, Kasahara H, Edmonson AM, Izumo S, Yacoub MH, Barton PJ, Gourdie RG. Elevated expression of Nkx-2.5 in developing myocardial conduction cells. *Anat Rec.* 2001;263(3):307-313.

17. Blaschke RJ, Hahurij ND, Kuijper S, Just S, Wisse LJ, Deissler K, Maxelon T, Anastassiadis K, Spitzer J, Hardt SE, Schöler H, Feitsma H, Rottbauer W, Blum M, Meijlink F, Rappold G, Gittenberger-de Groot AC. Targeted mutation reveals essential functions of the homeodomain transcription factor Shox2 in sinoatrial and pacemaking development. *Circulation.* 2007;115(14):1830-1838.

18. Moskowitz IP, Kim JB, Moore ML, Wolf CM, Peterson MA, Shendure J, Nobrega MA, Yokota Y, Berul C, Izumo S, Seidman JG, Seidman CE. A molecular pathway including Id2, Tbx5, and Nkx2-5 required for cardiac conduction system development. *Cell.* 2007;129(7):1365-1376.

19. Gittenberger-de Groot AC, Mahtab EA, Hahurij ND, Wisse LJ, de Ruiter MC, Wijffels MC, Poelmann RE. Nkx2.5-negative myocardium of the posterior heart field and its correlation with podoplanin expression in cells from the developing cardiac pacemaking and conduction system. *Anat Rec.* 2007;290(1):115-122.

20. de Ruiter MC, Gittenberger-de Groot AC, Wenink AC, Poelmann RE, Mentink MM. In normal development pulmonary veins are connected to the sinus venosus segment in the left atrium. *Anat Rec.* 1995;243(1):84-92.

21. Watanabe M, Timm M, Fallah-Najmabadi H. Cardiac expression of polysialylated NCAM in the chicken embryo: correlation with the ventricular conduction system. *Dev Dyn.* 1992;194(2):128-141.

22. Hamburger V, Hamilton HL. A series of normal stages in the development of the chick embryo. 1951. *Dev Dyn.* 1992;195(4):231-272.

23. Kolditz DP, Wijffels MC, Blom NA, van der Laarse A, Markwald RR, Schalij MJ, Gittenberger-de Groot AC. Persistence of functional atrioventricular accessory pathways in postseptated embryonic avian hearts: implications for morphogenesis and functional maturation of the cardiac conduction system. *Circulation.* 2007;115(1):17-26.

24. Van Mierop LH. Location of pacemaker in chick embryo heart at the time of initiation of heartbeat. *Am J Physiol.* 1967;212(2):407-415.

25. Kamino K, Hirota A, Fujii S. Localization of pacemaking activity in early embryonic heart monitored using voltage-sensitive dye. *Nature.* 1981;290(5807):595-597.

26. Mommersteeg MT, Hoogaars WM, Prall OW, de Gier-de Vries C, Wiese C, Clout DE, Papaioannou VE, Brown NA, Harvey RP, Moorman AF, Christoffels VM. Molecular pathway for the localized formation of the sinoatrial node. *Circ Res.* 2007;100(3):354-362.

27. Christoffels VM, Mommersteeg MT, Trowe MO, Prall OW, de Gier-de Vries C, Soufan AT, Bussen M, Schuster-Gossler K, Harvey RP, Moorman AF, Kispert A. Formation of the venous pole of the heart from an Nkx2-5-negative precursor population requires Tbx18. *Circ Res.* 2006;98(12):1555-1563.

28. Sedmera D, Wessels A, Trusk TC, Thompson RP, Hewett KW, Gourdie RG. Changes in activation sequence of embryonic chick atria correlate with developing myocardial architecture. *Am J Physiol Heart Circ Physiol.* 2006;291(4):H1646-1652.

29. Allen HJ. Glycogen in the chick embryo. *Biological Bulletin.* 1919;36:63-U66.

30. Kim Y, Yasuda M. The cardiac conducting system of the fowl. *Anatomia, histologia, embryologia.* 1979;8(2):138-150.

31. Gossrau R. The impulse conducting system of birds. Histochemical and electron microscopy studies. *Histochemie* 1968;13(2):111-159.

32. Dominguez JN, de la Rosa, A., Navarro, F., Franco, D., Aranega, A.E. Tissue distribution and subcellular localization of the cardiac sodium channel during mouse heart development. . *Cardiovasc Res.* 2008;78(1):45-52.

33. Boyett MR, Inada S, Yoo S, Li J, Liu J, Tellez J, Greener ID, Honjo H, Billeter R, Lei M, Zhang H, Efimov IR, Dobrynski H. Connexins in the sinoatrial and atrioventricular nodes. *Adv Cardiol.* 2006;42:175-197.

34. Du Y, Huang X, Wang T, Han K, Zhang J, Xi Y, Wu G, Ma A. Downregulation of neuronal sodium channel subunits Nav1.1 and Nav1.6 in the sinoatrial node from volume-overloaded heart failure rat. *Pflugers Arch.* 2007;454(3):451-459.

35. Yoo S, Dobrzynski H, Fedorov VV, Xu SZ, Yamanushi TT, Jones SA, Yamamoto M, Nikolski VP, Efimov IR, Boyett MR. Localization of Na+ channel isoforms at the atrioventricular junction and atrioventricular node in the rat. *Circulation.* 2006;114(13):1360-1371.

36. Marshall JJ. On the development of the great anterior veins in man and mammalia: including an account of certain remnants of foetal structures found in the adult, a comparative view of these great veins in the different mammalia, and an analysis of their occasional peculiarities in the human subject. *Philos Trans R Soc Lond.* 1850;140:133-169.

37. Virágh S, Challice CE. The development of the conduction system in the mouse embryo heart. II. Histogenesis of the atrioventricular node and bundle. *Dev Biol.* 1977;56(2):397-411.

38. Gourdie RG, Harris BS, Bond J, Justus C, Hewett KW, O'Brien TX, Thompson RP, Sedmera D. Development of the cardiac pacemaking and conduction system. *Birth Defects Res C Embryo Today.* 2003;69(1):46-57.

39. Patten BM. Initiation and early changes in the character of the heart beat in vertebrate embryos. *Physiol Rev.* 1949;29(1):31-47.

40. Argüello C, Alanís J, Pantoja O, Valenzuela B. Electrophysiological and ultrastructural study of the atrioventricular canal during the development of the chick embryo. *J Mol Cell Cardiol.* 1986;18(5):499-510.

41. Kim JS, Virágh S, Moorman AF, Anderson RH, Lamers WH. Development of the myocardium of the atrioventricular canal and the vestibular spine in the human heart. *Circ Res.* 2001;88(4):395-402.

42. Wessels A, Markman MW, Vermeulen JL, Anderson RH, Moorman AF, Lamers WH. The development of the atrioventricular junction in the human heart. *Circ Res.* 1996;78(1):110-117.

43. James TN. The internodal pathways of the human heart. *Progr Cardiovasc Dis.* 2001;43(6):495-535.

44. Anderson RH, Ho SY, Becker AE. Anatomic boundaries between the atrioventricular node and the atrioventricular bundle. *J Cardiovasc Electrophysiol.* 1998;9(2):225-228.

45. Spach MS, Lieberman M, Scott JG, Barr RC, Johnson EA, Kootsey JM. Excitation sequences of the atrial septum and the AV node in isolated hearts of the dog and rabbit. *Circ Res.* 1971;29(2):156-172.

46. Li J, Greener ID, Inada S, Nikolski VP, Yamamoto M, Hancox JC, Zhang H, Billeter R, Efimov IR, Dobrzynski H, Boyett MR. Computer three-dimensional reconstruction of the atrioventricular node. *Circ Res.* 2008;102(8):975-985.

47. Polymeropoulos KP, Rodriguez LM, Timmermans C, Wellens HJ. Images in cardiovascular medicine. Radiofrequency ablation of a focal atrial tachycardia originating from the Marshall ligament as a trigger for atrial fibrillation. *Circulation*. 2002;105(17):2112-2113.

48. Betts TR, Ho SY, Sanchez-Quintana D, Roberts PR, Anderson RH, Morgan JM. Three-dimensional mapping of right atrial activation during sinus rhythm and its relationship to endocardial architecture. *J Cardiovasc Electrophysiol*. 2002;13(11):1152-1159.

Online Data Supplement

Experimental Preparations

All animal experiments were approved by the Committee on Animal Welfare of the Leiden University Medical Center (LUMC), Leiden, the Netherlands. Animal experiments were conducted in compliance with the Guide for the Care and Use of Laboratory Animals (NIH Publication No.85-23, revised 1996). Fertilized eggs of the Japanese quail (*Coturnix coturnix japonica*, Leiden University Medical Center, The Netherlands) and white leghorn chick (*Gallus domesticus*) were incubated blunt end up at 37.5°C and 80% humidity. Embryos were staged according to the Hamburger-Hamilton (HH) criteria.[1]

Ex-Ovo Extracellular Electrode Recordings – Technical Features & Recording Protocol

In total, extracellular electrode recordings were performed at HH20-30 in wildtype embryonic chick (n=34) and quail (n=33) hearts (group A, HH20-30, n=37; group B, HH24-27, n=38; group C, HH28-30, n=21). The experimental preparations were placed in a custom-built, fluid-heated, temperature-controlled tissue bath and superfused with carbogenated (95% O_2 and 5% CO_2) Tyrode's solution (30 ± 0.1°C) with the following composition (mmol/l): NaCl 130, KCl 4, KH_2PO_4 1.2, $MgSO_4$ 0.6, $NaHCO_3$ 20, $CaCl_2$ 1.5, glucose 10 (pH 7.35).

Unipolar extracellular electrogram recording was subsequently performed, as previously described,[2, 3] by consistently positioning 3 tungsten-recording electrodes (tip:1-2μm; impedance 0.5-1.0MΩ, WPI Inc., Berlin, Germany) on the left atrium (LA), right atrium (RA) and left ventricular apex (LVA) (Figure 1). A silver reference electrode was placed in the tissue bath.

In short, the experimental preparations were allowed to equilibrate for 10 minutes before starting the recording protocol. Recordings in embryonic hearts with a spontaneous heart rate (HR) of < 60 bpm were considered non-physiological and excluded from the present study.

Definitions

In extracellular electrogram recording, a mean difference in local depolarization time between two recording electrodes of ≥1 ms was considered significant.[2, 3] In all experiments, a stable 1:1 relation between atrial and ventricular activation was assured to be present. The time difference between LA activation and the location of earliest ventricular activation was denominated as the AV interval.

Immunohistochemistry

After completion of extracellular electrogram recordings, the hearts were removed from the Tyrode's solution and fixated in a 4% paraformaldehyde solution for 24 hours, dehydrated and embedded in paraffin. Subsequently, 36 chick and 28 quail (HH19–36) hearts were serially sectioned in the frontal plane at 5 μm, transferred to albumin/glycerin-coated objective slides. After deparaffinization and rehydration, the sections were prepared for standard Periodic-Acid-Schiff (PAS) staining or for immunohistochemical staining by treatment with 0.3% H_2O_2 in phosphate buffered saline (PBS) for 20 minutes to smother endogenous peroxidase activity.

Routine immunohistochemical staining was subsequently performed by overnight incubation with the primary antibody; rabbit primary antibody against Myosin-Light-Chain 2 atrium (MLC2a) (Kubalak) diluted 1:5000, goat primary antibody against Nkx2.5 (Abcam, ab-266) diluted 1:3000 rabbit primary antibody against Cx43 (Abcam, ab-407) diluted 1:200 and goat primary antibody against SCN5a (Nav1.5)(Santa Cruz, Sc-23174) diluted 1:200 in PBS with 0.05% Tween-20 and 1% Bovine Serum Albumin (BSA) (Sigma Aldrich, USA) in a humified chamber.

After rinsing in PBS and PBS-Tween, the sections were incubated with Goat-anti-Rabbit IgG labeled with biotin (GAR-Biotin, Vector Laboratories, USA, BA-100) or Horse anti-Goat IgG labeled with biotin (HAG-biotin, Vector Laboratories, USA) diluted 1:200 and 1:66 Goat-serum (Vector Laboratories, USA, PK 6100) or Horse-serum (Vector Laboratories, USA) diluted 1:66 in PSB-Tween for 40 minutes. Goat/Horse serum was used to block aspecific binding of the secondary antibody. After rinsing in PBS and PBS-Tween, the sections were incubated with ABC-reagent, which consisted of reagent A diluted 1:100 and reagent B diluted 1:100 in PBS, in a humified chamber for 40 minutes. After rinsing with PBS, PBS-Tween and tris/maleate pH 7.6, the sections were incubated with 3,3'-diaminobenzidin (DAB, Sigma-Aldrich Chemie, USA, D5637) in a concentration of 400 mg/l with 4 droplets of H_2O_2 acting as a catalyzer, for 5 minutes. After incubation with DAB, the sections were rinsed with H_2O-demi and counterstained with 0.1% Heamatoxylin (Merck, Darmstadt, Germany) for 10 seconds. Finally, the sections were rinsed with tap water for 10 minutes, dehydrated and mounted in Entellan (Merck, Darmstadt, Germany).

Statistical Analysis

The symmetry of the distribution was determined by determining the Skewness value. Heart rates and AV interval were compared between groups using the 2-tailed Student *t* test for normally distributed values. For comparison of categorical variables (atrial activation sequences), the χ^2-test was applied. A *P* value <0.05(2-tailed) was considered statistically significant. All analyses were performed using the Statistical Package for Social Studies version 12.0 (SPSS Inc, Chicago, Ill).

The authors had full access to the data and take responsibility for its integrity. All authors have read and agree to the manuscript as written.

References

1. Hamburger V, Hamilton HL. A series of normal stages in the development of the chick embryo. 1951. *Dev Dyn.* 1992;195(4):231-272.
2. Kolditz DP, Wijffels MC, Blom NA, van der Laarse A, Hahurij ND, Lie-Venema H, Markwald RR, Poelmann RE, Schalij MJ, Gittenberger-De Groot AC. Epicardium-Derived Cells in Development of Annulus Fibrosis and Persistence of Accessory Pathways. *Circulation.* 2008.
3. Kolditz DP, Wijffels MC, Blom NA, van der Laarse A, Markwald RR, Schalij MJ, Gittenberger-de Groot AC. Persistence of functional atrioventricular accessory pathways in postseptated embryonic avian hearts: implications for morphogenesis and functional maturation of the cardiac conduction system. *Circulation.* 2007;115(1):17-26.

PART III

CLINICAL ASPECTS OF SUPRAVENTRICULAR TACHYCARDIA IN NEONATES AND CHILDREN

Chapter 8

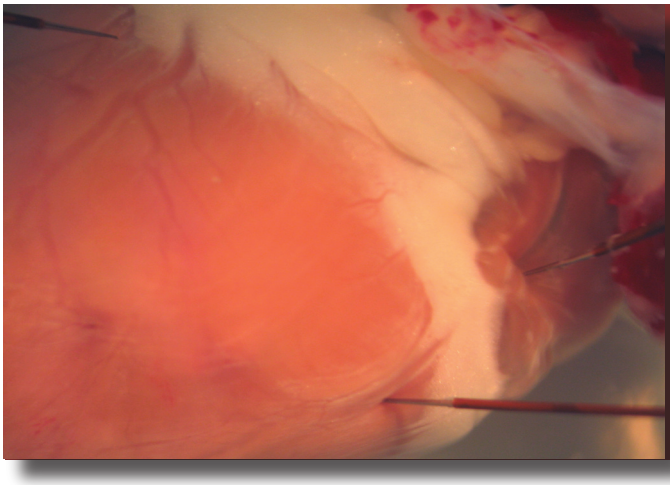

Denise P.Kolditz[1]
Nico A.Blom[2]
Regina Bökenkamp[2]
Marianne Bootsma[1]
Katja Zeppenfeld[1]
Martin J. Schalij[1]

[1]Department of Cardiology, Leiden University Medical Center
[2]Department of Pediatric Cardiology, Leiden University Medical Center

Radiofrequency Catheter Ablation as Treatment for Children with Cardiac Arrhythmias: Favourable Results after a Mean of 4 Years

Ned Tijdschr Geneeskd.
2005;149(24):1339-46

Article is written in Dutch:

Katheterablatie met Radiofrequente Energie ter Behandeling van Kinderen met Hartritmestoornissen: Gunstige Resultaten na Gemiddeld 4 Jaar

Abstract

Objective. Analysis of long-term results with radiofrequency catheter ablation (RF ablation) in children.

Design. Retrospective.

Method. Data were analysed from all 118 pediatric patients B 18 years old who underwent RF ablation at the Leiden University Medical Center (LUMC), the Netherlands, during the period 1 December 1992-31 May 2004.

Results. The group consisted of 60 boys and 58 girls with a mean age of 12.7 years (SD: 4.6). They underwent 140 RF ablation procedures for 122 disorders. Indications for RF ablation were: failure or side effects of antiarrhythmic medication (45%), patient/parent choice (45%), cardiomyopathy or life-threatening arrhythmia (8%), and impending surgery for a congenital heart defect (2%). The mean follow-up interval was 4 years (SD: 3.2; range: 1.2 months-11.3 years). The final total success rate for RF was 93% (n = 110). 19 patients (16%) underwent a total of 22 repeat procedures. Recurrences occurred after a mean period of 2.3 months (SD: 2.5) following successful RF ablation. Major complications (2nd degree AV block) occurred in 2 patients. During follow-up, no evidence was found of new arrhythmias or of coronary artery lesion development as the result of RF ablation. There was no difference between the < 10 years of age group and the C 10 years of age group in terms of final success rate (93% vs. 93%; p = 0.914) and complication rate (3% vs. 7%,p = 0.680).

Conclusion. The long-term outcome of pediatric patients who underwent RF ablation was good. RF ablation in young children (< 10 years) was found to be safe and effective. These results demonstrate that it is also possible to curatively treat this group of patients with RF ablation in specialized centers.

Samenvatting

Doel. Analyse van de langetermijnresultaten van katheterablatie met radiofrequente energie (RF ablatie) bij kinderen.
Opzet. Retrospectief.
Methode. Van alle 118 kinderen in de leeftijd van 0-18 jaar die in de periode 1 december 1992-31 mei 2004 in het Leids Universitair Medisch Centrum (LUMC) een RF ablatie ondergingen, werden de gegevens geanalyseerd.
Resultaten. De groep bestond uit 60 jongens en 58 meisjes met een gemiddelde leeftijd van 12,7 jaar (SD: 4,6). Zij hadden in totaal 140 RF ablaties voor 122 aandoeningen ondergaan. De indicaties voor RF ablatie waren: falen van of bijwerkingen van antiarrhythmica (45%), keuze van patiënt/ouder(s) (45%), cardiomyopathie of levensbedreigende hartritmestoornissen (8%), voorgenomen chirurgie voor aangeboren hartafwijkingen (2%). De follow-upduur was gemiddeld 4 jaar (SD: 3,2; uitersten: 1,2 maand-11,3 jaar). Het uiteindelijke totale succespercentage van RF ablatie was 93 (n = 110). Er ondergingen 19 patiënten (16%) in totaal 22 tweede of derde ingrepen. Recidieven traden gemiddeld 2,3 maanden (SD: 2,5) na een succesvolle RF ablatie op. Belangrijke complicaties (tweedegraads AV blok) kwamen voor bij 2 patiënten. Er waren geen aanwijzingen voor het optreden van nieuwe aritmieën of voor het ontstaan van coronairlaesies na RF ablatie tijdens de follow-upperiode. Tussen de groep kinderen < 10 jaar (n = 29; 25%) en de groep kinderen ≥ 10 jaar (n = 89; 75%) bestond geen verschil in het uiteindelijke succespercentage (93 versus 93%; p = 0,914) en in het totale complicatierisico (3 versus 7%; p = 0,680).
Conclusie. De langetermijnresultaten van RF ablatie bij kinderen waren goed. Ook bij jonge kinderen (< 10 jaar) was RF ablatie veilig en effectief, wat ruimte biedt om in gespecialiseerde centra ook deze groep curatief met RF ablatie te behandelen.

Introductie

Supraventriculaire tachycardieën (SVT's) vormen, met een geschatte prevalentie van 0,4-1,0%, de belangrijkste groep hartritmestoornissen bij kinderen.[1] In ongeveer tweederde van de gevallen treedt de aritmie voor het eerst op vóór de geboorte of in de eerste levensmaanden. Bij een groot deel van deze jonge kinderen verdwijnen de SVT-episoden spontaan na het eerste levensjaar, maar ze kunnen rond de puberteit terugkeren. Indien de eerste presentatie op oudere leeftijd optreedt, blijven de SVT-episoden in het algemeen bestaan.[2, 3]

Men spreekt van een SVT wanneer de boezem en/of de atrioventriculaire knoop bij het mechanisme van de tachycardie zijn betrokken. Paroxismale atrioventriculaire 're-entry'-tachycardieën (AVRT's), ofwel cirkeltachycardieën tussen boezem en kamer op basis van een extra myocardverbinding, vormen de belangrijkste groep SVT's bij kinderen (**Figuur 1**). Rond de puberteit komen ook de atrioventriculaire nodale re-entrytachycardieën steeds vaker voor, waarbij er cirkeltachycardieën bestaan tussen een snel en langzaam geleidend pad in de atrioventriculaire knoop. Chronische vormen van SVT zoals 'permanent junctional reciprocating' tachycardie en ectopische atriale tachycardie zijn veel zeldzamer, maar zijn typisch voor jonge patiënten en kunnen leiden tot een ernstige gedilateerde cardiomyopathie.[2, 4]

De belangrijkste therapie voor hartritmestoornissen bestond aanvankelijk uit het chronisch gebruik van antiarrhythmica. Begin jaren negentig van de vorige eeuw werd echter katheterablatie met radiofrequente energie (RF ablatie) geïntroduceerd als nieuwe behandelingsmethode voor hartritmestoornissen, naast de bestaande chirurgische behandeling en katheterablatie met hoogenergetische gelijkstroomschokken.[5] RF ablatie wordt inmiddels bij volwassen patiënten op grote schaal succesvol toegepast. Tevens is het indicatiegebied het afgelopen decennium sterk uitgebreid.[6]

In 1990 werd de eerste succesvolle RF ablatie bij een kind beschreven[7] en sedertdien zijn verscheidene studies gepubliceerd waarin goede kortetermijnresultaten van RF ablatie bij kinderen worden beschreven.[8-15] Deze gunstige resultaten hebben ertoe geleid dat ook de indicaties voor RF ablatie bij kinderen de afgelopen tien jaar veranderd zijn. Op de kinderleeftijd vormde het falen van medicamenteuze therapie aanvankelijk de belangrijkste indicatie voor RF ablatie. Tegenwoordig wordt RF ablatie beschouwd als een goed alternatief voor medicamenteuze therapie bij kinderen vanaf 5-8 jaar. In veel gevallen heeft RF ablatie de voorkeur van de patiënt en/of de ouders bij oudere kinderen.[2, 16, 17]

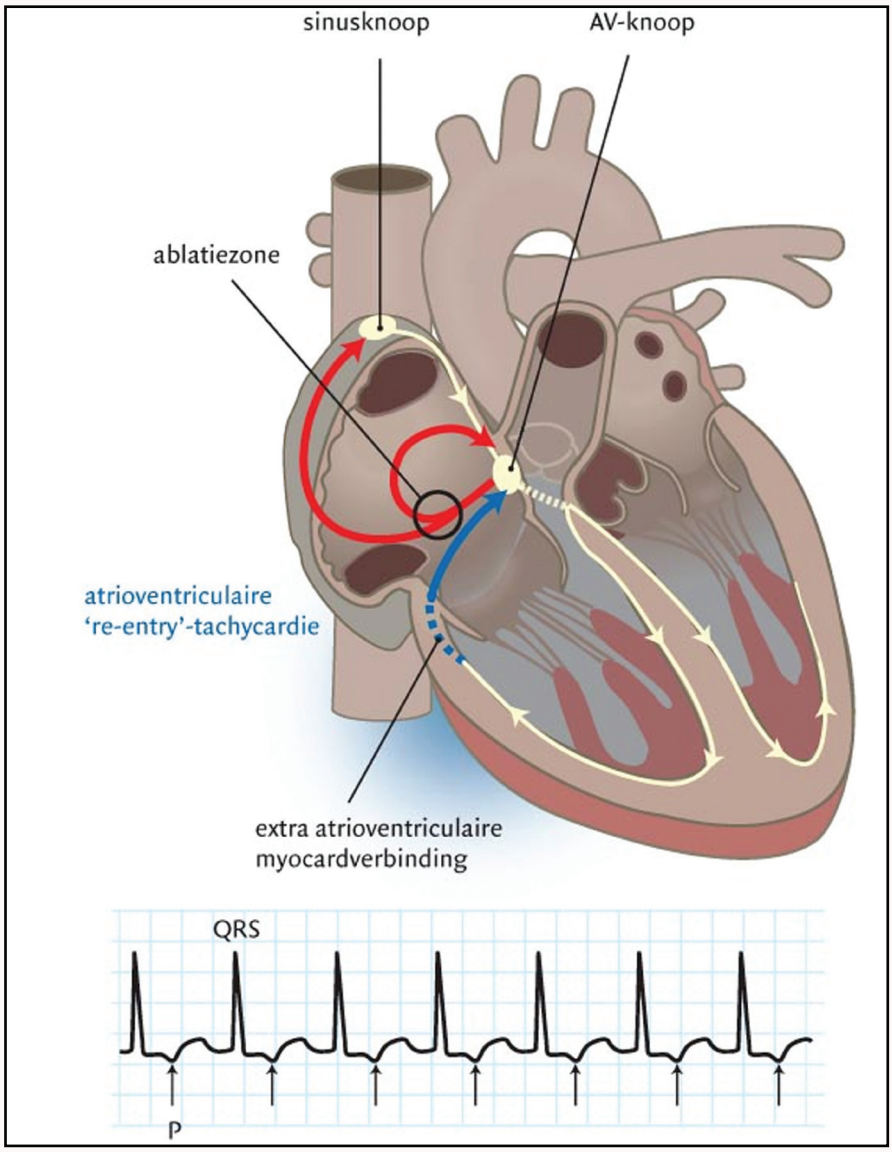

Figuur 1. Schematische weergave van het mechanisme van een orthodrome atrioventriculaire 're-entry'-tachycardie (AVRT). Deze vorm van SVT komt veruit het meeste voor bij kinderen. Er ontstaat een cirkeltachycardie tussen de boezems en de kamers ten gevolge van een extra atrioventriculaire myocardverbinding rond de tricuspidalis-of mitralisklep. Bij een orthodrome AVRT wordt het antegrade pad van de cirkel gevormd door de AV-knoop en het retrograde pad door de extra verbinding. Op het ECG is een regelmatige smalle QRS-complextachycardie zichtbaar met de P-top achter het QRS-complex. Door radiofrequente energie af te geven via de tip van een stuurbare katheter kan de extra myocardverbinding worden onderbroken.

Desalniettemin zijn er argumenten om met name bij jonge kinderen terughoudend te zijn in het toepassen van RF ablatie. Grote studies hebben aangetoond dat de kans op ernstige complicaties als gevolg van RF ablatie, waaronder zelfs sterfte, verhoogd is bij jonge kinderen.[10, 11, 18]

Uit dierexperimenteel onderzoek is tevens gebleken dat RF laesies in immatuur myocard op de lange termijn in afmeting toenemen en aritmogene substraten zouden kunnen vormen; ook kan RF stroom laesies in de coronairarteriën veroorzaken.[19-21]

Het werkelijke risico op late complicaties na RF ablatie bij kinderen, alsmede de effectiviteit op de lange termijn, is tot op heden onvoldoende aangetoond. Het is nu meer dan 11 jaar geleden dat in het Leids Universitair Medisch Centrum (LUMC) het eerste kind een RF ablatie onderging. In de hier beschreven studie analyseerden wij de resultaten en de follow-upgegevens van alle kinderen die sindsdien binnen ons centrum een RF ablatie ondergingen.

Methode

In de periode 1 december 1992-31 mei 2004 ondergingen 118 kinderen (leeftijd: 0-18 jaar) in het LUMC een RF ablatie. De gegevens van deze kinderen werden retrospectief geanalyseerd.

RF ablatietechniek

Elektrofysiologisch onderzoek en RF ablatie vonden bij alle patiënten gedurende dezelfde procedure plaats onder heparinisatie (100 E/kg lichaamsgewicht). Bij jonge kinderen werden de procedures verricht onder algehele anesthesie en bij kinderen vanaf 13-14 jaar werd veelal gekozen voor lokale anesthesie met sedatie. Bij een standaardprocedure werden via de V. femoralis rechts of links 3 tot 4 diagnostische elektrodekatheters (4, 5 of 6 Fr) en een RF ablatiekatheter (7 Fr) in het hart geplaatst. Bij zuigelingen en jonge kinderen werd gebruikgemaakt van een ablatiekatheter met een 5 Fr en 4 mm tip (5 Fr Medtronic RF Marinr; Medtronic Inc, Minneapolis, MN, VS) en werd het aantal intracardiale katheters beperkt tot 2 of zelfs tot 1 katheter en werd voor atriale stimulatie via de slokdarm een elektrodekatheter geplaatst (**Figuur 2**). Na bepaling van het mechanisme van de aritmie en de lokalisatie van het aritmogene substraat door middel van geprogrammeerde elektrische stimulatie, mappingtechnieken en röntgendoorlichting werd de tip van de stuurbare RF katheter op het aritmogene substraat geplaatst. Door temperatuurgecontroleerde (maximale tiptemperatuur: 60-70°C) afgifte van RF energie (300-750 kHz) aan de tip van de ablatiekatheter vond coagulatie van het aritmogene substraat plaats. Bij kinderen met aangeboren hartafwijkingen en postoperatieve atriale tachycardieën werd gebruikgemaakt van een driedimensionaal elektro-anatomisch mappingsysteem (CARTO; Biosense Webster Inc, Waterloo, België).[22]

Vervolgonderzoek

Na de RF ablatie werd de patiënt gedurende 12 h gehepariniseerd (15 E/kg lichaamsgewicht/h) en onder telemetriebewaking 1 nacht ter observatie gehouden. De dag na de ingreep werden een elektrocardiogram en echocardiogram gemaakt, waarna ontslag volgde. Poliklinische controles vonden plaats na 2 tot 3 maanden en na 1 jaar. Na deze controles werd de patiënt/ouder(s) gevraagd om in het geval van klachten direct een nieuwe poliklinische afspraak te maken.

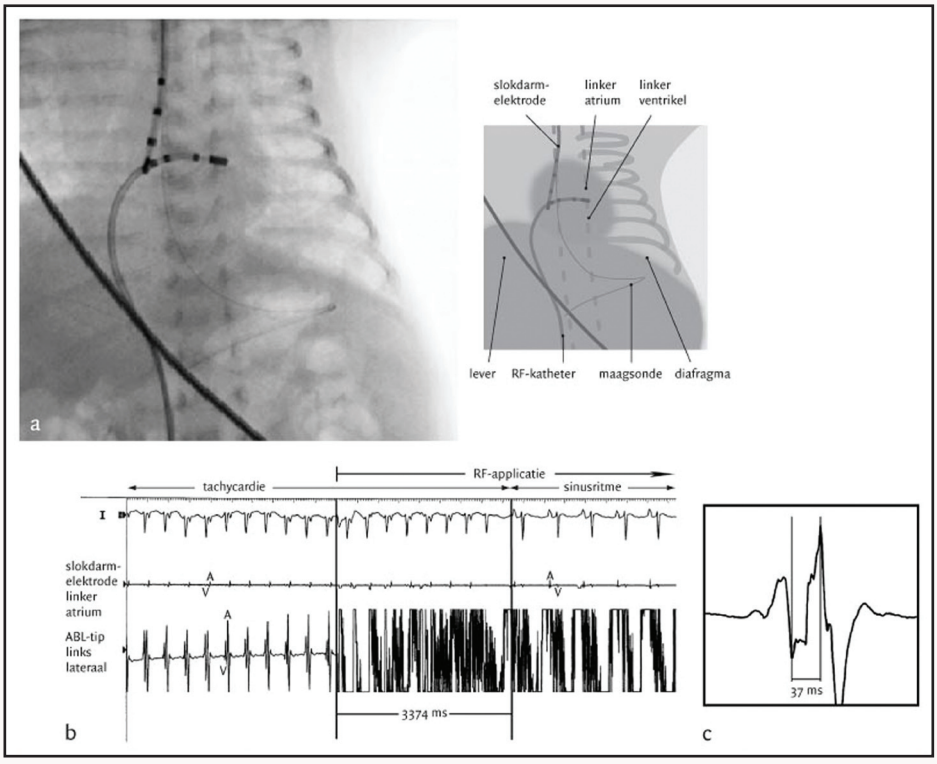

Figuur 2. Katheterablatie met radiofrequente energie ('RF-ablatie') bij een patiënt van 1,5 maand oud met een lichaamsgewicht van 2,1 kg en het Wolff-Parkinson-White-syndroom. (**a**) Röntgendoorlichting tijdens de procedure. Een slokdarmelektrode werd gebruikt voor atriale stimulatie en een 5 Fr RF-ablatiekatheter met een 4 mm tip werd via het open foramen ovale in het linker atrium op de linkslateraal gelegen extra verbinding geplaatst. (**b**) Oppervlakte-ECG-afleiding I en elektrodekathetersignalen voor en tijdens de behandeling. Mapping en RF-applicatie vonden plaats tijdens tachycardie. De RF-ablatiekathetertip (ABL-tip) is precies op de extra verbinding geplaatst, hetgeen af te leiden is uit het korte VA-interval in deze afleiding (**c**). De extra verbinding viel na ongeveer 3 s uit. V = ventriculair elektrogram, A = atriaal elektrogram, de VA-tijd op de slokdarmelektrode is 80 ms, die op de ABL-tip 37 ms.

Definities

Het initiële succespercentage werd gedefinieerd als het percentage RF ablaties waarbij het aritmogene substraat met elektrofysiologisch onderzoek niet meer aantoonbaar was aan het einde van de behandeling. Het uiteindelijke succespercentage werd gedefinieerd als het percentage patiënten dat na één of meer RF ablaties zonder antiarrhythmica vrij was van recidieven en bij wie het aritmogene substraat met elektrofysiologisch onderzoek na afloop van de laatste behandeling niet meer aantoonbaar was.

Statistische analyse

De gegevens worden gepresenteerd als gemiddelden met standaarddeviatie of als medianen met spreiding. De $\chi 2$-toets en de t-toets voor twee steekproeven werden gebruikt om de resultaten te vergelijken. Bij $p < 0,05$ (tweezijdig) werd een verschil als significant beschouwd. Het tijdsinterval van RF ablatie tot het optreden van een recidief werd geanalyseerd met de Kaplan-Meier-methode.

Resultaten

Demografische gegevens en diagnosen

De groep bestond uit 60 jongens en 58 meisjes, die in totaal 140 RF ablatieprocedures ondergingen voor 122 aandoeningen. De demografische gegevens en de diagnosen zijn weergegeven in **Tabel 1**. De gemiddelde duur van de follow-up was 4 jaar (SD: 3,2; uitersten: 1,2 maand-11,3 jaar) en de follow-upgegevens van alle 118 patiënten waren in ons bestand aanwezig.

diagnose	aantal patiënten (%)	gemiddelde leeftijd in jaren (SD; uitersten)	gemiddelde gewicht in kg (SD; uitersten)	aantal kinderen met aangeboren hartafwijkingen
atrioventriculaire 're-entry'-tachycardie	97 (80)	12,3 (4,7; 0,1-18,9)	46,7 (18,8; 2,1-85,0)	8
Wolff-Parkinson-White-syndroom	51 (42)	12,7 (4,8; 0,1-18,9)	49,5 (19,2; 2,1-85,0)	5
verborgen extra verbinding	37 (30)	12,5 (4,2; 0,1-18,7)	46,3 (16,6; 3,7-73,0)	2
'permanent junctional reciprocating' tachycardie	6 (5)	5,9 (3,2; 2,6-10,3)	23,0 (10,1; 14,0-40,0)	0
Mahaim-tachycardie	3 (3)	12,7 (4,0; 9,9-15,5)	51,3 (26,5; 32,5-70,0)	1
AV-nodale re-entrytachycardie	9 (7)	16,2 (2,5; 11,5-18,5)	66,6 (15,6; 44,0-90,0)	0
intra-atriale re-entrytachycardie	8 (7)	15,6 (4,0; 6,2-18,5)	53,5 (16,8; 20,2-70,9)	6
ectopische-atriale tachycardie	4 (3)	13,6 (3,6; 9,4-18,3)	56,1 (20,5; 28,0-75,0)	0
ventriculaire tachycardie	4 (3)	12,7 (2,5; 10,6-16,1)	57,1 (15,7; 42,0-73,0)	0
totaal*	118	12,7 (4,6; 0,1-18,9)	49,0 (18,9; 2,1-90,0)	14

Tabel 1. Demografische gegevens van de 118 patiënten die een RF-ablatie hadden ondergaan in de periode 1 december 1992-31 mei 2004, Leids Universitair Medisch Centrum. * het aantal en het percentage patiënten per diagnose van het totaal aantal patiënten, ** het aantal en het percentage patiënten met een aangeboren hartafwijking per diagnose, *** 4 patiënten hadden 2 verschillende diagnosen en komen in meer dan 1 groep voor: 2 patiënten met AV-nodale re-entrytachycardie en ectopische-atriale tachycardie, 1 patiënt met een verborgen extra verbinding en Wolff-Parkinson-White-syndroom, 1 patiënt met Wolff-Parkinson-White-syndroom en Mahaim tachycardie.

De indicaties voor RF ablatie waren: het falen van/bijwerkingen van antiarrhythmica (n = 63; 45%), de keuze van patiënt/ouder(s) (63; 45%), cardiomyopathie of levensbedreigende hartritmestoornissen (11; 8%), en voorgenomen chirurgie voor aangeboren hartafwijkingen (3; 2%).

Röntgendoorlichtings- en behandeltijd

De röntgendoorlichtingstijd was gemiddeld 38,9 min (SD: 26,0) en de gemiddelde tijd die nodig was voor de ingreep was 186 min (SD: 84,2).

Succespercentage

De RF ablatie was initieel succesvol bij 106 (90%) van de 118 patiënten (**Figuur 3**). Er ondergingen 19 patiënten (16%) een tweede ingreep en 3 van deze 19 patiënten een derde ingreep wegens het falen van de eerste behandeling, de aanwezigheid van een tweede aritmogeen substraat of het optreden van een recidief. Van deze 19 hadden 15 een AVRT. Uiteindelijk werd de aritmie bij 110 van de 118 (93%) patiënten definitief succesvol behandeld met RF ablatie (zie **Figuur 3**). Het initiële en uiteindelijke succespercentage verschilde per diagnose (zie **Tabel 2**).

Het initiële succespercentage van RF ablatie voor AVRT verschilde per lokalisatie van de extra verbinding. In totaal was 90% (101/112) van de RF ablaties voor AVRT succesvol. Er was geen statistisch significant verschil in succespercentage tussen rechts, septaal en links gelokaliseerde extra verbindingen: respectievelijk 86% (24/28) versus 84% (27/32) versus 96% (50/52) (p = 0,219).

Complicaties

Met de ingreep samenhangende geringe complicaties kwamen voor bij 5 (4%) patiënten: nabloeding in de lies (n = 4) en pericardeffusie (n = 1). Belangrijke complicaties kwamen voor bij 2 (2%) patiënten; bij beiden ontstond een tweedegraads AV blok. Bij geen van de patiënten traden late complicaties op, met name werden geen nieuwe aritmieën of symptomen passend bij coronairlaesies gevonden.

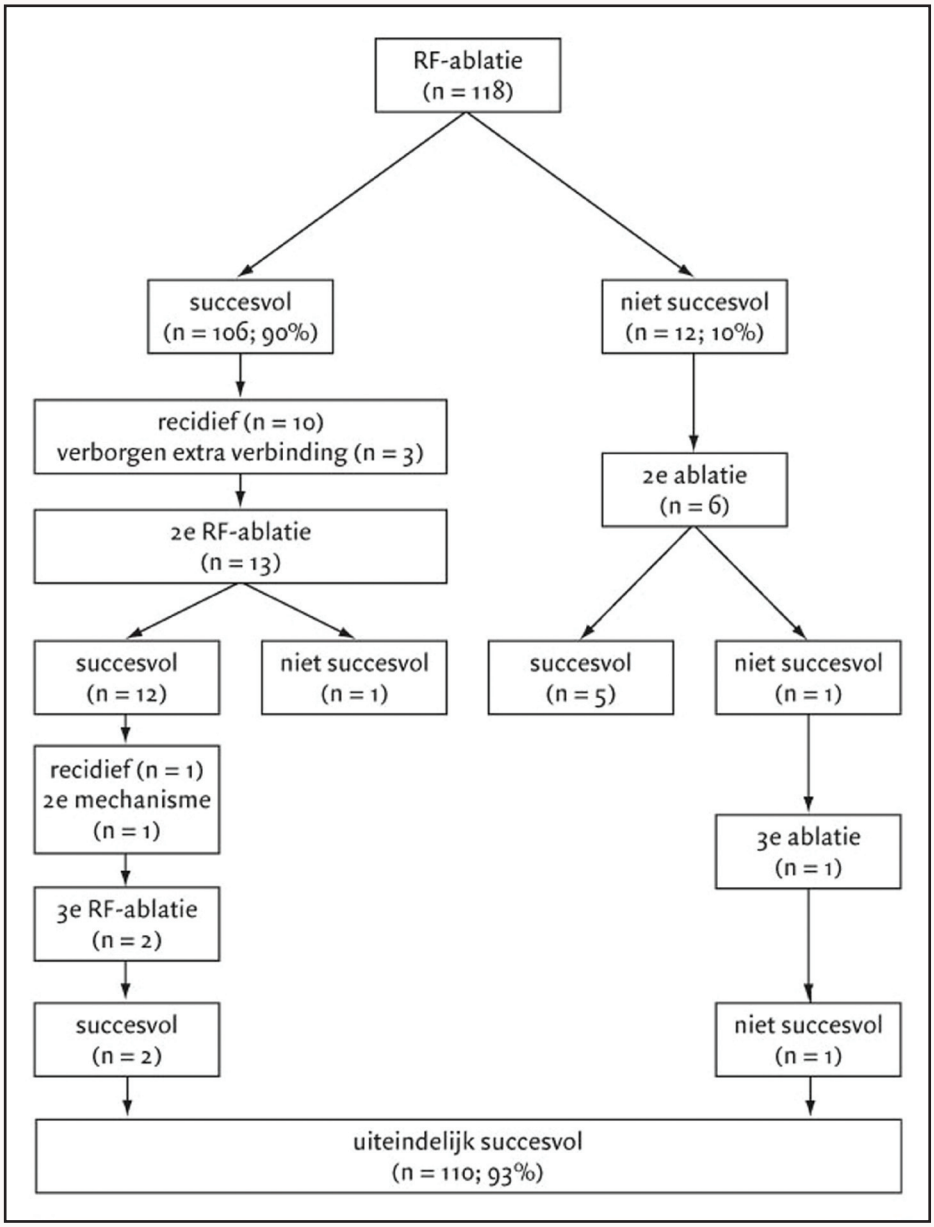

Figuur 3. Schematische weergave van het klinische beloop bij de 118 patiënten die een katheterablatie met radiofrequente energie ('RF-ablatie') hadden ondergaan in de periode 1 december 1992-31 mei 2004, Leids Universitair Medisch Centrum.

diagnose	aantal (%) patiënten*		
	totaal	succesvol behandeld	
		initieel†	uiteindelijk‡
atrio-ventriculaire 're-entry'-tachycardie	97	86 (89)	92 (95)
Wolff-Parkinson-White(WPW)-syndroom	51	44 (86)	48 (94)
verborgen extra verbinding	37	36 (97)	37 (100)
'permanent junctional reciprocating' tachycardie	6	5 (83)	5 (83)
Mahaim-tachycardie	3	1 (33)	2 (67)
AV-nodale re-entrytachycardie	9	9 (100)	9 (100)
intra-atriale re-entrytachycardie	8	7 (88)	7 (88)
ectopische-atriale tachycardie	4	4 (100)	4 (100)
ventriculaire tachycardie	4	2 (50)	2 (50)

Tabel 2. Succespercentages van katheterablatie met radiofrequente energie bij de 118 kinderen die deze hadden ondergaan in de periode 1 december 1992-31 mei 2004, Leids Universitair Medisch Centrum *4 patiënten hadden 2 verschillende aandoeningen en komen in meer dan 1 groep voor: 2 patiënten met AV-nodale re-entry tachycardie en ectopische-atriale tachycardie, 1 patiënt met een verborgen extra verbinding en WPW-syndroom, en 1 patiënt met WPW-syndroom en Mahaim-tachycardie. †Het initiële succespercentage werd gedefinieerd als het percentage RFablaties waarbij het aritmogene substraat met elektrofysiologisch onderzoek niet meer aantoonbaar was aan het einde van de behandeling. ‡Het uiteindelijke succespercentage werd gedefinieerd als het percentage patiënten dat na één of meer RF-ablaties zonder antiarrhythmica vrij was van recidieven en bij wie het aritmogene substraat met elektrofysiologisch onderzoek na afloop van de laatste behandeling niet meer aantoonbaar was.

Recidieven

Na 18 van de in totaal 125 initieel succesvolle RF ablaties (14%) deed zich een recidief voor. Recidieven traden gemiddeld 2,3 maanden (SD: 2,5) na een succesvolle RF ablatie op; 6 maanden na een succesvolle RF ablatie werden geen recidieven meer geobserveerd.

Recidieven na RF ablatie voor AVRT

Na 10 van de in totaal 101 initieel succesvolle RF ablaties voor AVRT (10%) deed zich een recidief voor. De Kaplan-Meier-analyse voor afwezigheid van recidief na een succesvolle RF ablatie voor AVRT is weergegeven in **Figuur 4**. Recidieven traden gemiddeld 1,8 maanden (SD: 1,5) na een succesvolle RF ablatie op.

Vroeg (december 1992-2000) versus laat tijdperk (2001-mei 2004)

In het vroege tijdperk (8,1 jaar) werden in totaal 69 RF ablaties uitgevoerd en in het late tijdperk (3,4 jaar) 71. Het percentage initieel succesvolle RF ablaties in het vroege tijdperk was 86 (59/69) en in het late 93 (66/71) (p = 0,154). De gemiddelde doorlichtingstijd in de late periode was significant lager dan in de vroege: 32,4 (SD: 22,1) versus 45,4 (SD: 28,2) min (p = 0,003). Ook de gemiddelde proceduretijd was in het late tijdperk significant lager dan in het vroege: 156,20 (SD: 60,9) versus 217,7 (SD: 93,7) min (p < 0,0001). Het percentage complicaties was in het vroege tijdperk 6 (4/69) en in het late 4 (3/71) (p = 0,670).

Samenhang van de leeftijd met de resultaten van RF ablatie

Tussen de groep kinderen < 10 jaar (n = 29; 25%) en de groep kinderen ≥ 10 jaar (n = 89; 75%) was geen verschil in het uiteindelijke totale succespercentage: 93 (27/29) en 93 (83/89) (p = 0,914). Hetzelfde gold voor het totale complicatierisico: 3 (1/29) versus 7 (6/89) (p = 0,680).

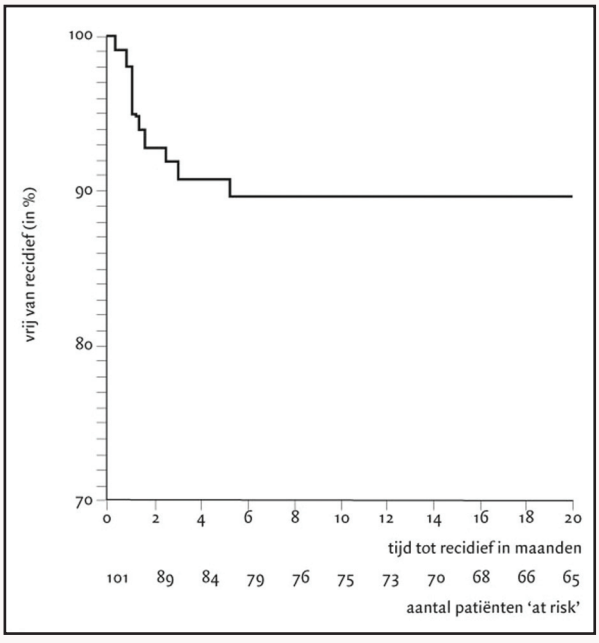

Figuur 4. Kaplan-Meier-analyse voor het vrij van recidief zijn na een geslaagde katheterablatie met radiofrequente energie wegens atrioventriculaire 're-entry'-tachycardieën (n = 101 ablaties bij 97 patiënten) in de periode 1 december 1992-31 mei 2004, Leids Universitair Medisch Centrum.

Beschouwing

In deze studie beschrijven wij de resultaten van RF ablatie bij kinderen na een gemiddelde follow-upduur van 4 jaar. Het merendeel van ons cohort (n = 97; 80%) bestond uit kinderen met een AVRT. Het uiteindelijke succespercentage binnen het gehele cohort was 93, waarbij 19 patiënten (16%) een tweede behandeling ondergingen en 3 van hen een derde. Het eerste recidief trad gemiddeld na 2,3 maanden (SD: 2,5) op en 6 maanden na een succesvolle RF ablatie werden geen nieuwe recidieven meer geobserveerd. Bij 2 kinderen trad een tweedegraads AV blok als belangrijke complicatie van de RF ablatieprocedure op.

Deze resultaten zijn vergelijkbaar met de kortetermijnresultaten van andere pediatrische studies in één centrum.[13, 15] In de multicenterstudie van de North American Pediatric Radiofrequency Catheter Ablation Registry, tot op heden het grootste onderzoek in de literatuur, vond men 3% belangrijke complicaties.[11]

Inmiddels neemt het complicatiepercentage met de groeiende ervaring verder af. Het complicatierisico van RF ablatie bij kinderen is aanzienlijk lager dan het risico op het optreden van levensbedreigende proaritmie bij chronisch gebruik van klasse-I- en klasse-III-antiarrhythmica of het potentiële risico van de hartritmestoornis zelf.[23-25] Zo had in onze studie 8% van de patiënten ernstige cardiomyopathie gekregen als gevolg van een chronische tachycardie of reanimatie ondergaan wegens atriumfibrillatie met snel kamervolgen bij het Wolff-Parkinson-White-syndroom.

Onlangs werd in een studie naar de langetermijnresultaten van RF ablatie bij 24 kinderen met een structureel normaal hart na een mediane follow-upduur van 10 jaar een uiteindelijk totaal succespercentage van 100 gerapporteerd. Bijna de helft (46%) van de patiënten onderging echter een tweede ingreep. Recidieven traden over het algemeen binnen 6 maanden op, terwijl bij 17% van de patiënten jaren na de RF ablatie nog recidieven optraden.[9]

Er bestaan belangrijke argumenten om met name bij jonge kinderen terughoudend te zijn bij het toepassen van RF ablatie. De kans op ernstige complicaties, waaronder ook sterfte, zou met name bij kinderen < 15 kg lichaamsgewicht verhoogd zijn,[10, 11, 18] hoewel deze bevinding in een recentere publicatie niet werd bevestigd.[8] In onze studie was geen verschil aantoonbaar in het succes- en complicatiepercentage tussen kinderen < 10 jaar en ≥ 10 jaar en ook bij de relatief beperkte groep jonge kinderen (< 2 jaar of < 15 kg lichaamsgewicht) verliepen de behandelingen succesvol en ongecompliceerd.

Uit een recente studie is gebleken dat de kans op ernstige complicaties na RF ablatie bij jonge kinderen samenhangt met de totale dosis RF stroom per kilogram lichaamsgewicht.[26] Bij deze jongste groep patiënten blijft voorzichtigheid derhalve geboden, mede gezien het gunstige spontane natuurlijke beloop van de meeste hartritmestoornissen bij kinderen < 1 jaar.[2, 4, 27] Door aanpassingen in de RF ablatietechniek, zoals het gebruik van slechts 1 of 2 kleine intracardiale katheters in combinatie met een slokdarmelektrode voor atriale stimulatie en een lagere hoeveelheid RF energie, kunnen de risico's op complicaties zoveel mogelijk verkleind worden.

Bij proefdieronderzoek met jonge biggen is aangetoond dat als gevolg van RF ablatie coronairlaesies kunnen ontstaan, hetgeen ook incidenteel bij jonge kinderen is gerapporteerd.[19, 20, 28, 29] Bovendien werd bij lammeren aangetoond dat RF laesies in immatuur myocard in grootte toe kunnen nemen gedurende de groei en aritmogene substraten zouden kunnen vormen.[21] Een belangrijke bevinding in onze studie is dat er ook op langere termijn geen klinische aanwijzingen zijn voor het optreden van nieuwe aritmieën als gevolg van de RF laesies in het groeiende hart of voor het ontstaan van vroege of late coronairlaesies na RF ablatie.

Een beperking van onze follow-up is dat er geen routinematige 24-uur-Holter-registraties vervaardigd zijn en dat de kinderen binnen onze cohort geen coronairangiografieën hebben ondergaan, waardoor het optreden van nieuwe aritmieën of het bestaan van subklinische coronairlaesies niet geheel uitgesloten kan worden. Tevens zou het aantal recidieven mogelijk onderschat kunnen zijn, daar de patiënt en/of de ouders, na de poliklinische controle 1 jaar na de RF ablatieprocedure, gevraagd werd zelf contact met ons op te nemen in het geval van recidiverende klachten.

Hoewel de gemiddelde röntgendoorlichtingstijd gedurende de studieperiode statistisch significant afgenomen is, blijft het risico op het ontstaan van maligniteiten zeker bij kinderen een punt van zorg. Het risico op het ontstaan van een maligniteit na het ondergaan van 1 uur röntgendoorlichting bij volwassenen bedraagt 0,1%.[30] De voortschrijdende ontwikkelingen op het gebied van non-fluoroscopische mappingtechnieken bieden echter perspectief op een verdere reductie van de röntgendoorlichtingstijd tijdens RF ablatieprocedures in de toekomst.

Conclusie

De ervaring die in de afgelopen jaren met RF ablatie bij kinderen is opgedaan, heeft in goede langetermijnresultaten geresulteerd. Ook bij jonge kinderen (< 10 jaar) is RF ablatie op lange termijn veilig en effectief. Dit biedt de ruimte om in gespecialiseerde centra ook deze groep patiënten curatief met RF ablatie te behandelen.

Belangenconflict

Geen gemeld.

Financiële ondersteuning

Geen gemeld.

Literatuur

1. Lubbers WJ, Losekoot TG, Anderson RH, Wellens HJ. Paroxysmal supraventricular tachycardia in infancy and childhood. *Eur J Cardiol.* 1974;2(1):91-99.

2. Bauersfeld U, Pfammatter JP, Jaeggi E. Treatment of supraventricular tachycardias in the new millennium--drugs or radiofrequency catheter ablation? *Eur J Pediatr.* 2001;160(1):1-9.

3. Weindling SN, Saul JP, Walsh EP. Efficacy and risks of medical therapy for supraventricular tachycardia in neonates and infants. *Am Heart J.* 1996;131(1):66-72.

4. Wren C. The presentation of arrhythmias. In: Wren C, Campbell, R.W.F., ed. *Paediatric cardiac arrhythmias.* New York: Oxgord University Press; 1996:1-15.

5. Wellens HJ. Application of radiofrequency energy as a new treatment method for arrhythmias. *Ned Tijdschr Geneeskd.* 1991;135(36):1624-1625.

6. Morady F. Catheter ablation of supraventricular arrhythmias: state of the art. *PACE.* 2004;27(1):125-142.

7. Van Hare GF, Velvis H, Langberg JJ. Successful transcatheter ablation of congenital junctional ectopic tachycardia in a ten-month-old infant using radiofrequency energy. *PACE.* 1990;13(6):730-735.

8. Blaufox AD, Felix GL, Saul JP, Registry PCA. Radiofrequency catheter ablation in infants </=18 months old: when is it done and how do they fare?: short-term data from the pediatric ablation registry. *Circulation.* 2001;104(23):2803-2808.

9. Collins KK, Chiesa NA, Dubin AM, Van Hare GF. Clinical outcomes of children with normal cardiac anatomy having radiofrequency catheter ablation > or =10 years earlier. *Am J Cardiol.* 2002;89(4):471-475.

10. Kugler JD, Danford DA, Deal BJ, Gillette PC, Perry JC, Silka MJ, Van Hare GF, Walsh EP. Radiofrequency catheter ablation for tachyarrhythmias in children and adolescents. The Pediatric Electrophysiology Society. *N Engl J Med.* 1994;330(21):1481-1487.

11. Kugler JD, Danford DA, Houston K, Felix G. Radiofrequency catheter ablation for paroxysmal supraventricular tachycardia in children and adolescents without structural heart disease. Pediatric EP Society, Radiofrequency Catheter Ablation Registry. *Am J Cardiol.* 1997;80(11):1438-1443.

12. Kugler JD, Danford DA, Houston KA, Felix G, Society PRARotPRARotPE. Pediatric radiofrequency catheter ablation registry success, fluoroscopy time, and complication rate for supraventricular tachycardia: comparison of early and recent eras. *J Cardiovasc Electrophysiol.* 2002;13(4):336-341.

13. Tanel RE, Walsh EP, Triedman JK, Epstein MR, Bergau DM, Saul JP. Five-year experience with radiofrequency catheter ablation: implications for management of arrhythmias in pediatric and young adult patients. *J Pediatr.* 1997;131(6):878-887.

14. Van Hare GF, Javitz H, Carmelli D, Saul JP, Tanel RE, Fischbach PS, Kanter RJ, Schaffer M, Dunnigan A, Colan S, Serwer G, Society PE. Prospective assessment after pediatric cardiac ablation: demographics, medical profiles, and initial outcomes. *J Cardiovasc Electrophysiol.* 2004;15(7):759-770.

15. Van Hare GF, Witherell CL, Lesh MD. Follow-up of radiofrequency catheter ablation in children: results in 100 consecutive patients. *J Am Coll Cardiol.* 1994;23(7):1651-1659.

16. Friedman RA, Walsh EP, Silka MJ, Calkins H, Stevenson WG, Rhodes LA, Deal BJ, Wolff GS, Demaso DR, Hanisch D, Van Hare GF. NASPE Expert Consensus Conference: Radiofrequency catheter ablation in children with and without congenital heart disease. Report of the writing committee. North American Society of Pacing and Electrophysiology. *PACE.* 2002;25(6):1000-1017.

17. Wren C. Catheter ablation in paediatric arrhythmias. *Arch Dis Child.* 1999;81(2):102-104.

18. Schaffer MS, Gow RM, Moak JP, Saul JP. Mortality following radiofrequency catheter ablation (from the Pediatric Radiofrequency Ablation Registry). Participating members of the Pediatric Electrophysiology Society. *Am J Cardiol.* 2000;86(6):639-643.

19. Bökenkamp R, Wibbelt G, Sturm M, Windhagen-Mahnert B, Bertram H, Hausdorf G, Paul T. Effects of intracardiac radiofrequency current application on coronary artery vessels in young pigs. *J Cardiovasc Electrophysiol.* 2000;11(5):565-571.

20. Paul T, Bökenkamp R, Mahnert B, Trappe HJ. Coronary artery involvement early and late after radiofrequency current application in young pigs. *Am Heart J.* 1997;133(4):436-440.

21. Saul JP, Hulse JE, Papagiannis J, Van Praagh R, Walsh EP. Late enlargement of radiofrequency lesions in infant lambs. Implications for ablation procedures in small children. *Circulation.* 1994;90(1):492-499.

22. de Groot NM, Schalij MJ. Treatment of intra-atrial reentry tachycardia by catheter ablation, using three-dimensional electro-anatomical map of the atrial activation pattern. *Ned Tijdschr Geneeskd.* 2001;145(25):1214-1218.

23. Bootsma M, van der Wall EE, Schalij MJ. Risk of ventricular fibrillation in patients with Wolff-Parkinson White syndrome. *Ned Tijdschr Geneeskd.* 2003;147(15):708-714.

24. Fish FA, Gillette PC, Benson DW. Proarrhythmia, cardiac arrest and death in young patients receiving encainide and flecainide. The Pediatric Electrophysiology Group. *J Am Coll Cardiol.* 1991;18(2):356-365.

25. Pfammatter JP, Paul T, Lehmann C, Kallfelz HC. Efficacy and proarrhythmia of oral sotalol in pediatric patients. *J Am Coll Cardiol.* 1995;26(4):1002-1007.

26. Blaufox AD, Paul T, Saul JP. Radiofrequency catheter ablation in small children: relationship of complications to application dose. *PACE.* 2004;27(2):224-229.

27. Case C. Radiofrequency catheter ablation of arrhythmias in infants and small children. *Prog Pediatr Cardiol.* 2000;11(1):77-82.

28. Bertram H, Bökenkamp R, Peuster M, Hausdorf G, Paul T. Coronary artery stenosis after radiofrequency catheter ablation of accessory atrioventricular pathways in children with Ebstein's malformation. *Circulation.* 2001;103(4):538-543.

29. Paul T, Kakavand B, Blaufox AD, Saul JP. Complete occlusion of the left circumflex coronary artery after radiofrequency catheter ablation in an infant. *J Cardiovasc Electrophysiol.* 2003;14(9):1004-1006.

30. Calkins H, Niklason L, Sousa J, el-Atassi R, Langberg J, Morady F. Radiation exposure during radiofrequency catheter ablation of accessory atrioventricular connections. *Circulation.* 1991;84(6):2376-2382.

Chapter 9

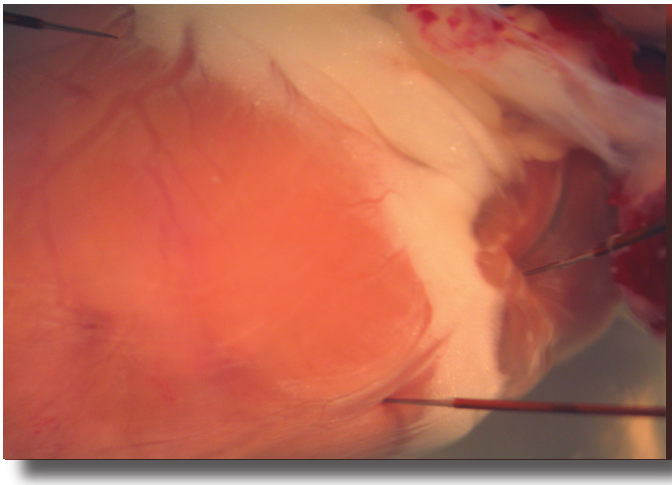

Denise P. Kolditz[1]
Nico A. Blom[2]
Regina Bökenkamp[2]
Martin J. Schalij[1]

[1]Department of Cardiology, Leiden University Medical Center
[2]Department of Pediatric Cardiology, Leiden University Medical Center

Low-Energy Radiofrequency Catheter Ablation as Therapy for Supraventricular Tachycardia in a Premature Neonate

Eur J Pediatr 2005;164(9):559-562

Abstract

A hydropic premature neonate was born at 32 weeks of gestation after successful direct fetal amiodarone therapy via cordocentesis for incessant supraventricular tachycardia. After birth the tachycardia could not be controlled despite high doses of amiodarone and flecainide and the patient developed severe respiratory and circulatory failure. After three weeks, weighing 2 kg, he underwent successful and uncomplicated radiofrequency catheter ablation of a left free-wall accessory pathway using low-energy RF application.

Introduction

Fetal hydrops associated with tachyarrhythmia results in high prenatal and postnatal morbidity and mortality.[1, 2] After failure of maternal drug therapy with either digoxin, sotalol or flecainide, direct amiodarone fetal therapy can be considered.[3, 4] After birth, supraventricular tachycardias usually respond well to antiarrhythmic drug therapy, although combined therapies are occasionally necessary to control the arrhythmia.[2, 5]

Accessory pathways form the most common substrate for tachycardia in fetuses and newborns and more than two-thirds of cases remain free of symptoms by the age of one year.[1, 6] Radiofrequency catheter ablation (RFCA) is rarely necessary in this age group and considerable concerns exist about RFCA in neonates.[7] In the present report we describe a successful radiofrequency catheter ablation procedure to control drug-refractory tachycardia in a 2 kg premature neonate only using low-energy RFCA.

Case report

At 24 weeks of gestation fetal tachycardia was diagnosed in a 30-year-old female. M-mode echocardiography demonstrated a regular tachycardia of 260 beats/min. with 1:1 atrio(A)ventricular(V) association and a short VA-time suggesting an atrioventricular reciprocating tachycardia. Despite combined maternal digoxin/flecainide therapy and later combined digoxin/sotalol therapy, tachycardia of 220 beats/min. persisted and severe fetal hydrops developed.

At 28 weeks of gestation, conversion to sinus rhythm was achieved by two direct fetal amiodarone injections via cordocentesis (10 mg and 15 mg) combined with a maternal amiodarone loading dose of 1.2 g/day for 48 hours. Additionally, fetal paracentesis was performed to reduce the amount of ascites. The fetus remained in sinus rhythm the following 4 weeks and the maternal amiodarone dose was reduced to 200 mg/day.

Figure 1. The boy with severe hydrops fetalis, weighing 1.7 kg, after delivery by caesarian section at 32 weeks of gestation (printed with parental informed consent).

Premature rupture of the membranes was the indication for a caesarian section at 32 weeks of gestation and a boy was born with severe hydrops (**Figure 1**). He required mechanical ventilation and developed idiopathic respiratory distress syndrome (IRDS). Thyroid suppletion was instituted for mild hypothyroidism, most probably due to the fetal amiodarone therapy. The electrocardiogram (ECG) at birth revealed normal sinus rhythm without pre-excitation but tachycardia recurred within 24 hours. The ECG showed regular small QRS complex tachycardia with retrograde negative P-waves in I, II and AVL, suggesting an orthodromic atrioventricular reciprocating tachycardia through a left free-wall accessory pathway (**Figure 2**).

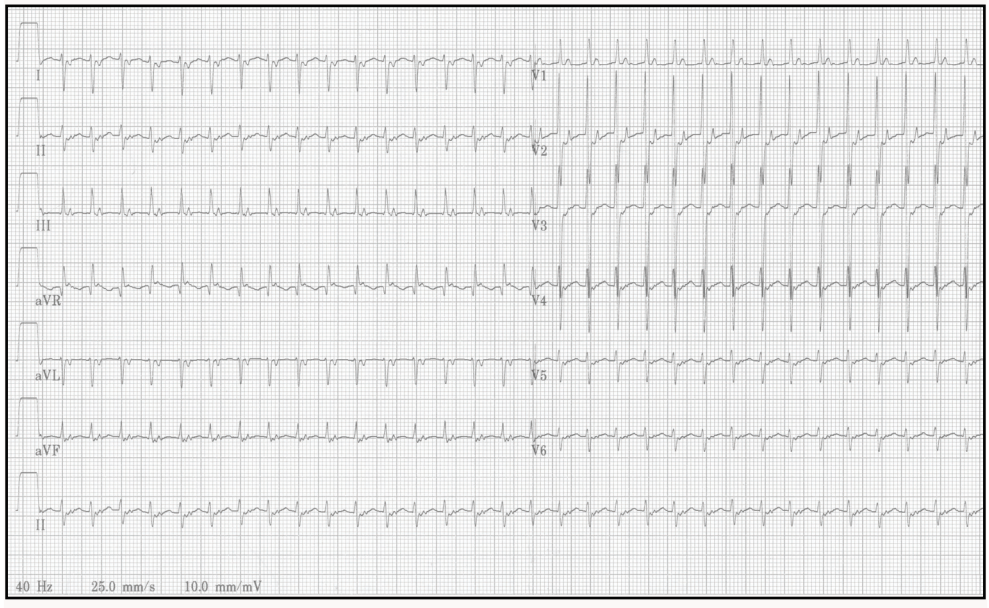

Figure 2. The electrocardiogram (ECG) 24 hours after birth revealing regular small complex tachycardia with retrograde negative P-waves in I, II and AVL, suggesting a left free-wall accessory pathway.

Combined therapy with digoxin and propranolol failed and intravenous amiodarone therapy (10mg/kg/day) was successfully re-instituted postnatally. Hydrops regressed and the boy, weighing 1.7 kg, was successfully weaned from the ventilator. However, incessant tachycardia (220 beats/min.) recurred and could not be controlled with high dose of amiodarone (20 mg/kg/day) eventually combined with flecainide (0.2 mg/kg/uur). The child developed severe congestive heart failure and required mechanical ventilation.

At 36 weeks of gestation radiofrequency catheter ablation was considered as ultimate therapy. At the time of the procedure, the child was three weeks of age and weighed 2 kg. A single standard 5 Fr, 4mm tip deflectable quadripolar catheter (RF Marinr, Medtronic Inc. Minneapolis, MN, USA) was introduced through the right femoral vein for mapping, pacing and ablation and a 5 Fr quadripolar electrode catheter (Josephson quadripolar catheter, Medtronic Inc.) was positioned into the esophagus for left atrial recordings and stimulation. The mapping catheter was easily positioned into the left atrium through a patent foramen ovale (**Figure 3A**).

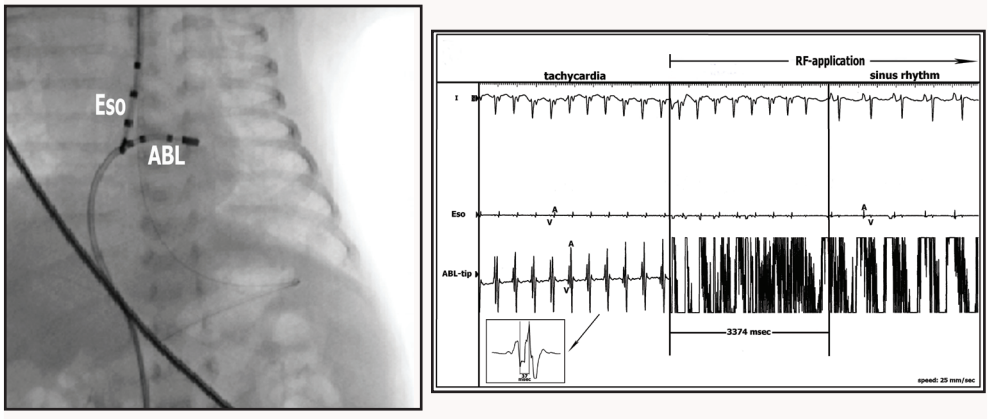

Figure 3. **A.** Radiograph recorded during the RFCA-procedure. A 5 Fr RFCA-catheter (ABL) was placed anterogradely through the patent foramen ovale and a second electrode catheter was placed in the esophagus (Eso) for atrial recordings and stimulation.
B. Mapping and radiofrequency catheter ablation during incessant tachycardia. The negative retrograde P-wave was visible in lead I of the surface-ECG. The esophagus-electrode showed both left ventricular (V) and left atrial (A) electrograms. The bipolar electrogram of the tip of the ablation catheter (ABL-tip) showed the earliest atrial activation and the shortest VA-interval (37 msec.) at the posterolateral part of the mitral ring. Radiofrequency energy immediately terminated tachycardia. Total RF-energy application time was 33 seconds. V-pacing demonstrated VA-dissociation.

Mapping was performed during incessant tachycardia (cycle length 310 ms.) and confirmed the diagnosis of orthodromic tachycardia through a left free-wall accessory pathway. The shortest VA-interval (37 msec.) during tachycardia was delineated as the most favorable site for ablation. Only one application of radiofrequency energy of 30 seconds with a temperature- and power limit of 55 ˚C and 25 W respectively, caused immediate termination of the tachycardia (**Figure 3B**) and subsequent ventricular pacing demonstrated VA-dissociation. Total procedural time was 35 minutes and fluoroscopy time was 6 minutes.

Post-procedural echocardiography showed an echodense "RFCA lesion" of the left atrium of 2 x 3 mm. just above the posterolateral part of the mitral ring (**Figure 4**). There was no mitral regurgitation or pericardial effusion. He was successfully weaned from the ventilator within one week but required oxygen therapy because of bronchopulmonary dysplasia for 8 months.

The echodense lesion in the left atrium could no longer be identified after the age of 3 months. Echocardiography (6 monthly) showed good systolic left ventricular function (shortening fraction 35%) and normal regional wall motions. Color flow Doppler echocardiography showed patency of the circumflex artery and no clinical symptoms nor electrocardiographic (ECG) findings of ischemia were found during follow-up. Thyroid suppletion was successfully discontinued at the age of 9 months and latest follow-up at 18 months showed normal psychomotor development.

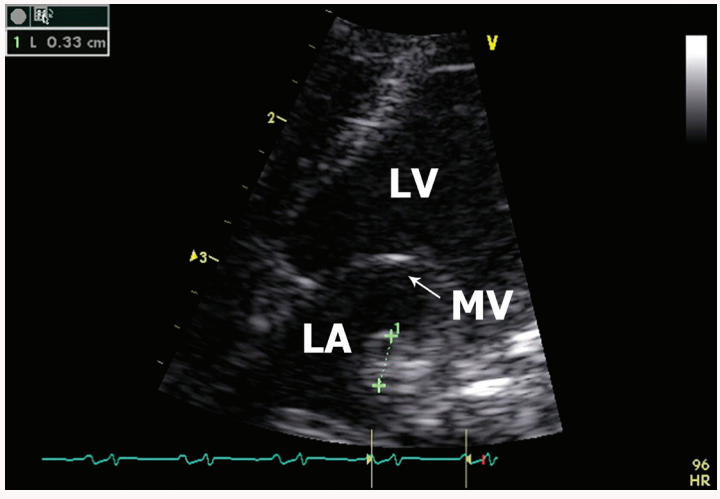

Figure 4. Post-procedural echocardiogram showing a echodense "RFCA-lesion" of the left atrium (LA) of 2 x 3 mm. just above the posterolateral part of the mitral ring. (LV = left ventricle, MV = mitral valve).

Discussion

The natural course of supraventricular tachycardia in fetuses or neonates is usually benign.[5] The most common tachyarrhythmias are those that involve accessory pathways that appear to resolve in more than sixty percent of cases by the time the child is 1 year of age.[1, 5, 6] RFCA is rarely indicated in this age group and should be restricted to cases in which Class Ic as well as Class III drugs are ineffective and the tachycardia causes hemodynamic compromise.[7]

There are significant concerns to perform RFCA in neonates and infants. Several studies have shown a greater complication-rate for RFCA in children weighing <15 kg,[8, 9] although this increased risks could not be confirmed in the most recent large series of the Pediatric RFCA Registry.[10]

However, the registry of a very small number of procedure-related late deaths after the ablation procedure suggests caution in the use of RFCA in young children.[8, 9, 11] Furthermore, both right and left coronary lesions have been reported during RFCA procedures in infants and young children.[12, 13] Experimental animal data have shown that RF lesions in the developing myocardium may have the potential to expand with time and effect coronary perfusion.[14-16]

The previously described RFCA procedures in neonates and infants in literature, were usually performed with 5 Fr or 7 Fr, 4 mm tip RF catheters and standard RFCA applications of 25 to 50 W power-limit in a temperature-controlled mode of 60 to 70 °C of 15 to 30 seconds.[12, 17-19]

We describe a premature hydropic neonate with respiratory and circulatory failure as a result of a drug-refractory tachycardia, involving a left free-wall accessory pathway. This patient was converted to sinus rhythm in utero by direct fetal amiodarone therapy via cordocentesis. Incessant tachycardia recurred shortly after birth despite combined amiodarone and flecainide therapy and RFCA was indicated as the last remaining option.

This case is one of the youngest premature neonates in whom RFCA has been performed. RFCA was successful with a 5 Fr, 4 mm tip RF catheter using one single RF application of 30 seconds with a power limit of 30 W in a temperature-controlled mode of 55 ˚C. Despite the single low-energy RF application post-procedural echocardiography demonstrated a clear 2 x 3 mm. echodens lesion of the left atrium. Follow-up echocardiography showed normal left ventricular function and no regional wall motion abnormalities.

At our institution the current practice is to use this low-energy RFCA approach in newborns and young infants < 10 kg as initial attempt to minimize

the risk of valvulair damage and coronary artery lesions. A recent study by Blaufox et al. showed that complications of RFCA in small infants appear to be related to the RF dose indexed for body size and this study also emphasises the importance to reduce the RF dose in this very young age group.[20] A further reason to minimize the RF lesion in small neonatal hearts comes from animal experiments showing an increase of RF lesion size in the immature heart of lambs during growth.[16]

In neonates and young infants RFCA is rarely indicated and should only be performed with extreme caution. In addition to the use of small 5 Fr RF catheters and a limited number of intracardiac catheters, low-energy RF application could further reduce the risk of major complications.

References

1. Naheed ZJ, Strasburger JF, Deal BJ, Benson DW, Gidding SS. Fetal tachycardia: mechanisms and predictors of hydrops fetalis. *J Am Coll Cardiol.* 1996;27(7):1736-1740.
2. Simpson JM, Sharland GK. Fetal tachycardias: management and outcome of 127 consecutive cases. *Heart.* 1998;79(6):576-581.
3. Jouannic JM, Delahaye S, Fermont L, Le Bidois J, Villain E, Dumez Y, Dommergues M. Fetal supraventricular tachycardia: a role for amiodarone as second-line therapy? *Prenat Diagn.* 2003;23(2):152-156.
4. Kleinman CS, Nehgme RA. Cardiac arrhythmias in the human fetus. *Pediatr Cardiol.* 2004;25(3):234-251.
5. Bauersfeld U, Pfammatter JP, Jaeggi E. Treatment of supraventricular tachycardias in the new millennium--drugs or radiofrequency catheter ablation? *Eur J Pediatr.* 2001;160(1):1-9.
6. Ko JK, Deal BJ, Strasburger JF, Benson DW. Supraventricular tachycardia mechanisms and their age distribution in pediatric patients. *Am J Cardiol.* 1992;69(12):1028-1032.
7. Friedman RA, Walsh EP, Silka MJ, Calkins H, Stevenson WG, Rhodes LA, Deal BJ, Wolff GS, Demaso DR, Hanisch D, Van Hare GF. NASPE Expert Consensus Conference: Radiofrequency catheter ablation in children with and without congenital heart disease. Report of the writing committee. North American Society of Pacing and Electrophysiology. *PACE.* 2002;25(6):1000-1017.
8. Kugler JD, Danford DA, Deal BJ, Gillette PC, Perry JC, Silka MJ, Van Hare GF, Walsh EP. Radiofrequency catheter ablation for tachyarrhythmias in children and adolescents. The Pediatric Electrophysiology Society. *N Engl J Med.* 1994;330(21):1481-1487.
9. Kugler JD, Danford DA, Houston K, Felix G. Radiofrequency catheter ablation for paroxysmal supraventricular tachycardia in children and adolescents without structural heart disease. Pediatric EP Society, Radiofrequency Catheter Ablation Registry. *Am J Cardiol.* 1997;80(11):1438-1443.
10. Blaufox AD, Felix GL, Saul JP. Radiofrequency catheter abltion in infants <18 months old: when is it done and how do they fare ? *Circulation.* 2001;104:2803-2808.
11. Schaffer MS, Gow RM, Moak JP, Saul JP. Mortality following radiofrequency catheter ablation (from the Pediatric Radiofrequency Ablation Registry). *Am J Cardiol.* 2000;86:639-643.

12. Bertram H, Bökenkamp R, Peuster M, Hausdorf G, Paul T. Coronary artery stenosis after radiofrequency catheter ablation of accessory atrioventricular pathways in children with Ebstein's malformation. *Circulation.* 2001;103(4):538-543.

13. Paul T, Kakavand B, Blaufox AD, Saul JP. Complete occlusion of the left circumflex coronary artery after radiofrequency catheter ablation in an infant. *J Cardiovasc Electrophysiol.* 2003;14(9):1004-1006.

14. Bökenkamp R, Wibbelt G, Sturm M, Windhagen-Mahnert B, Bertram H, Hausdorf G, Paul T. Effects of intracardiac radiofrequency current application on coronary artery vessels in young pigs. *J Cardiovasc Electrophysiol.* 2000;11(5):565-571.

15. Paul T, Bökenkamp R, Mahnert B, Trappe HJ. Coronary artery involvement early and late after radiofrequency current application in young pigs. *Am Heart J.* 1997;133(4):436-440.

16. Saul JP, Hulse JE, Papagiannis J, Van Praagh R, Walsh EP. Late enlargement of radiofrequency lesions in infant lambs. Implications for ablation procedures in small children. *Circulation.* 1994;90(1):492-499.

17. Brugada J, Closas R, Ordóñez A, Mabrok M, Grecu M, Mercé J, Mortera C. Radiofrequency catheter ablation of an incessant supraventricular tachycardia in a premature neonate. *PACE.* 2002;25(5):866-868.

18. Osborn DA, Lau KC, Uther JB, Coughtrey H, Rochefort MJ. Radiofrequency catheter ablation in a haemodynamically compromised premature neonate with hydrops fetalis. *J Paediatr Child Health.* 1999;35(4):406-408.

19. Berul CI, Hill SL, Wang PJ, Marx GR, Fulton DR, Estes NA. Neonatal radiofrequency catheter ablation of junctional tachycardias. *J Interv Card Electrophysiol* 1998;2(1):91-100.

20. Blaufox AD, Paul T, Saul JP. Radiofrequency catheter ablation in small children: relationship of complications to application dose. *PACE.* 2004;27(2):224-229.

Chapter

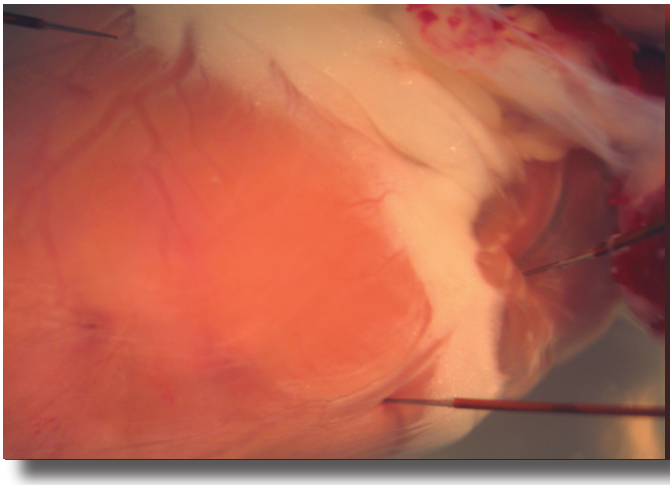

10

Denise P. Kolditz[1,2]

[1]Department of Cardiology, Leiden University Medical Center
[2]Department of Anatomy and Embryology, Leiden University Medical Center

Summary, Conclusions & Future Perspectives

Samenvatting, Conclusies & Toekomstperspectieven

Summary, Conclusions & Future Perspectives

Summary

The General Introduction in **Chapter 1** of this thesis provides an overview of structural cardiogenesis and the development of the cardiac conduction system (CCS) in avians (with references to equivalent mouse and human developmental timelines). Next, developmental transitions in impulse propagation and the construction of the individual components of the specialized CCS and the atrioventricular node (AVN) in particular, are shortly outlined. Current concepts on the transitions in ventricular activation sequences during cardiogenesis are subsequently discussed, preceded by a description of the changes in electrocardiograms (ECGs) during embryogenesis. Thereafter, contemporary knowledge on the development of the isolating annulus fibrosis, the key structure involved in accessory pathway (AP) persistence, in relation to general CCS development is reviewed. Subsequently, relevant general characteristics of the different animal models and the immunohistochemical markers used in this thesis are briefly outlined. Following the description of the structural basics of cardiogenesis, attention is focused on current knowledge of clinical SVTs in neonates and children and the treatment of these arrhythmias.

After the General Introduction, this thesis is divided in 3 main parts. In **PART I** of this thesis, both the (patho) physiological development of the isolating annulus fibrosus cordis and the etiological origin of clinical AP mediated atrioventricular (AV) reentrant tachycardia (AVRT) in children and adults is analyzed in experimental animal (quail and mouse) models and human histological sections. Subsequently, **PART II** of this thesis describes historical and contemporary concepts on the ontogeny of the AVN, followed by an experimental (quail/chick) study postulating a new concept on the developmental origin of the AVN and in particular the slow pathway of the AVN in relation to the etiology of AV nodal reentrant tachycardia (AVNRT). Finally, in **PART III** of this thesis therapeutical clinical issues in pediatric supraventricular tachycardia (SVT) will be outlined.

PART I

In **Chapter 2**, the physiological development of the isolating annulus fibrosus cordis was studied in the Japanese quail (*Coturnix coturnix japonica*) model. Ventricular activation patterns were deducted from *ex-ovo* extracellular

electrogram recordings in both the embryonic (n=80; HH stage 30-44) and adult (n=6; 5-6 months old) quail heart and correlated to the developmental morphology of the insulating AV annulus. Functionally, premature activation of the ventricular base indicating impulse propagation through persistent APs bypassing the AVN was found to remain possible at near-hatching stages of quail development. Morphological data in 16 embryonic and 1 adult quail heart confirmed this functional analysis by demonstrating persistent muscular AV connections coursing through the fibrous annulus in the embryonic heart until the last stages of development, while the adult heart demonstrated complete fibrous annular isolation. Longitudinal analysis revealed that these persistent APs decreased both in number ($p=0.004$) and width ($p=0.179$) at increasing developmental stages and were mainly found in the posteroseptal region of the heart. Furthermore, the region of these persistent APs was found to stain positive for periostin, a non-myocardial marker used to visualize cells with a fibrous identity, suggesting that these pathways eventually loose their myocardial phenotype, indicating an extended physiological process of perinatal completion of AV ring isolation. Results from this study support the hypothesis that persistent APs bypassing the AVN remain present and functional at late post-septated stages of embryonic development, possibly providing a physiological substrate for transient AVRTs in postnatal life, which is suggested to provide an etiological explanation for the clinical observation that AVRTs in human neonates are known to spontaneously disappear before the age of one year in the vast majority of cases.

In **Chapter 3**, the pathological development of the isolating annulus fibrosus cordis was studied in a Japanese quail (*Coturnix coturnix japonica*) model in which the migration of Epicardium-Derived-Cells (EPDCs) was mechanically inhibited by inserting a small piece of eggshell membrane between the dorsal wall of the embryonic HH stage 15-18 heart and the pericardial villi by *in-ovo* microsurgery. After reincubation, *in-ovo* electrocardiograms (ECGs) were subsequently recorded in normal (n=12) and EPDC-inhibited (n=12) HH stage 38-42 quail eggs. Additionally, ventricular activation patterns were deducted from *ex-ovo* extracellular electrogram recordings in both normal (n=45) and EPDC-inhibited (n=12) quail hearts at HH stages 38-42 and correlated to the developmental morphology of the insulating atrioventricular (AV) annulus. Functionally, in a subgroup of EPDC-inhibited embryos *in-ovo* ECGs demonstrated the 3 main electrocardiographic features of ventricular preexcitation syndromes: 1) a short

PR-interval, 2) a delta wave and 3) a prolonged QRS-complex. Furthermore, *ex-ovo* electrograms demonstrated premature activation of the ventricular base in all EPDC-inhibited hearts. Morphologically, the presence of posteroseptal APs was reconfirmed in normal quail hearts and was also confirmed in the EPDC-inhibited hearts. The EPDC-inhibited hearts however additionally demonstrated relatively broad APs in the right and left lateral free wall regions. Periostin staining was found in the regions where EPDCs are known to be present, for example in the epicardium, the endocardial AV cushions, the epicardial AV sulcus, the atrial and ventricular subendocardium, the interstitial fibroblasts and around the AV junction. While the posteroseptal APs stained positive for periostin, the broad lateral APs in EPDC-inhibited hearts were periostin negative. EPDCs thus seem essential for proper formation of the isolating annulus fibrosis, since inhibition of EPDC-migration during cardiogenesis results in marked defects in the annulus fibrosis with persistence of broad APs, functionally giving rise to ventricular preexcitation. While under physiological conditions small septal APs in the wildtype heart temporarily remain functionally active, broad lateral APs in the EPDC-inhibited heart might provide a pathological substrate for postnatally persistent APs and AVRTs into childhood or adult life.

Following this experimental study, an editorial in response to the experimental data described in this chapter written by Siew Yen Ho from the Department of Cardiac Morphology and the National Heart & Lung Institute of the Imperial College London and the Royal Brompton Hospital in the United Kingdom, is presented to provide additional background of state-of-the art knowledge on APs from a developmental point of view.

In **Chapter 4**, the physiological development of the isolating annulus fibrosus cordis was studied in the wildtype mouse (strain: C57B16/Jico and CD1) model to extrapolate avian data to mammalian development. Ventricular activation patterns were deducted from *ex-ovo* extracellular electrogram recordings in the 11.5-18.5 dpc embryonic (n=48) mouse heart and correlated to the morphology of the developing AV annulus in all hearts (n=48). In this study, the annulus fibrosis was shown to develop in the AV junctional myocardium, which was devoid of connexin-43 (Cx43). Similarly to the embryonic avian heart, persistent APs giving rise to premature activation of the ventricular base could also be found during mouse heart development. These persistent APs were devoid of Cx43, indicating an AV junctional myocardial origin, and were at early post-septated

stages mainly found around both the mitral and tricuspid orifice, while at late post-septated stages AP number had significantly ($p<0.001$) decreased around the mitral valve annulus. Similar to avians, periostin expression was found in the epicardium, the endothelial lining of the ventricular and atrial trabeculae, the subendocardial cushions, the interstitial fibroblast and around the AV junction. In contrast to the avian heart, in the mouse heart periostin expression could not be found in the Cx43 negative cardiomyocytes of the AP itself, while high levels of periostin were found in the fibroblasts adjacent to or in the APs. While these persistent APs significantly decreased in number ($p=0.003$) and size ($p=0.035$) at consecutive developmental stages, APs could still be found at late post-septated stages of mammalian heart development. Similarly to avian cardiogenesis, the physiological perinatal presence of APs in the mammalian heart, may provide transient substrates for neonatal AVRT.

In **Chapter 5**, the presence and specific locations of accessory pathways (APs) were systematically investigated in relation to the physiological developmental morphology of the isolating annulus fibrosis in human cardiogenesis. Immunohistochemical sections of 45 human embryonic, fetal and neonatal hearts from 4 to 36 weeks of development (avians ~HH 14-46, mouse ~E 10-19) were analyzed for AP number and location. While the annulus fibrosis was already laid down around 10 to 11 weeks of human gestation (avians ~ HH 21-27, mouse ~ E 12.5-13.5), numerous APs crossing the isolating AV ring could still be found mainly at both the left and right lateral AV junction up to the end of the second trimester of pregnancy. In the second and third trimester, the left AV annulus became firmly isolated by a thick layer of fibrous tissue, while the right AV annulus only demonstrated weak isolation frequently consisting only of very thin layers of fibrous tissue. As a consequence, up to 20 weeks of human gestation (avians ~HH 40, mouse ~E 17) APs near the lateral side of the tricuspid valve remained present. These right-sided APs frequently seemed to be located in close proximity to the right AV ring bundle, which is part of the temporary embryological specialized AV conduction axis. Furthermore, small myocardial extensions crossing the isolating annulus fibrosis connecting the developing AVN with the ventricular septal myocardium were found, remaining present until birth corresponding to previously described phenomenon of foetal dispersion of the AVN. In this study we confirmed our data from previous avian and mammalian studies and concluded that in human embryos isolation of the annulus fibrosis is normally completed postnatally, leaving mostly right-sided

persistent APs in the foetal heart which may act as substrates for transient AVRT in foetuses or neonates.

PART II

In **Chapter 6**, a review of historical and contemporary knowledge on the anatomy, physiology and ontogeny of the AVN and its atrial inputs is provided. Furthermore, structural AV nodal development and the cellular electrophysiology of the developing AV junction in relation to the adult AVN and the concept of AV nodal conduction dichotomy are discussed. While the electrophysiological substrates for AVNRT are well known, the anatomical correlates forming the reentry circuit have still remained incompletely understood. Although recent marker studies have provided some clues to the developmental origin of the AVN, its physiology, structural boundaries and ontogeny still remain puzzling.

This review is followed by **Chapter 7**, describing an experimental avian (quail and chick) study, in which a new concept on the developmental origin of the AVN is postulated. In this study, spatiotemporal changes in atrial activation sequences in the embryonic avian (*Japanese quail* and *white leghorn chick*) heart (HH stages 19-36, n=96) were correlated to developmental morphology (n=64). Around HH stage 19-22, bilateral morphologically distinct myocardial regions could be identified surrounding the proximal myocardial part of the left cardinal vein (LCV) and the proximal myocardial part of the right cardinal vein (RCV). These bilateral regions were both characterized by MLC2a positivity, Nkx2.5 negativity and relatively low levels of Cx43, Nav1.5 and glycogen compared to the surrounding myocardium. Although the proximal myocardial part of the right cardinal vein (RCV) corresponds to the primordium of the sinoatrial node (SAN), the proximal myocardial part of the left cardinal vein (LCV) was hypothesized to contribute to the developing AV nodal tissues. Until HH stage 27, the distinct LCV tissues were positioned caudodorsally to the left atrium and functionally a left-sided dominant pacemaker could still be found in a considerable number of cases (21%), while unilateral impulse initiation was already expected in the SAN region in the right atrium. After HH stage 28, impulse initiation in the left atrium could however no longer be found, perfectly correlating to the morphological observation that around HH stage 29-30 the LCV was already transposed to the right and submerged in the right atrium to become the coronary sinus (CS), while the myocardium surrounding the proximal LCV became positioned around the CS ostium in the slow pathway region of the adult AVN. In this study, we

demonstrated that the LCV tissues provide an important functional contribution to the AVN Anlagen in the slow pathway region.

PART III

In **Chapter 8**, the long-term results of radiofrequency catheter ablation (RF ablation) in 118 paediatric patients, who underwent 140 RF ablation procedures for 122 substrates of supraventricular arrhythmias, were analyzed retrospectively. Indications for RF ablation were: failure or side effects of antiarrhythmic medication (45%), patient/parent choice (45%), cardiomyopathy or life-threatening arrhythmia (8%), and impending surgery for congenital heart defects (2%). In this study, we concluded that the long-term outcome of pediatric patients who underwent RF ablation was favorable in terms of success, recurrence and complication rates. Additionally, RF ablation in young children (< 10 years) was found to be as safe and effective as RF ablation procedures in older children and adolescents (10-18 years). These results demonstrate that it is also possible to curatively and safely treat this young group of pediatric patients with RF ablation in specialized centers.

Finally, in **Chapter 9**, an illustrative case report of incessant accessory pathway (AP) mediated SVT in a premature neonate with hydrops foetalis, is presented. While RF ablation in neonates and young infants is rarely indicated and only should be performed with extreme caution, in this case RF ablation was indicated as the last remaining option. A hydropic premature neonate was born at 32 weeks of gestation after successful direct fetal amiodarone therapy via cordocentesis for incessant supraventricular tachycardia. After birth tachycardia could not be controlled despite high doses of amiodarone and flecainide and the patient developed severe respiratory and circulatory failure. After three weeks, weighing 2 kg, he underwent successful and uncomplicated RF ablation of a left free-wall accessory pathway using low-energy RF application.

Conclusions

- Accessory pathways (APs) bypassing the isolating annulus fibrosis and atrioventricular node (AVN) are structural remnants of the embryonic AV junctional myocardium and remain morphologically present and functional in avian and mammalian hearts at late post-septated stages of embryonic development and might provide a transient physiological substrate for AV reentrant tachycardia (AVRT) in perinatal life.

- Epicardium-Derived-Cells (EPDCs) are essential for proper formation of the isolating annulus fibrosis.

- Inhibition of EPDC-migration during cardiogenesis results in marked defects in the isolating annulus fibrosis with persistence of broad APs, functionally resulting in ventricular preexcitation, possibly providing a pathological mechanism for postnatally persistent APs and AVRTs into childhood or adult life.

- Periostin is a profibrogenic extracellular matrix protein strongly expressed in collagen-rich fibrous connective tissues. Expression of periostin in the annulus fibrosis in the region around myocardial APs in the avian and mammalian developing heart, seems to indicate their ultimate perinatal fate.

- In humans, up to 20 weeks of gestation, APs remain present and are mainly found around the tricuspid valve annulus and are frequently located in close proximity to the right AV ring bundle, which is part of the temporary embryological specialized AV conduction axis.

- In the developing avian heart bilateral functional pacemakers are temporarily present in the right and left cardinal vein myocardium, while ultimately the right sinoatrial nodal (SAN) primordium becomes the prevailing pacemaker.

- The myocardium surrounding the proximal part of the left cardinal vein (LCV) in the embryonic avian heart provides an important contribution to the slow pathway region of the developing heterogeneous AVN.

- The long-term outcome of pediatric patients who underwent RF ablation is favorable in terms of success, recurrence and complication rate.

- While RF ablation in neonates and young infants (<10 years of age) is rarely indicated and only should be performed with extreme caution, RF ablation can safely be indicated as a last remaining option in experienced centers.

Future Perspectives

By studying avian, mammalian and human cardiogenesis we have been able to unravel some clues on the physiological and pathological development of the isolating annulus fibrosis and the atrioventricular node (AVN). From these studies it is clear that with respect to the developing annulus fibrosis and cardiac conduction system (CCS), physiology and pathology are divided by a very thin line. While we demonstrated that normally isolation of the annulus fibrosis is completed postnatally, established an essential role for EPDCs in normal annulus fibrosis development, postulated a new concept on AV nodal development and identified (immuno)histochemical markers such as PAS-staining, the antibodies MLC2a, Nkx2.5, periostin, Cx43 and Nav1.5, suited to study these processes, several aspects of normal and abnormal annulus fibrosis formation and AV nodal development remain unanswered. Although we analyzed the developmental process of annulus fibrosis formation in both avian and mammalian models and extrapolated these data to human sections, it remains to be determined how the postulated functional implications can be translated to clinically relevant issues. Furthermore, the conundrum of whether accessory pathways (APs) presenting later in life also represent postnatally persistent APs temporarily remaining functionally quiescent or represent *de novo* occurring APs growing through newly developed holes in the annulus fibrosis, still remains.

To tackle these and other questions, future research in this field will be aimed at more elaborate studies of atrial and ventricular activation patterns in the developing and adult heart by using Multi-Electrode-Array (MEA) recordings and optical mapping with voltage sensitive dyes. Knowledge of the cellular electrophysiology of the persistent APs and postulated AV nodal primordial tissues, described in this thesis, by analyzing intracellular electrophysiology with patch clamping would further aid in our understanding of the functional implications of current and future experimental findings. Future research will furthermore be aimed at the application of (new) genetically engineered animal models (such as the podoplanin-KO and Shox2-KO mouse model) and identification and exploration of the expression of (new) myocardial (such as Nkx2.5) and CCS markers (such as Islet-1 and Id-2) and their interaction.

The studies described in this thesis have illustrated that in future research the analysis of structure-function relations is key to unraveling the developmental mechanisms underlying annulus fibrosis formation, AP persistence and AV nodal development and will provide a translational benchmark to successfully interpret clinically relevant aspects in cardiac arrhythmias.

With respect to the clinical research on pediatric supraventricular tachycardias and therapeutic options described in this thesis, currently ongoing large prospective pediatric studies will provide the next step and more insight in evaluation of the clinical presentation of pediatric SVTs and treatment strategies in this specific age group.

Samenvatting, Conclusies & Toekomstperspectieven

Samenvatting

De algemene inleiding in **Hoofdstuk 1** van dit proefschrift geeft een overzicht van de structurele cardiogenese en de ontwikkeling van het cardiale geleidingssysteem in het vogelmodel (met referenties naar equivalente ontwikkelingsstadia in het muismodel en de mens). Vervolgens worden de ontwikkelingsbiologische transities in de voortgeleiding van de elektrische impuls en de aanleg van de verschillende elementen van het gespecialiseerde geleidingssysteem en met name de atrioventriculaire knoop (AV knoop) uiteengezet. Aansluitend worden de veranderingen in het embryonale elektrocardiogram tijdens de embryogenese en de huidige ideeën betreffende de transities in ventriculaire activatiesequenties tijdens de cardiogenese besproken. Daarna wordt de huidige kennis van de ontwikkeling van de isolerende annulus fibrosis, een structuur die belangrijk is bij het persisteren van accessoire verbindingen, in relatie tot de ontwikkeling van het gespecialiseerde geleidingssysteem, bediscussieerd. Vervolgens worden relevante algemene karakteristieken van de verschillende diermodellen en de (immuno)histochemische markers (antilichamen), die zijn gebruikt in de experimentele studies beschreven in dit proefschrift, uiteengezet. Na deze beschrijving van de structurele basis van de cardiogenese, volgt er een uiteenzetting over de huidige klinische kennis betreffende supraventriculaire tachycardieën (SVTs) bij neonaten en kinderen en de behandeling van deze ritmestoornissen.

Na de algemene inleiding, is dit proefschrift verdeeld in 3 delen. In **DEEL I** van dit proefschrift, wordt zowel de fysiologische als de pathofysiologische ontwikkeling van de isolerende annulus fibrosus cordis en de etiologie van klinische door accessoire verbindingen gemedieerde atrioventriculaire (AV) reentry tachycardieën (AVRTs) bij kinderen en volwassenen structureel en functioneel geanalyseerd in verschillende experimentele diermodellen (kwartels, kippen en muizen) en in humane histologische en immunohistochemische coupes. Daarna worden in **DEEL II** van dit proefschrift allereerst de historische en huidige opvattingen betreffende de ontogenese van de AV knoop besproken. Aansluitend wordt een experimentele studie (in het kwartel en kipmodel) gepresenteerd, waarin een nieuw concept betreffende de ontwikkelingsbiologische oorsprong van de AV knoop en het slow pathway gebied van de AV knoop in relatie tot de etiologie van AV nodale reentry tachycardieën (AVNRTs) wordt gepostuleerd.

Afsluitend, worden in **DEEL III** van dit proefschrift therapeutische en andere klinische aspecten van SVTs bij kinderen besproken.

DEEL I

In **Hoofdstuk 2**, werd de fysiologische ontwikkeling van de isolerende annulus fibrosus cordis bestudeerd in de Japanse kwartel (*Coturnix coturnix japonica*). Ventriculaire activatiesequenties werden afgeleid van *ex-ovo* extracellulair opgenomen electrogrammen in zowel het embryonale (n=80; HH stadium 30-44) als volwassen (n=6; 5-6 maanden) kwartelhart en gecorreleerd aan de ontwikkelingsbiologische morfologie van de isolerende annulus fibrosis. Functioneel bleek premature activatie van de ventriculaire basis als uiting van impuls voortgeleiding door persisterende accessoire verbindingen, op te kunnen treden tot de laatste stadia van de embryonale kwartel ontwikkeling. Morfologische data verkregen uit 16 embryonale en 1 volwassen kwartelhart bevestigde de functionele data en liet persisterende musculaire AV verbindingen door gaten in de isolerende annulus zien, terwijl in het volwassen hart complete continuïteit in de fibreuze annulus geobserveerd werd. Longitudinale analyse toonde aan dat deze persisterende accessoire verbindingen zowel in aantal ($p=0.004$) als in volume ($p=0.179$) afnamen met toenemend ontwikkelingsstadium en voornamelijk in de posteroseptale regio van het embryonale hart gelokaliseerd waren. Deze persisterende accessoire verbindingen bleken positief te kleuren voor het proteïne periostin, een non-myocardiale marker die gebruikt werd om cellen met een fibreuze identiteit te visualiseren, wat suggereert dat deze verbindingen uiteindelijk hun fibreuze identiteit zullen verliezen en daarmee aangeeft dat het proces van AV ring isolatie onder fysiologische omstandigheden pas postnataal gecompleteerd wordt. De resultaten van deze studie ondersteunen de hypothese dat persisterende accessoire verbindingen die de AV knoop zowel morfologisch als elektrofysiologisch passeren, structureel en functioneel aanwezig kunnen blijven tot op late post-gesepteerde stadia van de embryonale hartontwikkeling en op deze manier een fysiologisch substraat voor voorbijgaande AVRTs in het postnatale leven zouden kunnen vormen, wat mogelijk een etiologische verklaring zou kunnen geven voor de klinische observatie dat AVRTs in humane neonaten in de meerderheid van de gevallen spontaan lijken te verdwijnen voor de leeftijd van 1 jaar.

In **Hoofdstuk 3**, werd de pathofysiologische ontwikkeling van de isolerende annulus fibrosus cordis bestudeerd in een experimenteel model in de Japanse

kwartel (*Coturnix coturnix japonica*), waarin de migratie van 'Epicardium-Derived-Cells' (EPDCs) mechanisch geïnhibeerd werd door de positionering van een klein stukje eierschaalmembraan tussen de dorsale wand van het embryonale kwartelhart en de pericardiale villi van het Pro-Epicardiale-Orgaan (PEO) op ontwikkelingsstadium HH 15-18, met behulp van *in-ovo* microchirurgie. Na reïncubatie, werden *in-ovo* electrocardiogrammen (ECGs) opgenomen in normale (n=12) en EPDC-geïnhibeerde (n=12) HH stadium 38-42 kwarteleieren. Aanvullend werden ventriculaire activatiesequenties afgeleid van *ex-ovo* extracellulaire electrogram opnamen in zowel het normale (n=45) als het EPDC-geïnhibeerde (n=12) kwartelhart op HH stadia 38-42 en gecorreleerd aan de ontwikkelingsbiologische morfologie van de isolerende annulus fibrosis. In een subgroep van EPDC-geïnhibeerde embryonen lieten de *in-ovo* ECGs de 3 belangrijkste electrocardiografische karakteristieken van ventriculaire pre-excitatie syndromen zien: 1) een verkort PR-interval, 2) een delta golf en 3) een verlengd QRS-complex. *Ex-ovo* electrogrammen brachten aan het licht dat premature activatie van de ventriculaire basis in alle EPDC-geïnhibeerde embryonen voorkwam. Morfologisch kon ook in deze studie bevestigd worden dat er in het normale kwartelhart met name posteroseptaal gelokaliseerde accessoire verbindingen aanwezig zijn, welke ook in de EPDC-geïnhibeerde harten terug gevonden kunnen worden. In de EPDC-geïnhibeerde harten bleken echter additionele en relatief brede accessoire verbindingen in de rechter en linker laterale vrije myocardwand aanwezig te zijn. Periostin positiviteit werd gevonden in alle regionen van het hart waar ook EPDCs aanwezig zijn, zoals in het epicard, de endocardiale AV kussens, de epicardiale AV sulcus, het atriale en ventriculaire subendocard, de interstitiële fibroblasten en rondom de AV overgang. Hoewel de posteroseptale accessoire verbindingen positief voor periostin kleurden, bleek er rondom de brede laterale accessoire verbindingen in het EPDC-geïnhibeerde hart geen periostin expressie te zijn. Aan de hand van deze studie kunnen we concluderen dat EPDCs essentieel zijn voor een adequate formatie van de isolerende annulus fibrosis, daar inhibitie van de migratie van EPDCs tijdens de cardiogenese resulteert in grote defecten in de annulus fibrosis en het persisteren van brede accessoire verbindingen, die functioneel verantwoordelijk lijken te zijn voor het optreden van ventriculaire pre-excitatie.

Hoewel onder fysiologische omstandigheden smalle posteroseptale accessoire verbindingen tijdelijk functioneel actief blijven, zouden bredere lateraal gelokaliseerde accessoire verbindingen in het EPDC-geïnhibeerde hart mogelijk een pathologisch substraat voor postnataal persisterende accessoire verbindingen en AVRTs tot op de kinderleeftijd of volwassenheid kunnen vormen.

Na de beschrijving van deze experimentele studie, volgt een editorial dat geschreven is in antwoord op de resultaten van deze studie door Siew Yen Ho van de 'Department of Cardiac Morphology and the National Heart & Lung Institute of the Imperial College London and the Royal Brompton Hospital ' uit het Verenigd Koninkrijk, waarin additionele 'state-of-the-art' kennis betreffende accessoire verbindingen vanuit een ontwikkelingsbiologisch oogpunt wordt beschreven.

In **Hoofdstuk 4**, werd de fysiologische ontwikkeling van de isolerende annulus fibrosus cordis bestudeerd in het wildtype muismodel (stam C57B16/Jico en CD1) om de data uit het vogelmodel te kunnen extrapoleren naar een zoogdiermodel. Met behulp van *ex-ovo* electrogrammen werden ventriculaire activatiesequenties afgeleid in het embryonale muizenhart (n=48) op de ontwikkelingsstadia E 11.5 – 18.5 dpc en gecorreleerd aan de morfologie van de zich ontwikkelende annulus fibrosis in alle elektrofysiologisch geanalyseerde harten (n=48). In deze studie hebben we laten zien dat de annulus fibrosis zich ontwikkelt in het embryonale AV junctionele myocard, waar geen connexine 43 (Cx43) tot expressie wordt gebracht. Net als in het kwartelhart, bleken persisterende accessoire verbindingen en functionele premature activatie van de ventriculaire basis ook tijdens de cardiogenese in de muis te bestaan. De persisterende accessoire verbindingen in het embryonale muizenhart bleken overblijfselen van het AV junctionele myocard te zijn, omdat deze verbindingen net als het AV junctionele myocard ook geen Cx43 tot expressie brachten. Op vroege post-gesepteerde stadia van de hartontwikkeling in de muis bleken de accessoire verbindingen voornamelijk rondom zowel de mitralis als tricuspidalis klep annulus gelokaliseerd te zijn, terwijl de hoeveelheid accessoire verbindingen rondom de mitraalklep annulus significant ($p<0.001$) afnam in het laat post-gesepteerde muizenhart. Net als in het kwartelmodel, werd expressie van periostin in het muizenmodel gevonden in het epicardium, de endotheliale bekleding van het atriale en ventriculaire myocard, de interstitiële fibroblasten, de endocardiale AV kussens, de epicardiale AV sulcus en de AV overgang. In de muis bleken de myocardiale Cx43 negatieve

cardiomyocyten van de accessoire verbindingen in tegenstelling tot de kwartel zelf geen periostin tot expressie te brengen, terwijl hoge concentraties periostin wel in de fibroblasten aangrenzend aan en in de accessoire verbindingen gevonden werd. Hoewel de accessoire verbindingen ook in de muis significant afnamen in zowel aantal (p=0.003) als volume (p=0.035) op toenemende ontwikkelingsstadia, bleken persisterende accessoire verbindingen aanwezig te zijn tot op late gepostspeteerde stadia van de zoogdierontwikkeling. Vergelijkbaar met het vogelmodel, zou de fysiologische perinatale aanwezigheid van accessoire verbindingen in het muizenhart een tijdelijk substraat voor AVRTs in het perinatale leven kunnen vormen.

In **Hoofdstuk 5**, werd de aanwezigheid en specifieke lokalisatie van accessoire verbindingen tijdens de humane cardiogenese in relatie tot de fysiologische ontwikkeling van de isolerende annulus fibrosis bestudeerd. Immunohistochemische coupes van 45 humane embryonale, foetale en neonatale harten van 4 tot 6 weken gestatie (vogels ~HH stadium 14-46, muis ~E 10-19) werden geanalyseerd op het aantal en de locatie van accessoire verbindingen. Hoewel de annulus fibrosis in beginsel reeds aanwezig was rond 10 à 11 weken humane gestatie (vogels ~HH 21-27, muis ~E12.5-13.5), bleken multipele accessoire verbindingen de isolerende AV ring van zowel de linker als rechter annulus fibrosis te passeren tot aan het einde van het tweede trimester van de zwangerschap. Tijdens het tweede en derde trimester van de zwangerschap, was de linker annulus fibrosis reeds goed geïsoleerd door een dikke laag fibreus weefsel, terwijl de rechter AV annulus op dit ontwikkelingsstadium nog slechts zwak geïsoleerd was door een zeer dunne laag fibreus weefsel. Als gevolg hiervan, bleken er tot 20 weken humane gestatie (vogels ~HH 40, muis ~E17) accessoire verbindingen rond de laterale zijde van de tricuspidaalklep annulus aanwezig te zijn. Deze rechts gelokaliseerd accessoire verbindingen waren vaak in nabijheid van de rechter AV ring bundel, welke onderdeel uitmaakt van het tijdelijke embryonale gespecialiseerde AV geleidingssysteem, gelokaliseerd. Naast deze klassieke accessoire verbindingen bleken er in het zich ontwikkelende humane hart tot aan de geboorte ook myocardiale extensies te zijn die de zich ontwikkelende AV knoop met het myocard van het ventrikelseptum verbonden via gaten in de annulus fibrosis, corresponderend met het eerder beschreven fenomeen van foetale dispersie van de AV knoop. In deze studie hebben we onze morfologische data van eerdere dierexperimentele studies in het vogel en muismodel kunnen bevestigen en laten zien dat zoals gepostuleerd ook

in het humane hart de completering van de annulus fibrosis pas postnataal geschied, waarbij voornamelijk rechts gelokaliseerde persisterende accessoire verbindingen aanwezig blijven in het embryonale hart tot op late stadia van de ontwikkeling en zo mogelijk als substraat voor tijdelijke AVRTs bij foetussen of neonaten zouden kunnen functioneren.

DEEL II

In **Hoofdstuk 6**, werd een review betreffende de historische en huidige kennis omtrent de anatomie, fysiologie en ontogenese van de AV knoop en zijn atriale inputs gepresenteerd. Ook de structurele ontwikkeling van de AV knoop en de cellulaire elektrofysiologie van de embryonale AV overgang in relatie tot de volwassen AV knoop en het concept van AV nodale conductie dichotomie werden in dit hoofdstuk besproken. Hoewel het elektrofysiologisch substraat voor AVNRT uitgebreid bekend is, zijn de anatomische equivalenten die het reentry circuit vormen, grotendeels onbekend gebleven. Alhoewel recente markerstudies enige aanwijzingen betreffende de ontwikkelingsbiologische oorsprong van de AV knoop hebben gegeven, blijft de fysiologie, de structurele begrenzing en de ontogenese van de AV knoop grotendeels een raadsel.

Dit review wordt gevolgd door een experimentele studie in het kippen en kwartelmodel in **Hoofdstuk 7**, waarin een nieuw concept betreffende de ontwikkelingsbiologische oorsprong van de AV knoop werd gepostuleerd. In deze studie, werden spatiotemporele veranderingen in atriale activatiesequenties in het embryonale vogelhart (*Japanse kwartel* en *witte Leghorn kip*, HH stadia 19-36, n=96) gecorreleerd aan de morfologie van het zich ontwikkelende hart (n=64). Rond HH stadium 19-22, werden bilaterale morfologisch onderscheidbare gebieden van myocardweefsel geïdentificeerd rondom het proximale myocardiale deel van de linker en rechter cardinaalvenen. Deze bilaterale gebieden werden beiden gekarakteriseerd door MLC2a positiviteit, Nkx2.5 negativiteit en relatief lage concentraties connexine 43, Nav1.5 en glycogeen vergeleken met het aangrenzende atriale myocard. Hoewel het proximale myocardiale deel van de rechter cardinaalvene (RCV) correspondeert met het primordium van de sinusknoop (SAN), werd gehypothetiseerd dat het proximale deel van de linker cardinaalvene (LCV) een contributie levert aan de formatie van de AV knoop. Tot op HH stadium 27, bleven de LCV weefsels caudodorsaal aan het linker atrium gepositioneerd en bleek er functioneel een duidelijke links-zijdige dominante pacemaker te zijn in 21% van de functioneel geanalyseerde harten, terwijl op

deze stadia unilaterale impuls initiatie verwacht werd in de SAN in het rechter atrium. Na HH stadium 28, werd impuls initiatie in het linker atrium echter niet langer gevonden, wat perfect bleek te correleren aan de morfologische observatie dat rond HH stadium 28-30 de LCV reeds naar rechts getranspositioneerd was om in de basis van het rechter atrium de sinus coronarius (CS) te vormen, terwijl het myocard rondom het proximale deel van de LCV hierdoor gepositioneerd werd rondom het CS ostium in het slow pathway gebied van de toekomstig volwassen AV knoop. In deze studie hebben we laten zien dat de weefsels van de LCV een belangrijke functionele contributie aan de aanleg van de AV knoop in het slow pathway gebied lijken te leveren.

DEEL III

In **Hoofdstuk 8**, werden de langetermijnresultaten van radiofrequente katheterablatie (RF ablatie) in 118 pediatrische patiënten, die 140 RF ablatie procedures ondergingen voor 122 substraten voor supraventriculaire tachycardieën (SVTs), retrospectief geanalyseerd. De indicaties voor deze procedures waren: het falen of bijwerkingen van anti-arrhythmica (45%), keuze van patiënt/ouders (45%), cardiomyopathie of levensbedreigende aritmieën (8%) of naderende chirurgie voor congenitale hartdefecten (2%). In deze studie werd geconcludeerd dat de langetermijn uitkomst van pediatrische patiënten die RF ablatie hadden ondergaan wat betreft succespercentage, recidieven en complicatierisico gunstig is. Tevens bleek RF ablatie bij jongere kinderen (< 10 jaar) net zo veilig en effectief te zijn als RF ablatie bij oudere kinderen en adolescenten (10-18 jaar). Deze resultaten laten zien dat het in gespecialiseerde centra ook goed mogelijk is om de jongste pediatrische SVT patiënten curatief en veilig te behandelen met RF ablatie.

In **Hoofdstuk 9**, werd een illustratief case report beschreven over het optreden van 'incessant SVTs' gemedieerd door een persisterende accessoire verbinding in een premature neonaat met hydrops foetalis. Hoewel RF ablatie bij neonaten en jonge kinderen zelden geïndiceerd is en enkel uitgevoerd dient te worden met inachtneming van maximale veiligheidsmaatregelen, werd in deze casus gekozen voor RF ablatie als laatste therapeutische optie. De hydropische neonaat werd geboren op 32 weken gestatie na een tijdelijke succesvolle directe foetale amiodarone-therapie via de navelstreng. Na de geboorte bleek de tachycardie echter oncontroleerbaar ondanks hoge doseringen amiodarone en flecaïnide, waarna de patiënt ernstig respiratoir en circulatoir falen ontwikkelde.

Drie weken na de geboorte, met een lichaamsgewicht van 2 kg, onderging deze patiënt een succesvolle en ongecompliceerde RF ablatieprocedure waarbij een accessoire verbinding in de linker vrije wand als substraat voor de SVTs werd gevonden en behandeld met low-energy RF applicatie.

Conclusies

- Accessoire verbindingen die de isolerende annulus fibrosis en atrioventriculaire knoop (AV knoop) passeren zijn structurele overblijfselen van het embryonale AV junctionele myocard en blijven morfologisch aanwezig en functioneel in het kwartel en muizen hart tot op late post-gesepteerde stadia van de embryonale ontwikkeling en zouden een tijdelijk fysiologisch substraat voor AV reentry tachycardieën (AVRTs) in het perinatale leven kunnen vormen.

- Epicardium-Derived-Cells (EPDCs) zijn essentieel voor een adequate formatie van de isolerende annulus fibrosis.

- Inhibitie van EPDC-migratie tijdens de cardiogenese resulteert in grote defecten in de annulus fibrosis met het persisteren van brede accessoire verbindingen tot gevolg, die functioneel kunnen zorgen voor ventriculaire pre-excitatie en mogelijk een pathologisch mechanisme vormen voor postnataal persisterende accessoire verbindingen en AVRTs op de kinderleeftijd of volwassen leeftijd.

- Periostin is een profibrogeen extracellulair matrix proteïne dat sterk tot expressie komt in collageenrijk fibreus weefsel. Expressie van periostin in de annulus fibrosis rondom myocardiale accessoire verbindingen in het embryonale kwartel en muizen hart, lijkt het postnatale lot van deze verbindingen aan te geven.

- Tijdens de humane ontwikkeling, tot op 20 weken gestatie, blijken accessoire verbindingen met name rondom de tricuspidaalklep annulus aanwezig te blijven en zijn vaak in nabijheid van de rechter AV ring bundel, die onderdeel uitmaakt van het tijdelijke embryonale gespecialiseerde AV geleidingssysteem, gelokaliseerd.

- In het zich ontwikkelende vogelhart zijn er initieel tijdelijk bilateraal functionele pacemakers aanwezig in het rechter en linker cardinaalvene myocard, waarna het rechter sinoatriale knoop myocard in de rechter cardinaalvene de dominante pacemaker zal worden.

- Het myocard rondom het proximale deel van de linker cardinaalvene (LCV) in het embryonale vogelhart levert een belangrijke bijdrage aan het slow pathway gebied van de zich ontwikkelende heterogene AV knoop.

- De langetermijnuitkomst van pediatrische patiënten die een RF ablatie hebben ondergaan is wat betreft successpercentage, recidieven en complicatierisico gunstig.

- Hoewel RF ablatie bij neonaten en jonge kinderen (<10 jaar) zelden geïndiceerd is en enkel uitgevoerd dient te worden met maximale voorzichtigheid, kan RF ablatie als veilig laatste alternatief geïndiceerd zijn in gespecialiseerde centra.

Toekomstperspectieven

Door bestudering van de cardiogenese in het vogel, muizen en humane hart hebben we enkele aanwijzingen betreffende de fysiologische en pathologische ontwikkeling van de isolerende annulus fibrosis en de AV knoop aan het licht kunnen brengen. Uit deze studies is gebleken dat fysiologie en pathologie bij de ontwikkeling van de annulus fibrosis en het centrale geleidingssysteem nauw aan elkaar verbonden. Hoewel we hebben laten zien dat isolatie van de annulus fibrosis normaal gesproken pas postnataal gecompleteerd wordt, een essentiële rol voor EPDCs in de formatie van de annulus fibrosis hebben aangetoond, een nieuw concept betreffende de ontwikkeling van de AV knoop hebben gepostuleerd en bruikbare (immuno)histochemische markers zoals PAS-staining en de antilichamen MLC2a, Nkx2.5, periostin, Cx43 en Nav1.5, hebben geïdentificeerd voor de analyse van deze processen, blijven verscheidene aspecten van normale en abnormale annulus fibrosis formatie en AV knoop ontwikkeling onbeantwoord. Alhoewel we het ontwikkelingsbiologische proces van annulus fibrosis formatie zowel in het vogel en als in het muizenmodel hebben onderzocht en deze data hebben geëxtrapoleerd naar onderzoek in humane coupes, blijft de vraag bestaan hoe de gepostuleerde functionele implicaties getransleerd kunnen worden naar klinisch relevante problemen. Ook het conundrum betreffende de vraag of accessoire verbindingen die zich pas later in het leven presenteren tevens verbindingen zijn die postnataal zijn blijven bestaan maar tijdelijk functioneel verborgen zijn gebleven of dat deze verbindingen *de novo* zijn ontstaan en door nieuw ontwikkelde gaten in de annulus fibrosis zijn gegroeid, blijft bestaan.

Om deze en andere onderzoeksvragen verder te kunnen analyseren, zal toekomstig onderzoek op dit terrein met name gericht zijn op additionele analyse van atriale en ventriculaire activatiesequenties in het zich ontwikkelende en volwassen hart met behulp van nieuwere technieken zoals Multi-Electrode-Array (MEA) opnamen en optical mapping door toepassing van voltage sensitieve kleurstoffen. Ook kennis betreffende de cellulaire elektrofysiologie van de persisterende accessoire verbindingen en de gepostuleerde AV nodale primordiale weefsels, zoals beschreven in dit proefschrift, door analyse van de intracellulaire elektrofysiologie met behulp van patch clamp opnames, zal meer licht schijnen op de functionele implicaties van onze huidige en toekomstige experimentele bevindingen. Toekomstig onderzoek zal ook gericht zijn op de toepassing van (nieuwe) genetisch gemodificeerde diermodellen (zoals bv. de podoplanine-KO muis of Shox2-KO muis) en de identificatie en exploratie van

de expressie van (nieuwe) myocardiale markers (zoals Nkx2.5) en markers voor het cardiale geleidingssysteem (zoals Islet-1 en Id-2) en hun onderlinge interacties. De studies in dit proefschrift hebben in ieder geval laten zien dat een systematische analyse van de anatomie in relatie tot de functionaliteit ook fundamenteel zal zijn in toekomstig onderzoek naar de ontwikkelingsbiologische mechanismen die ten grondslag liggen aan de formatie van de annulus fibrosis en AV knoop ontwikkeling en uiteindelijk een translationele basis zal vormen om klinisch relevante aspecten van cardiale arritmieën succesvol te kunnen interpreteren.

Wat betreft het klinisch onderzoek naar pediatrische SVTs en de therapeutische opties beschreven in dit proefschrift, is de verwachting dat huidige lopende grote prospectieve pediatrische studies een volgende stap in de evaluatie van de klinische presentatie en het bepalen van behandelingsstrategieën zullen vormen.

List of Publications

Full Papers

Kolditz DP, Blom NA, Bökenkamp R, Schalij MJ. Low-energy radiofrequency catheter ablation as therapy for supraventricular tachycardia in a premature neonate. **Eur J Pediatr. 2005 Sep;164(9):559-62**.

Kolditz DP, Blom NA, Bökenkamp R, Bootsma M, Zeppenfeld K, Schalij MJ. Radiofrequency catheter ablation for treating children with cardiac arrhythmias: favorable results after a mean of 4 years. **Ned Tijdschr Geneeskd. 2005 Jun;149(24):1339-46. Erratum in: Ned Tijdschr Geneeskd. 2005 Jul;149(29):1656**.

Kolditz DP, Wijffels MCEF, Blom NA, van der Laarse A, Markwald RR, Schalij MJ, Gittenberger-de Groot AC. Persistence of functional atrioventricular accessory pathways in post-septated embryonic avian hearts: implications for morphogenesis and functional maturation of the cardiac conduction system. **Circulation. 2007 Jan 2;115(1):17-26**.

Kolditz DP, Wijffels MCEF, Blom NA, van der Laarse A, Hahurij ND, Lie-Venema H, Markwald RR, Poelmann RE, Schalij MJ, Gittenberger-de Groot AC. Epicardium-derived cells (EPDCs) in annulus fibrosis development and persistece of accessory pathways. **Circulation. 2008 Mar 25;117(12):1508-17**.

Hahurij ND, Blom NA, Kolditz DP, Bökenkamp R, Markwald RR, Schalij MJ, Poelmann RE, Gittenberger-De Groot AC. Accessory atrioventricular myocardial connections in the developing human heart, relevance for perinatal supraventricular tachycardias. **Circulation. 2008. Jun 3;117(22):2850-8**.

Heleen Lie-Venema, Ismail Eralp, Roger R. Markwald, Nynke M.S. van den Akker, Denise P. Kolditz, Maurits C.E.F. Wijffels, Robert E. Poelmann, Ad J.J.C. Bogers, Adriana C. Gittenberger-de Groot. Periostin expression by epicardium-derived cell (EPDCs) is involved in the development of the fibrous heart skeleton. **Differentiation. 2008 Sep;76(7):809-19.**

Kolditz DP, Schalij MJ, Gittenberger-de Groot AC. Development of the Atrio-Ventricular Conduction Axis in Relation to Cardiac Arrhythmia Etiology. (**Submitted**)(see also, **Chapter 6**, *this thesis*)

Kolditz DP, Vicente-Steijn R, Pijnappels DA, Jongbloed MR, Poelmann RE, Martin J. Schalij,Adriana C. Gittenberger-de Groot. Development of the Atrioventricular Node from Heterogeneous Primordia: Implications for the Anatomical Correlate of the Slow-Pathway. (**Submitted**)(see also, **Chapter 7**, *this thesis*)

Hahurij ND, Kolditz DP, Blom NA, Bokenkamp R, Markwald RR, Schalij MJ, Poelmann RE, Gittenberger-de Groot AC. Functional Accessory Atrioventricular myocardial pathways in mouse heart development: Basis for transient perinatal supraventricular tachycardias. (**Submitted**) (see also, **Chapter 4**, *this thesis*)

Vicente-Steijn R, Kolditz DP, Mahtab EAF, Bax NAM, van der Graaf LM, Schalij MJ, Poelmann RE, Gittenberger-de Groot AC, Jongbloed MRM. Dual Pacemaker Activity in the Developing Chick Heart and Correlation with the Expression of RhoA in the Developing Cardiac Conduction System. (**Submitted**)

Peer-Reviewed Abstracts

Kolditz DP, Blom NA, Schalij MJ, Bootsma M, Bökenkamp R, Zeppenfeld K. Long-term efficacy and safety of pediatric radiofrequency catheter ablation as treatment for cardiac arrhythmias. *Annual autumn meeting Netherlands society of Cardiology, Ermelo, The Netherlands, October 2004.*

Kolditz DP, Blom NA, Schalij MJ, Bootsma M, Bökenkamp R, Zeppenfeld K. Resultaten en follow-up van katheterablatie met radiofrequente energie bij kinderen. *Annual meeting Netherlands society of Pediatrics, Veldhoven, The Netherlands.* **Tijdschrift voor Kindergeneeskunde. 2004;S1:52.**

Kolditz DP, Wijffels MCEF, Schalij MJ, Gittenberger-de Groot AC. Persistence of primitive functional atrioventricular conduction pathways bypassing the AV node and insulating annulus fibrosis in post-septated embryonic avian hearts. *Annual autumn meeting Netherlands society of Cardiology, Ermelo, The Netherlands, October 2005.*

Kolditz DP, Wijffels MCEF, Blom NA, van der Laarse A, Markwald RR, Gittenberger-de Groot AC, Schalij MJ. Persistence of Functional, Periostin Positive, Myocardial Accessory Pathways in Embryonic Avian Hearts at Late Post-Septational Stages of Embryonic Development. *The 13th Annual Weinstein Cardiovascular Development congress, St. Petersburg, Florida, May 2006.*

Kolditz DP, Wijffels MCEF, Blom NA, van der Laarse A, Markwald RR, Gittenberger-de Groot AC, Schalij MJ. Persistence of Functional, Periostin Positive, Myocardial Accessory Pathways in Embryonic Avian Hearts at Late Post- Septational Stages of Embryonic Development. *European Society of Cardiology congress, Barcelona, Spain, September 2006.* **European Heart Journal 2006;27(1):414.**

Kolditz DP, Wijffels MCEF, Blom NA, van der Laarse A, Markwald RR, Gittenberger-de Groot AC, Schalij MJ. The role of Epicardium-Derived-Cells (EPDCs) in atrioventricular isolation and development of the specialized cardiac conduction system: implications for AV reentrant tachycardias. *Annual autumn meeting Netherlands society of Cardiology, Ermelo, The Netherlands, October 2006.*

Kolditz DP, Wijffels MCEF, Blom NA, van der Laarse A, Markwald RR, Schalij MJ, Gittenberger-de Groot AC. Persistence of Primitive Functional Accessory Atrio-Ventricular (AV) Conduction Pathways in Post-Septated Embryonic Avian Hearts and The Role of Epicardium-Derived-Cells (EPDCs) in Atrio-Ventricular Isolation: Implications for AV Reentrant Tachycardias. *Working group on Cardiovascular research the Netherlands (WCN) congress, Amsterdam, The Netherlands, November 2006.*

Kolditz DP, Wijffels MCEF, Blom NA, van der Laarse A, Markwald RR, Gittenberger-de Groot AC, Schalij MJ. The role of epicardium-derived-cells (EPDCs) in atrio-ventricular (AV)-isolation: implications for AV reentrant tachycardias. *28th Annual Scientific Sessions Heart Rhythm Society (HRS), Denver, Colorado, USA, May 2007.* **Heart Rhythm. 2007;4(5):S109.**

Hahurij ND, Blom NA, Kolditz DP, Wijffels MCEF, Bökenkamp R, Markwald RR, Schalij MJ, Poelmann RE, Gittenberger-de Groot. Accessory atrioventricular myocardial connections in the developing human heart, relevance for perinatal supraventricular tachycardias. *28th Annual Scientific Sessions Heart Rhythm Society (HRS), Denver, Colorado, USA, May 2007.* **Heart Rhythm. 2007;4(5): S44.**

Hahurij ND, Blom NA, Kolditz DP, Wijffels MCEF, Bökenkamp R, Markwald RR, Schalij MJ, Poelmann RE, Gittenberger-de Groot AC. Presence of accessory pathways in the developing human heart, possible explanation for fetal and neonatal atrioventricular reentrant tachycardias. *42rd Annual Meeting of the Association for European Paediatric Cardiology (AEPC), Warsaw, Poland, May 2007.* **Cardiology in the Young 2007;17(1):26.**

Kolditz DP, Wijffels MCEF, Blom NA, van der Laarse A, Markwald RR, Gittenberger-de Groot AC, Schalij MJ. The role of epicardium-derived-cells (EPDCs) in atrio-ventricular (AV)-isolation: implications for AV reentrant tachycardias. *EUROPACE congress, Lisboa, Portugal, June 2007.* **European Heart Journal. 2007;28:103.**

Kolditz DP, Wijffels MCEF, van der Laarse A, Markwald RR, Gittenberger-deGroot AC, Schalij MJ. Epicardium-Derived-Cells in annulus fibrosis development and persistence of accessory atrioventricular pathways. *European Society of Cardiology (ESC) congress, Vienna, Austria, September 2007.* **European Heart Journal. 2007;28:102.**

Hahurij ND, Blom NA, Kolditz DP, Wijffels MCEF, Bökenkamp R, Markwald RR, Schalij MJ, Poelmann RE, Gittenberger-de Groot AC. Presence of accessory AV pathways in human fetuses, substrate for fetal supraventricular tachycardias. *European Society of Cardiology (ESC) congress, Vienna, Austria, September 2007.* **European Heart Journal. 2007;28:102.**

Kolditz DP, Schalij MJ, Blom NA, van der Laarse A, Markwald RR, Poelmann RE, Gittenberger-de Groot AC. Persistence of Accessory Atrioventricular Pathways in Post-Septated Embryonic Avian Hearts and The Role of Epicardium-Derived-Cells (EPDCs) in Annulus Fibrosis Formation: Implications for AV Reentrant Tachycardias. *Bi-Annual Meeting of the ESC Working Group on Developmental Anatomy and Pathology, Bari, Italy, March 2008.*

Kolditz DP, Pijnappels DA, Blom NA, Hahurij ND, Gittenberger-de Groot AC, Schalij MJ. Embryonic Development of the Atrio-Ventricular Node from Triple AV Nodal Primordia in Relation to Arrhythmia Etiology. *29th Annual Scientific Sessions Heart Rhythm Society (HRS), San Fransisco, California, USA, May 2008.* **Heart Rhythm. 2008;5:S7.**

Hahurij ND, Kolditz DP, Bökenkamp R, Markwald RR, Schalij MJ, Poelmann RE, Gittenberger-de Groot AC, Blom NA. Functional accessory atrioventricular myocardial pathways in mouse heart development: basis for perinatal supraventricular tachycardias. *29th Annual Scientific Sessions Heart Rhythm Society (HRS), San Fransisco, California, USA, May 2008.* **Heart Rhythm. 2008;5:S40.**

Kolditz DP, Pijnappels DA, Blom NA, Hahurij ND, Gittenberger-de Groot AC, Schalij MJ. Embryonic Development of the Atrio-Ventricular Node from Triple AV Nodal Primordia in Relation to Arrhythmia Etiology. *43rd Annual Meeting of the Association for European Paediatric Cardiology (AEPC), Venice, Italy, May 2008.* **Cardiology Young. 2008;18(1):1-106.**

Hahurij ND, Kolditz DP, Bökenkamp R, Markwald RR, Schalij MJ, Poelmann RE, Gittenberger-de Groot AC, Blom NA. **Accessory atrioventricular pathways** in normal mouse heart development, possible explanation for perinatal atrioventricular reentrant tachycardias. *43rd Annual Meeting of the Association for European Paediatric Cardiology (AEPC), Venice, Italy, May 2008.* **Cardiology Young. 2008;18:1-106.**

Kolditz DP, Blom NA, Van Der Laarse A, Markwald RR, Gittenberger-De Groot AC, Schalij MJ. **Periostin expression on the annulus fibrosis in relation to** accessory pathway persistence. *European Society of Cardiology (ESC) congress, Munich, Germany, September 2008.* **European Heart Journal. 2008;29:362-363.**

Kolditz DP, Vicente-Steijn R, Pijnappels DA, Jongbloed MRM, Blom NA, Van Der Laarse A, Poelmann RE, Schalij MJ, Gittenberger-De Groot AC. **Embryonic** development of the Atrio-Ventricular Node (AVN) from triple AV Nodal primordia in relation to arrhythmia etiology. *European Society of Cardiology (ESC) congress, Munich, Germany, September 2008.* **European Heart Journal.2008;29:651**.

Hahurij ND, Kolditz DP, Bokenkamp R, Markwald RR, Schalij MJ, Poelmann RE, Gittenberger-De Groot AC, Blom NA. **Functional accessory atrioventricular** myocardial pathways in mouse heart development; basis for perinatal supraventricular tachycardias. *European Society of Cardiology (ESC) congress, Munich, Germany, September 2008.* **European Heart Journal. 2008;29:652.**

Scientific Awards

First price in recognition of best oral presentation entitled "Long-term efficacy and safety of pediatric radiofrequency catheter ablation as treatment for cardiac arrhythmias," annual autumn meeting Netherlands society of Cardiology, Ermelo, The Netherlands, October 2004

First price in recognition of best oral presentation entitled "Persistence of primitive functional atrioventricular conduction pathways bypassing the AV node and insulating annulus fibrosis in post-septated embryonic avian hearts," annual autumn meeting Netherlands society of Cardiology, Ermelo, The Netherlands, October 2005

First price in recognition of best oral presentation entitled "The role of Epicardium-Derived-Cells (EPDCs) in atrioventricular isolation and development of the specialized cardiac conduction system: implications for AV reentrant tachycardias," annual autumn meeting Netherlands society of Cardiology, Ermelo, The Netherlands, October 2006

Council on Basic Cardiovascular Science (CBCS) award from the ESC Working Group on Developmental Anatomy and Pathology, in recognition of best oral presentation, entitled "Persistence of Accessory Atrioventricular Pathways in Post-Septated Embryonic Avian Hearts and The Role of Epicardium-Derived-Cells (EPDCs) in Annulus Fibrosis Formation: Implications for AV Reentrant Tachycardias," at the Bi-Annual Meeting of the Working Group on Developmental Anatomy and Pathology, Bari, Italy, March 2008.

Travel award from the ESC Council on Basic Cardiovascular Science at the European Society of Cardiology congress 2008, Munich, Germania, September 2008.

Curriculum Vitae

De auteur van dit proefschrift werd geboren op 6 mei 1982 te Maassluis. In 2000 behaalde zij haar Gymnasiumdiploma aan de Scholengemeenschap Spieringshoek te Schiedam. Hierna startte zij met haar opleiding Geneeskunde aan de Universiteit Leiden. In 2004 startte zij met een klinisch wetenschappelijk doctoraal afstudeeronderzoek naar de behandeling van supraventriculaire ritmestoornissen bij kinderen onder begeleiding van Dr. N.A. Blom (Kindercardiologie) en Prof. dr. M.J. Schalij (Cardiologie). In augustus 2004 behaalde zij haar doctoraalexamen en zette tijdens de co-schappenfase van haar studie haar wetenschappelijk onderzoek voort. In juni 2005 startte zij vervolgens met haar pre-klinische promotietraject onder begeleiding van Prof. dr. M.J. Schalij (Cardiologie) en Prof. dr. A.C. Gittenberger-de Groot (Anatomie& Embryologie) naar de etiologie van supraventriculaire ritmestoornissen en heeft dit gedurende de eerste 2 jaren gecombineerd met de afronding van haar co-schappen. Na haar artsexamen in september 2007, heeft zij het laatste jaar van haar promotietraject fulltime aan haar onderzoek gewerkt, waarvan dit proefschrift het resultaat is.

Tijdens haar afstudeeronderzoek en promotieperiode won zij in oktober 2004, 2005 en 2006 de prijs voor de beste presentatie op het najaarscongres van de Nederlandse Vereniging Voor Cardiologie (NVVC), ontving in maart 2008 een prijs van de 'Council on Basic Cardiovascular Science (CBCS)' van de 'ESC Working Group on Developmental Anatomy and Pathology' voor de beste presentatie op het 2-jaarlijkse congres van de 'ESC Working Group on Developmental Anatomy and Pathology' en ontving in september 2008 een Travel Grant van de 'European Society of Cardiology (ESC)'.

Per 1 januari 2009 is zij begonnen met de opleiding Cardiologie vanuit het Leids Universitair Medisch Centrum (LUMC) (opleider Prof. dr. E.E. van der Wall), welke werd aangevangen met het B-jaar Cardiologie (opleider Dr. B.J.M. Delamarre) in het HAGA ziekenhuis te Den Haag. Daarna zal zij haar vooropleiding Interne Geneeskunde in het Rijnland ziekenhuis te Leiderdorp (opleider Dr. M.J.F.M. Janssen) volgen, waarna zij in 2012 weer zal terugkeren naar het LUMC om de A-jaren van haar opleiding af te ronden. Naast het vervolgen van de klinische opleiding Cardiologie, hoopt zij zich in de toekomst bezig te blijven houden met (basaal) wetenschappelijk onderzoek.

Curriculum Vitae

The author of this thesis was born May 6th 1982 in Maassluis, the Netherlands. In 2000 she graduated and received her Gymnasium diploma from the 'Scholengemeenschap Spieringshoek' in Schiedam, whereafter she started studying Medicine at the University of Leiden. In 2004 she started a clinically oriented scientific research project concerning the treatment of paediatric supraventricular arrhythmias under supervision of Dr. N.A. Blom (Pediatric Cardiology) and Prof. Dr. M.J.Schalij (Cardiology) to complete the Bachelor part of her study in August 2004. During her interships, she continued her research and in June 2005 she started her pre-clinical PhD-research under supervision of Prof. dr. M.J. Schalij (Cardiologie) and Prof. dr. A.C. Gittenberger-de Groot (Anatomy & Embryology) on the etiology of supraventricular arrhythmias in children and adults and worked on this PhD-research for 2 years in parallel to finishing the remainder of her internships. After her medical degree in September 2007, she completed the remaining part of her PhD-project fulltime, of which this thesis is the result.

During her research project as a medical student and during her PhD-research she received the first price in recognition of best oral presentation at the annual autumn meeting of the Netherlands Society of Cardiology (NVVC) in October 2004, 2005 and 2006, received the Council on Basic Cardiovascular Science (CBCS) award in recognition of best oral presentation from the ESC Working Group on Developmental Anatomy and Pathology in March 2008 and was awarded a Travel Grant from the European Society of Cardiology (ESC) in September 2008.

As of January 1st 2009 she started her Cardiology training at the Leiden University Medical Center (LUMC) (Prof. dr. E.E. van der Wall), which commenced with the B-year of Cardiology at the HAGA-hospital in The Hague (Dr. B.J.M. Delamarre) and will be followed by the pre-Cardiology phase of Internal Medicine at the Rijnland Hospital in Leiderdorp (Dr. M.J.F.M. Janssen) after which she will return to the LUMC for the last part of her training in 2012. Besides completing her Cardiology training, she hopes to remain active in (basic) scientific work.